2
4-28-82

MASTER

NUREG/CR-2456
ORNL-5848

ornl

OAK
RIDGE
NATIONAL
LABORATORY

UNION
CARBIDE

NUREG/CR--2456

DE82 013357

Experimental Investigations of Uncovered-Bundle Heat Transfer and Two-Phase Mixture-Level Swell Under High-Pressure Low-Heat-Flux Conditions

T. M. Anklam
R. J. Miller
M. D. White

Prepared for the U.S. Nuclear Regulatory Commission
Office of Nuclear Regulatory Research
Under Interagency Agreements DOE 40-551-75 and 40-552-75

OPERATED BY
UNION CARBIDE CORPORATION
FOR THE UNITED STATES
DEPARTMENT OF ENERGY

DISCLAIMER

Printed in the United States of America. Available from
National Technical Information Service
U.S. Department of Commerce
5285 Port Royal Road, Springfield, Virginia 22161

Available from

GPO Sales Program
Division of Technical Information and Document Control
U.S. Nuclear Regulatory Commission
Washington, D.C. 20555

NUREG/CR-2456
ORNL-5848
Dist. Category R2

Contract No. W-7405-eng-26

NUREG/CR--2456

DE82 013357

Engineering Technology Division

EXPERIMENTAL INVESTIGATIONS OF UNCOVERED-BUNDLE HEAT TRANSFER AND TWO-PHASE MIXTURE-LEVEL SWELL UNDER HIGH-PRESSURE LOW-HEAT-FLUX CONDITIONS

(Final Report for THTF Tests 3.09.10I-N and 3.09.10AA-FF)

T. M. Anklam R. J. Miller
M. D. White

Manuscript Completed — March 12, 1982
Date Published — March 1982

Prepared for the
U.S. Nuclear Regulatory Commission
Office of Nuclear Regulatory Research
Under Interagency Agreements DOE 40-551-75 and 40-552-75

NRC Fin No. B0125

Prepared by the
OAK RIDGE NATIONAL LABORATORY
Oak Ridge, Tennessee 37830
operated by
UNION CARBIDE CORPORATION
for the
DEPARTMENT OF ENERGY

MGW

THIS PAGE

WAS INTENTIONALLY

LEFT BLANK

CONTENTS

Page

ACKNOWLEDGMENTS v

LIST OF SYMBOLS vii

ABSTRACT 1

1. INTRODUCTION 1

2. TEST NOMENCLATURE 3

3. FACILITY DESCRIPTION 4

3.1 Flow Circuit Description 4

3.2 Bundle Description 7

3.3 Differential Pressure Instrumentation 12

3.4 Summary 12

4. EXPERIMENTAL PROCEDURES 14

5. UNCOVERED BUNDLE HEAT TRANSFER 15

5.1 Background 15

5.2 General Theory 15

5.2.1 Convection heat transfer 15
5.2.2 Radiation heat transfer 19
5.2.3 Spacer grid effects 20

5.3 Presentation of Results 20

5.3.1 Summary of test conditions 20
5.3.2 Temperature and heat transfer coefficient profiles 22
5.3.3 Radiation heat transfer 31
5.3.4 Correlation of convective component of heat transfer 34
5.3.5 Addition of radiation to selected convective correlations 40
5.3.6 Evaluation of reactor vendor correlations 45

6. TWO-PHASE MIXTURE LEVEL SWELL 55

6.1 Review of Experimental Procedure 55

6.2 General Theory 55

6.3 Data Reduction and Analysis 61

6.3.1 Two-phase mixture level 61
6.3.2 Beginning of saturated boiling 61
6.3.3 Mass flow and volumetric vapor generation rate 61
6.3.4 Void fraction 62

	Page
6.3.5 Collapsed liquid level	63
6.3.6 Uncertainties	63
6.4 Presentation of Results	63
6.4.1 Summary of test conditions	63
6.4.2 Void fraction profiles	65
6.4.3 Comparisons between experimental and predicted mixture level	73
6.4.4 Two-phase mixture level swell	78
7. SUMMARY	81
REFERENCES	83
APPENDIX A. ANALYTICAL METHODOLOGY	85
APPENDIX B. UNCOVERED BUNDLE HEAT TRANSFER RESULTS	99
APPENDIX C. UNCERTAINTIES METHODOLOGY	249
APPENDIX D. VOID FRACTION DATA	251

ACKNOWLEDGMENTS

In the conduct of a large experimental and analytical program, there are always a great many individuals whose contributions should be recognized. The dedicated efforts of the entire Blowdown Heat Transfer Program staff are reflected in this report. The authors express their sincere appreciation to the following personnel:

M. C. Adair	A. F. Johnson	D. Reed
J. L. Bartley	R. W. McCulloch	R. D. Stulting
D. H. Cook	G. S. Mailen	J. W. Teague, Jr.
W. G. Craddick	D. G. Morris	R. E. Textor
R. D. Dabbs	C. B. Mullins	H. E. Trammell
R. L. Durall	R. W. Murphy	B. J. Veazie
S. S. Gould	L. J. Ott	J. D. White
H. W. Hoffman	H. R. Payne	G. L. Yoder
J. E. Robinson	W. Ragan, Jr.	

The authors wish to express special thanks to D. F. Hunt and M. S. Thompson for their work on data management and graphics, to C. R. Hyman for his valuable suggestions and comments, and to D. K. Felde, J. E. Wolfe and D. J. Fraysier for their skillful operation of the THTF.

THIS PAGE

WAS INTENTIONALLY

LEFT BLANK

LIST OF SYMBOLS

A_1, A_2, A_3, ...	Constants
A_F	Flow area
a_1	Ratio of bundle-flow area at grid to normal bundle-flow area when viewed from upstream
a_2	Ratio of projected mixing vane area to normal grid area when viewed from upstream
C_o	Concentration parameter
C_p	Specific heat
D	Diameter
D_H	Hydraulic diameter
F	Geometric view factor
F_d	Modified Froude number
F_{froth}	Function describing enhancement of heat transfer near froth level
F_{grid}	Function describing enhancement of heat transfer near spacer grid
G	Mass flux
g	Gravitational acceleration
Gr	Grashof number
h	Enthalpy or heat transfer coefficient
I	Electrical current
j	Superficial velocity
k	Thermal conductivity
L	Length
L/D	Length-to-diameter ratio
M	Mass
$\dot{M}$	Mass flow
Nu	Nusselt number
P	Pressure
p	Perimeter
Pr	Prandtl number
$\dot{Q}$	Volumetric flow
q	Heat flow
q'	Heat flow/length

q''	Heat flux
r	Electrical resistance
Re	Reynolds number
S	Mixture-level swell
T	Temperature
t	Time
V'	Volume/length
V_{gj}	Mean-weighted drift velocity
$VVF_{2-\phi}$	Volumetric vapor flux evaluated at two-phase mixture level
X	Transverse coordinate
Z	Axial coordinate
Z_{CLL}	Collapsed liquid level
Z_{sat}	Start of saturated boiling length
$Z_{2-\phi}$	Two-phase mixture level
α	Absorptivity or void fraction
β	Coefficient of volume expansion
ε	Emissivity
χ	Quality
μ	Viscosity
ν	Dynamic viscosity
ϕ	Angle of mixing vane with respect to axial direction
ρ	Density
Σ	Laplace length
σ	Boltzmann's constant or surface tension

Subscripts

bub	Bubble
conv	Convective
cor	Correlation
cr	Critical
CW	Cold wall
EOHL	End of heated length
exp	Experimental

f	Film or saturated liquid depending on context
FRS	Fuel rod simulator
g	Saturated vapor
H	Hydraulic
l	Liquid
lam	Laminar
m	Measured
mw	Modified wall
rad	Radiation
ref	Reference
sat	Saturated
ss	Stainless steel
std	Standard
TC	Thermocouple
tot	Total
tur	Turbulent
v	Vapor
w	Wall

EXPERIMENTAL INVESTIGATIONS OF UNCOVERED-BUNDLE HEAT TRANSFER AND TWO-PHASE MIXTURE-LEVEL SWELL UNDER HIGH-PRESSURE LOW HEAT-FLUX CONDITIONS

T. M. Anklam R. J. Miller
M. D. White

ABSTRACT

Results are reported from a series of uncovered-bundle heat transfer and mixture-level swell tests. Experimental testing was performed at Oak Ridge National Laboratory in the Thermal Hydraulic Test Facility (THTF). The THTF is an electrically heated bundle test loop configured to produce conditions similar to those in a small-break loss-of-coolant accident.

The objective of heat transfer testing was to acquire heat transfer coefficients and fluid conditions in a partially uncovered bundle. Testing was performed in a quasi-steady-state mode with the heated core 30 to 40% uncovered. Linear heat rates varied from 0.32 to 2.22 kW/m·rod (0.1 to 0.68 kW/ft·rod). Under these conditions peak clad temperatures in excess of 1050 K (1430°F) were observed, and total heat transfer coefficients ranged from 0.0045 to 0.037 W/cm²·K (8 to 65 Btu/h·ft²·°F). Spacer grids were observed to enhance heat transfer at, and downstream of, the grid. Radiation heat transfer was calculated to account for as much as 65% of total heat transfer in low-flow tests. It is recommended that a reference temperature correlation, based on the modified wall Reynolds number, be used to predict convective heat transfer in the range $2000 \leq Re_{mw} \leq 10{,}000$.

Results of mixture-level swell testing showed that the relative expansion of the boiling length caused by the presence of vapor voids (mixture-level swell) was linearly related to the total core volumetric vapor generation rate. Assessment of commonly used local void-fraction models indicated that of the correlations examined, the Yeh void correlation was best suited for use under the subject test conditions.

1. INTRODUCTION

Under sponsorship of the U.S. Nuclear Regulatory Commission, Oak Ridge National Laboratory (ORNL) has experimentally and analytically investigated rod bundle heat transfer under high-pressure low heat-flux conditions. Experimental work has centered on four areas: (1) quasi-steady-state uncovered-bundle heat transfer, (2) two-phase mixture-level swell under high-pressure low heat-flux conditions, (3) high-pressure core reflood, and (4) high-pressure transient bundle boiloff.

The experimental work was performed in the Thermal-Hydraulic Test Facility (THTF) at ORNL. The THTF is a high-pressure bundle thermal-hydraulics loop. It contains a 64-rod electrically heated bundle with internal dimensions typical of a 17 x 17 pressurized-water reactor (PWR) fuel assembly. Testing was performed in two series. The first series, run in January 1980, consisted of six uncovered-bundle heat transfer and mixture-level swell tests and six high-pressure reflood tests.[1-3] After extensive THTF instrumentation upgrading, the second series was run in November 1980. The series consisted of 6 uncovered-bundle heat transfer tests, 12 high-pressure mixture-level swell tests, 5 high-pressure reflood tests, and 5 transient bundle boiloff tests.

This report presents the results and analyses of the uncovered-bundle heat transfer and mixture-level swell tests run in November 1980. Reflood and bundle boiloff test results and analyses can be found in Ref. 4. Major topics to be discussed in the uncovered-bundle heat transfer section include a presentation of experimentally determined heat transfer coefficients, local fluid conditions, correlation of convective heat transfer data, comparison of experimental heat transfer coefficients to existing heat transfer correlations, and a discussion of the effects of spacer grids on heat transfer.

Topics to be covered in the section on mixture-level swell include a presentation of experimentally determined axial void-fraction profiles, comparisons between commonly used local void-fraction predictive models and experimental data, and a critique of selected void-fraction models and their ability to predict the two-phase mixture level in an uncovered bundle.

Report appendixes contain descriptions of analytical methodologies and detailed listings of heat transfer and mixture-level swell data. The report begins with a description of test nomenclature.

2. TEST NOMENCLATURE

The intent of this section is to familiarize the reader with the test naming conventions used at ORNL. All of the uncovered bundle tests run at ORNL are named in the following format:

test 3.ab.cdE,

where 3 refers to THTF Bundle 3, ab is a two-digit test series identifier, cd is a two-digit identifier that defines the generic type of test run, and E is a letter or letters denoting a particular test within the generic test type cd. A specific example would be

test 3.09.10K,

where 09 denotes that the test was run in the 9th series of tests run on THTF bundle 3. The number 10 denotes that the test is designed to study thermal hydraulics under high-pressure low heat-flux conditions, and K denotes that it is the 11th type-10 test to be run. The first uncovered-bundle test series was test series 02, and the second series was 09.

3. FACILITY DESCRIPTION

Experimental testing was performed at ORNL in the THTF. The THTF is a large high-pressure nonnuclear thermal-hydraulics loop. System configuration was designed to produce a thermal-hydraulic environment similar to that expected in a small-break loss-of-coolant accident (SBLOCA).

3.1 Flow Circuit Description

Figure 1 is an illustration of the THTF in small-break test configuration. Flow leaves the main coolant pump and passes through FE-3, a 2-in. turbine meter. On leaving FE-3, flow enters the inlet flow manifold. The flow manifold is divided into two parallel flow lines: a 1/2-in. line used to meter very low flow rates and a 3/4-in. flooding line used for the higher flows experienced during reflood. The entire inlet-flow manifold was constructed of high-pressure stainless steel tubing. Volumetric flow rates in the low-flow 1/2-in. inlet line were measured by FE-18A (a low-flow orifice meter), and FE-250 and FE-260 (1/2-in. turbine meters). The two inlet lines converge at the injection manifold, from which fluid passes directly into the lower plenum. Fluid does not pass through a downcomer. Flow proceeds upward through the heated bundle and exits through the bundle outlet spool piece. Spool piece measurements include pressure, temperature, density, volumetric flow, and momentum flux. When outlet flow rates were very low the volumetric flow was measured by a bank of low-flow orifice meters downstream of the outlet spool piece. On leaving the orifice manifold, flow passes through a heat exchanger and returns to the pump inlet.

System pressure was controlled via the loop pressurizer. The pressurizer was partially filled with subcooled water, and nitrogen cover gas was used to control pressure. The system pressure could be controlled more easily by filling or venting nitrogen than by the conventional flashing and condensation of saturated water and steam.

Flow was injected directly into the lower plenum and did not pass through a downcomer. The shroud-plenum annulus (Fig. 2) was used in earlier THTF testing as an internal downcomer but was isolated from the primary flow circuit in these tests. The shroud-plenum annulus pressure was equalized with the system pressure. This was accomplished by connecting the bottom of the annulus region to the pressurizer surge line and the top of the annulus to the test section outlet. The line between the annulus and pressurizer was opened, and the line between the annulus and test section outlet was closed during the initial boiloff phase of steady-state testing. This allowed any vapor generated by boiling in the annulus to displace liquid into the pressurizer. Note that the displacement of liquid causes the mixture levels in the downcomer and bundle to equalize, which is why installation of a line between the pressurizer and downcomer was advantageous. However, once mixture levels had equalized, leaving this line open was no longer advantageous. The reason is that the steam flow through the outlet causes a substantial pressure drop between the test section and pressurizer. If the annulus was in communication with

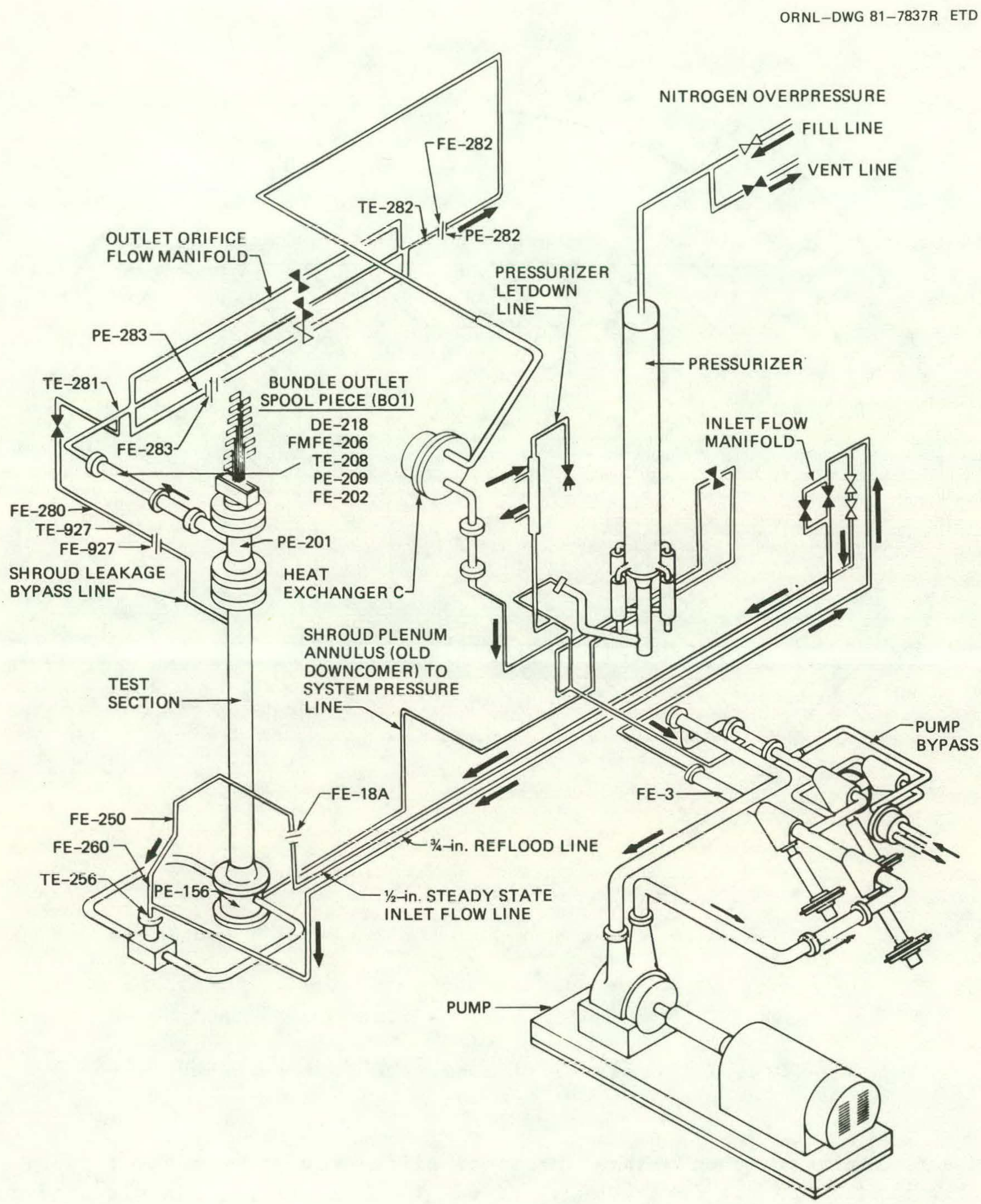

Fig. 1. THTF in small-break test configuration.

ORNL–DWG 82–4875 ETD

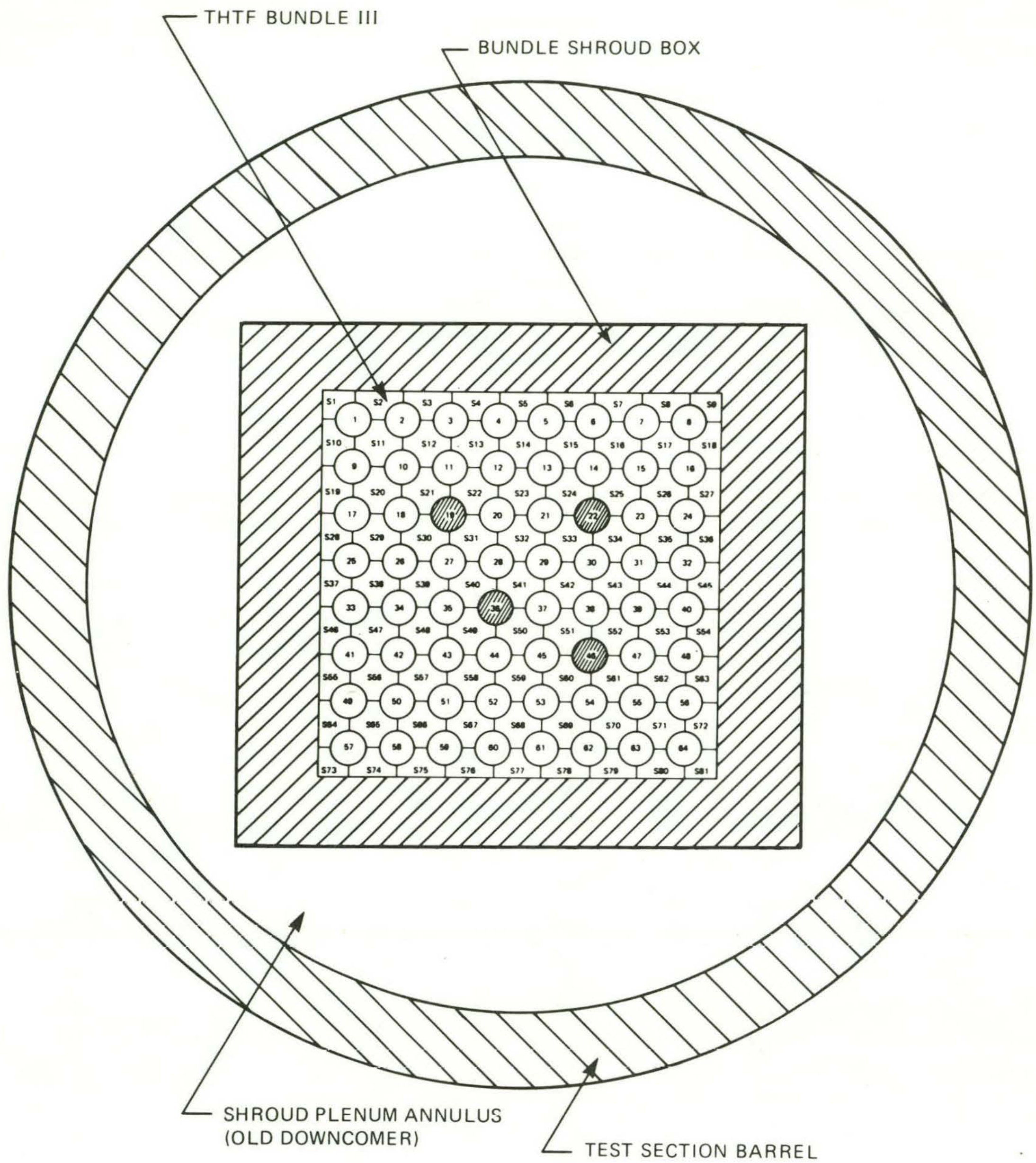

Fig. 2. Cross section of THTF test section.

the pressurizer, then a large pressure difference between the test section bundle and the downcomer would exist. This large pressure difference has been observed to cause substantial leakage from the bundle to the annulus. To minimize this leakage, the line between the pressurizer and annulus was closed after mixture-level equalization had taken place. To maintain pressure equalization, the shroud bypass line, which connects the top of the shroud annulus to the test outlet, was opened (Fig. 1). As a final step to minimize the possibility of leakage from bundle to annulus, the shroud bypass line was closed shortly before data were taken. The annulus was then completely isolated from the rest of the system, thus providing the least opportunity for undesired leakage.

3.2 Bundle Description

The THTF test section contains a 64-rod electrically heated bundle. Figure 3 is a cross section of the bundle. The four unheated rods were designed to represent control-rod guide tubes in a nuclear fuel assembly. Rod diameter and pitch are typical of a 17 x 17 fuel assembly.

ORNL–DWG 77-5718D

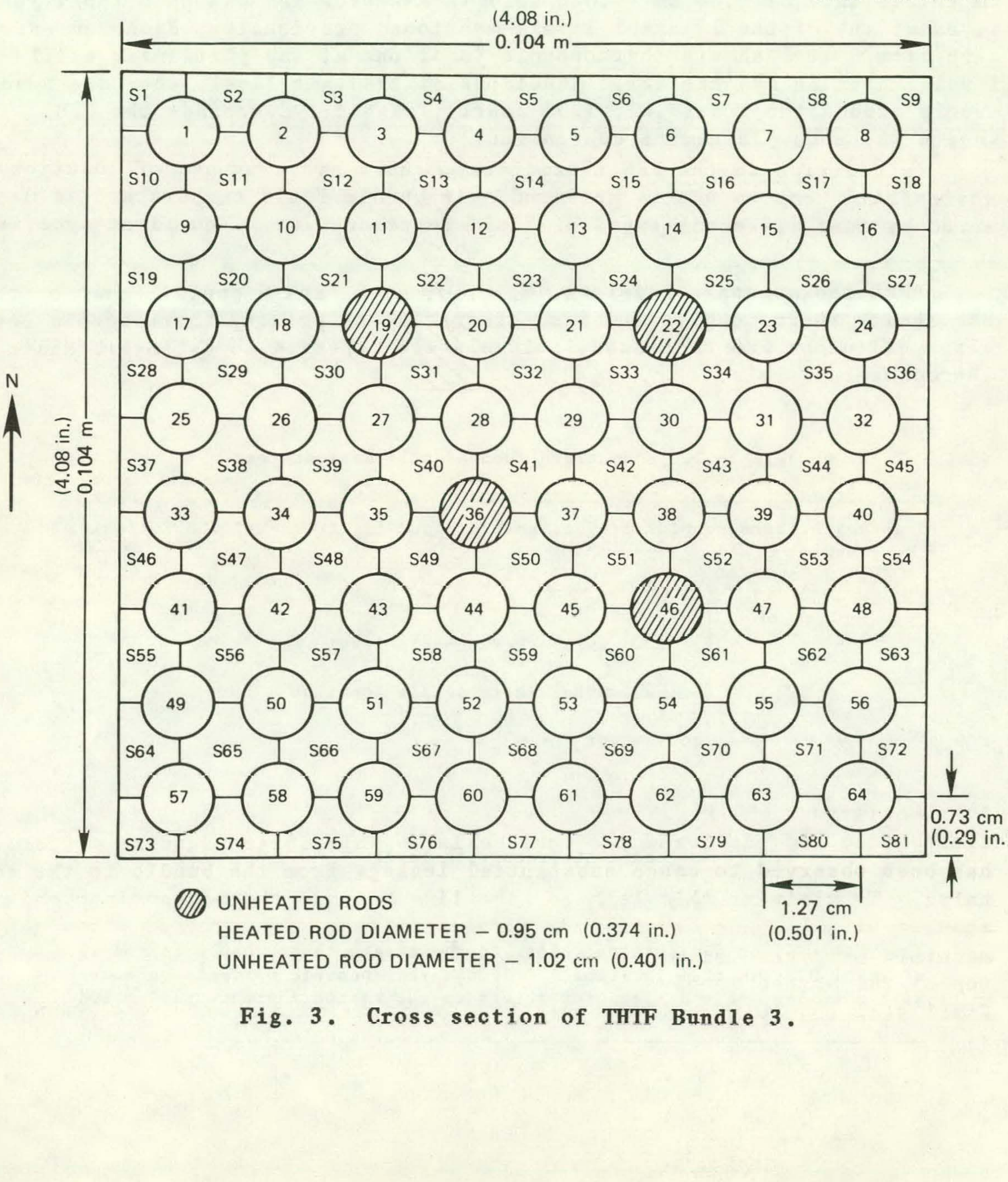

Fig. 3. Cross section of THTF Bundle 3.

Figure 4 is an axial profile of the THTF bundle that illustrates the positions of spacer grids and fuel rod simulator (FRS) thermocouples. The heated length is 3.66 m (12 ft), and a total of 25 FRS thermocouple levels are distributed over that length. An FRS thermocouple level refers to an axial location where a selected number of FRSs are instrumented with sheath thermocouples.* Note that the upper third of the bundle is more heavily instrumented than the lower portion. For most tests the two-phase mixture level is in the top 1/3 of the heated length. The additional instrumentation in the top 1/3 of the bundle is used to better define the mixture-level position. In addition, the increased instrumentation near the spacer grids can be used to ascertain to what extent spacer grids affect heat transfer.

A drawing of an FRS cross section is shown in Fig. 5. Each FRS has 12 sheath and 4 center thermocouples. The thermocouples are either 0.05 cm (0.020 in.) or 0.04 cm (0.016 in.) in diameter and can have their junctions at any of the 25 axial levels mentioned previously. Each rod can have from 0 to 3 sheath thermocouple junctions at any particular axial level. When an FRS has three junctions at the same level, they are spaced evenly around the rod (i.e., 120° apart). Table 1 describes the FRS sheath thermocouple naming convention.

In addition to the FRS thermometry, there are a number of locations where fluid temperature is measured. In-bundle fluid temperature is measured by four different types of fluid thermocouples. The first type is

---

*FRS thermocouple levels A, B, C, D, E, F, and G contain most of the FRS sheath thermocouples and are referred to as primary thermocouple levels. All other FRS thermocouple levels are referred to as intermediate thermocouple levels.

Table 1. Rod-sheath thermocouple designations

Rod-sheath thermocouples are designated according to one of the following two schemes:

1. TE – 3 17 A D
   - D — axial thermocouple level
   - A — azimuthal thermocouple location
   - 17 — rod number

2. TE – 3 54 F8
   - F8 — axial thermocouple level
   - 54 — rod number

Thus, this first designation refers to the sheath thermocouple in rod 17 at level D, azimuthal location A. If the thermocouple designation ends with a number, this designation refers to the sheath thermocouple in rod 54 at level F8.

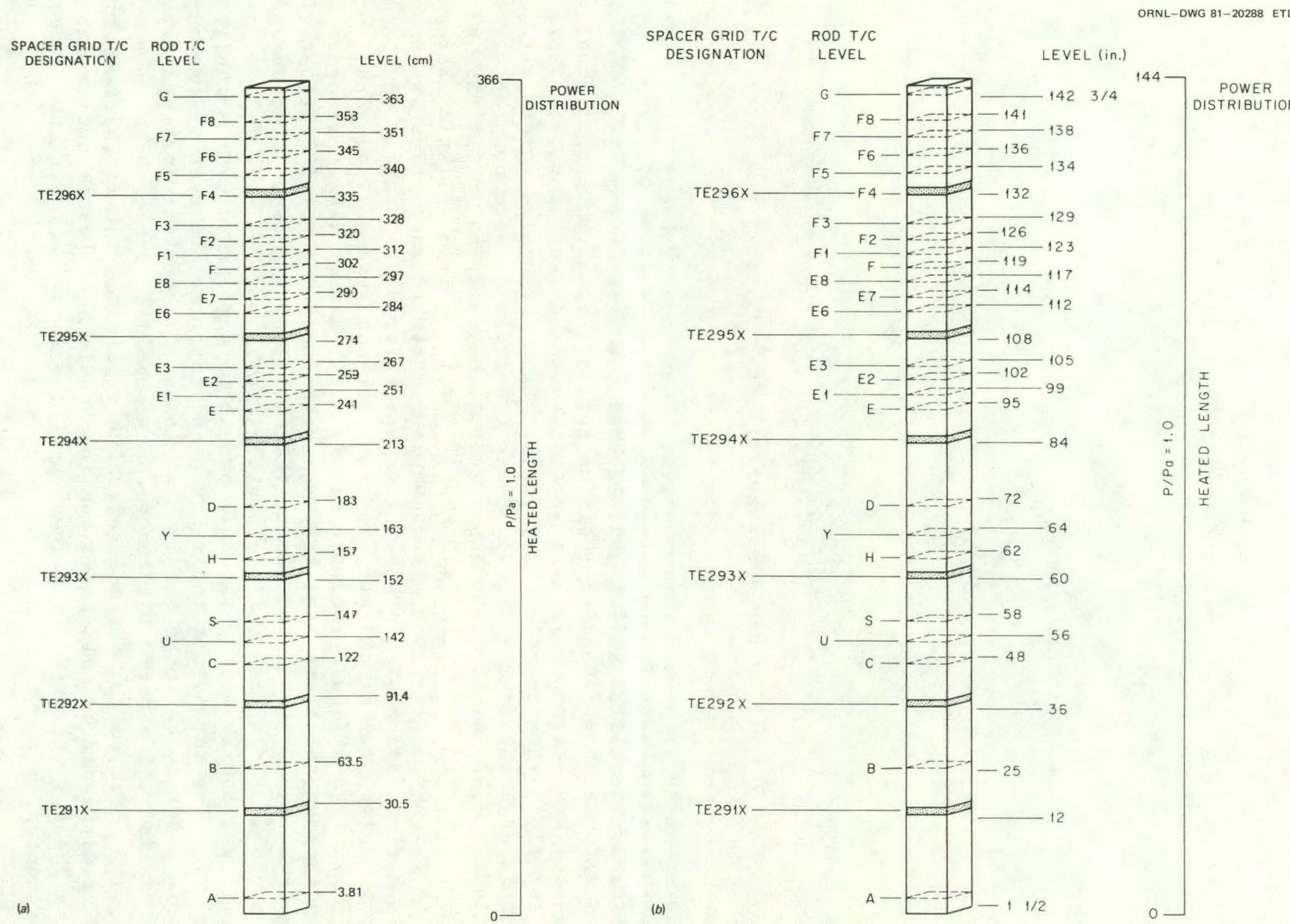

Fig. 4. Axial location of spacer grids and FRS thermocouples. (a) Metric units; (b) English units.

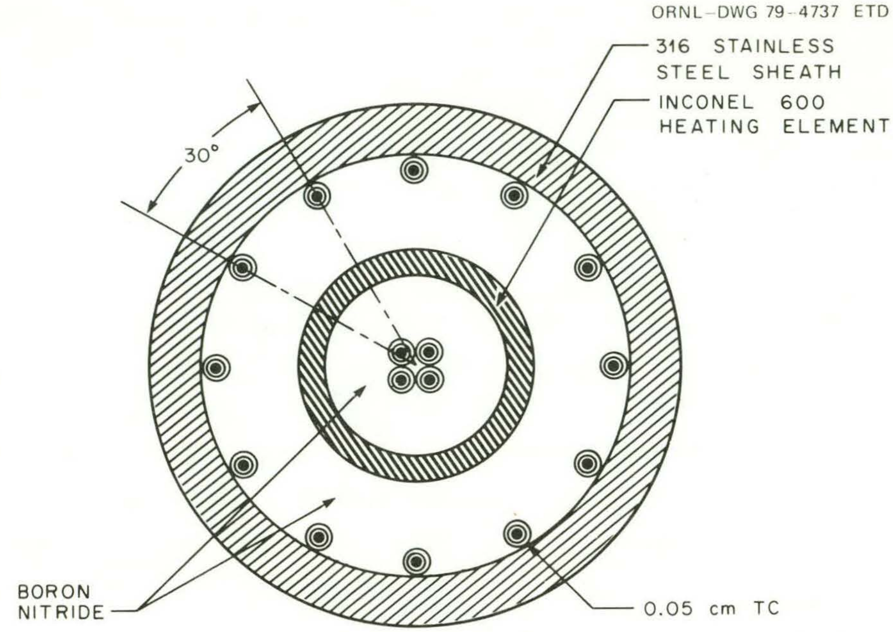

Fig. 5. Simplified cross section of a typical fuel rod simulator.

a thermocouple array-rod thermocouple. These are exposed* fluid thermocouples that project from unheated rods. Thermocouple array-rod thermocouples are installed at 1.83, 2.41, 3.02, and 3.62 m (72, 95, 119, and 142.5 in.) above the beginning of the heated length (BOHL). The second type of fluid thermocouple is a shroud box fluid thermocouple. These are exposed fluid thermocouples that project from the bundle shroud into subchannels adjacent to the shroud. Shroud box fluid thermocouples are installed at 0.38, 0.64, 1.22, 1.83, 2.41, 3.02, and 3.61 m (15, 25, 48, 72, 95, 119, and 142 in.) above BOHL. The third type of fluid thermocouple is a spacer grid fluid thermocouple. These thermocouples are exposed fluid thermocouples that project from spacer grids. Spacer grid fluid thermocouples project slightly upstream of each spacer grid. The fourth and final type of fluid thermocouple is a subchannel rake thermocouple. These thermocouples are attached to a rake located several centimeters above the end of the heated length (EOHL). They are used in measuring the cross-sectional temperature distribution.

As previously noted, the THTF bundle is surrounded by a shroud box (Fig. 2). The shroud box walls have been instrumented with thermocouples in order to estimate bundle heat losses. A typical instrumentation site consists of a pair of thermocouples embedded in the shroud box wall (Fig. 6). Because the thermocouples are separated, the radial temperature gradient can be calculated and the bundle heat losses estimated. Figure 7 shows the axial locations where the shroud box walls have been instrumented.

---

*Exposed in this context does not mean that the thermocouple junction actually contacts the fluid. The junction is encased in a stainless steel sheath but does not have a droplet shield.

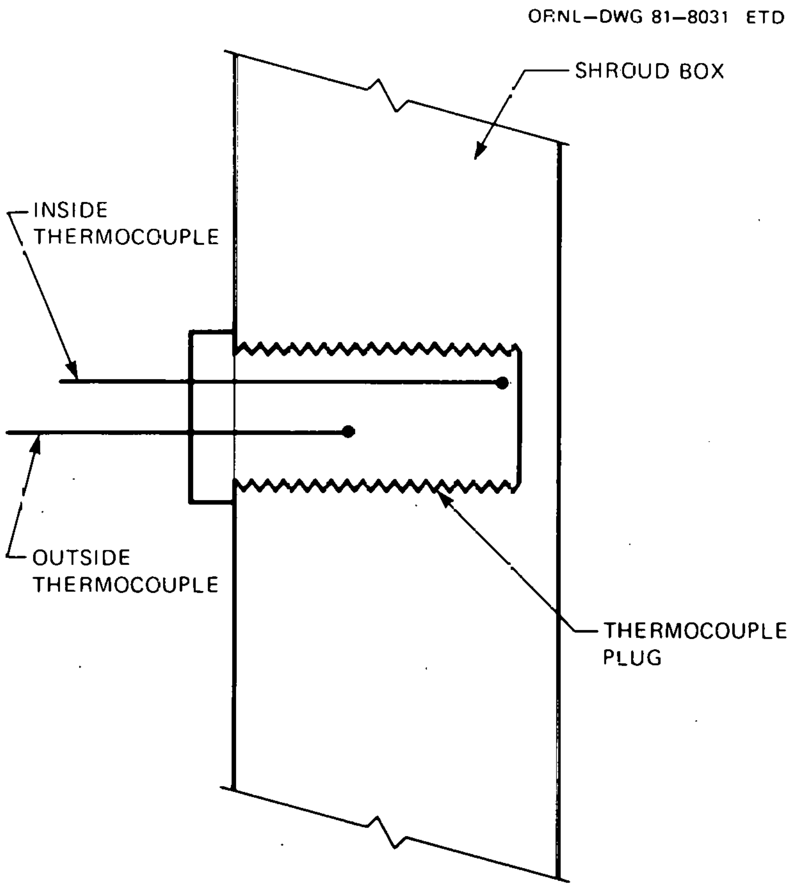

Fig. 6. Shroud-wall thermocouple configuration.

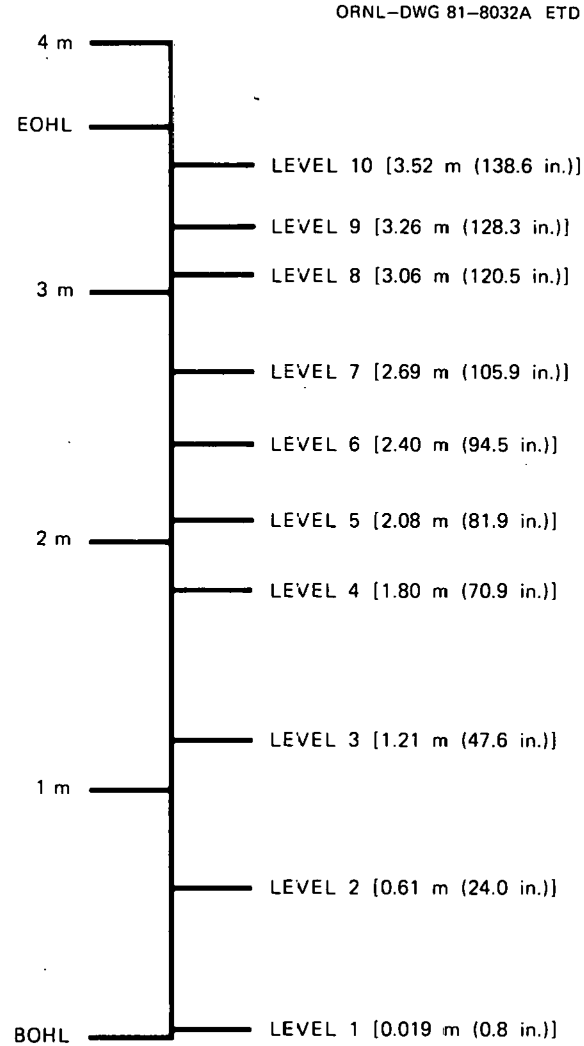

Fig. 7. Axial location of shroud-wall thermometry.

3.3 Differential Pressure (ΔP) Instrumentation

A primary objective of this test series was to obtain mixture-level swell and void-fraction distribution data under high-pressure low heat-flux conditions. These data were obtained through the use of "stacked" ΔP cells. Figure 8 illustrates the ΔP measurement sites. Differential pressure cells PdE-180 through 188 are ranged from 0.0 to 0.63 m (0.0 to 25.0 in.) of standard water, and PdE-189 is ranged from 0.0 to 0.76 m (0.0 to 30.0 in.) of water. Spacing of the cells varies from 0.75 to 0.22 m (29.4 to 8.5 in.).

3.4 Summary

The THTF is a large and complex experimental facility, and a detailed discussion of it would be impractical in this report. However, this introduction should allow the reader to interpret the results to be presented. Key aspects of the THTF design have been summarized in Table 2; a more detailed description of the THTF may be found in Ref. 5.

Table 2. THTF design summary

Parameter	Quantity
Design pressure, MPa (psia)	17.2 (2500)
Pump capacity, m^3/s (gpm)	0.044 (700)
Heated length, m (ft)	3.66 (12.0)
Power profile	Flat
FRS diameter, cm (in.)	0.95 (0.374)
Lattice	Square
Pitch, cm (in.)	1.27 (0.501)
Subchannel hydraulic diameter, cm (in.)	1.23 (0.48)
Number of heated rods	60
Number of unheated rods	4
Unheated rod diameter, cm (in.)	1.02 (0.40)
Bundle shroud configuration	Square
Bundle shroud thickness, 2 sides, cm (in.)	2.54 (1.0)
2 sides, cm (in.)	1.91 (0.75)
Number of grid spacers	7

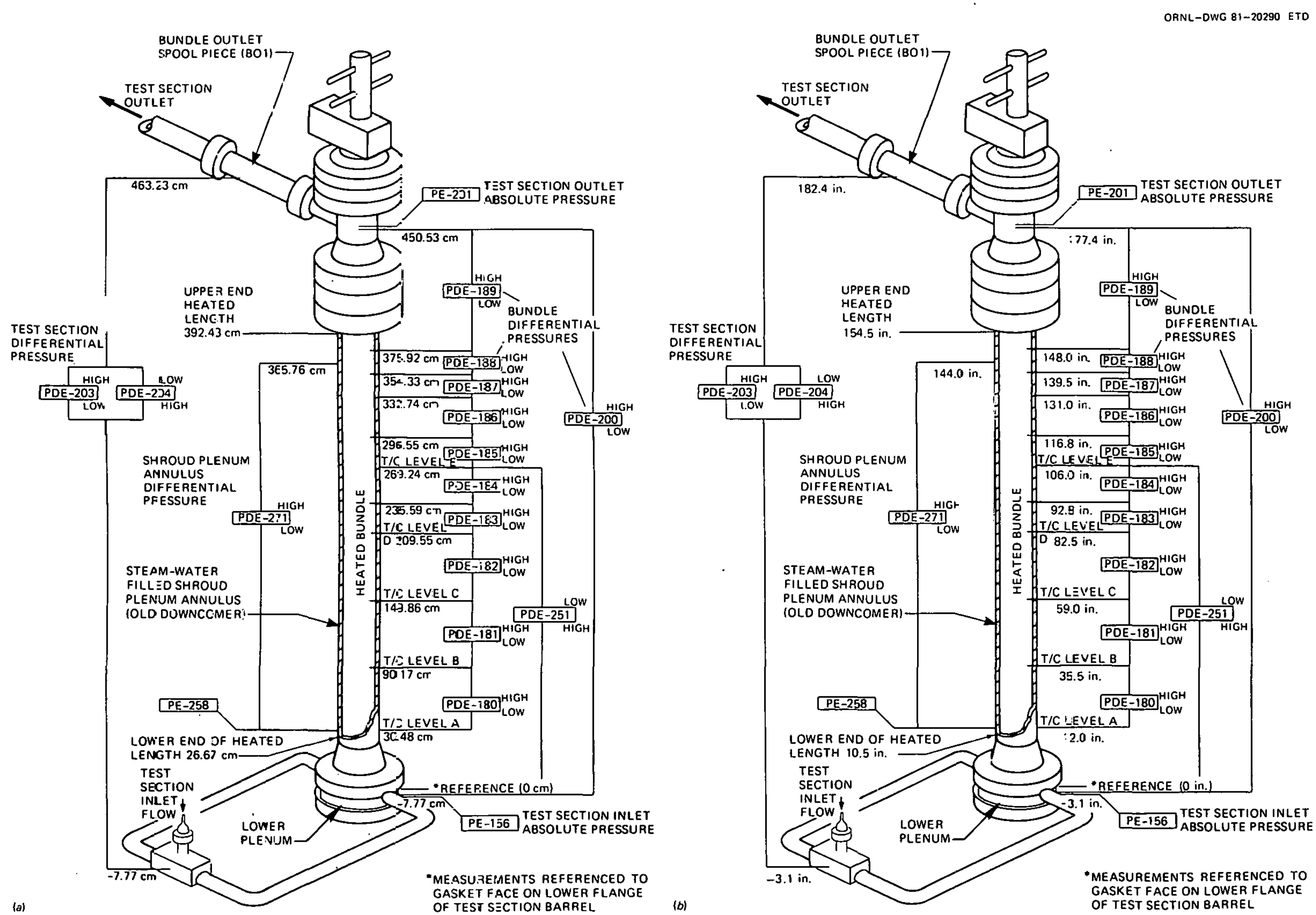

Fig. 8. THTF in-bundle pressure instrumentation. (a) Metric units; (b) English units.

4. EXPERIMENTAL PROCEDURES

As noted in the introduction, this report concerns the 6 uncovered-bundle heat transfer and 12 mixture-level swell tests run in November 1980. All of these tests were run within a 24-h period, which minimized the amount of time needed for preheating the THTF and enabled the use of a single instrumentation calibration. Preheating of the loop was accomplished by accumulating pump heat in the primary flow circuit. Preheating continued until a stable base loop temperature of 450 to 478 K (350 to 400°F) was obtained.

Once the desired base loop temperature and pressure had been established, the test section flow was reduced to a predetermined level. This was accomplished by closing the 3/4-in. inlet flooding line and metering flow through the 1/2-in. flow line (Fig. 1). Excess pump capacity was diverted through the pump bypass loop.

When the loop was properly configured, bundle power was applied and boiloff commenced. Excess volume was accumulated in the pressurizer, and nitrogen was vented from the pressurizer to maintain constant pressure. Eventually, the THTF settled into a quasi-steady state with the bundle partially uncovered and inlet flow just sufficient to make up for the liquid being vaporized. During this boiloff process, the valves in the lines from the shroud annulus to the pressurizer and test section outlet were left open. This aided in the rapid equalization of bundle and downcomer mixture levels.

When steady state was reached, the lines from the pressurizer to the shroud annulus and the line from the annulus to the test section outlet were closed, thus isolating the shroud annulus from the rest of the system. After an additional period of stabilization, bundle power was trimmed to produce peak FRS temperatures of about 1033 K (1400°F) (maximum temperature imposed by safety limits). This produced the maximum number of uncovered levels for the subject pressure and mass flow rate. Once again, the loop was allowed to stabilize, after which a 20-s data scan was taken. Data were recorded at a rate of 10 points per second per instrument. Once data had been acquired, the pressure, flow, and power were slowly changed to the next test point. In general, it was possible to do this without recovering the bundle.

5. UNCOVERED-BUNDLE HEAT TRANSFER

5.1. Background

Under certain SBLOCA scenarios, the nuclear reactor core is expected to undergo a slow quasi-steady boiloff transient. Figure 9 is a schematic of a nuclear reactor subchannel in a partially uncovered configuration. The core can be divided into a number of thermal-hydraulic regions. Fluid entering the bottom of the core can be subcooled or saturated, and heat transfer can take place by forced convection, free convection, subcooled boiling, or saturated nucleate boiling, depending on fluid temperature, pressure, velocity, and decay heat level. Above the entrance region, a saturated boiling region exists that extends upward to the fuel dryout elevation. In the vicinity of the dryout elevation, a relatively short "froth" region exists. In this region the reactor fuel is either dry or intermittently wetted. Liquid arises from oscillations in the liquid-free surface or by droplet ejection from the free surface as vapor bubbles burst. Heat transfer is primarily by convection to steam, intermittent liquid-wall interactions, and radiation to vapor and liquid. Finally, a dry steam-cooling region is entered. Little or no liquid is present in this region, because steam velocities near the liquid-free surface are too low to entrain a significant number of the ejected droplets. Heat transfer occurs primarily by convection and radiation to high-pressure superheated steam.

Of the four regions discussed, only the steam-cooling region has the potential for thermal damage to the reactor fuel. Thus, the ORNL uncovered-bundle heat transfer tests were designed to study heat transfer in the steam-cooling region under conditions and geometry similar to those expected in an SBLOCA.

5.2 General Theory

In the steam-cooling region, three heat transfer mechanisms dominate: (1) convection from heated surface to superheated vapor, (2) radiation from heated surface to high-pressure vapor and unheated structures, and (3) local enhancement of heat transfer caused by the effect of spacer grids.

5.2.1 Convection heat transfer

Convection heat transfer may be forced-convection dominated, free-convection dominated, or of a mixed-convective nature. Apparently, no generally accepted transition criteria have been developed for rod bundle heat transfer.[6] However, work in vertical tubes resulted in a flow regime map based on the Reynolds number and the product (GrPr) (D/L) (Ref. 7). The map appears in Fig. 10; all vapor properties are evaluated at the film temperature, and the characteristic dimension for the Grashof number is the tube diameter. The applicability of a flow map based on tube geometry

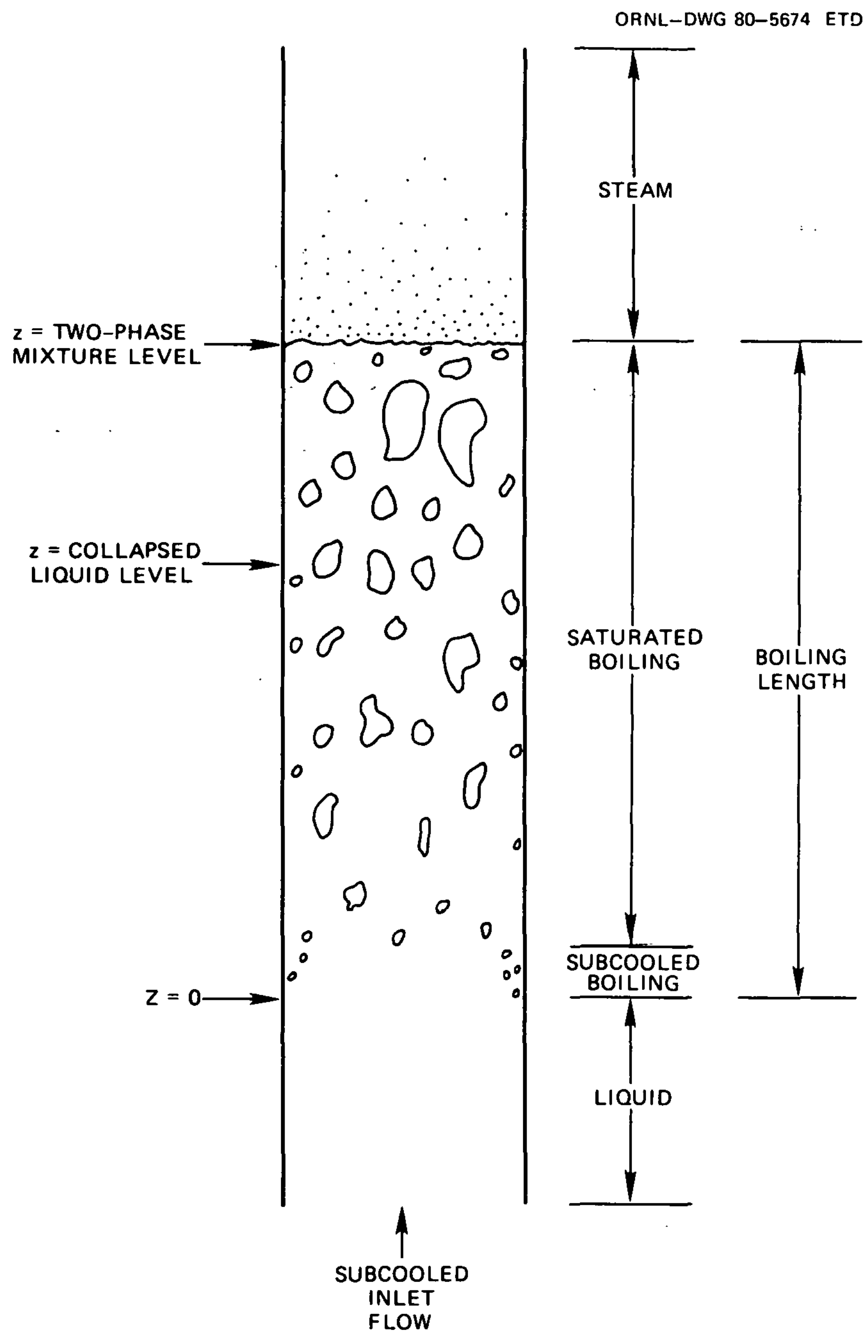

Fig. 9. Schematic of a nuclear reactor subchannel in a partially uncovered configuration.

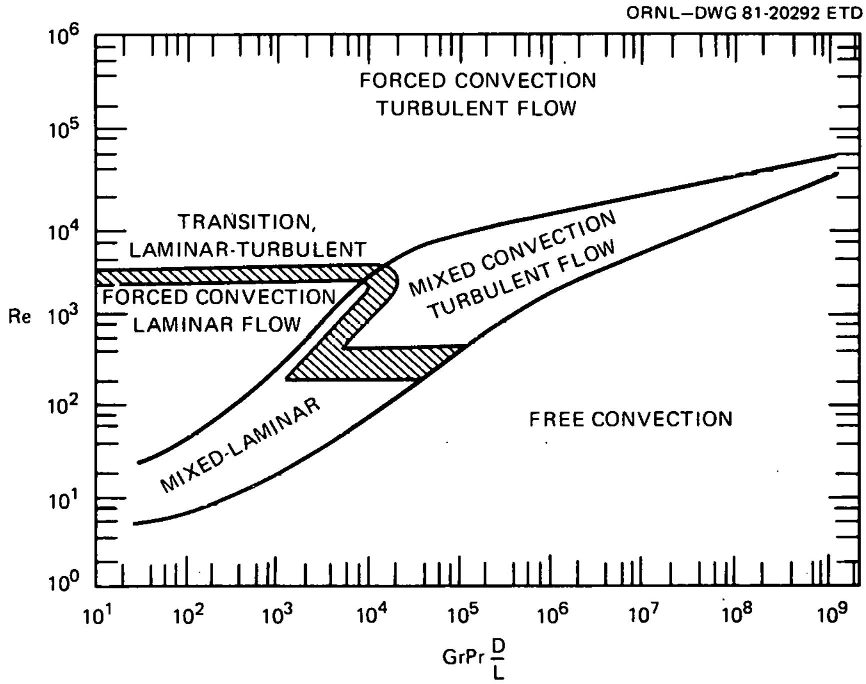

Fig. 10. Flow regime map for heat transfer in vertical tubes taken from B. Metais and E. R. G. Eckert, *J. Heat Transfer*, p. 295 (May 1964).

to a rod bundle is questionable. However, it does provide general guidance to possible flow regimes.

A number of steam-cooling experiments have been performed that resulted in the proposal of several convective heat transfer correlations. A series of six high-pressure low-flow uncovered-bundle heat transfer tests were performed at ORNL in January 1980 (Ref. 1). The tests spanned a pressure range from 2.6 to 7.1 MPa (375 to 1030 psia) and a range of linear heat rates from 0.8 to 1.4 kW/m·rod (0.24 to 0.43 kW/ft·rod). Rod bundle geometry was similar to a 17 x 17 PWR fuel assembly (pitch-to-diameter ratio of 1.34), and the axial power profile was uniform.

The resulting heat transfer data spanned a range of bulk vapor Reynolds numbers from 3500 to 10,500. Maximum rod surface temperatures exceeded 1000 K (1340°F) and rod-to-steam temperature ratios were as high as 1.6. It was concluded that, because of the large temperature ratios, convective heat transfer was substantially affected by vapor property variations across the boundary layer.[1] A convective heat transfer correlation based on the modified wall Reynolds number was recommended:

$$Nu_w = 0.021\ Re_{mw}^{0.8}\ Pr_w^{0.4}\ ; \qquad (1)$$

$$Re_{mw} \equiv \frac{GD_H}{\mu_w}\left(\frac{\rho_w}{\rho_v}\right) .$$

Evaluation of the vapor properties at the heated surface temperature adjusts the correlation for effects caused by vapor property variations.

Selection of the modified wall Reynolds number as a basis for correlating large temperature-ratio convective data was supported by a number of previous experiments run in tube geometry.[1] These studies demonstrated that an extensive body of large temperature-ratio convective data over a wide range of Reynolds numbers could successfully be correlated through the use of the modified wall Reynolds number. The specific form of Eq. (1) was derived from a theoretical modification of the McEligot correlation[8] and was not the result of a regression on ORNL data.

A comprehensive set of steam-cooling correlations has been proposed by the FLECHT Analysis Group. The correlations were derived from FLECHT-SEASET unblocked-bundle steam-cooling test data.[9] These tests were run under low-pressure low-temperature ratio conditions ($T_w/T_v \leq 1.1$) in a rod bundle with a pitch-to-diameter ratio of 1.33. All tests were probably forced-convection dominated. The correlations were originally based on vapor properties evaluated at the mean vapor temperature. However, recent comparisons with high-pressure high-temperature transient boiloff data obtained from the G-2 facility reinforce the contention that the vapor properties should be evaluated at the heated surface temperature.[10] The most recent versions of the correlations are based on the modified wall Reynolds number:

$$\frac{Nu_w}{F_{froth}F_{grid}} = 13.7\ Pr_w^{1/3} \qquad (Re_{mw} \leq 2000)\ , \tag{2}$$

$$\frac{Nu_w}{F_{froth}F_{grid}} = 0.0797\ Re_{mw}^{0.677}\ Pr_w^{1/3} \qquad (2000 \leq Re_{mw} \leq 25{,}200)\ , \tag{3}$$

$$\frac{Nu_w}{F_{froth}F_{grid}} = 0.023\ Re_{mw}^{0.8}\ Pr_w^{1/3} \qquad (Re_{mw} \geq 25{,}200)\ . \tag{4}$$

The functions F_{froth} and F_{grid} are intended to account for enhancement of heat transfer in the froth region and by spacer grids.

Several other correlations merit inclusion because of their widespread use. The first is the McEligot correlation:

$$Nu_v = 0.021\ Re_v^{0.8}\ Pr_v^{0.4} \left(\frac{T_v}{T_w}\right)^{0.5}\ , \tag{5}$$

where all vapor properties are evaluated at the mean temperature, and the temperature ratio is intended to correct for property variations across the boundary layer. The McEligot correlation was developed from a series of large temperature-ratio convection tests that spanned a vapor Reynolds number range from 1450 to 45,000 (Ref. 8). Note that the heat transfer media in these tests were air, nitrogen, and helium. Therefore, the test results are not strictly applicable to a steam-cooling experiment. Because the gases in the McEligot experiments were all essentially ideal gases, the gas property variations are modeled well by power law approximations. The result is that Eq. (5) is equivalent to a reference temperature correlation where the vapor properties evaluated at the surface temperature are approximated by the vapor properties at the mean temperature multiplied by the temperature ratio raised to an appropriate power. Summation of the exponents for all of the properties results in the exponent of 0.5 on the temperature ratio. In the case of high-pressure steam, the property variations do not always conform to power law approximations. Accordingly, a reference temperature correlation is more appropriate, because vapor properties are explicitly evaluated at the reference temperature rather than through power law approximations. Equation (1) is roughly equivalent to the McEligot correlation for the case of heat transfer to essentially ideal gases.[1]

The last convective correlation to be discussed is the Heineman correlation for fully developed flow.[11]

$$Nu_f = 0.0133\ Re_f^{0.84}\ Pr_f^{0.33}\ . \qquad (6)$$

The Heineman correlation was developed from a series of high-pressure steam cooling tests in tube and square-duct geometry. The rod-to-steam temperature differences extant in these tests were large. However, the results may not be strictly applicable to low-flow steam-cooling tests, because the minimum Reynolds number of 20,000 was quite large for a reactor core boiloff.

5.2.2 Radiation heat transfer

Because of the high-temperature high-pressure conditions expected in a reactor core boiloff, the effect of thermal radiation should not be ignored. Calculation of the radiation heat transfer coefficient in the steam-cooling region is relatively straightforward. Because few, if any, droplets exist in the steam-cooling region, only radiation to water vapor at the high-pressure limit and radiation to unheated structure need be considered.

Radiation to high-pressure steam can be calculated using the Hottel empirical method:[12]

$$q''_{rad} = \varepsilon'\sigma(T_w^4 - T_v^4)\ ,$$

and

$$\varepsilon' = \left[\frac{1}{\varepsilon_w} + \frac{1}{\alpha_v(T_w)} - 1\right]^{-1}\ , \qquad (7)$$

where the absorptivity of the vapor is evaluated at the heated surface temperature. Radiation to unheated structure can be estimated through the use of a multinode radiation model with an absorbing vapor. Radiation properties of high-pressure steam can be evaluated from the Ludwig and Ferrisso chart.[13] Appendix A contains further details concerning the radiation calculations for the subject tests.

5.2.3 Spacer grid effects

Previous experimental work has shown that spacer grids can have marked effects on local heat tranfer.[14] Relevant work in this area has been performed by Yao et al.,[15] who have correlated the enhancement of heat transfer in terms of (1) distance from the grid, (2) blockage ratio of the grid and mixing vanes, (3) blockage ratio of the mixing vane with respect to the normal grid area, and (4) angle of the mixing vane with respect to the axial direction. The resulting correlation is

$$\frac{Nu}{Nu_o} = \{1 + 5.55\ a_1^2\ \exp[-0.13(Z - Z_{grid})/D_H]\}$$

$$\times\ \{1 + a_2^2\ \tan^2\phi\ \exp[-0.034(Z - Z_{grid})/D_H]\}^{0.4}\ , \quad (8)$$

where Nu_o is the Nusselt number with no enhancement.

5.3 Presentation of Results

5.3.1 Summary of test conditions

Table 3 summarizes the test conditions for the quasi-steady-state uncovered-bundle heat transfer test series. The table indicates that three tests were run at roughly 4.1 MPa (600 psia) and three tests at roughly 7.2 MPa (1050 psia). The three tests at each of the primary pressure levels were designed to span a range of linear powers. Original plans called for running tests at 0.33, 0.98, and 1.97 kW/m (0.1, 0.3, and 0.6 kW/ft). However, problems in measuring the extremely low volumetric flow associated with the 7.2-MPa low-power test made running at the somewhat higher linear power level of 0.46 kW/m (0.14 kW/ft) necessary. In all other tests the deviations from the originally intended power levels were a result of fine tuning the flow and power to achieve an optimal degree of bundle uncovering.

Mixture level varied considerably from test to test. This variation occurred because test procedure specified that the maximum core uncovering be achieved while maintaining a peak clad temperature of roughly 1033 K (1400°F). At high power levels this constraint allowed uncovering of only 25 to 30% of the bundle, while at low power roughly 40% of the bundle could be uncovered.

The steam-cooling region was defined as the region at or above the lowest primary thermocouple level experimentally indicating the presence

Table 3. Summary of uncovered-bundle heat transfer test conditions[a]

Test	System pressure [MPa (psia)]	Linear power/rod [kw/m (kw/ft)]	Mass flux [$kg/m^2 \cdot s$ ($lb_m/h \cdot ft^2$) x 10^{-4}]	Mixture level [m (ft)]	Steam cooling region [m (ft)]	Vapor Reynolds number (BOSCR)[b]	Vapor Reynolds number (EOSCR)[c]	Fractional heat loss	Heat transfer regime (BOSCR)[b,d]	Heat transfer regime (EOSCR)[c,d]
3.09.10I	4.5 (650)	2.22 (0.68)	29.7 (2.19)	2.62 (8.6)	3.02–3.62 (9.91–11.88)	16,600	12,200	0.018	FCT	FCT
3.09.10J	4.2 (610)	1.07 (0.33)	12.7 (0.94)	2.47 (8.1)	3.02–3.62 (9.91–11.88)	6,700	5,000	0.052	MCT	FCT
3.09.10K	4.0 (580)	0.32 (0.10)	3.1 (0.23)	2.13 (7.0)	2.42–3.62 (7.94–11.88)	1,900	1,100	0.176	MCT	FCL
3.09.10L	7.5 (1090)	2.17 (0.66)	29.1 (2.15)	2.75 (9.0)	3.02–3.62 (9.91–11.88)	17,700	13,000	0.017	FCT	FCT
3.09.10M	7.0 (1010)	1.02 (0.31)	12.6 (0.93)	2.62 (8.6)	3.02–3.62 (9.91–11.88)	6,500	5,100	0.042	MCT	MCT
3.09.10N	7.1 (1030)	0.47 (0.14)	4.6 (0.34)	2.13 (7.0)	2.42–3.62 (7.94–11.88)	3,000	1,600	0.162	MCT	MCTR

[a] Numbers in this table have been rounded off. For precise listing of test conditions see Appendix B.

[b] BOSCR – beginning of steam-cooling region.

[c] EOSCR – end of steam-cooling region.

[d] Abbreviations are:
FCT – forced-convection turbulent
MCT – mixed-convection turbulent
FCL – forced-convection laminar
MCTR – mixed-convection transition to laminar

of dry superheated vapor, but at or below the EOHL. The steam-cooling region corresponds to the portion of the bundle for which heat transfer calculations have been performed.

Table 3 also presents the bulk vapor Reynolds number evaluated at the beginning of the steam-cooling region and at the upper end of the steam-cooling region for each test. Because the only parameter in the vapor Reynolds number that changes with elevation is the vapor viscosity, the Reynolds numbers shown correspond to the range of Reynolds numbers encountered in a particular test. The range of vapor Reynolds numbers encountered in the test series was from 1100 to 17,700. In a forced-convection dominated system this range of Reynolds numbers would indicate that the test series spanned from the laminar regime to the lower bound of the fully turbulent regime. However, because of the large temperature differences and low flows encountered in these tests, buoyancy forces may affect convective heat transfer.

Flow can also be forced-convection dominated, free-convection dominated, or of a mixed-convective nature. Table 3 lists the heat transfer regimes (as inferred from Fig. 10) at the beginning and end of the steam-cooling region for each test. The flow development length L was assumed to start at the top of the closest spacer grid.

The entire steam-cooling region appears to be in simple forced-convection dominated turbulent flow in only two of the six tests. In the other four tests at least part of the steam-cooling region appears to be in mixed convection. Note that in three of the tests (10K, 10N, and 10J) a flow transition is indicated. Test 10K indicates laminarization in the upper part of the steam-cooling region. Test 10N indicates a movement from a mixed turbulent regime at the bottom of the steam-cooling region toward a mixed transition to laminar regime at the top of the bundle, and test 10J undergoes a transition to turbulent forced convection in the upper portion of the bundle.

Because Fig. 10 was developed from tube experiments, the inferred flow regimes should not be taken too literally. However, convective heat transfer under high-pressure uncovered-bundle conditions can clearly be quite complex. A large number of flow regimes is possible, and flow transitions within the steam-cooling region may occur. Accordingly, empirical correlations that treat low-flow steam cooling as a simple forced-convection dominated system should be used with caution, because the underlying physics of convective heat transfer may be quite complex. Correlations that ignore this complexity may fit certain subsets of data quite well but may fail when extrapolated to regimes not supported by data.

5.3.2 Temperature and heat transfer coefficient profiles

Figures 11–22 are the bundle cross-section average vapor and FRS temperature profiles and associated heat transfer coefficient profiles for each test. The methodology used to compute these profiles and other parameters relevant to the heat transfer analysis appears in Appendix A. However, a point concerning the calculation of vapor temperature bears mention.

5.3.2.1 Calculation of vapor temperature. Vapor temperature was computed by two different methods. In one method, the vapor temperature

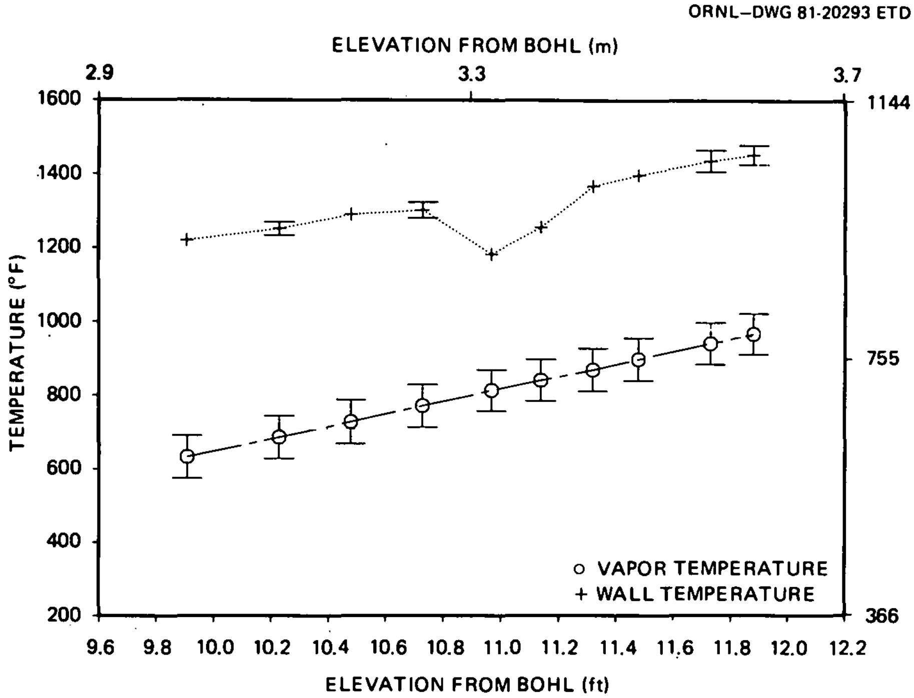

Fig. 11. Temperature profile for test 3.09.10I.

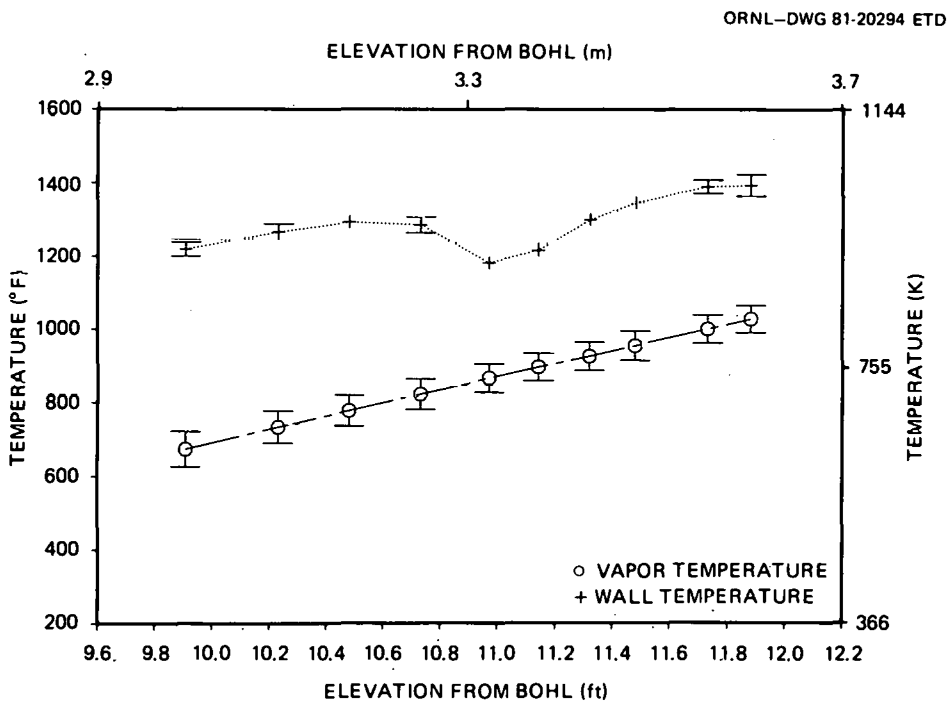

Fig. 12. Temperature profile for test 3.09.10J.

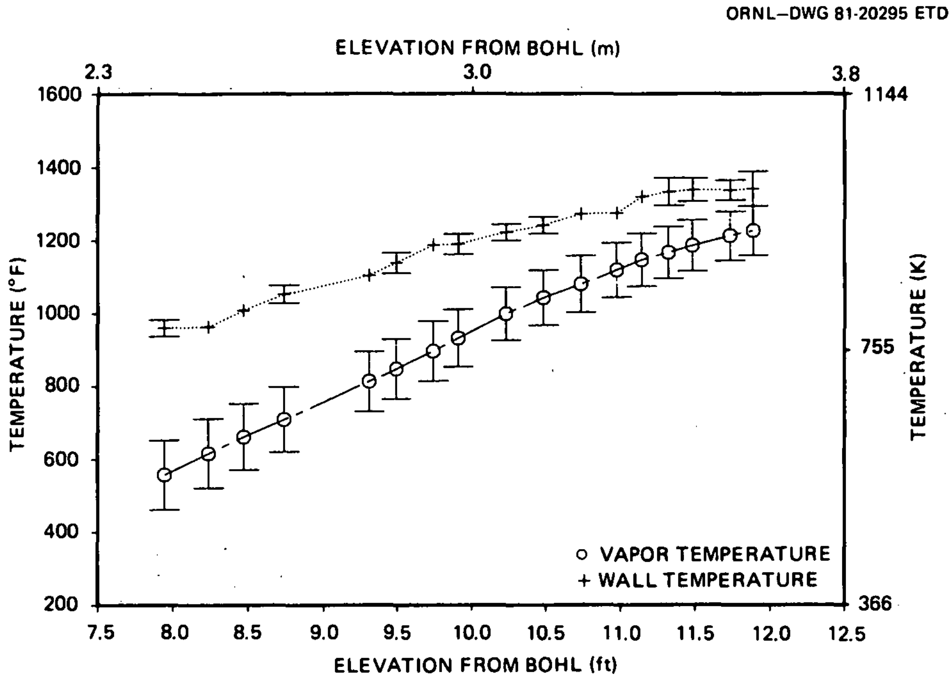

Fig. 13. Temperature profile for test 3.09.10K.

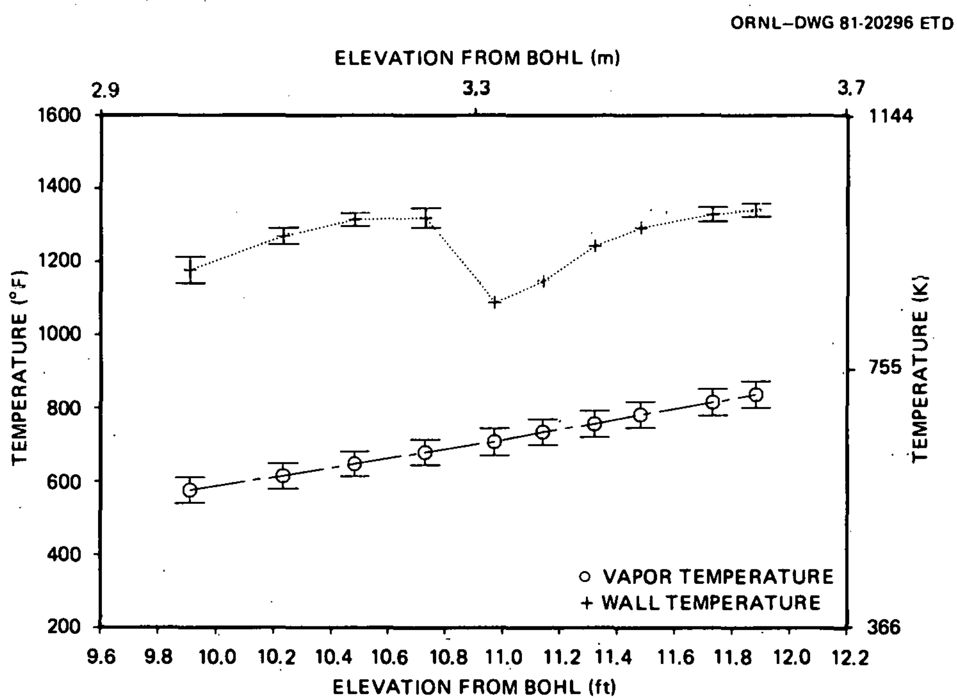

Fig. 14. Temperature profile for test 3.09.10L.

ORNL–DWG 81-20297 ETD

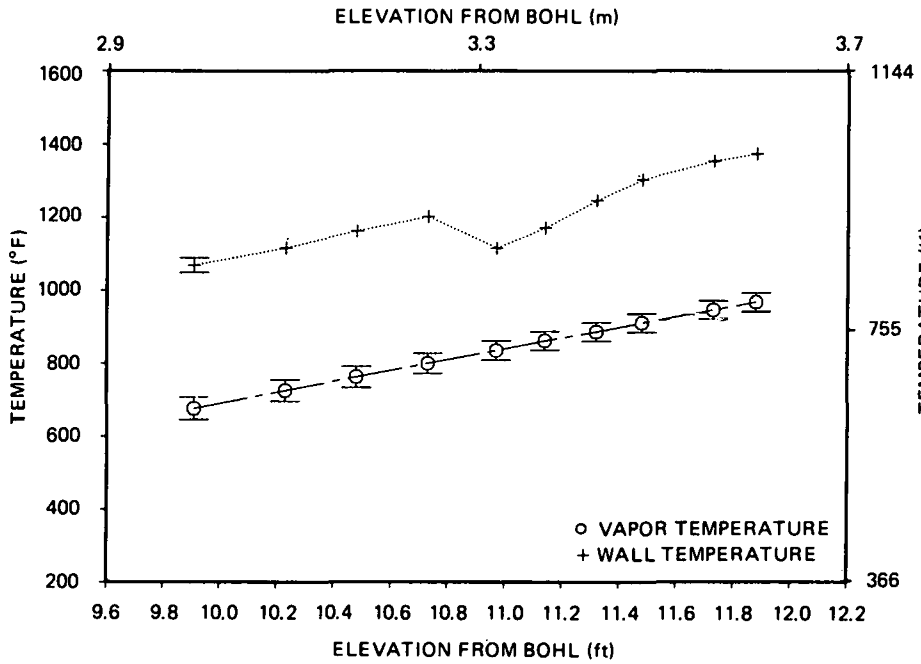

Fig. 15. Temperature profile for test 3.09.10M.

ORNL–DWG 81-20298 ETD

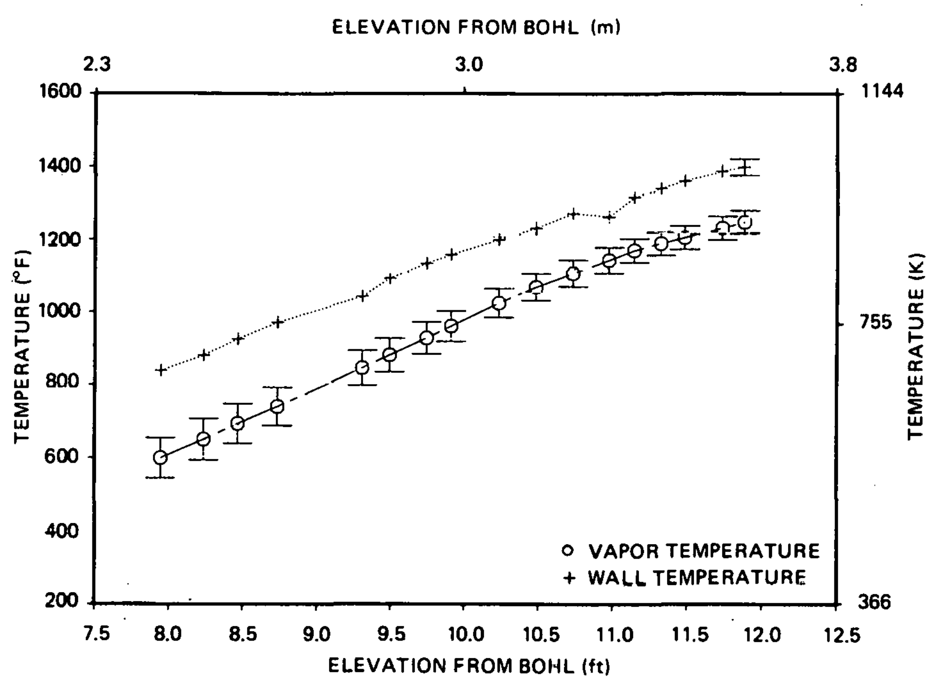

Fig. 16. Temperature profile for test 3.09.10N.

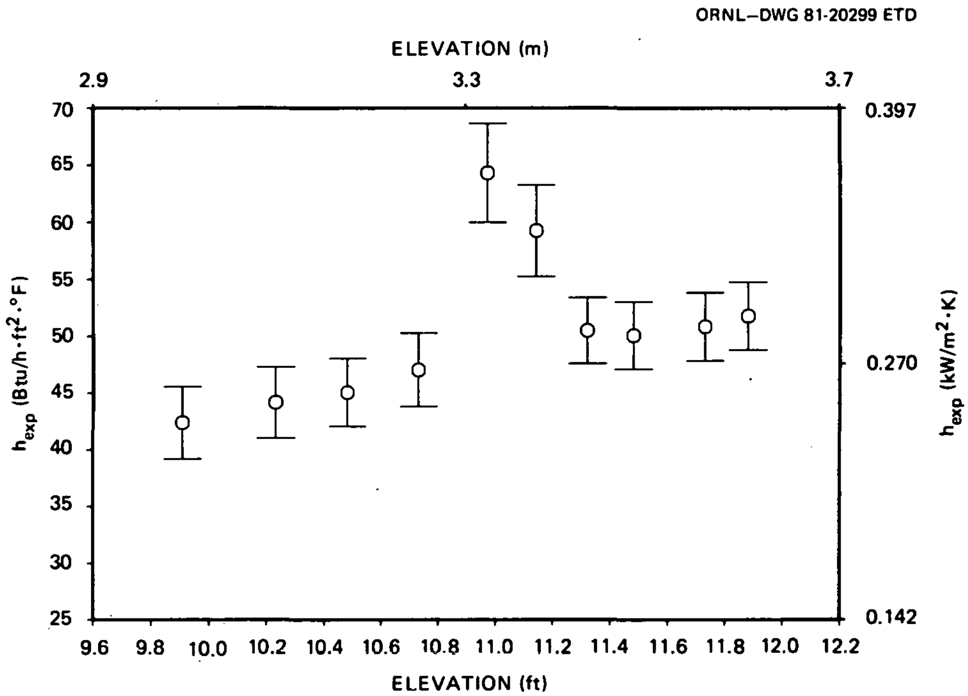

Fig. 17. Experimental heat transfer coefficient profile for test 3.09.10I.

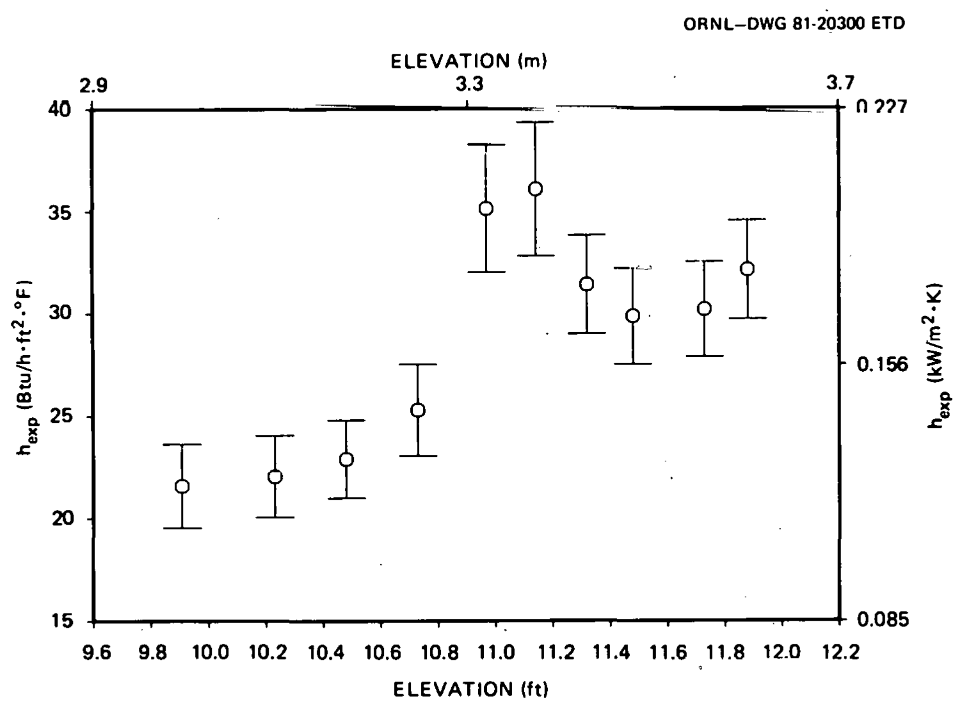

Fig. 18. Experimental heat transfer coefficient profile for test 3.09.10J.

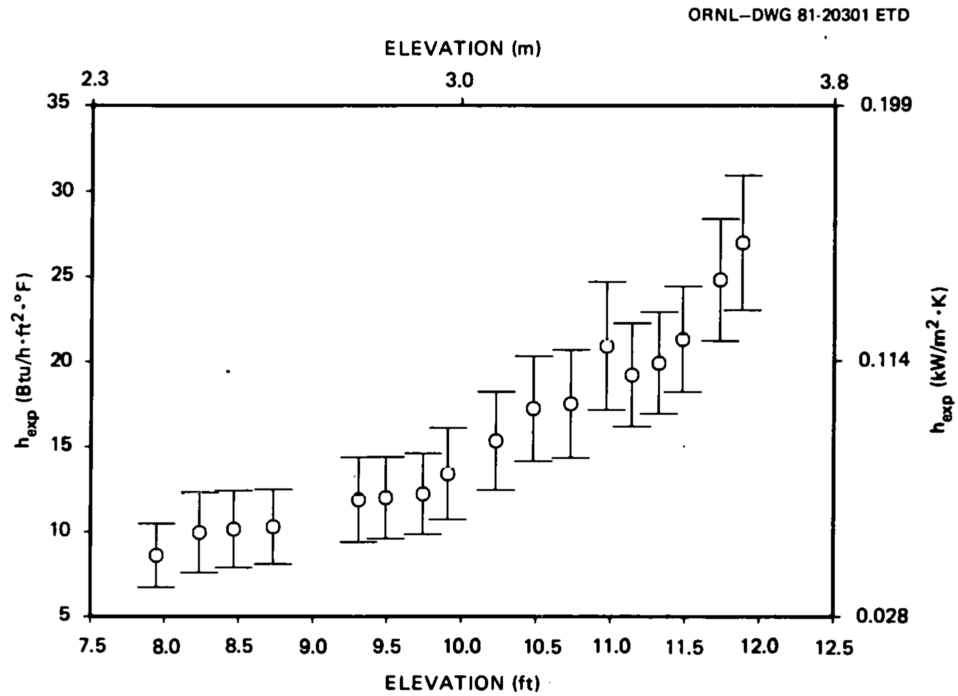

Fig. 19. Experimental heat transfer coefficient profile for test 3.09.10K.

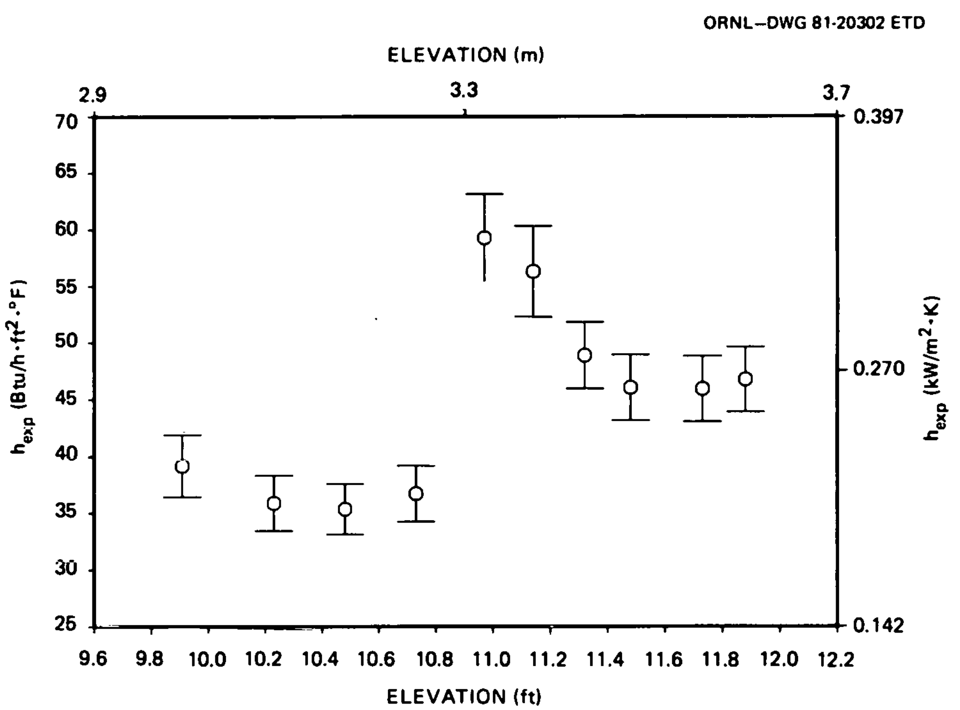

Fig. 20. Experimental heat transfer coefficient profile for test 3.09.10L.

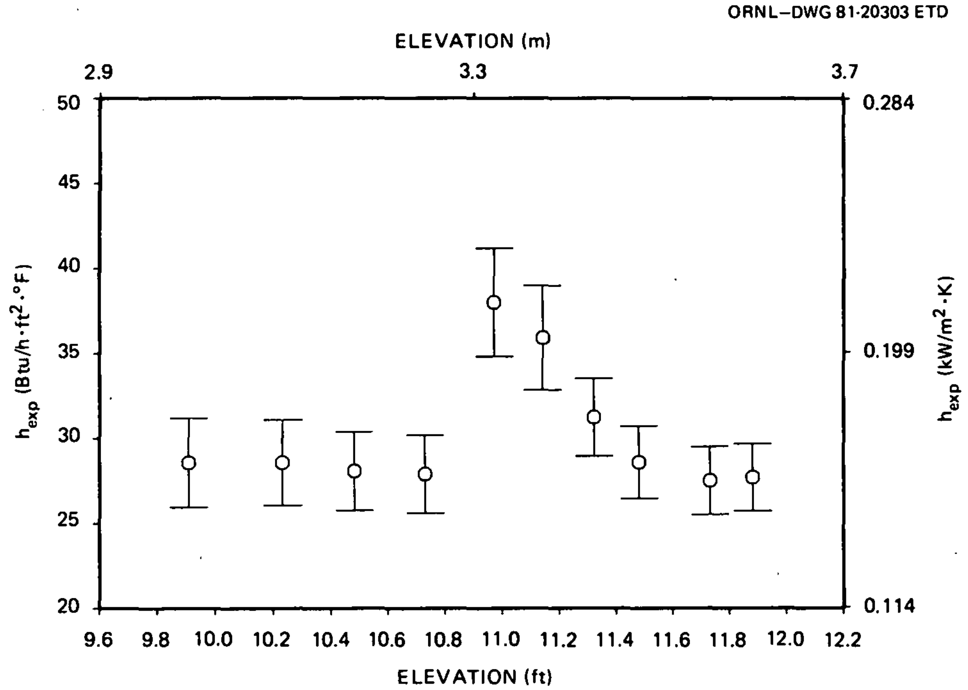

Fig. 21. Experimental heat transfer coefficient profile for test 3.09.10M.

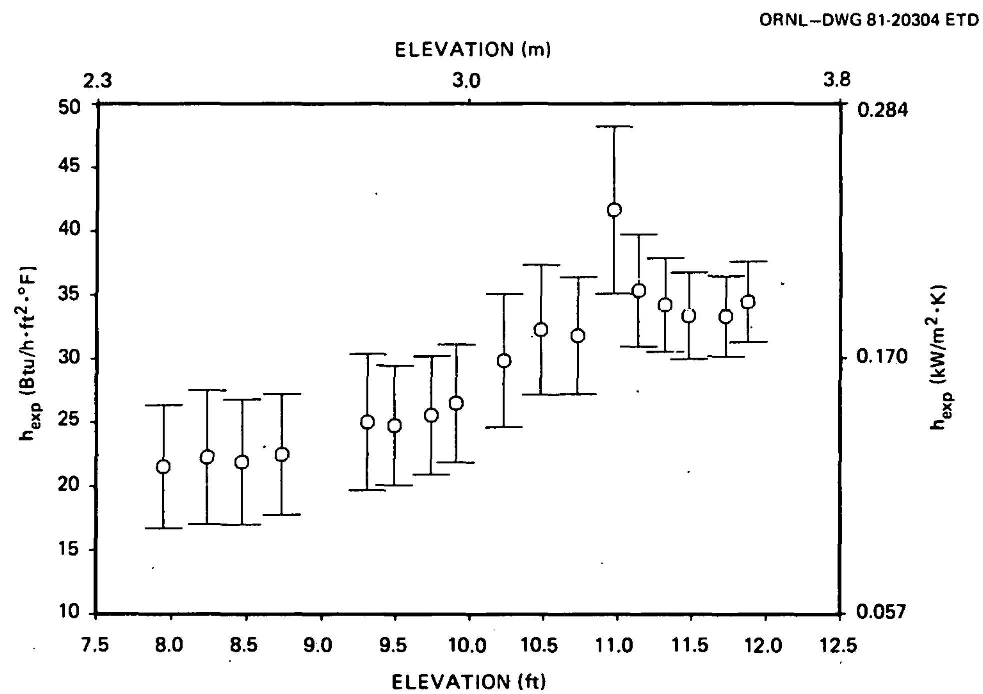

Fig. 22. Experimental heat transfer coefficient profile for test 3.09.10N.

was based on local vapor temperature measurements made by the thermocouple array rods (Sect. 3.2). In the other method, an energy balance was employed to back calculate the vapor temperature in the heated bundle from the vapor temperature measured at the EOHL by the subchannel thermocouple rake. When heat transfer coefficients were calculated using the two methods, excellent consistency was observed for the high mass-flux tests. In other words, heat transfer coefficients based on an energy-balance vapor temperature agreed well with those based on local vapor temperature measurements. Unfortunately, at very low flow rates the two methods diverged widely. A difference in heat transfer coefficients of 500% was not uncommon. Of the two methods discussed, the energy balance method appears to yield the most reasonable results, because heat transfer coefficients calculated from local vapor temperature measurements are extraordinarily high for the flow rates extant. As an example, test 10K at the 2.42-m (7.94-ft) elevation was calculated to have a local-measurement-based Nusselt number of about 40 for a vapor Reynolds number of roughly 1900. If an energy balance is used for the same case, the Nusselt number is roughly 4.0, which is more consistent with a vapor Reynolds number typical of laminar flow. The reason for this discrepancy is not fully understood. However, installation and fabrication problems are suspected, because a new type of thermocouple array rod was installed shortly before testing. Because of the nonphysical nature of the local-measurement-based heat transfer coefficients at low flow, an energy-balance-based vapor temperature was used for all heat transfer calculations.

5.3.2.2 Temperature profiles. Calculated vapor temperature profiles for the six heat transfer tests appear in Figs. 11–16. The profiles show that vapor temperatures varied from a minimum of about 561 K (550°F) to a maximum of 950 K (1250°F). The profiles also show that, except for tests 10K and 10N, vapor temperature increased relatively linearly with elevation. The variation of vapor temperature with elevation was a result of both bundle heat input and heat losses. In tests 10I, J, L, and M bundle heat losses were small compared with the heat input (<5%). Accordingly, the axially uniform heat input dominated the temperature profile, and a relatively linear increase in vapor temperature with elevation occurred. This was not the case in tests 10K and N where heat losses were roughly 17% of bundle power. In tests 10K and N, the vapor temperature rise in the lower portion of the steam-cooling region was linear. However, as vapor temperature rose so did heat losses. Therefore, heat losses in the upper portion of the steam-cooling region were greater than in the lower portion. As a result, the rate of vapor temperature rise with elevation decreased in the upper portion of the steam-cooling region.

Rod surface temperatures vary from a low of about 811 K (1000°F) to a high of 1061 K (1450°F) (Figs. 11–16).* The most notable feature of the FRS temperature profiles is the distinct drop in surface temperature at and downstream of spacer grids. The drop in temperature at the grid increases with an increasing Reynolds number. Test 10L ($13{,}000 \leq Re_v \leq 17{,}700$) shows the greatest effect with a reduction of 128 K (230°F). On

---

*If error bars are not present on figure, then uncertainty was smaller than the size of the symbol.

the other hand, test 10K ($1,100 \le Re_v \le 1,900$) shows no temperature drop at the grid.

As noted previously, the steam-cooling region was defined as being at or above the lowest primary thermocouple level where fluid thermocouples experimentally indicated the presence of dry superheated vapor. Therefore, enhancement of heat transfer at the grid is apparently caused by convective effects such as disruption of the thermal boundary layer and radiation to the grid, rather than by desuperheating of the vapor caused by contact with a wetted grid, as had been concluded by previous investigators.[14]

Fuel rod simulator to vapor ΔTs range from a low of ~63 K (114°F) to a high of 356 K (640°F). The low ΔTs were associated with the low-flow tests 10K and 10N, which indicates that in a late core boiloff [decay heat rates ≤ 0.5 kW/m (0.15 kW/ft)] the core average vapor and clad surface temperatures can be quite close. However, note that considerably larger ΔTs might be experienced in peak power subchannels where steam flow rates would be roughly the core average value, but decay heat levels would be considerably higher.

Higher flow and power tests show quite large rod-to-steam temperature differences; as large as 356 K (640°F) in test 10L. The large temperature differences indicate that correlation of the convective heat transfer data should account for vapor property variations across the thermal boundary layer.

5.3.2.3 Heat transfer coefficient profiles. Total heat transfer coefficients range from a low of roughly 0.0045 W/cm²·K (8 Btu/h·ft²·°F) in test 10K to a high of roughly 0.037 W/cm²·K (65 Btu/h·ft²·°F) in test I. As was discussed regarding temperature profiles, the influence of the grid was quite pronounced. The effect was most pronounced in test 10L where the heat transfer coefficient at the grid was increased by 64% over the location just below the grid. As expected from the temperature profiles, the effect of the grid was least in the low-flow low-power tests 10K and 10N.

The shape of the heat transfer profiles is the combined result of changes in convective heat transfer, radiative transfer, and grid effects. The axial variation in convective heat transfer tends to be dominated by variations in viscosity and vapor thermal conductivity. Viscosity increases with vapor temperature and thus elevation; this caused the vapor Reynolds number to decrease with elevation. Conductivity increases with vapor temperature and thus elevation as well. Therefore, increases in conductivity tend to offset decreases in Reynolds number. The result is that the convective heat transfer coefficient, excluding grid effects, can either increase or decrease with elevation, depending on the particular test conditions. In all tests with the exception of 10M the convective heat transfer coefficient is calculated to increase overall with respect to elevation. The radiative component of heat transfer increases with elevation in all tests.

The combined effects can sometimes produce surprising results. The heat transfer profile for test 10M, excluding grid effects, shows an almost constant heat transfer coefficient with elevation. This is true despite the fact that vapor Reynolds number and rod surface temperature are both changing with elevation. Apparently, the decrease in convective heat transfer is just offset by the increase in radiation heat transfer.

5.3.3 Radiation heat transfer

As noted in Sect. 5.2.2, thermal radiation is an important heat transfer mechanism under the high-temperature high-pressure conditions typical of a core uncovering. Most of the radiative transfer is from heated rods to high-pressure steam. Under high-pressure conditions steam is an excellent absorber for thermal radiation; absorption coefficients of 0.4 are not uncommon. In addition, a small fraction of the total power is radiated to unheated structures, which then dissipate the energy convectively. The methodology used to compute the radiative heat transfer to steam and unheated structure is discussed in Appendix A.

Figures 23–28 show the fractional radiative component of heat transfer as a function of elevation for each test. Radiative heat transfer is of the least significance in the high-power high-flow tests 10I and 10L where thermal radiation accounts for 10 to 25% of the total heat transfer. As flow and power are decreased, the fractional radiative component increases. Radiation is of most significance in test 10K, where it may account for as much as 65% of total heat transfer. Note that the fractional radiative component of heat transfer does not necessarily increase with elevation despite the increase in surface temperature. In fact, in test 10K it decreases. This decrease results from a number of factors including increases in the convective component of heat transfer with elevation, lower rod-to-steam temperature differences (Fig. 13), and decreases in vapor absorptivity with increasing surface temperature. Thus, radiative

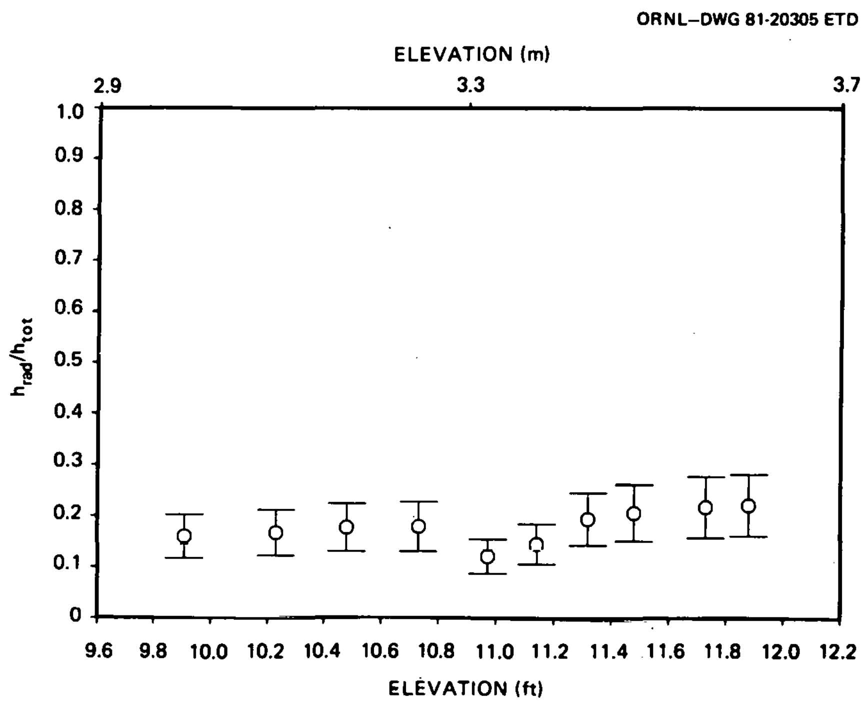

Fig. 23. Radiative fraction of total heat transfer vs elevation: test 3.09.10I.

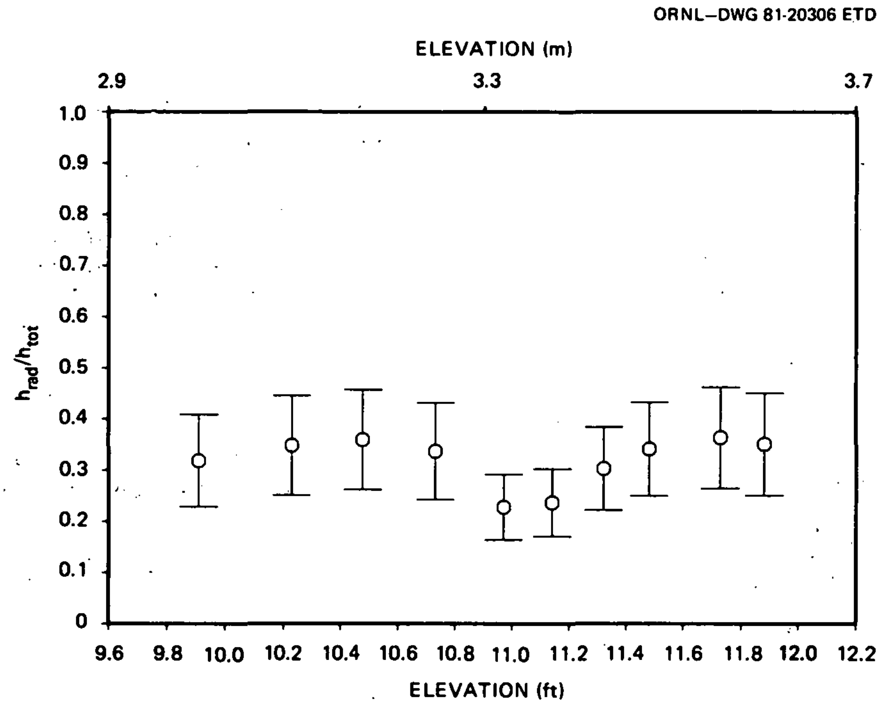

Fig. 24. Radiative fraction of total heat transfer vs elevation; test 3.09.10J.

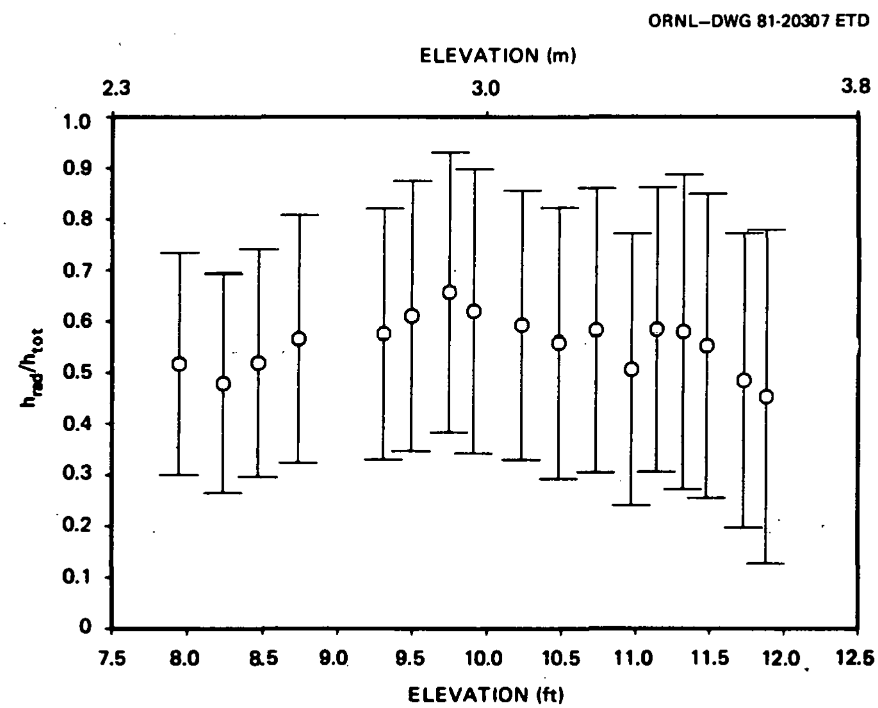

Fig. 25. Radiative fraction of total heat transfer vs elevation; test 3.09.10K.

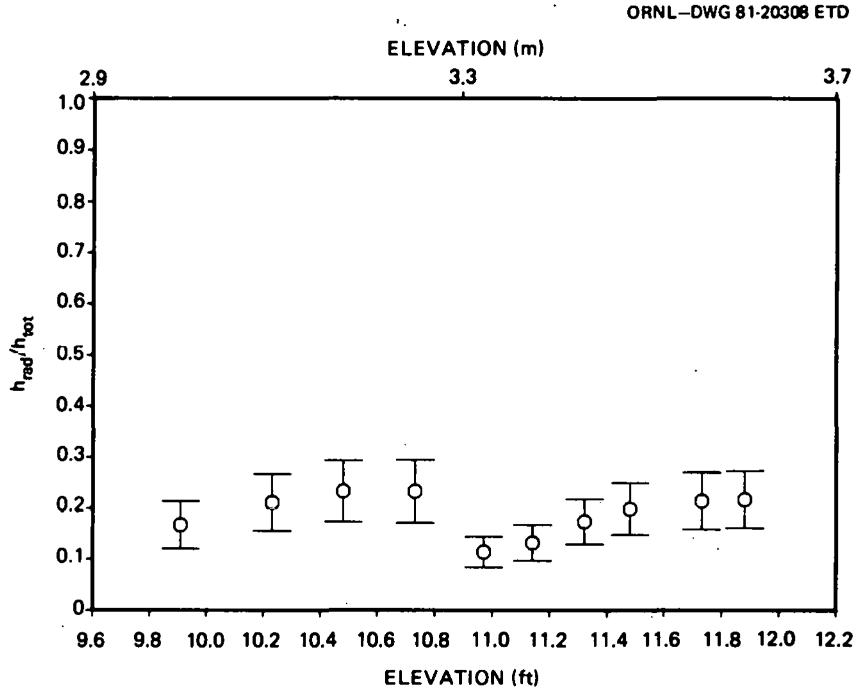

Fig. 26. Radiative fraction of total heat transfer vs elevation; test 3.09.10L.

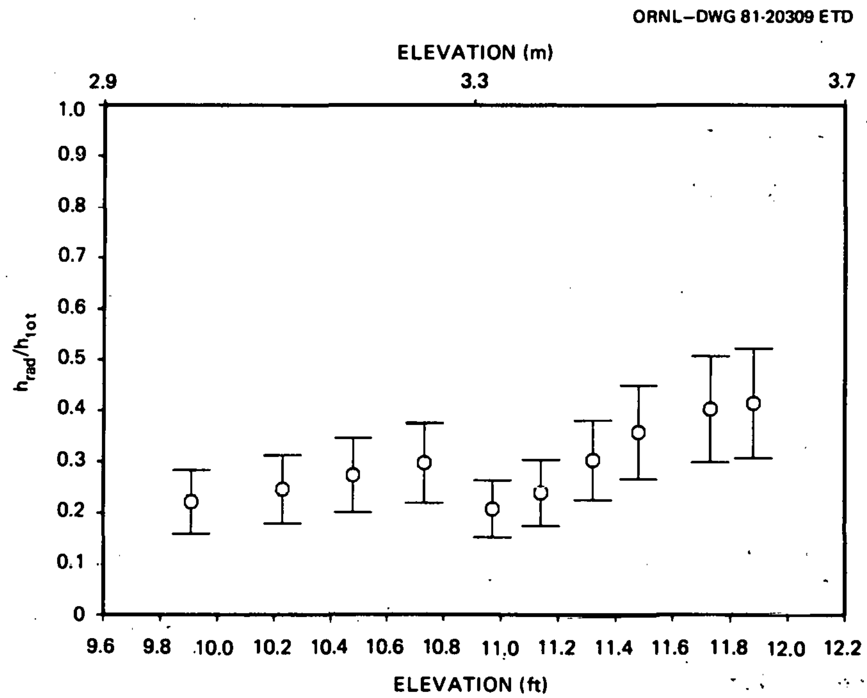

Fig. 27. Radiative fraction of total heat transfer vs elevation; test 3.09.10M.

ORNL–DWG 81-20289 ETD

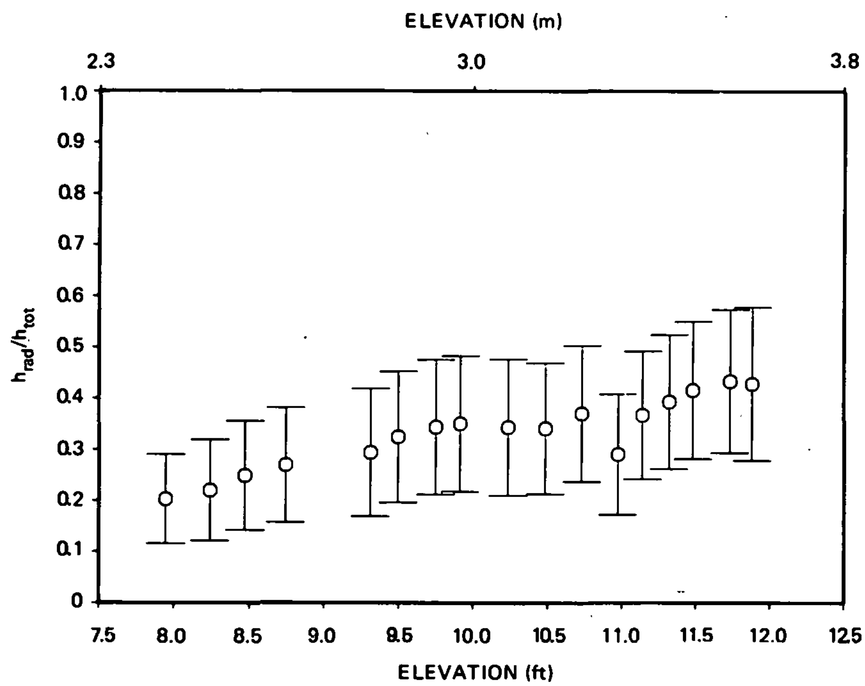

Fig. 28. Radiative fraction of total heat transfer vs elevation; test 3.09.10N.

heat transfer is not always of greater significance in the high-temperature upper portion of the steam-cooling region.

5.3.4 Correlation of convective component of heat transfer

5.3.4.1 Comparison of data with proposed correlations. As noted in Sect. 5.2.1, several correlations have been proposed or have been routinely used to correlate convective heat transfer under low-flow steam-cooling conditions. All of the correlations are of (or equivalent to) the form

$$\frac{Nu_{R_1}}{F} = C\ Re_{R_2}^{a}\ Pr_{R_3}^{b}\ , \tag{9}$$

where R_1, R_2, and R_3 refer to different reference temperatures at which vapor properties are evaluated. The function F corrects for entrance effects, spacer grids, and/or proximity to the froth level. All of the correlations implicitly assume that the steam-cooling region is forced-convection dominated.

The purpose of this section is to compare the experimentally determined convective heat transfer coefficients with selected correlations.

In addition, the convective data will be examined for evidence of transitions between forced-convection dominated and mixed-convection heat transfer regimes.

The data to be examined are composed of heat transfer coefficients obtained from the first small-break heat transfer test series run in January 1980 and the second series, run in November 1980. All heat transfer coefficients were computed as bundle cross-sectional averages. The convective heat transfer coefficients were formulated as

$$h_{conv} = h_{total} - h_{rad} , \tag{10}$$

where h_{total} was the experimentally determined heat transfer coefficient and h_{rad} was the computed radiation heat transfer coefficient. Details of the calculational procedures appear in Appendix A.

As previously discussed, spacer grids may substantially enhance heat transfer at and downstream of the grid. However, in the analysis of an actual reactor accident, the spacer grids cannot a priori be assumed to mitigate the consequences of core uncovering. Therefore, assessing the convective heat transfer at locations not affected by the grids is of primary importance. Thus, data that appear in the comparisons have been screened for proximity to spacer grids.

All data less than 18 L/Ds downstream or 6 L/Ds upstream of the spacer grids have been removed from the comparisons. Yao's correlation, when applied to ORNL spacer grids (which do not have mixing vanes), indicates that enhancement of local heat transfer at 18 L/Ds should be less than 5% of nominal [see Eq. (8)].* In addition, all steam-cooling data to be presented were acquired at locations far enough from the froth level so that enhancement of heat transfer caused by the froth was insignificant.

The first comparison (Fig. 29) is a log-log plot of $Nu_v/Pr_v^{0.4}$ vs Re_v, which is overlaid with a line representing the Dittus-Boelter correlation and the line $Nu_v/Pr_v^{0.4} = 4.0$. For vapor Reynolds numbers greater than 4000, the data roughly parallel the Dittus-Boelter correlation. However, the correlation systematically overpredicts the data. In addition, the data groupings show considerable scatter. This raises the possibility that mechanisms other than simple forced convection may be influencing heat transfer.

The data at vapor Reynolds numbers less than 3000 show a large amount of scatter and, particularly in the lowest Reynolds number data, quite large relative uncertainties. The large uncertainties at low flow are caused primarily by two factors. First, the low-flow tests were also the lowest power tests, rod-to-steam temperature differences were relatively small. Therefore, modest uncertainties in vapor temperature and rod surface temperature translate into large relative uncertainties in temperature difference and heat transfer coefficient. Second, uncertainty in the radiation heat transfer coefficients affects uncertainty in the convective heat transfer coefficients [Eq. (10)]. Uncertainty in radiation

---

*Flow blockage ratio for ORNL spacer grids is 0.284.

ORNL–DWG 81-20291 ETD

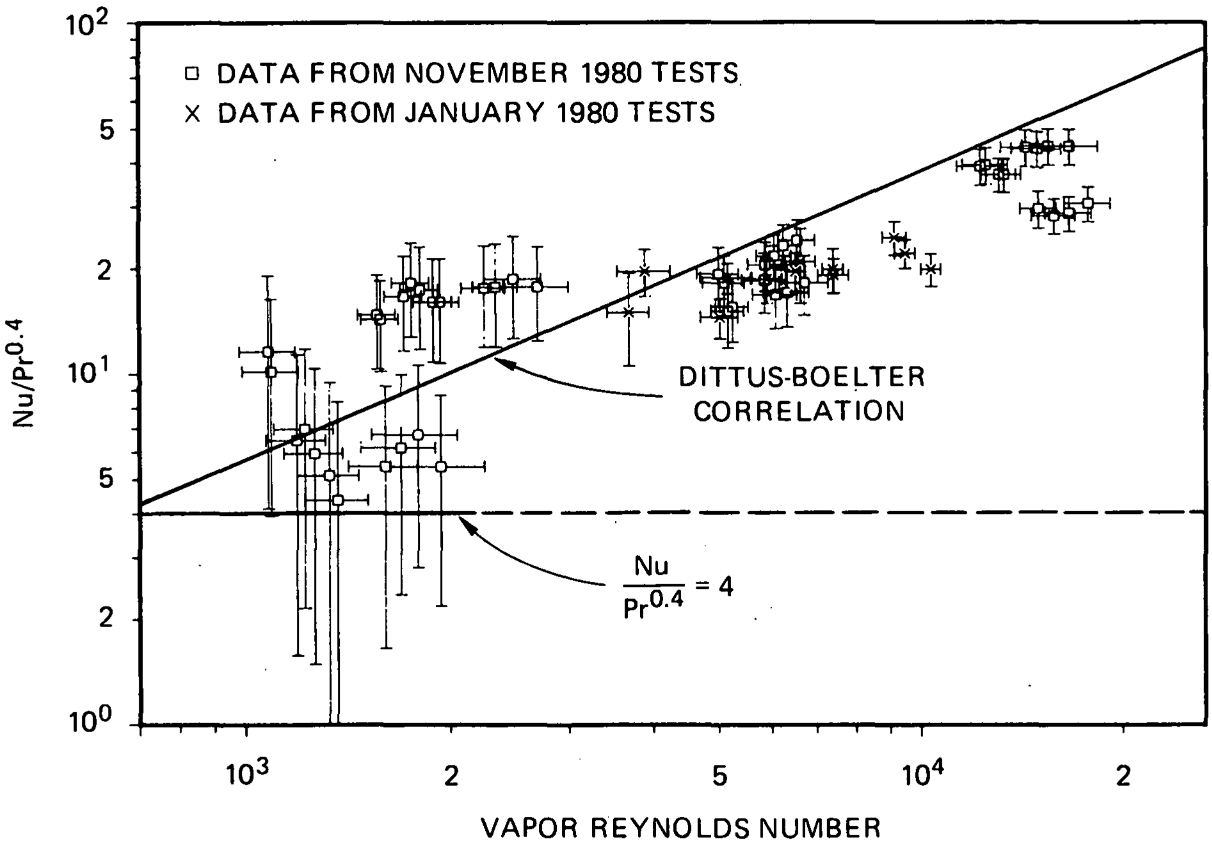

Fig. 29. $Nu/Pr^{0.4}$ vs vapor Reynolds number; all vapor properties evaluated at vapor temperature.

heat transfer is large for all tests. However, radiation is a much larger fraction of the total heat transfer in the low-flow tests. Thus, the uncertainty in radiation heat transfer has a greater influence on total uncertainty in convective heat transfer coefficients in the low-flow tests.

Despite these large uncertainties, the low-flow data do not appear compatible with a simple forced-convection heat transfer model. Note that the data set from test 10N ($1500 \leq Re_v \leq 3000$) lies well above the Dittus-Boelter correlation, despite the fact that the Reynolds number range is typical of forced-convection laminar or transition to turbulent flow. In addition, data from test 10K appear to be well below the test 10N data, although they overlap in Reynolds numbers. These deviations were not a total surprise, as Fig. 10 indicated that most of the convective data below a vapor Reynolds number of 3000 would be in a mixed-convection regime.

The second comparison (Fig. 30) examines the same data set, but in this case all steam properties were evaluated at the film temperature. Evaluation at the film temperature adjusts the data for vapor property variations across the boundary layer. The data are overlaid with lines

ORNL–DWG 81-20310 ETD

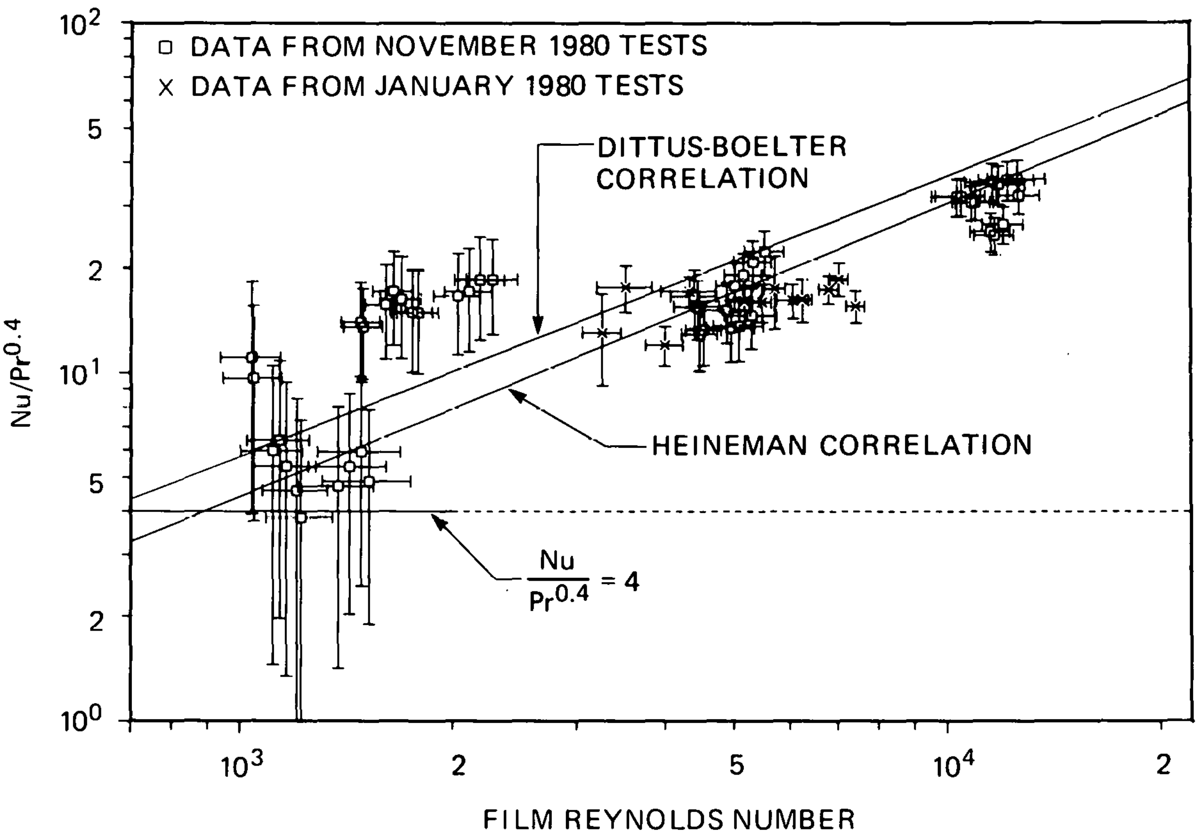

Fig. 30. $Nu/Pr^{0.4}$ vs film Reynolds number; all vapor properties evaluated at film temperature.

representing the Dittus-Boelter correlation, the Heineman correlation, and the constant 4.0.*

Note that the use of the film temperature to evaluate vapor properties produces somewhat tighter groupings of the data. This is best illustrated by comparing the highest Reynolds number group of data in Figs. 29 and 30. Use of the film temperature results in a significant consolidation of the group. This reinforces the notion that, because of the large temperature differences, vapor property variations are important.

---

*The Heineman correlation appears in a slightly modified form in that the Prandtl number is evaluated with exponent 0.4 rather than 0.333. Because the Prandtl number is so close to 1.0, this modification is not significant. Also, Heineman recommends an (L/D) correction for (L/D) $<$ 60. The (L/D) correction is not significant in these comparisons because the data were screened for proximity to grids. If the (L/D) correction were included, it would result in no more than a 5% change in the Nu.

As in the first comparison, the Dittus-Boelter correlation systematically overpredicts the higher Reynolds number data; the Heineman correlation fits the data better. However, significant scatter in the higher Reynolds number data remains. As in the first comparison a large amount of scatter exists in the low Reynolds number data and a simple forced-convection heat transfer model does not appear to describe the experimental observations.

The third comparison (Fig. 31) examines the data in terms of the modified wall Reynolds number and the ratio $Nu/Pr^{0.4}$ where all properties were evaluated at the heated surface temperature. The data are overlaid with lines representing Eq. (1), the FLECHT correlations, and the line $Nu/Pr^{0.4} = 4$.*

The use of the modified wall Reynolds number results in further consolidation of the data groups. This is most evident in the lowest Reynolds number group where the data collapse almost to a vertical line. Equation (1) fits the data reasonably well at modified wall Reynolds numbers greater than 2000. The correlation does not appear to be appropriate for modified wall Reynolds numbers less than 2000. The FLECHT correlation tends to systematically overpredict the data for Reynolds numbers greater than 2000. At Reynolds numbers less than 2000 the FLECHT correlation is in approximate agreement with the test 10N results but clearly overpredicts the test 10K results. The constant 4.0 is probably a lower bound for the convective data at Reynolds numbers less than 2000.

5.3.4.2 Discussion of results. In summary, several points bear discussion. The first and most important is that evidence exists that a simple forced-convection heat transfer model may not be appropriate under conditions similar to those expected in a high-pressure core uncovering. Conventional forced-convection correlations fit the data reasonably well down to modified wall Reynolds numbers of 2000. However, at Reynolds numbers less than 2000 marked deviations from a forced-convection model may occur. Data acquired from test 10K at an almost constant modified-wall Reynolds number of 900 show a Nusselt number of about 4.0 at the bottom of the steam-cooling region. This is consistent with the Nusselt number for laminar flow in a tube with uniform heat flux. However, the Nusselt number increases considerably with elevation, exceeding 10 at the top of the steam-cooling region. This occurs despite the fact that the modified wall Reynolds number remains at roughly 900 over the entire steam-cooling region. The data from test 10N have a mean Nusselt number of about 14 despite the fact that the modified wall Reynolds number is about 1400. A considerable body of data acquired at Reynolds numbers between 3000 and 4000 have Nusselt numbers less than 14; thus, the low flow data apparently do not conform to a simple forced-convection model.

---

*Because the data displayed in Fig. 31 were taken from locations well removed from the froth level and spacer grids, the functions F_{froth} and F_{grid} [see Eqs. (2), (3), and (4)] in the FLECHT correlations were set equal to 1.0. In addition, the Prandtl number in the FLECHT correlation was evaluated with an exponent of 0.4 rather than 0.333. Because the Prandtl number is close to 1.0, this is not significant.

ORNL–DWG 81-20311 ETD

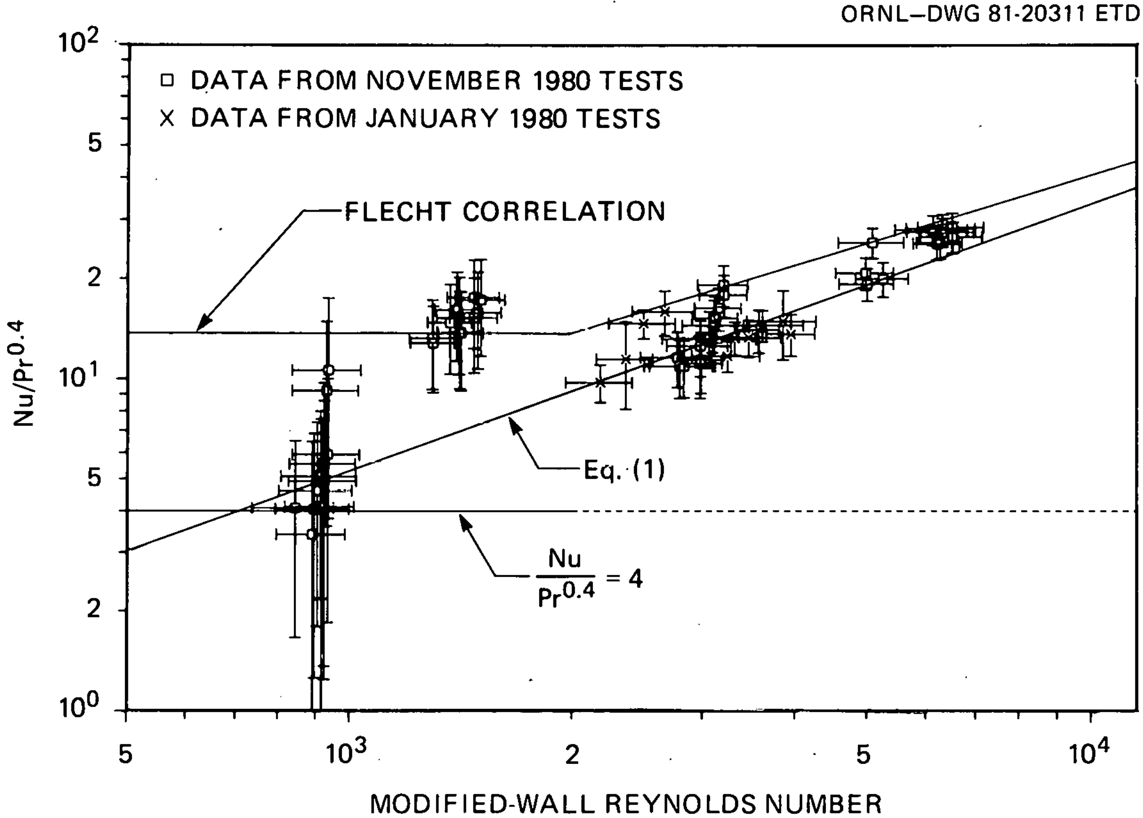

Fig. 31. $Nu/Pr^{0.4}$ vs modified wall Reynolds number; all vapor properties evaluated at heated surface temperature.

The most likely cause of the deviations observed at low flow seems to be a transition to a mixed-convection- or free-convection-dominated regime. The Metais and Eckert chart (Fig. 10) indicates that both tests run at modified wall Reynolds numbers less than 2000 should be at least partially in a mixed-convootive regime. However, this should not be taken as a validation of the chart; the flow regime map was developed for vertical tubes. To what extent the rod bundle geometry and spacer grids might affect flow transitions is not known. One deviation from the chart is immediately evident in test 10K. The Metais and Eckert chart indicates mixed-convection turbulent flow at the bottom of the steam-cooling region with transition to forced-convection laminar near the top of the region. The data would indicate just the opposite, with a Nusselt number typical of laminar forced convection at the bottom of the steam-cooling region and a Nusselt number indicating enhanced heat transfer near the top of the region. Separate rod bundle experiments are apparently needed to accurately delineate flow transitions in rod bundle geometry.

The second point concerns the selection of an appropriate set of heat transfer correlations. For modified wall Reynolds numbers greater than 2000 and less than 10,000, two correlations predict the data reasonably well: Eq. (1) and the Heineman correlation. A quantitative differentiation between the two correlations will be made in the next section. Note that buoyancy effects may not be limited to the data below modified wall Reynolds numbers of 2000. Mixed-convection effects may account for some of the scatter observed in the higher Reynolds number data. However, deviations from forced-convection correlations are not marked, and use of simple forced-convection correlations is probably adequate.

The situation is not as clear for modified wall Reynolds numbers less than 2000. The data seem to indicate that substantial enhancement of heat transfer over that expected in laminar forced convection is possible. However, the enhancing mechanisms and possible flow regime boundaries are not well understood. The FLECHT correlation for laminar flow matches the test 10N data quite well; however, it overpredicts some of the test 10K data by a wide margin. At this point, recommendation of a best-estimate correlation for modified wall Reynolds numbers less than 2000 is not possible. A best-estimate correlation should at least have theoretical underpinnings that can explain the wide variations in $Nu/Pr^{0.4}$ observed at low flow. In addition, given the possible complexity of convective heat transfer at low flow and the difficulty in obtaining accurate experimental data, a best-estimate correlation should be supported by a substantial data base acquired over a wide range of flows, temperatures, and rod-to-steam temperature differences. Given the current state of knowledge, setting $Nu/Pr^{0.4} = 4.0$ is probably advisable for modified-wall Reynolds numbers less than 2000. All properties are evaluated at the heated surface temperature. The results from tests 10K and 10N indicate that this should provide a conservative estimate of the heat transfer coefficient.

Finally, although the majority of the data could be fit reasonably well simply by adjusting the exponents and coefficients in the proposed correlations, this is not advisable for several reasons. As discussed, evidence exists that several flow regimes may be represented by the data. A single regression of the data would ignore the underlying physics and invite problems if the resulting correlation were used outside of the parametric ranges supported by data. In addition, the data are not in a parametric form, because in the THTF, with its radially uniform power profile, both vapor generation rate and surface heat flux are controlled by bundle power. Thus, the high steam-flow tests have a tendency to be the large rod-to-steam temperature difference tests. As noted earlier, temperature difference can substantially affect convective heat transfer because of vapor property variations.

5.3.5 Addition of radiation to selected convective correlations

As discussed in the previous section, Eq. (1) and Heineman correlations fit the majority of the convective heat transfer data for modified-wall Reynolds numbers greater than 2000. As a final step in data correlation, calculated radiation heat transfer coefficients were added to the convective heat transfer coefficients calculated by these two correlations and the McEligot correlation [Eq. (5)]. The McEligot correlation has been commonly used in steam-cooling applications and is roughly equivalent to Eq. (1) for the case of heat transfer to essentially ideal gases.[1] Thus it is of interest to determine to what extent, if any, the nonidealities of high-pressure steam affect the selection of an optimal convective heat transfer correlation. The radiation heat transfer coefficients were computed using methods outlined in Appendix A.

Note that this step in the correlation process is somewhat trivial, because the convective heat transfer coefficients were computed by subtracting the calculated radiation heat transfer coefficients from the experimentally determined total heat transfer coefficients. Thus, correlations that predict the convective heat transfer well are also expected, when combined with the radiation heat transfer model, to predict total heat transfer coefficients well.

The comparisons are presented in Figs. 32–34. The data base used in the comparisons is the same as used in the convective heat transfer comparisons (i.e., screened for proximity to spacer grids). The comparisons appear as the ratio of the correlation-computed total heat transfer coefficient to the experimentally determined total heat transfer coefficient

ORNL–DWG 81-20312 ETD

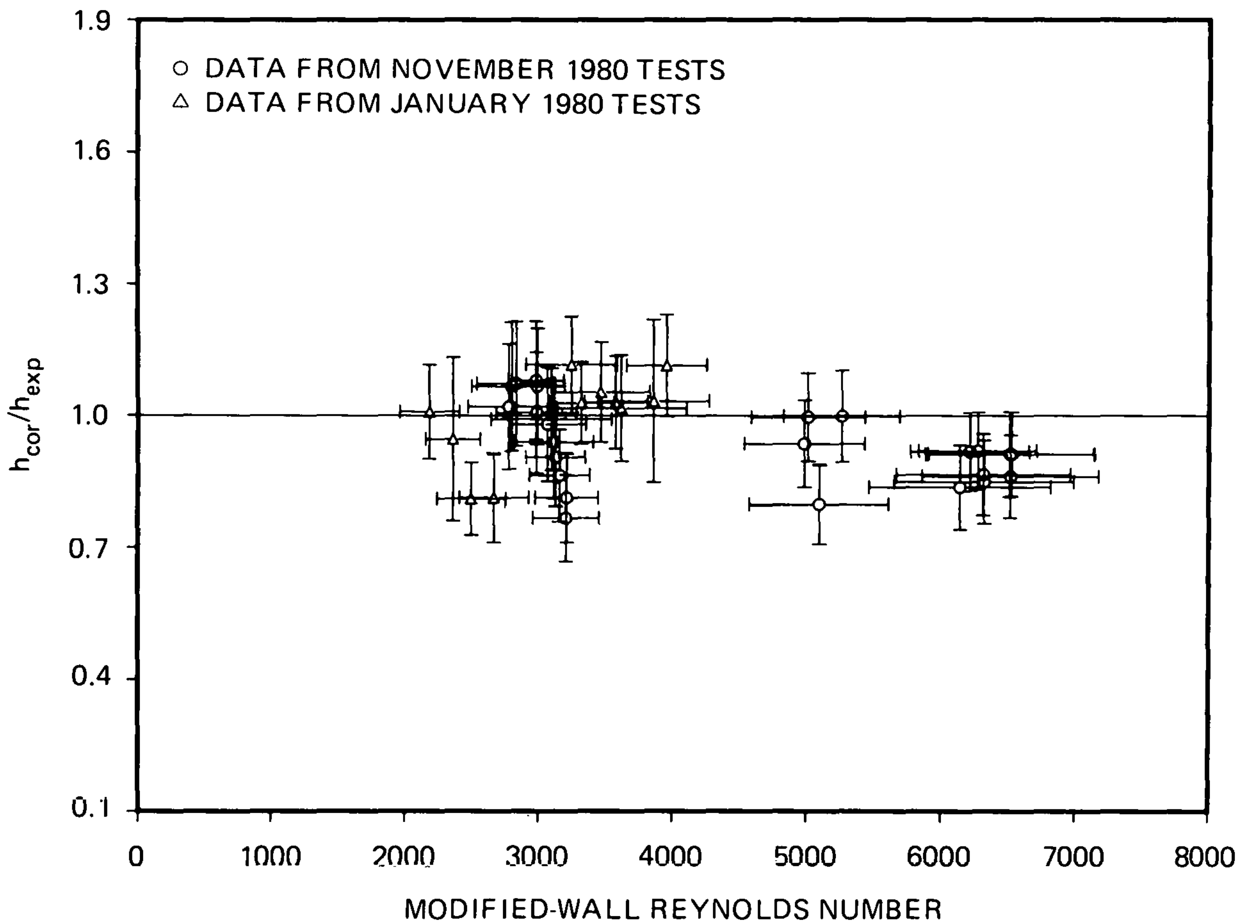

Fig. 32. Ratio of predicted total heat transfer coefficient to experimentally determined heat transfer coefficient vs modified wall Reynolds number; convective component of heat transfer computed from Eq. (1).

ORNL–DWG 81-20313 ETD

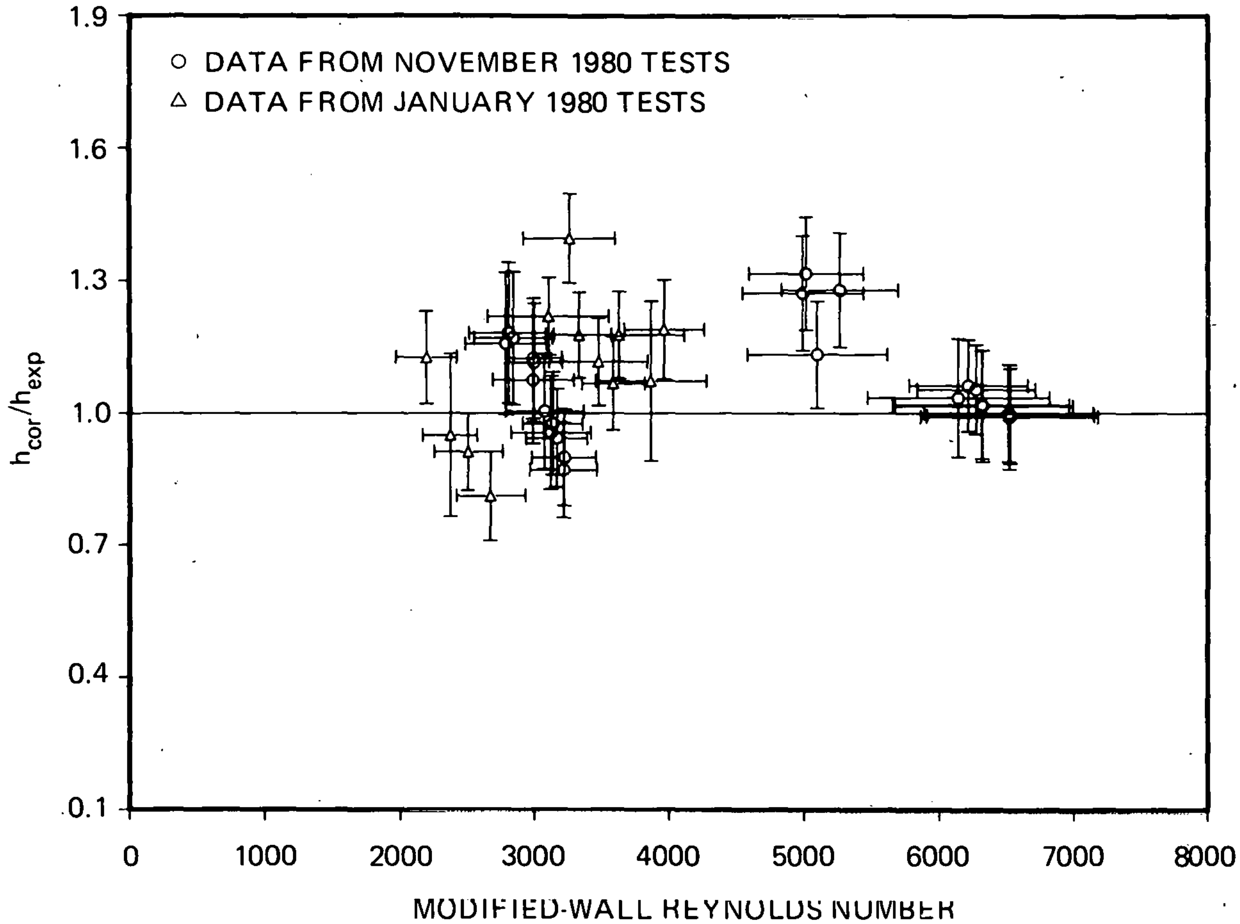

Fig. 33. Ratio of predicted total heat transfer coefficient to experimentally determined heat transfer coefficient vs modified wall Reynolds number; convective component of heat transfer computed from Heineman correlation.

vs the modified wall Reynolds number. Appendix B contains specific numerical values of predicted and experimental heat transfer coefficients, including those at elevations where spacer grid enhancement is present.

A statistical breakdown of the three comparisons appears in Table 4, which indicates that all of the correlations predict the data quite well. The recommended correlation is Eq. (1), which had the lowest standard error and smallest maximum overprediction.

The second choice would be the McEligot correlation, as its predictions are quite similar to those of Eq. (1). The exception occurs when the temperature ratio is large and the steam is almost saturated. An example of this phenomenon is the data group at a modified-wall Reynolds number of roughly 5000. The vapor superheat for these data points varies from 11 to 68 K (19 to 122°F). The temperature ratios are roughly 1.6.

Table 4. Statistical breakdown for total heat transfer coefficient comparisons

Correlation	Standard error[a]	Percent point overpredicted	Percent point underpredicted	Maximum overprediction (%)	Maximum underprediction (%)
Equation (1)	0.11	39	61	12	22
Heineman	0.15	72	28	39	20
McEligot	0.13	53	47	30	19

[a] Standard error is defined as $SE = \sqrt{\dfrac{\sum_{i=1}^{N} [1.0 - (h_{cor}/h_{exp})]^2}{N}}$.

ORNL–DWG 81-20314 ETD

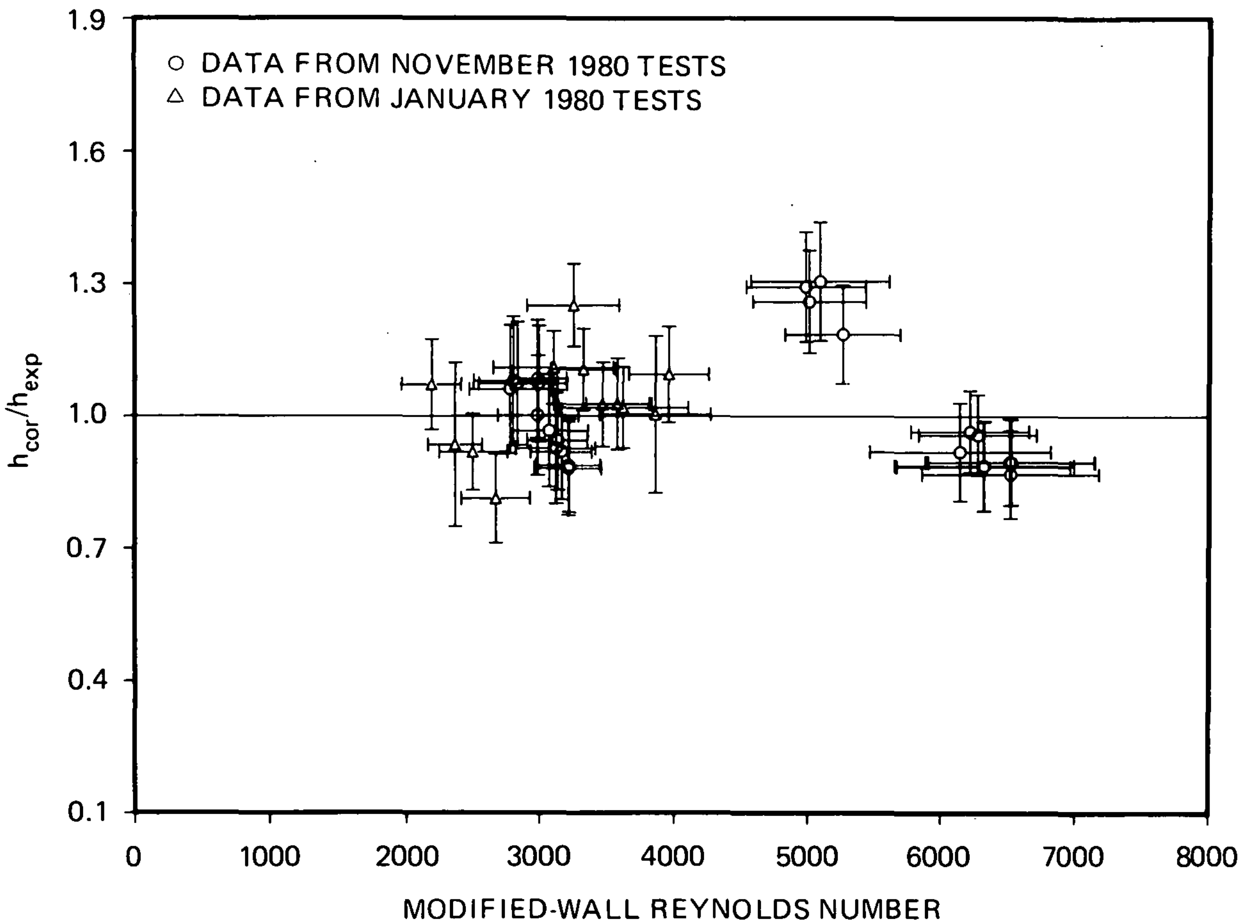

Fig. 34. Ratio of predicted total heat transfer coefficient to experimentally determined heat transfer coefficient vs modified wall Reynolds number; convective component of heat transfer computed from McEligot correlation.

The McEligot correlation overpredicts this data group by as much as 30%, while Eq. (1) predicts three of the four data points within measurement certainty.

This deviation occurs because the McEligot correlation relies on power law approximations for temperature-dependent vapor property variations. When the temperature ratio is large, property variations have a strong influence on convective heat transfer. If, at the same time, the vapor is near saturation, the power law approximations are invalid. Therefore, when property variations are important and when the vapor deviates significantly from an ideal gas, the McEligot correlation performs poorly. It was for precisely these conditions that Eq. (1) was originally developed. When the vapor is near ideal, Eq. (1) is roughly equivalent to the McEligot correlation; however, when the vapor is nonideal, the correlations diverge because Eq. (1) explicitly evaluates vapor properties at the heated surface temperature rather than relying on a power law approximation.

5.3.6 Evaluation of reactor vendor correlations

At the request of the U.S. Nuclear Regulatory Commission (NRC), ORNL has compared experimentally determined heat transfer coefficients with those predicted by nuclear reactor vendor correlations. The following vendor correlations were provided to ORNL by the NRC:

1. Westinghouse Electric Corp. (W)

All W correlations are of the form

$$h_{total} = h_{rad} + h_{conv} , \quad (11)$$

where h_{rad} is computed using a proprietary thermal radiation model for SBLOCAs and h_{conv} is the convective heat transfer coefficient computed from the following correlations:

For laminar flow ($Re_v < 3000$)

$$h_{conv} = \frac{3.66\ k_v}{D_H}\left(\frac{T_v}{T_w}\right)^{0.25} , \quad (12)$$

where k_v is the thermal conductivity of the steam evaluated at the vapor temperature, D_H is the hydraulic diameter, T_v is the vapor temperature, T_w is the rod surface temperature, and Re_v is the vapor Reynolds number.

For turbulent flow ($Re_v > 5000$)

$$h_{conv} = \frac{0.021\ k_v}{D_H} Re_v^{0.8}\ Pr_v^{0.4}\left(\frac{T_v}{T_w}\right)^{0.5} , \quad (13)$$

where Pr_v is the vapor Prandtl number.

For transition to turbulent flow ($3000 \leq Re_v \leq 5000$)

$$h_{conv} = h_{lam} + (h_{tur} - h_{lam})\left(\frac{Re_v - 3000}{5000 - 3000}\right) , \quad (14)$$

where h_{lam} is computed from Eq. (12) and h_{tur} is computed from Eq. (13) with $Re_v = 5000$.

2. Combustion Engineering Corporation (CE)

CE does not account for thermal radiation to steam, thus

$$h_{total} = h_{conv} \; . \tag{15}$$

For laminar flow

$$h_{conv} = \frac{1.86\ k_v}{D_H} \left(\frac{Re_v\ Pr_v\ D_H}{L - Z_L} \right)^{1/3} \left(\frac{\mu_v}{\mu_w} \right)^{0.14} , \tag{16}$$

where L is the elevation, Z_L is the two-phase mixture level, and μ is the viscosity of the steam.

For turbulent flow

$$h_{conv} = \frac{0.023\ k_v}{D_H}\ Re_v^{0.8}\ Pr_v^{0.4} \; . \tag{17}$$

For transition flow h_{conv} is computed from a proprietary interpolation between Eqs. (16) and (17).

3. Babcock and Wilcox Corp. (B&W)

B&W uses the Dittus-Boelter correlation for all Reynolds numbers. Radiation to steam is not accounted for:

$$h_{tot} = h_{conv} = \frac{0.023\ k_v}{D_H}\ Re_v^{0.8}\ Pr_v^{0.4} \; . \tag{18}$$

The data base for the comparisons is a composite of bundle cross-section average heat transfer coefficients from the first uncovered-bundle test series run in January 1980 and the second series run in November 1980. The data have been screened for proximity to spacer grids, as was done for convective heat transfer (Sect. 5.3.4). This prevents local enhancement of heat transfer by spacer grids from biasing the graphical comparisons. All comparisons are presented as the ratio of the correlation-predicted heat transfer coefficient to the experimentally determined total heat transfer coefficient vs the modified wall Reynolds number. The comparisons are shown in Figs. 35–41. Table 5 is a statistical breakdown for each correlation. Specific numerical values of vendor-predicted heat transfer coefficients, including those at elevations where spacer grid effects are present, appear in Appendix B.

Table 5. Statistical breakdown of vendor correlation comparisons

Vendor	Regime[a]	Standard error[b]	Percent points overpredicted	Percent points underpredicted
W	Turbulent	0.13	61	39
W	Transition	0.21	0	100
W	Laminar	0.41	0	100
B&W	All Re_v	0.38	17	83
CE	Turbulent	0.28	46	54
CE	Transition	0.37	7	93
CE	Laminar	0.71	0	100

[a] Regimes as prescribed by vendors.

[b] Standard error is a relative error defined as

$$SE = \sqrt{\frac{\sum_{i=1}^{N} [1.0 - (h_{cor}/h_{exp})_i^2]}{N}}$$

ORNL—DWG 81-20315 ETD

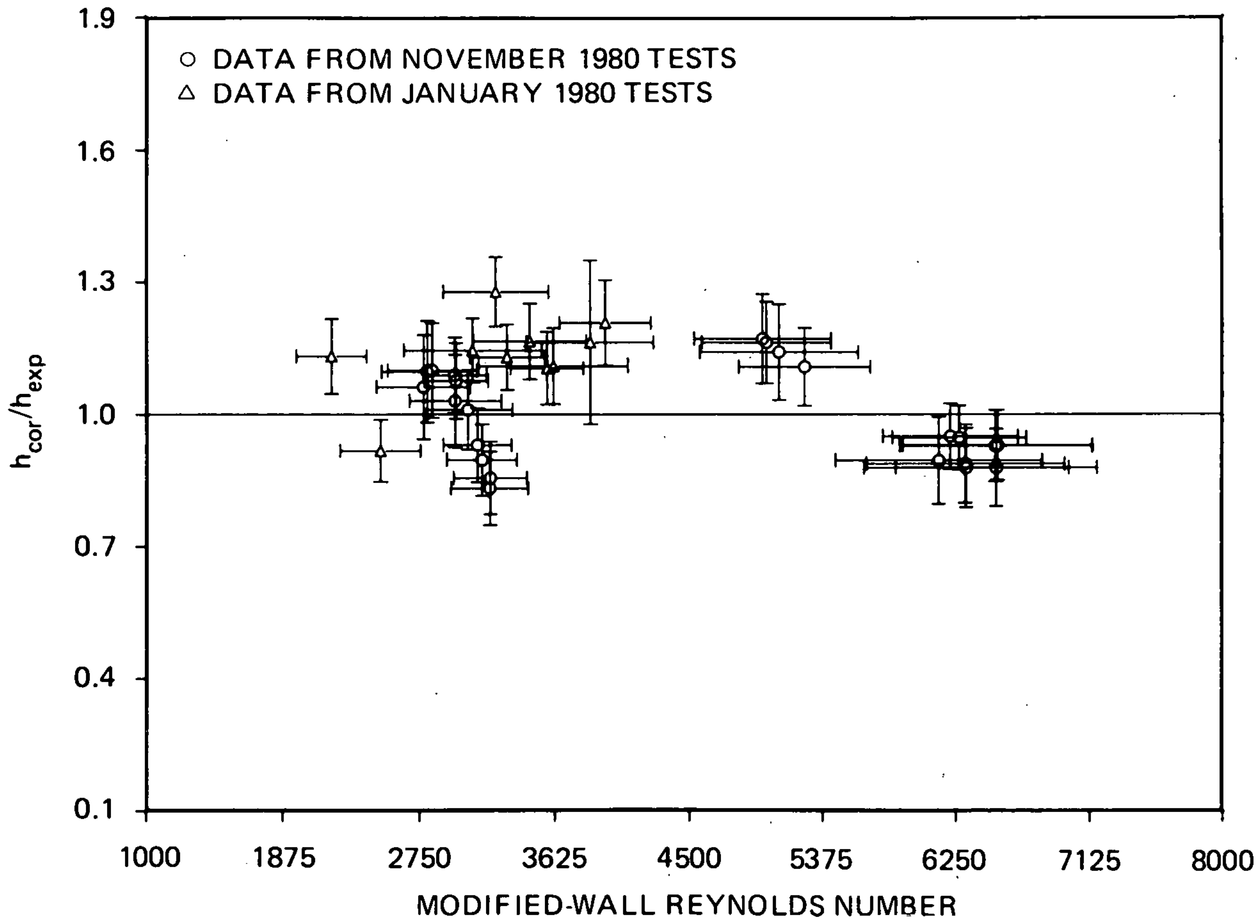

Fig. 35. Ratio of predicted total heat transfer coefficient to experimentally determined heat transfer coefficient vs modified wall Reynolds number; convective component of heat transfer computed from W correlation for turbulent flow.

ORNL—DWG 81-20316 ETD

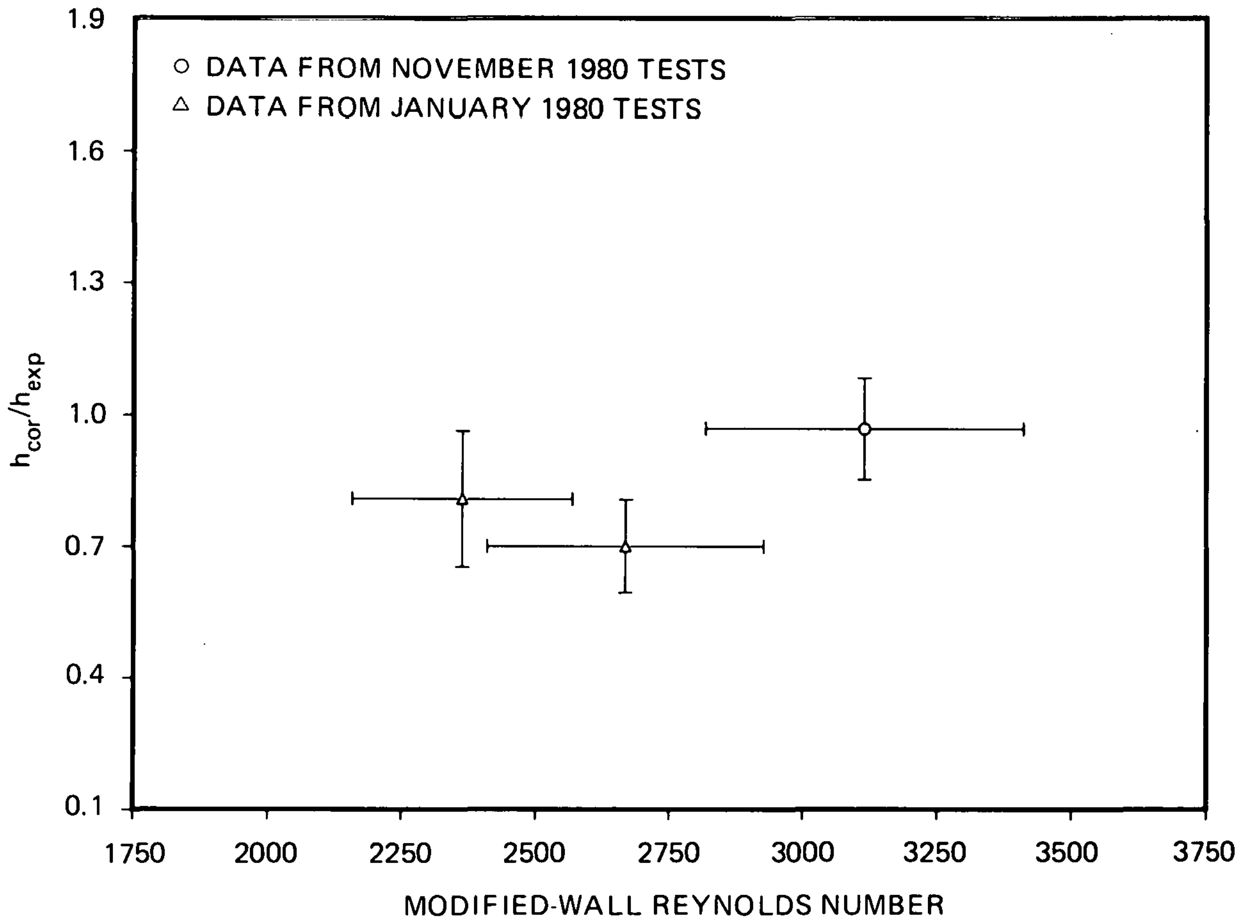

Fig. 36. Ratio of predicted total heat transfer coefficient to experimentally determined heat transfer coefficient vs modified wall Reynolds number; convective component of heat transfer computed from W correlation for transition flow.

ORNL–DWG 81-20317 ETD

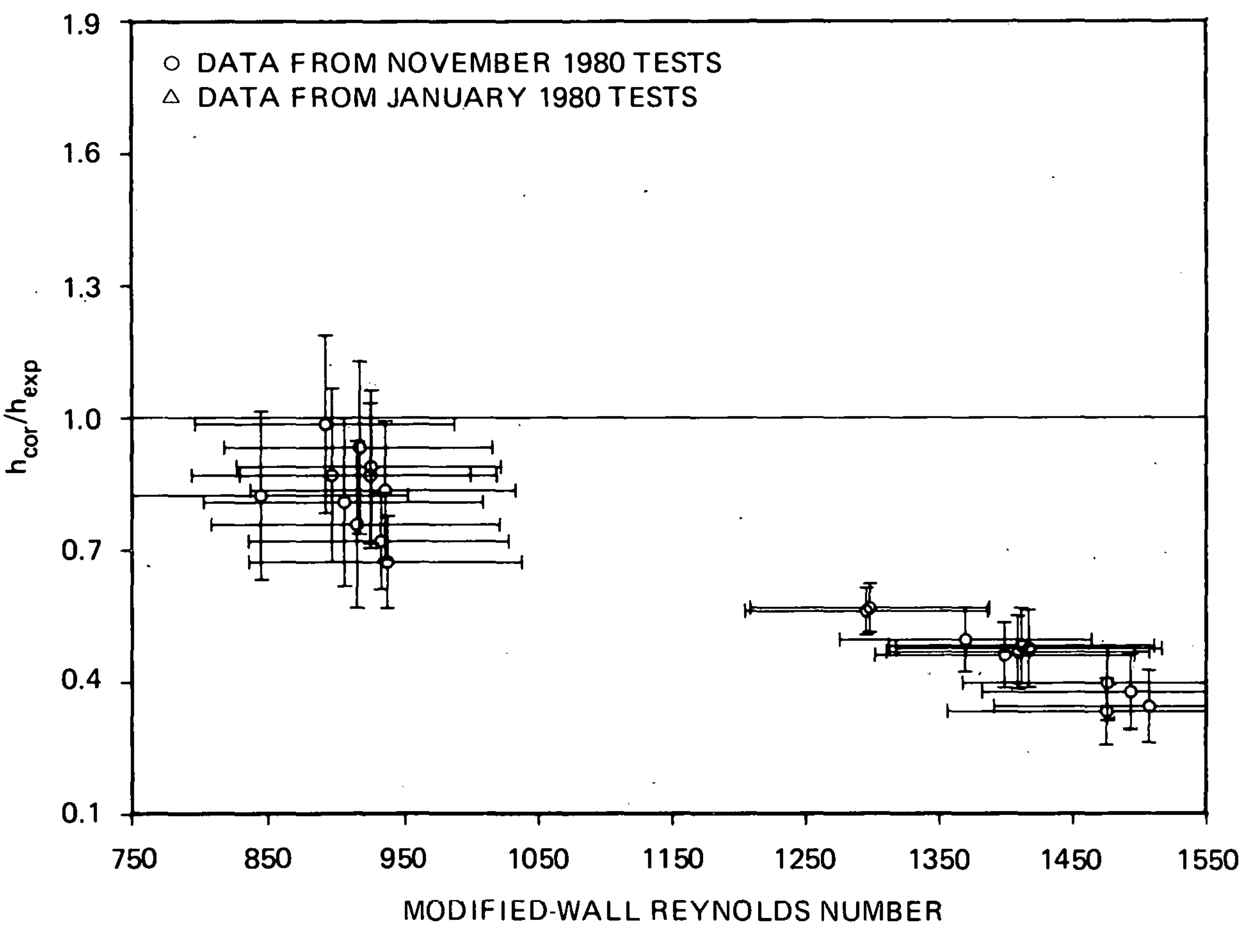

Fig. 37. Ratio of predicted total heat transfer coefficient to experimentally determined heat transfer coefficient vs modified wall Reynolds number; convective component of heat transfer computed from W correlation for laminar flow.

ORNL–DWG 81-20318 ETD

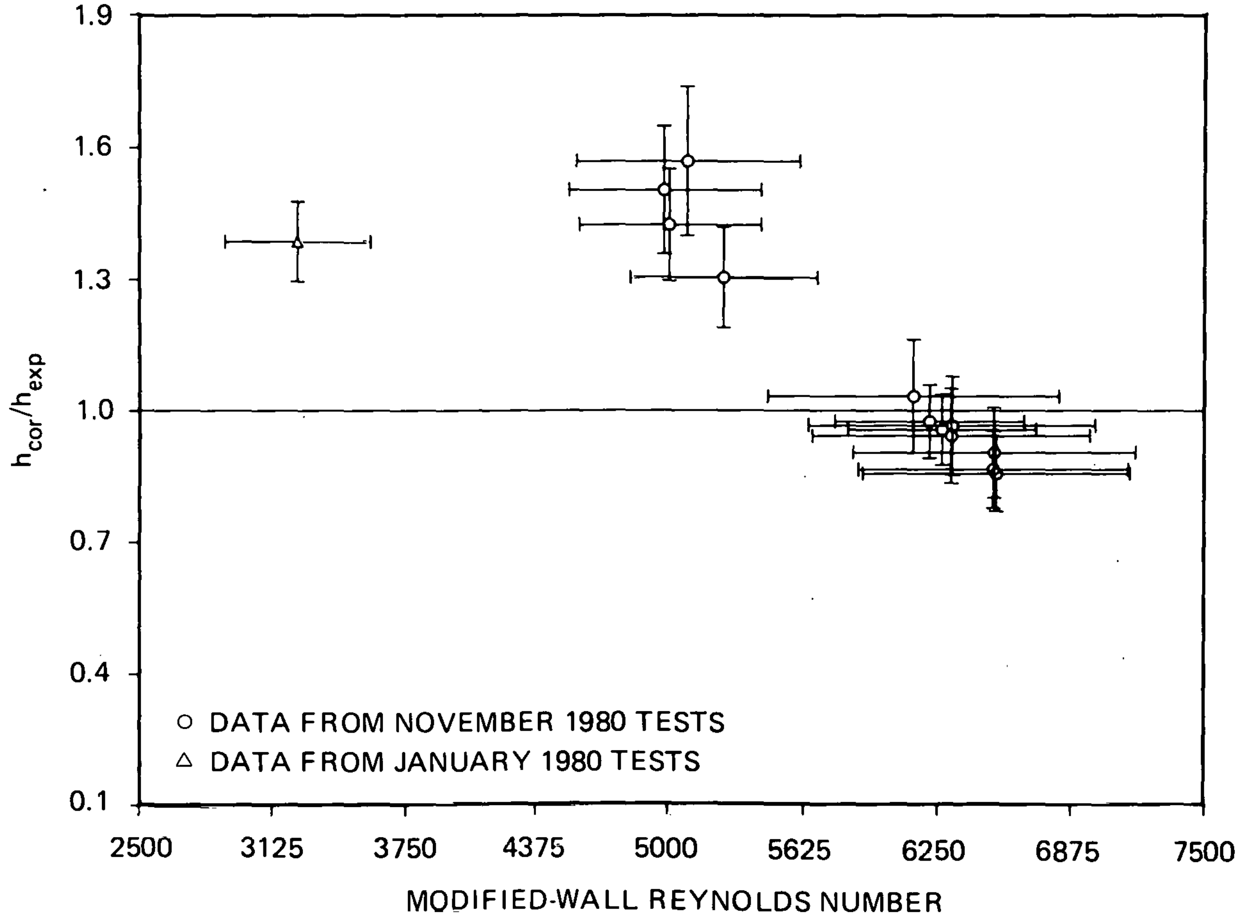

Fig. 38. Ratio of predicted total heat transfer coefficient to experimentally determined heat transfer coefficient vs modified wall Reynolds number; convective component of heat transfer computed from CE correlation for turbulent flow.

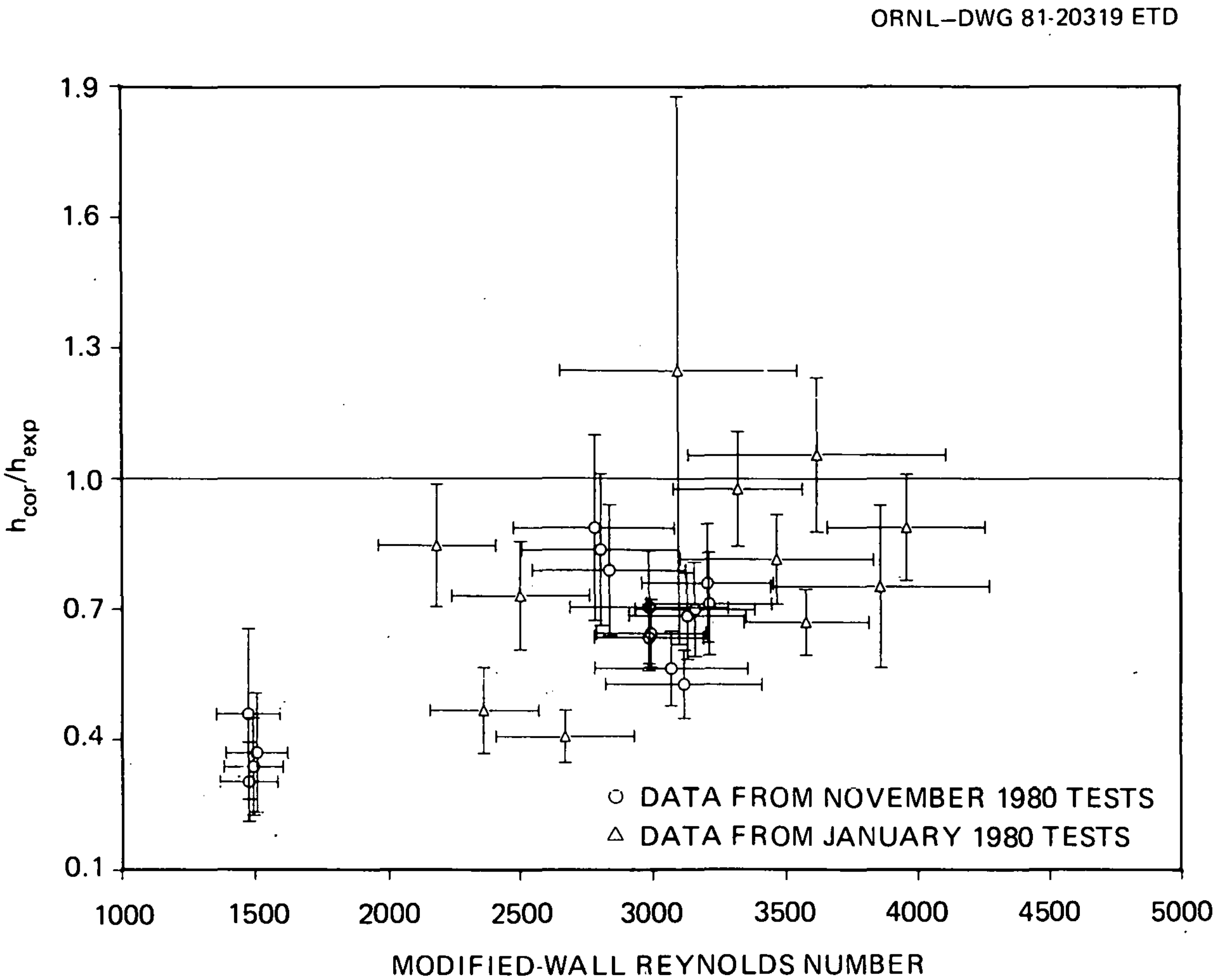

Fig. 39. Ratio of predicted total heat transfer coefficient to experimentally determined heat transfer coefficient vs modified wall Reynolds number; convective component of heat transfer computed from CE correlation for transition flow.

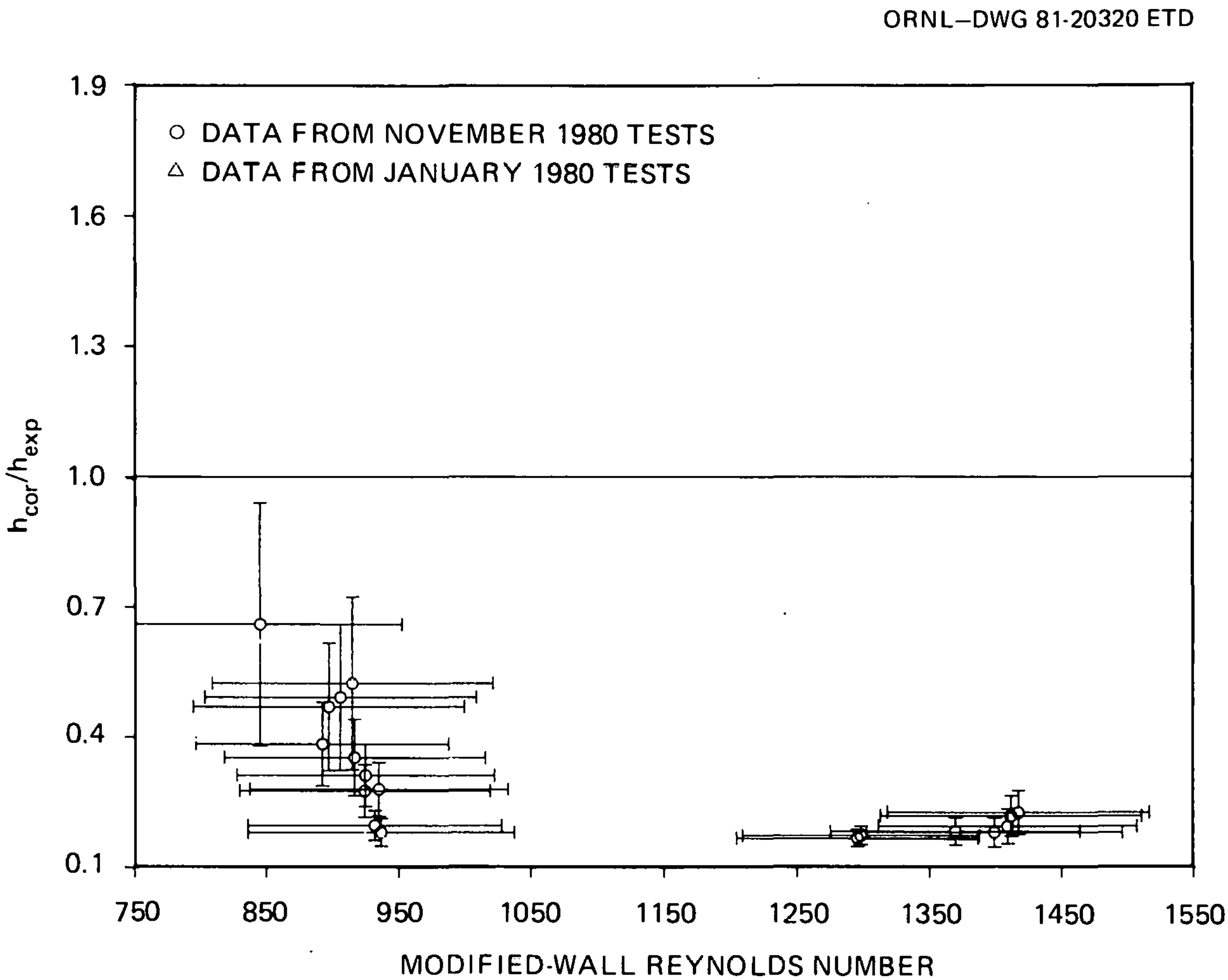

Fig. 40. Ratio of predicted total heat transfer coefficient to experimentally determined heat transfer coefficient vs modified wall Reynolds number; convective component of heat transfer computed from CE correlation for laminar flow.

ORNL–DWG 81-20321 ETD

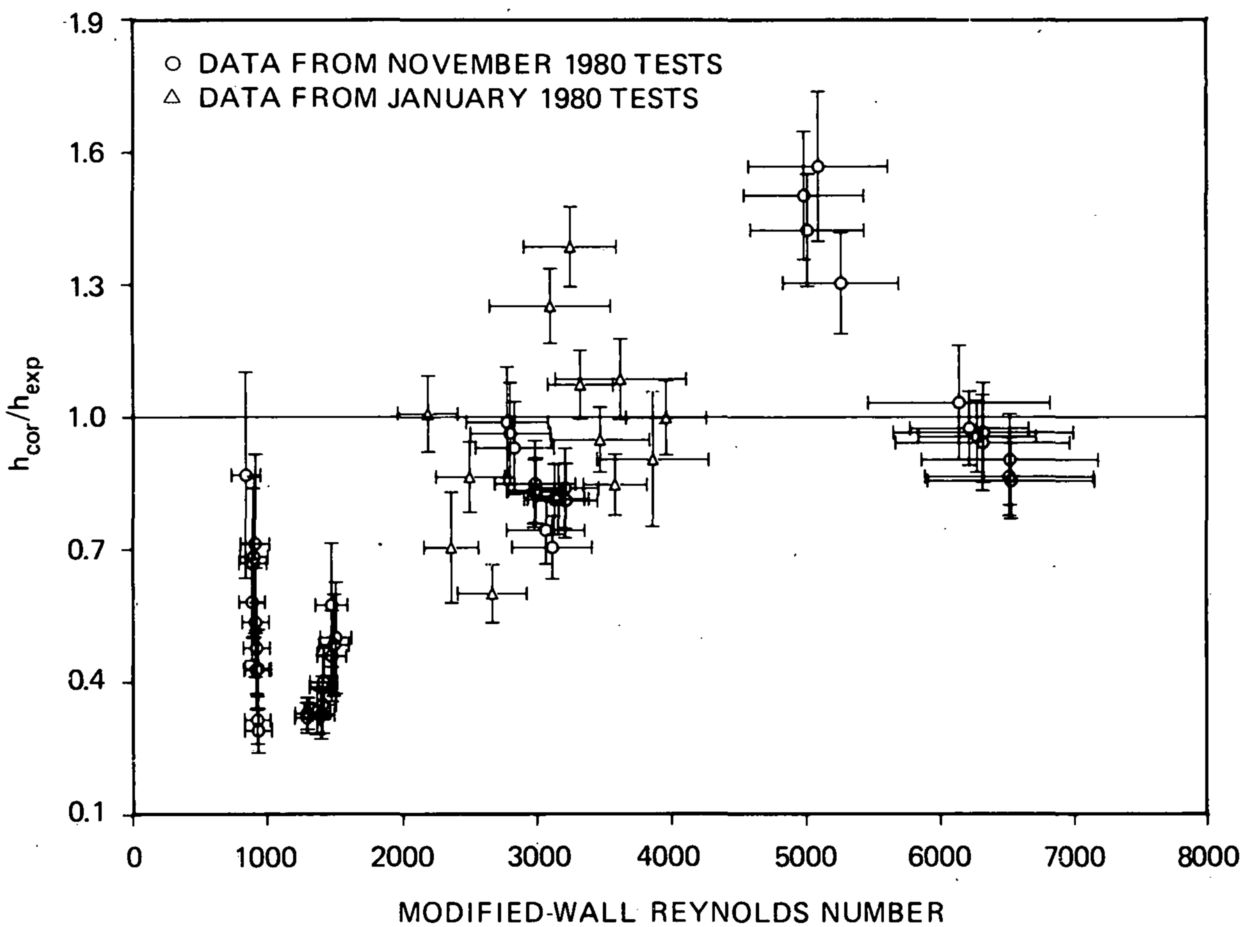

Fig. 41. Ratio of predicted total heat transfer coefficient to experimentally determined heat transfer coefficient vs modified wall Reynolds number; convective component of heat transfer computed from B&W correlation.

6. TWO-PHASE MIXTURE-LEVEL SWELL

This section presents the void-fraction data obtained from the 12 uncovered-bundle mixture-level swell tests. In addition, a critique of commonly used void-fraction models is included.

Six of the twelve tests to be discussed are the same as those used in heat transfer analysis (3.09.10I–N). The remaining six tests were run specifically to obtain void-fraction data (3.09.10AA–FF). In tests 3.09.10AA–FF, only the uppermost 10 to 15% of the bundle was uncovered. As such, most of the bundle was in saturated boiling, thus allowing the maximum amount of void-fraction data to be obtained in a single test. Because the mixture level was so high in the bundle, the tests were not suitable for uncovered-bundle heat transfer analysis.

6.1 Review of Experimental Procedure

The experimental procedure used in the uncovered-bundle tests was designed to allow acquisition of local void-fraction and mixture-level swell data. The test began with preheating of the THTF to the desired test section inlet temperature, reduction of inlet flow to the desired value, and application of bundle power. After a period of stabilization, the test section flow and bundle power were trimmed to place the mixture level at the desired height. Finally, when the system had stabilized and makeup flow was just sufficient to compensate for liquid being vaporized, quasi-steady-state data were taken.

The FRS bundle is instrumented with FRS sheath thermocouples at 25 elevations; most of these thermocouple "levels" are in the upper 30% of the bundle; therefore, the dryout elevation can be determined to within ± 0.08 m in the upper portion of the bundle. Axial void-fraction distributions were determined from the outputs of a set of stacked ΔP cells (Fig. 8).*

6.2 General Theory

Pictured in Fig. 9 is a schematic of a PWR subchannel during the uncovered phase of an SBLOCA. Void distribution was assumed to be radially uniform, and the Z-coordinate axis was taken parallel to the subchannel axis. The subchannel can be divided into three thermal-hydraulic regions: (1) a subcooled inlet region, (2) a saturated boiling region, and (3) a dry (or high-quality) steam-flow region. The subcooled boiling region was assumed to be negligibly small in comparison with the saturated boiling region, since surface heat fluxes typical of reactor decay-heat levels are low.

The zero coordinate was taken to be at Z_{sat} (i.e., $Z_{sat} = 0$), the elevation where saturated boiling begins. Other elevations important in

*PdE-189 failed prior to testing.

the analysis are the two-phase mixture level ($Z_{2\phi}$) and the collapsed-liquid level (Z_{CLL}). The two-phase mixture level, assumed to coincide with the FRS dryout level, is the maximum height above Z_{sat} where liquid is the continuous phase. The collapsed-liquid level is the elevation to which the mixture level would fall if all boiling ceased. Steam velocities in the subject tests were low, causing little or no liquid entrainment. Friction and form-loss pressure drops were negligible; thus, the collapsed-liquid level may also be interpreted as the hydrostatic head of the coolant inventory between Z_{sat} and $Z_{2\phi}$, as measured by the ΔP cells.

The mixture-level swell, defined as

$$S = \frac{Z_{2\phi} - Z_{CLL}}{Z_{CLL}} , \tag{19}$$

is a convenient parameter that interrelates the elevations of interest. Mixture swell is equal to the relative vertical expansion of the boiling length caused by the presence of vapor voids. If the mass inventory M is written in terms of the collapsed-liquid level

$$M = \rho_f A_F Z_{CLL} , \tag{20}$$

then the relationship between the mass inventory, swell, and two-phase mixture level is given by*

$$Z_{2\phi} = \frac{M}{\rho_f A_F} (S + 1) . \tag{21}$$

This formulation is significant because it relates the mass inventory to the elevation where core uncovering occurs. Below the mixture level the core remains in nucleate boiling, and heat transfer is sufficient to prevent thermal damage. In the uncovered region, heat transfer by steam cooling alone may not be sufficient to prevent thermal damage. An assessment of the severity of a hypothetical accident is dependent on the ability to predict the amount of core uncovering that would occur for a given coolant inventory loss; if mixture-level swell and mass inventory are known, the above equation allows this prediction.

The mixture-level swell and the local void fraction [$\alpha(Z)$] are related through the definition of the collapsed-liquid level:

$$Z_{CLL} = \int_0^{Z_{2\phi}} [1 - \alpha(Z)]dZ . \tag{22}$$

---

*To conform to conventional notation, the subscript f refers to saturated liquid, and g refers to saturated vapor.

Substitution of Eq. (22) into Eq. (19) yields the swell expressed as a function of the local void fraction and the mixture level.

As stated earlier, the objective of this analysis was to determine the void-fraction profile and mixture-level swell, and to compare them with the predictions of several local void-fraction models. The models chosen for evaluation were the drift-flux model (DFM) for churn-turbulent flow,[16] the Wilson bubble-rise model,[17] the Yeh empirical void correlation,[18] and the correlations derived by Gardner.[19]

In each of the models examined, the local void fraction can be written as a function of the local quality $[\chi(Z)]$. Because the axial power profile of the THTF is uniform, the quality was assumed to vary linearly from Z_{sat} to $Z_{2\phi}$, taking the values 0 and 1 (respectively) at the endpoints:

$$\chi(Z) = \frac{Z}{Z_{2\phi}} \ . \qquad (23)$$

Changing the independent variable in Eq. (22) from Z to χ yields

$$Z_{2\phi} = Z_{CLL} + Z_{2\phi} \int_0^1 \alpha(\chi) d\chi \ . \qquad (24)$$

Defining

$$I_\rho = \int_0^1 \alpha(\chi) d\chi \ , \qquad (25)$$

and with some algebraic manipulations, one finds that

$$S_\rho = \frac{I_\rho}{1 - I_\rho} \ . \qquad (26)$$

The predicted mixture-level swell S_ρ is independent of the observed collapsed-liquid and two-phase mixture levels. For the DFM and Wilson model, the relationship between the quality and the local void fraction is straightforward, and I_ρ is evaluated analytically. For the Yeh and Gardner correlations, it was easier to evaluate I_ρ numerically, using Simpson's rule.

The models examined are all based on the local volumetric vapor and liquid flux densities (j_g and j_f, respectively), which are dependent on the mass flow rate $\dot{M}$, the saturated water properties, and the local quality:

$$j_g = \frac{\chi(Z)\dot{M}}{\rho_g A_F} , \tag{27}$$

$$j_f = [1 - \chi(Z)] \frac{\dot{M}}{\rho_f A_F} , \tag{28}$$

and

$$j = j_g + j_f . \tag{29}$$

The only variable in any of the model equations that is a function of the position Z is the quality; because of this, the aforementioned change of variables in the model swell calculation is quite simple.

The DFM is the simplest model and is applicable when the relative velocity between phases is significant when compared with the superficial velocity j. The model expresses the local void fraction as

$$\alpha = \frac{j_g}{C_o j + V_{gj}} , \tag{30}$$

where C_o and V_{gj} are generally empirically derived. The specific form of the DFM used in these comparisons has been outlined by Sun in his paper on hydrodynamically controlled dryout.[16] The distribution parameter C_o corrects the void fraction for nonuniform radial effects; the equation used here is recommended for tubes and bundles by Lellouche and Zolotor:[16]

$$C_o = \left[0.82 + 0.18 \left(\frac{P}{P_{cr}}\right)\right]^{-1} . \tag{31}$$

The drift velocity V_{gj} is of the form for churn-turbulent flow:[16]

$$V_{gj} = 1.41 \left[\frac{\sigma g(\rho_f - \rho_g)}{\rho_f^2}\right]^{0.25} . \tag{32}$$

The Wilson bubble-rise model was developed from a series of experiments in which saturated steam was bubbled through columns of saturated water. The experiments were conducted in vessels of 10.2- and 48.3-cm (4.0- and 19-in.) diameters. The resulting correlation is based on the ratio of the Laplace length Σ to the hydraulic diameter D_H, the Froude number Fr, and a density ratio:

$$\alpha = C_1 \left(\frac{\Sigma}{D_H}\right)^{0.19} \left(\frac{\rho_g}{\rho_f - \rho_g}\right)^{0.32} Fr^{C_2} , \tag{33}$$

where

$C_1 = 0.136$ and $C_2 = 0.89$ if $Fr < 30.4$,
$C_1 = 0.75$ and $C_2 = 0.39$ if $Fr \geq 30.4$.

The Froude number was calculated using the Laplace length and the terminal bubble-rise velocity $V_{bub}(\chi)$:

$$Fr = \frac{V_{bub}^2(\chi)}{g\Sigma} , \tag{34}$$

where

$$V_{bub} = \frac{j_g}{\alpha} .$$

The Laplace length is defined as

$$\Sigma = \sqrt{\frac{\sigma}{g(\rho_f - \rho_g)}} . \tag{35}$$

The Yeh void correlation is an empirical model developed from a series of core uncovering experiments run at the Westinghouse Verification Test Facility. Tests were performed in a full-length 480-rod simulated fuel bundle. The dimensions were typical of 15 x 15 fuel assemblies. The tests were conducted at average rod powers from 0.33 to 1.32 kW/m (0.1 to 0.4 kW/ft), and system pressures varied from 0.7 to 2.8 MPa (100 to 400 psia). The correlation is based on the ratios of (1) saturated densities, (2) vapor to total superficial velocity, and (3) vapor superficial velocity to local vapor drift velocity:

$$\alpha = 0.925 \left(\frac{\rho_g}{\rho_f}\right)^{0.239} \left(\frac{j_g}{j}\right)^{0.6} \left(\frac{j_g}{j_{bcr}}\right)^{a} , \tag{36}$$

where

$$a = 0.67 \text{ if } \frac{j_g}{j_{bcr}} < 1.0 ,$$

$$a = 0.47 \text{ if } \frac{j_g}{j_{bcr}} \geq 1.0$$

and

$$j_{bcr} = 1.53 \left(\frac{g\sigma}{\rho_f}\right)^{0.25} . \tag{37}$$

The Gardner void-fraction correlation was developed from the data of several Russian and American experimenters, including Wilson. Gardner examined the data and correlations resulting from void-fraction tests using both water and Freon-12. He found large disparities between the various data sets and produced two correlations to fit as much of the data as possible. His model expresses the void fraction quadratically as a function of the ratio of the superficial velocity to drift velocity (F_d) and a dimensionless function of the water properties (P):

$$\frac{\alpha}{[1 - \alpha]^{0.5}} = C_1 \left(F_d P^{C_2}\right)^{0.67} , \tag{38}$$

where

$C_1 = 11.2$ and $C_2 = 0.30$ for the first correlation,
$C_1 = 1.70$ and $C_2 = 0.16$ for the second correlation;

and

$$F_d = \frac{1.41\ j_g}{V_{gj}} ; \qquad V_{gj} \text{ defined in Eq. (32)} \tag{39}$$

$$P = \left[\left(\frac{g\ \rho_g^2 \nu_f^2}{\sigma^3}\right) (\rho_f - \rho_g)\right]^{0.5} . \tag{40}$$

The second correlation was largely based on data in which the void fraction was determined by ΔP measurement, as was done in this study. The first correlation is primarily based on void fractions derived from gamma-ray density measurements. Gardner does not favor one correlation over the other, but in this case one might expect the second correlation to provide closer agreement than the first. Both correlations were examined; the first is referred to as G1 and the second as G2.

6.3 Data Reduction and Analysis

6.3.1 Two-phase mixture level

The two-phase mixture level was identified by observing the average temperature at the FRS thermocouple levels. The two-phase mixture level $Z_{2\phi}$ was assumed to be midway between the highest level where the average temperature indicated nucleate boiling and the lowest level where the average temperature indicated dryout. Those levels cooled by nucleate boiling had temperatures close to the saturation temperature, and the temperature excursion occurring at the dryout level is large and easily recognized. In the heavily instrumented top section of the bundle, the two-phase mixture level was determined to within ~±8.0 cm (±3.1 in.). If the dryout occurred in the lower two-thirds of the bundle where the thermocouple levels are widely spaced, the uncertainty became as large as ±30 cm (±11.8 in.).

6.3.2 Beginning of saturated boiling

Because the axial power profile of the bundle was uniform, the inlet enthalpy (h_{in}) and the saturated enthalpies (h_f and h_g) were used to locate Z_{sat} with respect to the BOHL (Fig. 9):

$$Z_{sat} = Z_{2-\phi} \left(\frac{h_f - h_{in}}{h_g - h_{in}} \right) , \qquad (41)$$

where both Z_{sat} and $Z_{2-\phi}$ are with respect to the BOHL.

6.3.3 Mass flow and volumetric vapor-generation rate

The volumetric flow was read from one of three instruments. The primary instrument used was FE-18A, a low-flow inlet orifice meter; if FE-18A was out of range, an outlet turbine meter (FE-202) was used. In cases of very low flow, an outlet-orifice flow meter (FE-283) was used. Multiplication by an appropriate density (determined from pressure and local temperature) produced mass flow rates. Because the tests were run under quasi-steady-state conditions, the mass flow rate divided by the saturated steam density is equal to the total volumetric vapor generation rate (VVG). A more general parameter is found when the VVG is divided by the test section flow area A_F. Assuming negligible entrainment, the result is the volumetric vapor superficial velocity at the two-phase mixture level. Past work at ORNL has shown a correlation between vapor superficial velocity at the mixture level and mixture-level swell.[3]

6.3.4 Void fraction

The void-fraction profile was calculated from the readings of the ΔP cells. Assuming negligible friction and form-loss pressure drops, the measured ΔP between the taps of a ΔP cell may be expressed as

$$\Delta P = \rho_{std}\, g h_m = \rho_{ref}\, g h_{ref} - \bar{\rho}\, g h_{ref} \,, \tag{42}$$

where

ρ_{std} = density of standard water,
ρ_{ref} = liquid density in ΔP cell cold-reference leg,
$\bar{\rho}$ = average density of the two-phase mixture between the cell taps,
h_{ref} = pressure tap separation,
h_m = ΔP cell reading in units of height of standard water,
g = local gravitational acceleration.

The average density of the two-phase mixture lying between the cell taps can be defined in terms of the saturated vapor density ρ_g, the saturated liquid density ρ_f, and the volume average void fraction $\bar{\alpha}$:

$$\bar{\rho} = \bar{\alpha}\rho_g + (1 - \bar{\alpha})\rho_f \,. \tag{43}$$

Substituting Eq. (42) into Eq. (43) and solving for the void fraction in terms of measured quantities yields the expression

$$\bar{\alpha} = \frac{\rho_{ref} - \dfrac{h_m}{h_{ref}}\rho_{std} - \rho_f}{(\rho_g - \rho_f)} \,. \tag{44}$$

Note that this void fraction is a volume average. In comparing it with the void fractions predicted by the models, we chose to assign the volume average void fraction to the midpoint between the ΔP cell taps. Fluid conditions used in the evaluation of the model void fractions were also evaluated at this elevation. The test facility had nine working ΔP cells; therefore, nine data points were calculated.

An average void fraction of zero was assigned to cells lying entirely below the saturation level Z_{sat}. The value of one was assigned to a cell if the calculated value exceeded one. For the cell containing the saturation level, an average void fraction was calculated only for the section above the saturation level; the evaluation elevation was thus changed (for plotting and comparison purposes) to the midpoint of the cell's two-phase region.

6.3.5 Collapsed-liquid level

The definition of the collapsed-liquid level was given in Sect. 6.2:

$$Z_{CLL} = \int_0^{Z_{2\phi}} [1 - \alpha(Z)]dZ \ . \tag{22}$$

Because the void fractions were determined as average values for segments along the Z-axis, the integral is replaced by a summation:

$$Z_{CLL} = \sum_{i=LB}^{9} (1 - \bar{\alpha})h_{ref_i} \ , \tag{45}$$

where LB is the number of the lowest ΔP cell with a nonzero average void fraction. For the ΔP cell containing the saturation level, the height above the saturation level is used in place of the full reference height.

6.3.6 Uncertainties

An explanation of how uncertainties were assigned to the derived quantities is given in Appendix C.

6.4 Presentation of Results

6.4.1 Summary of test conditions

Table 6 summarizes the test conditions for each of the 12 mixture-level swell and void distribution tests. For the sake of convenience, the tests can be divided into two pressure groups, one group of six tests run at roughly 4 MPa (580 psia) and another group of six at roughly 7.5 MPa (1088 psia). Henceforth, the data from these test groups will be referred to as the 4-MPa and 7.5-MPa data sets; however, note that considerable variation in pressure exists within each data set.

Experimentally observed two-phase mixture levels also fall into two groups. In tests 3.09.10I–N roughly 25 to 40% of the heated bundle was uncovered, while only 2 to 12% of the bundle was uncovered in tests 3.09.10AA–FF. This is reflective of the fact that tests 3.09.10I–N were

Table 6. Summary of mixture-level swell test conditions[a]

Test	System pressure [MPa (psia)]	Linear power/rod [kW/m (kW/ft)]	Vapor superficial velocity at mixture level [m/s (ft/s)]	Mixture level [m (ft)]	Collapsed-liquid level [m (ft)]	Beginning of boiling length [m (ft)]	Mixture-level swell
3.09.10I	4.50 (650)	2.22 (0.68)	1.30 ± 0.04 (4.25 ± 0.13)	2.62 ± 0.04 (8.60 ± 0.13)	1.34 ± 0.03 (4.39 ± 0.1)	0.36 ± 0.01 (1.18 ± 0.03)	1.30 ± 0.08
3.09.10J	4.20 (610)	1.07 (0.33)	0.61 ± 0.02 (1.99 ± 0.07)	2.47 ± 0.04 (8.10 ± 0.14)	1.62 ± 0.03 (5.31 ± 0.1)	0.27 ± 0.01 (0.89 ± 0.03)	0.63 ± 0.05
3.09.10K	4.01 (580)	0.32 (0.10)	0.15 ± 0.02 (0.50 ± 0.05)	2.13 ± 0.30 (6.98 ± 0.98)	1.62 ± 0.03 (5.31 ± 0.1)	0.28 ± 0.04 (0.92 ± 0.13)	0.38 ± 0.24
3.09.10L	7.52 (1090)	2.17 (0.66)	0.73 ± 0.02 (2.39 ± 0.06)	2.75 ± 0.09 (9.02 ± 0.29)	1.76 ± 0.03 (5.77 ± 0.1)	0.69 ± 0.02 (2.26 ± 0.07)	0.93 ± 0.12
3.09.10M	6.96 (1010)	1.02 (0.31)	0.37 ± 0.01 (1.20 ± 0.03)	2.62 ± 0.04 (8.60 ± 0.13)	1.89 ± 0.03 (6.20 ± 0.1)	0.55 ± 0.01 (1.80 ± 0.03)	0.54 ± 0.05
3.09.10N	7.08 (1030)	0.47 (0.14)	0.12 ± 0.01 (0.40 ± 0.04)	2.13 ± 0.03 (6.98 ± 0.98)	1.86 ± 0.03 (6.10 ± 0.1)	0.46 ± 0.07 (1.51 ± 0.23)	0.20 ± 0.24
3.09.10AA	4.04 (590)	1.27 (0.39)	1.04 ± 0.03 (3.40 ± 0.10)	3.42 ± 0.03 (11.23 ± 0.09)	2.00 ± 0.03 (6.56 ± 0.1)	0.56 ± 0.02 (1.84 ± 0.07)	0.98 ± 0.04
3.09.10BB	3.86 (560)	0.64 (0.20)	0.48 ± 0.02 (1.59 ± 0.07)	3.31 ± 0.04 (10.85 ± 0.12)	2.32 ± 0.03 (7.61 ± 0.1)	0.48 ± 0.02 (1.57 ± 0.07)	0.53 ± 0.03
3.09.10CC	3.59 (520)	0.33 (0.10)	0.40 ± 0.02 (1.31 ± 0.07)	3.60 ± 0.02 (11.80 ± 0.08)	2.88 ± 0.03 (9.45 ± 0.1)	0.41 ± 0.02 (1.34 ± 0.07)	0.29 ± 0.02
3.09.10DD	8.09 (1170)	1.29 (0.39)	0.46 ± 0.01 (1.50 ± 0.03)	3.23 ± 0.04 (10.61 ± 0.13)	2.39 ± 0.03 (7.84 ± 0.1)	0.90 ± 0.02 (2.95 ± 0.07)	0.57 ± 0.04
3.09.10EE	7.71 (1120)	0.64 (0.19)	0.27 ± 0.01 (0.88 ± 0.03)	3.47 ± 0.03 (11.40 ± 0.08)	2.85 ± 0.03 (9.35 ± 0.1)	0.92 ± 0.02 (3.02 ± 0.07)	0.32 ± 0.03
3.09.10FF	7.53 (1090)	0.32 (0.98)	0.12 ± 0.01 (0.40 ± 0.03)	3.23 ± 0.04 (10.61 ± 0.13)	2.90 ± 0.03 (9.51 ± 0.1)	0.86 ± 0.02 (2.82 ± 0.07)	0.16 ± 0.03

[a]Some rounding off of numbers has been done. Accordingly, conversions between metric and English and value of mixture-level swell may not appear to be exact.

run primarily to obtain heat transfer data. Thus, uncovering as much of the bundle as possible without exceeding peak temperature limits was desirable. In tests 3.09.10AA–FF high clad temperatures were not an objective. Accordingly, only the uppermost portion of the bundle was uncovered. This allowed for accurate determination of mixture level and, because of the close spacing of ΔP cells in the upper section of the bundle, better resolution of the axial void-fraction profile.

6.4.2 Void fraction profiles

Figures 42–53 present the experimentally derived void-fraction profiles overlaid with profiles computed from the four models discussed in Sect. 6.2. Note that error bars appear only on the experimentally derived void fractions, because the uncertainties in model-predicted void

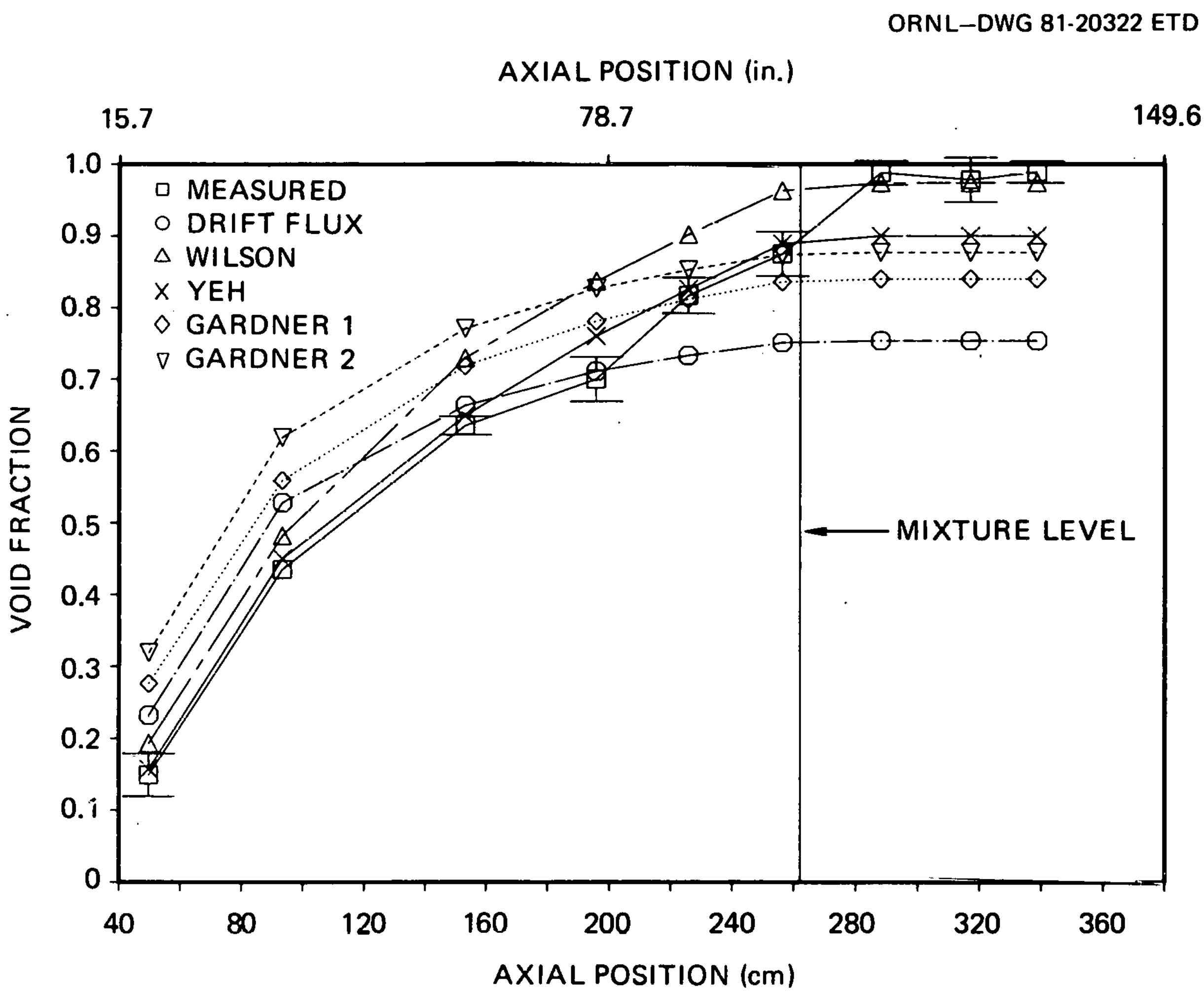

Fig. 42. Experimental and predicted void fraction profiles; test 3.09.10I.

ORNL—DWG 81-20323 ETD

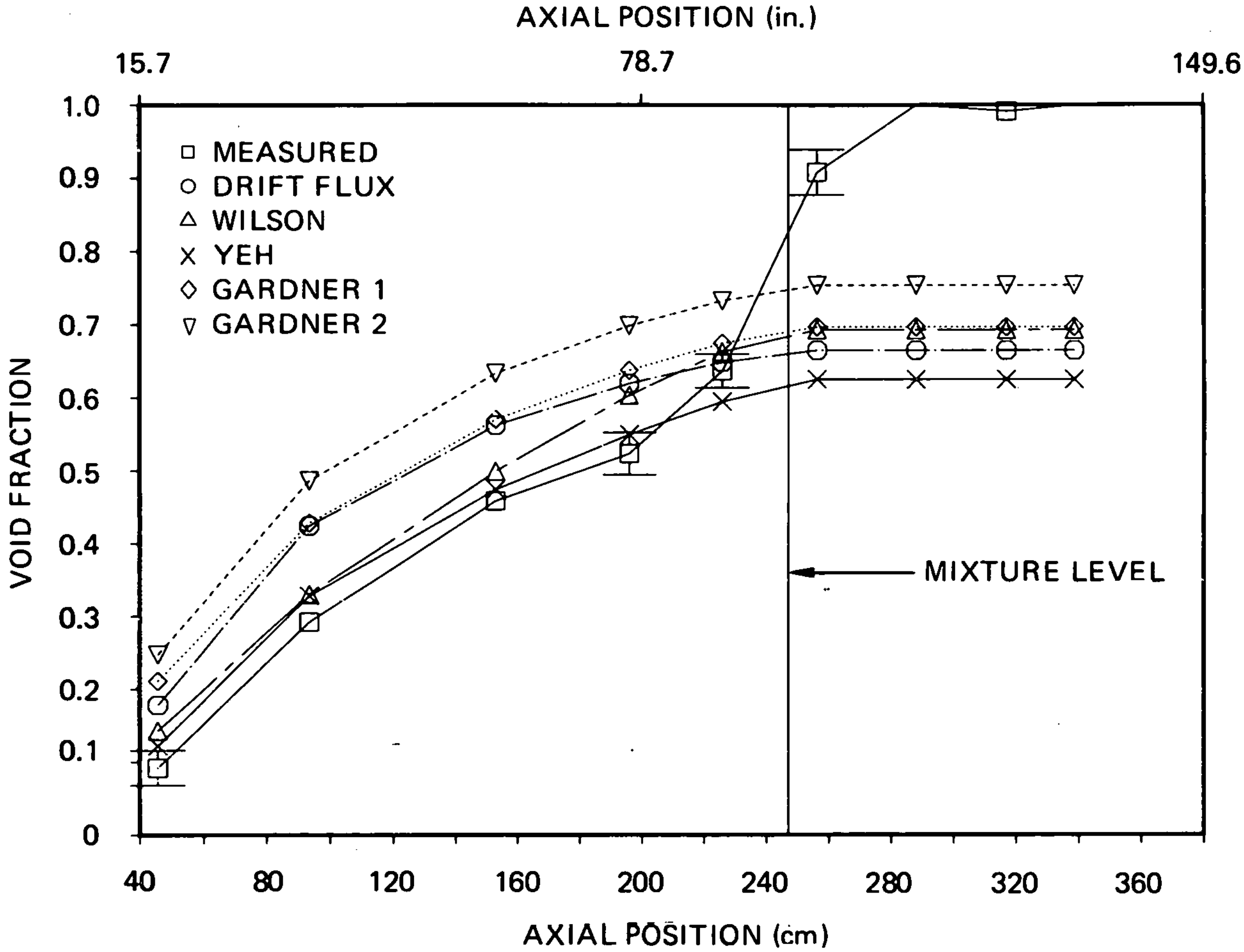

Fig. 43. Experimental and predicted void fraction profiles; test 3.09.10J.

fractions were negligible in comparison with the experimental uncertainties. If error bars do not appear on experimentally derived void fractions, then the uncertainty was smaller than the boundaries of the symbol used to denote void fraction. Also, note that if small measurement uncertainties caused the experimentally derived void fraction to be negative or greater than 1.0, then the void fraction was set to 0.0 or 1.0, respectively. Appendix D contains a detailed listing of the data appearing in Figs. 42–53.

Most of the experimental void profiles show several commonalities and parametric trends. All of the experimental profiles show very low or zero void fraction near the bottom of the heated length. This was expected because fluid in the lower portion of the bundle was either subcooled or of low quality. Void fraction then increased with elevation in a relatively linear or slightly parabolic manner. Slope of the void profile varied considerably from test to test with the steepest slopes associated with the highest volumetric vapor-generation rate tests. Finally,

ORNL–DWG 81-20324 ETD

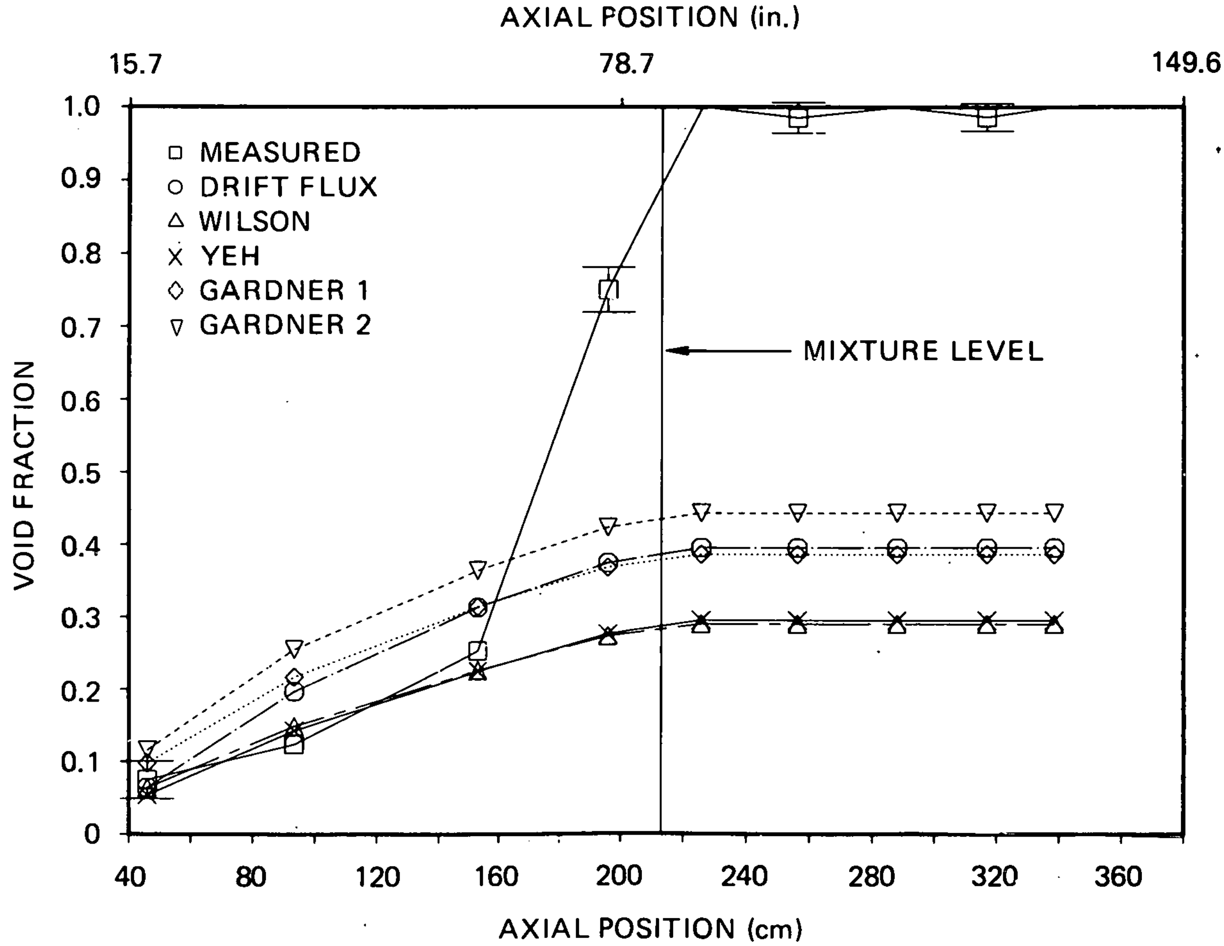

Fig. 44. Experimental and predicted void fraction profiles; test 3.09.10K.

at a location near the two-phase mixture level, a sharp increase in void fraction with elevation occurred. In this region void fraction rapidly approached 1.0, and FRS dryout occurred.

This "transition-to-dryout" region was well-defined in the lowest volumetric vapor-generation rate tests. This is evident in Fig. 53 where void fraction changed from roughly 0.3 to 1.0 over 50 cm (19.7 in.), which is quite an abrupt change when one considers that in the same test void fraction increased from 0 to 0.3 over 260 cm (103 in.). In higher vapor-generation rate tests the transition to dryout was not as distinct. In fact, in test 3.09.10I (Fig. 42) the transition region was hardly noticeable.

It also seems evident that the void fraction where transition to dryout occurred is dependent on volumetric vapor-generation rate. Figures 42–44 represent a series of tests at roughly constant pressure and varying volumetric vapor-generation rate. Test 3.09.10I (Fig. 42), with

ORNL–DWG 81-20325 ETD

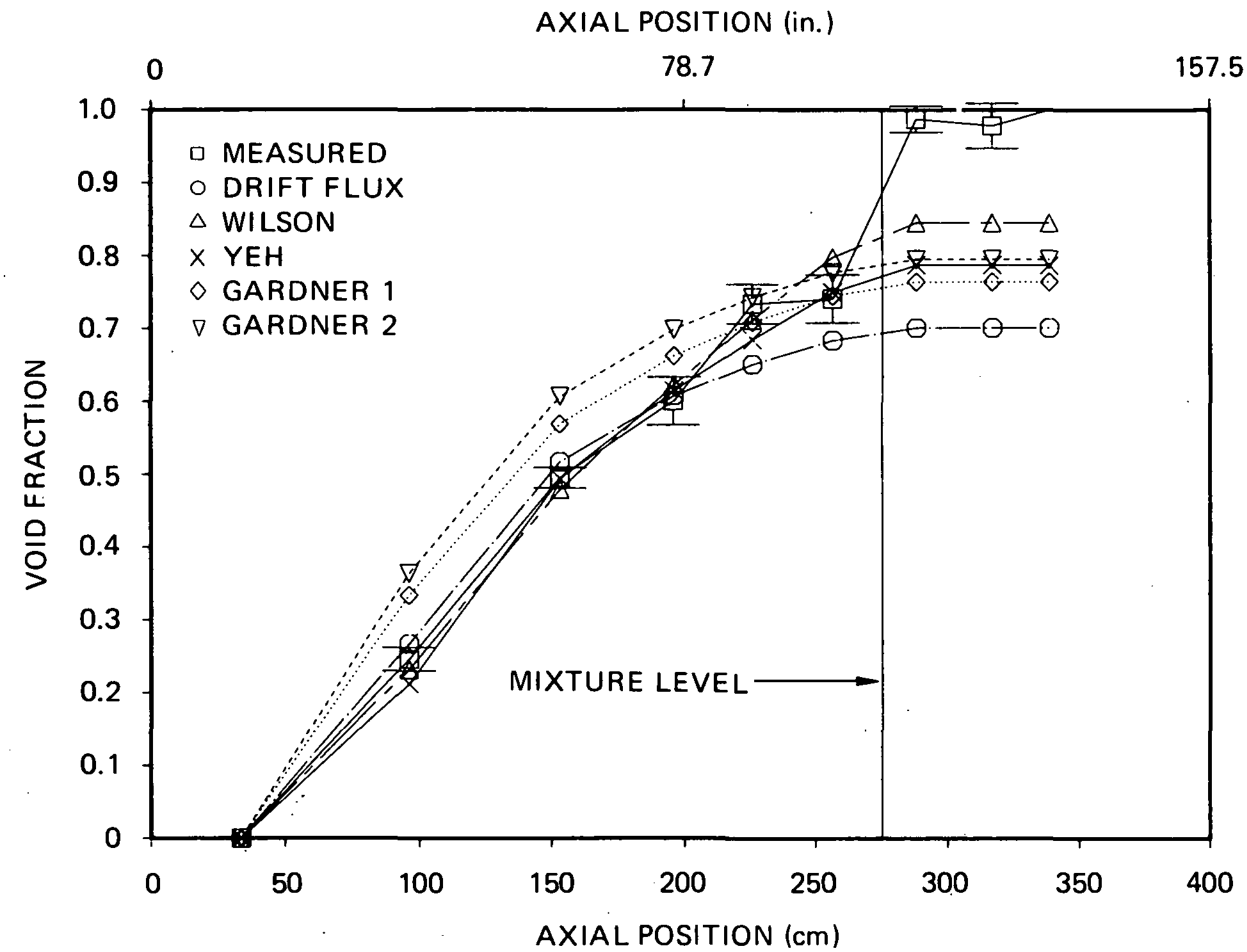

Fig. 45. Experimental and predicted void fraction profiles; test 3.09.10L.

the highest vapor-generation rate, did not show transition to dryout until a void fraction of roughly 0.85 had been reached. On the other hand, test 3.09.10K (Fig. 44), with the lowest vapor-generation rate, underwent transition to dryout at a void fraction of roughly 25%. This dependence can be predicted by a simple DFM.

The DFM expresses local void fraction as

$$\alpha = \frac{j_g}{C_o j + V_{gj}} \; . \tag{46}$$

In the subject tests j_ℓ is small as compared with j_g over most of the heated length. Accordingly, j can be approximated as j_g. The vapor

ORNL–DWG 81-20326 ETD

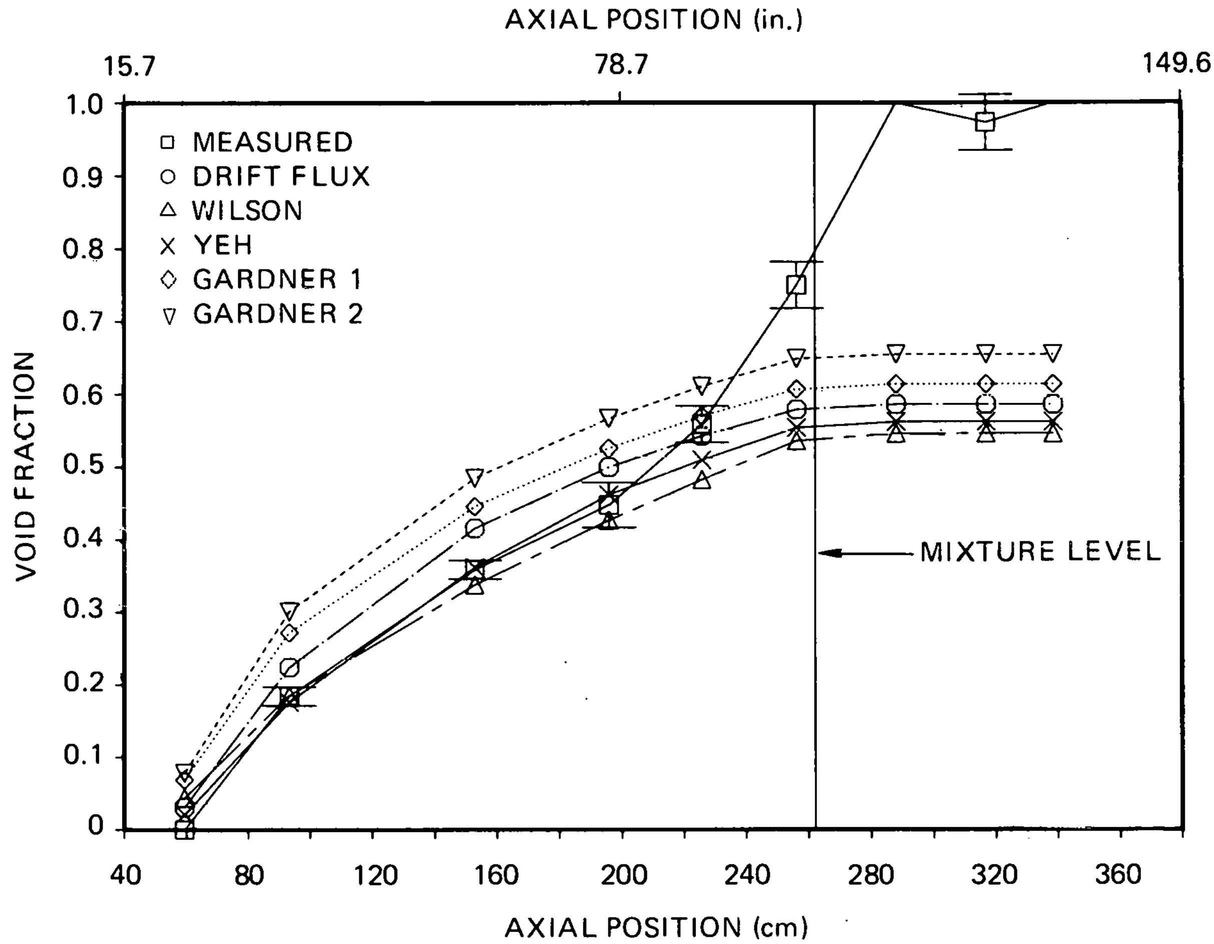

Fig. 46. Experimental and predicted void fraction profiles; test 3.09.10M.

superficial velocity can be written in terms of local quality X and the vapor superficial velocity evaluated at the two-phase mixture level $j_{2-\phi}$, such that $j_g = Xj_{2-\phi}$. Finally, Eq. (46) can be rewritten as

$$\alpha = \frac{\alpha_o}{C_o + V_{gj}/Xj_{2-\phi}} , \qquad (47)$$

where the no-slip void fraction α_o is j_g/j. If the assumption is made that for constant pressure C_o and V_{gj} are constant, then the maximum value of α is a function only of $j_{2-\phi}$. The superficial velocity at the mixture level is simply the volumetric vapor-generation rate/unit flow area. Therefore, for roughly constant pressure and a given flow regime,

ORNL–DWG 81-20327 ETD

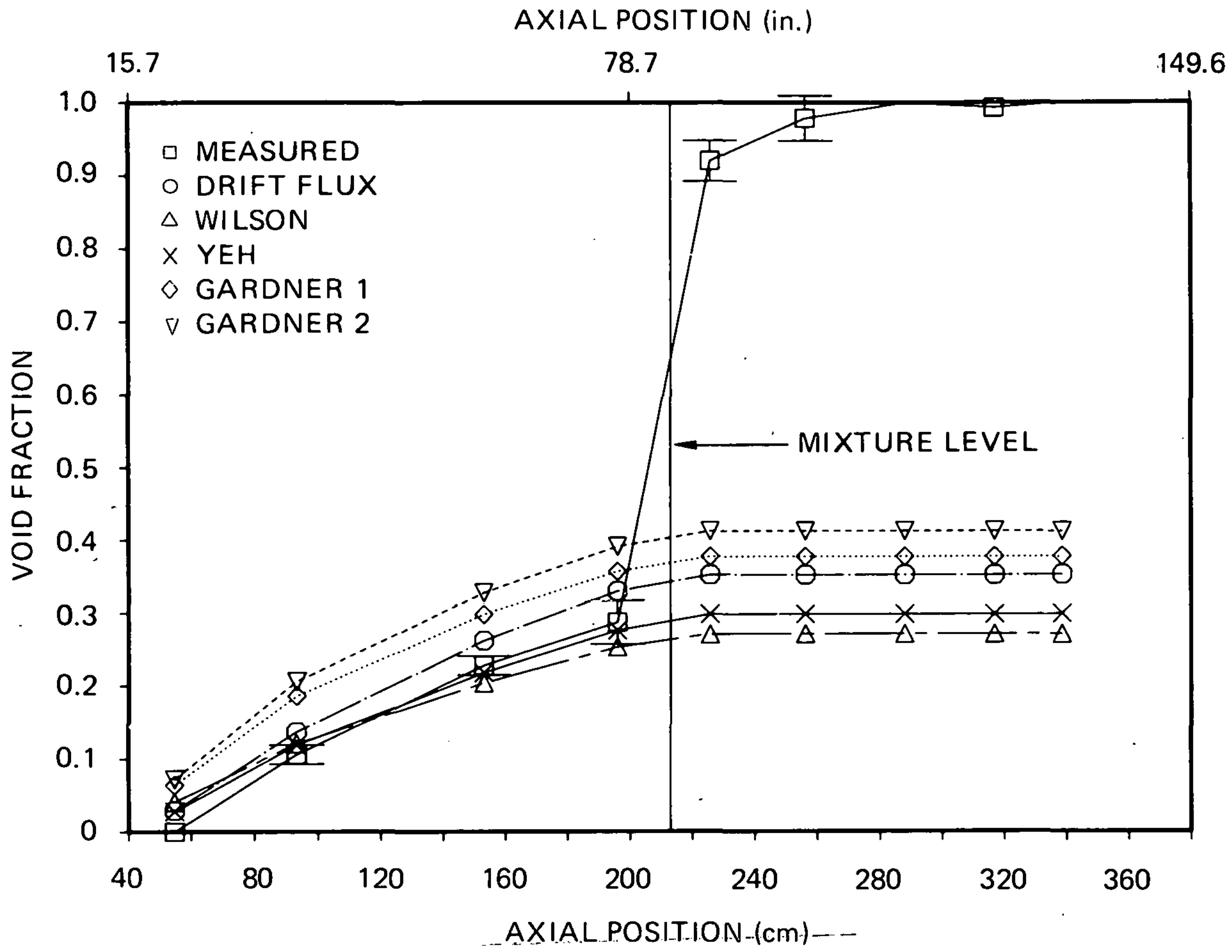

Fig. 47. Experimental and predicted void fraction profiles; test 3.09.10N.

the maximum void fraction increases with increasing volumetric vapor-generation rate. The only way to exceed the maximum is for C_o and V_{gj} to change, which implies a change in flow regime. As the liquid-vapor interface is approached, the void fraction must go to 1.0; therefore, a flow regime transition occurs. If $j_{2-\phi} \gg V_{gj}$ and C_o is close to 1.0, then the transition can occur at $\alpha \approx \alpha_o \approx 1.0$, and the transition-to-dryout region is not well-defined (Fig. 42). On the other hand, if $j_{2-\phi} < V_{gj}$, then the transition occurs at $\alpha < 1.0$, and the transition-to-dryout region can be quite distinct (Fig. 44).

The five local void-fraction models showed wide variance in their ability to predict the experimental data. Both of the Gardner correlations consistently overpredicted the data by a considerable margin. As a result, the Gardner correlations should probably not be used to predict local void fraction under conditions typical of these tests. The DFM for churn-turbulent flow predicted the data somewhat better than the Gardner

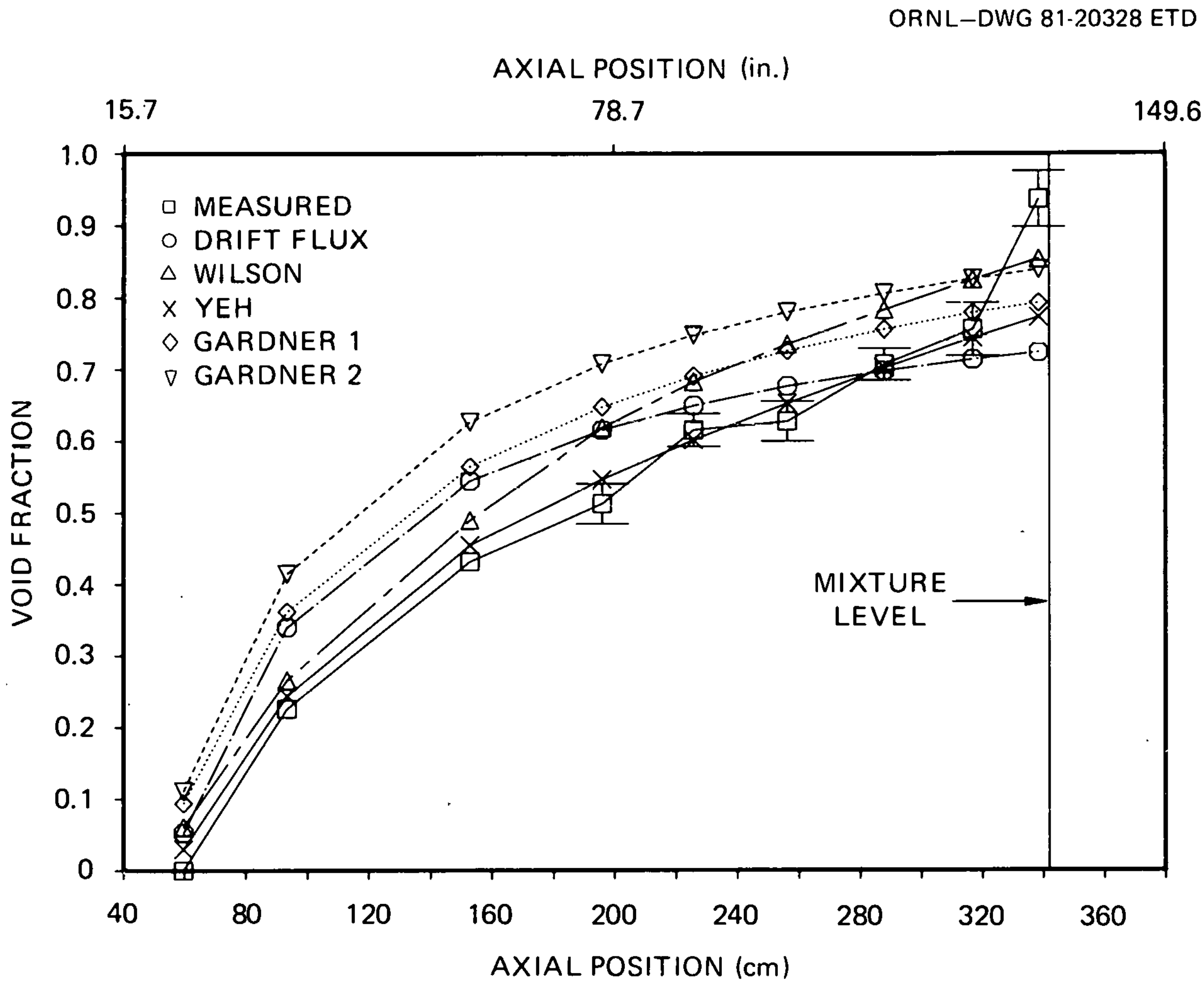

Fig. 48. Experimental and predicted void fraction profiles; test 3.09.10AA.

models. However, in several tests, the DFM consistently overpredicted void fraction near the bottom of the bundle and underpredicted the void fraction at higher elevations (Fig. 42). This implies that the value of V_{gj} that was used was too low, and C_o was too high. The models that appear best suited for use under the subject test conditions are the Wilson bubble-rise model and the Yeh void correlation. Of these two, the Yeh void correlation consistently provided the most accurate predictions. A quantitative distinction between the models will be made in Sect. 6.4.3. As might be expected, none of the correlations accurately predicted void fraction in the immediate vicinity of the mixture level.

Finally, all of the void fraction models in test 3.09.10CC overpredicted the data by a substantial margin (Fig. 50). In addition, the transition-to-dryout region was not evident, because the mixture level was well above the uppermost functioning ΔP cell tap. Consequently, the transition-to-dryout region was above the uppermost tap and could not be

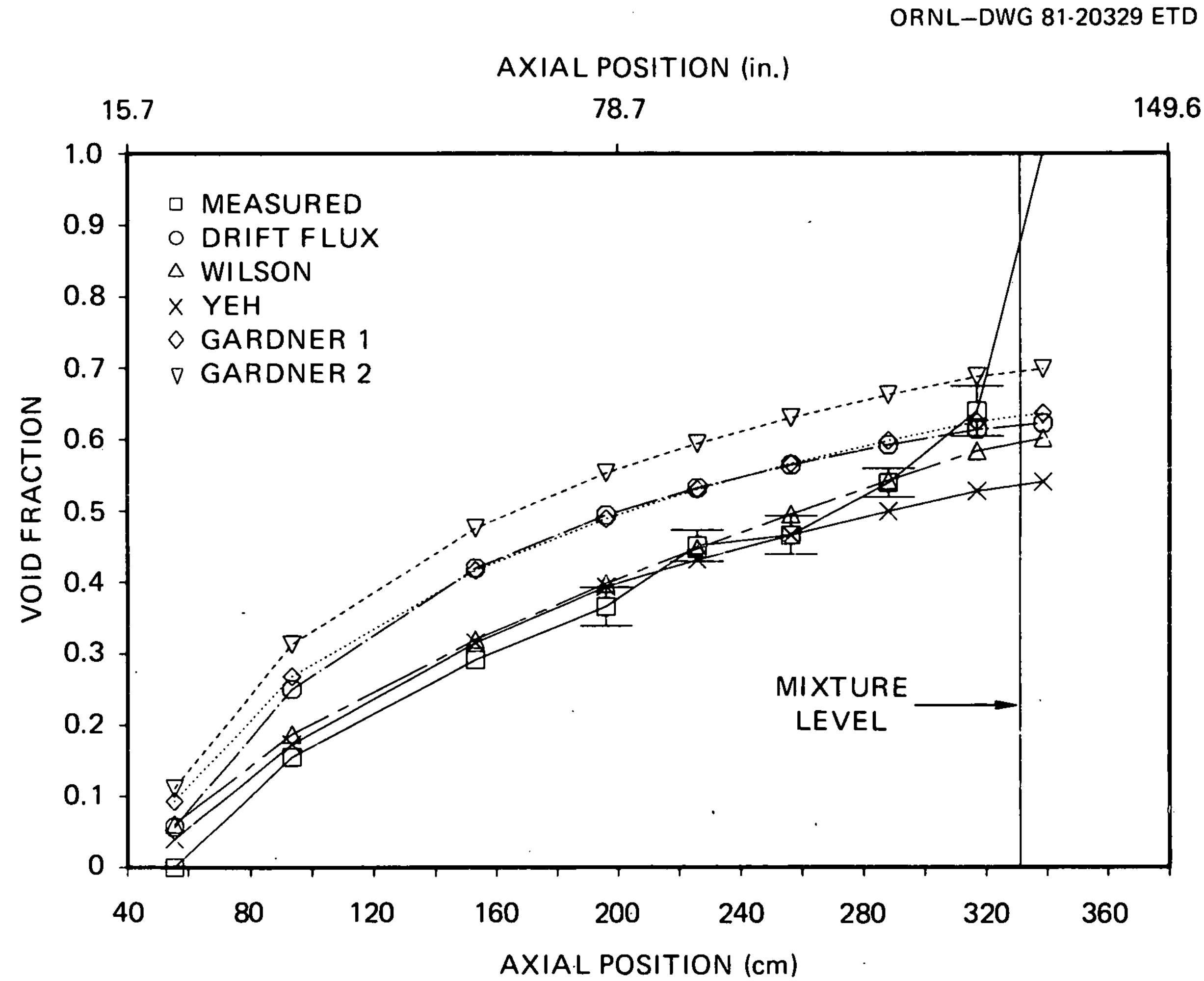

Fig. 49. Experimental and predicted void fraction profiles; test 3.09.10BB.

seen. The reason for the consistent overprediction of void fraction is not as clear. However, our suspicion is that, because the dryout elevation was so close to the EOHL, liquid was being discharged from the test section outlet. Because the calculation of vapor-generation rate assumed that all liquid was vaporized in the test section, the superficial velocities input to the predictive models would be too high, and an overprediction would result. Unfortunately, this cannot be confirmed because the test section outlet temperature remained slightly superheated throughout the test. This implies that, if liquid was discharged, then flow in the horizontal outlet pipe must have been stratified. The reason is that the outlet steam thermocouple was mounted at the pipe centerline; thus, if the outlet flow were dispersed, the thermocouple would quench. Given the uncertainties associated with test 3.09.10CC, disregarding the poor comparisons between the predictive models and data may be advisable.

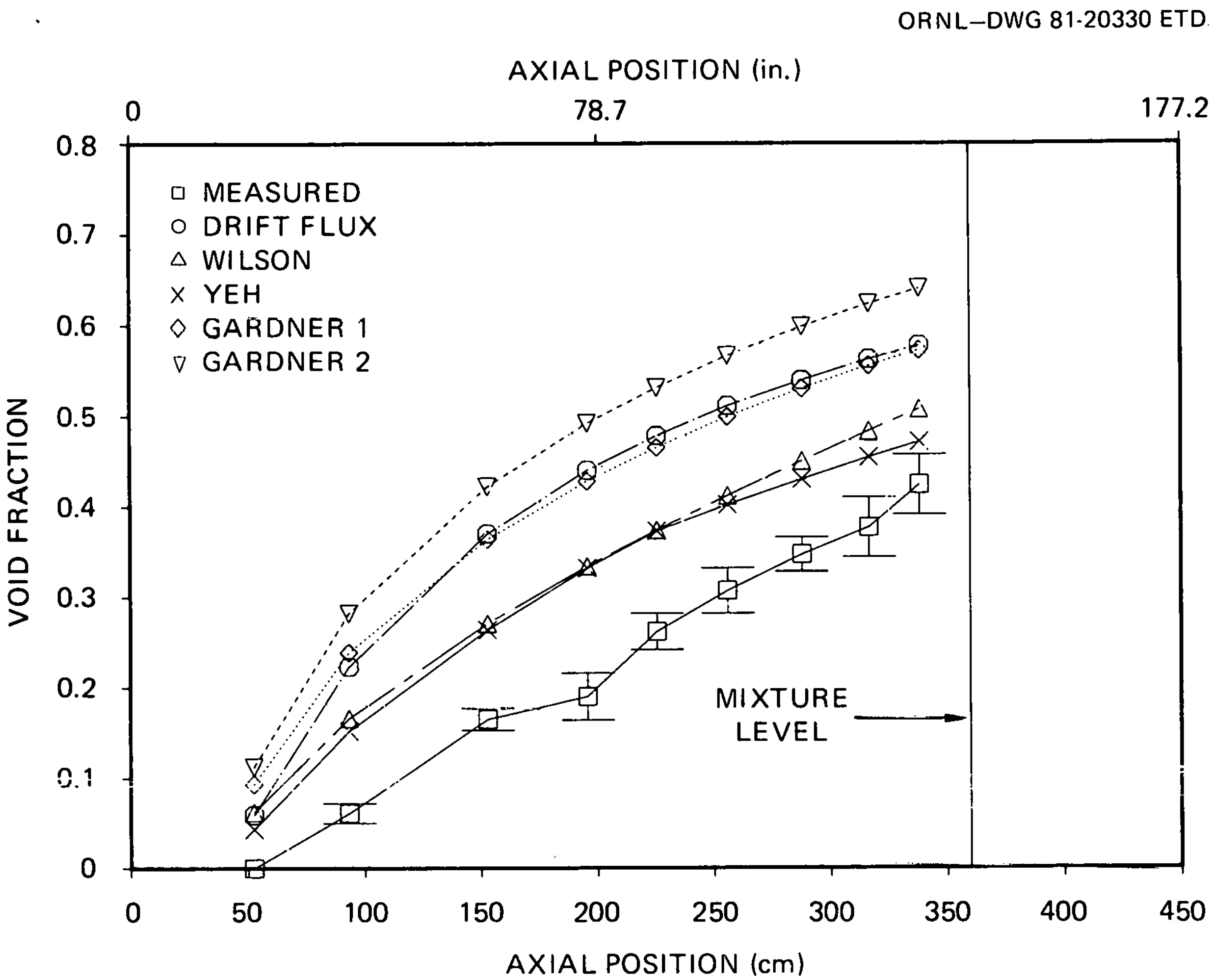

Fig. 50. Experimental and predicted void fraction profiles; test 3.09.10CC.

6.4.3 Comparisons between experimental and predicted mixture level

In the previous section four models were evaluated for their ability to predict experimentally derived void profiles under high-pressure low heat-flux conditions. In this section, selected correlations are evaluated for their ability to predict experimentally observed mixture levels. The predicted mixture levels were formulated in terms of local void fraction and experimentally derived collapsed-liquid level:

$$Z_{2-\phi_p} = Z_{CLL}(1 + S_p) = \frac{Z_{CLL}}{1 - I_p} , \quad (48)$$

ORNL–DWG 81-20331 ETD

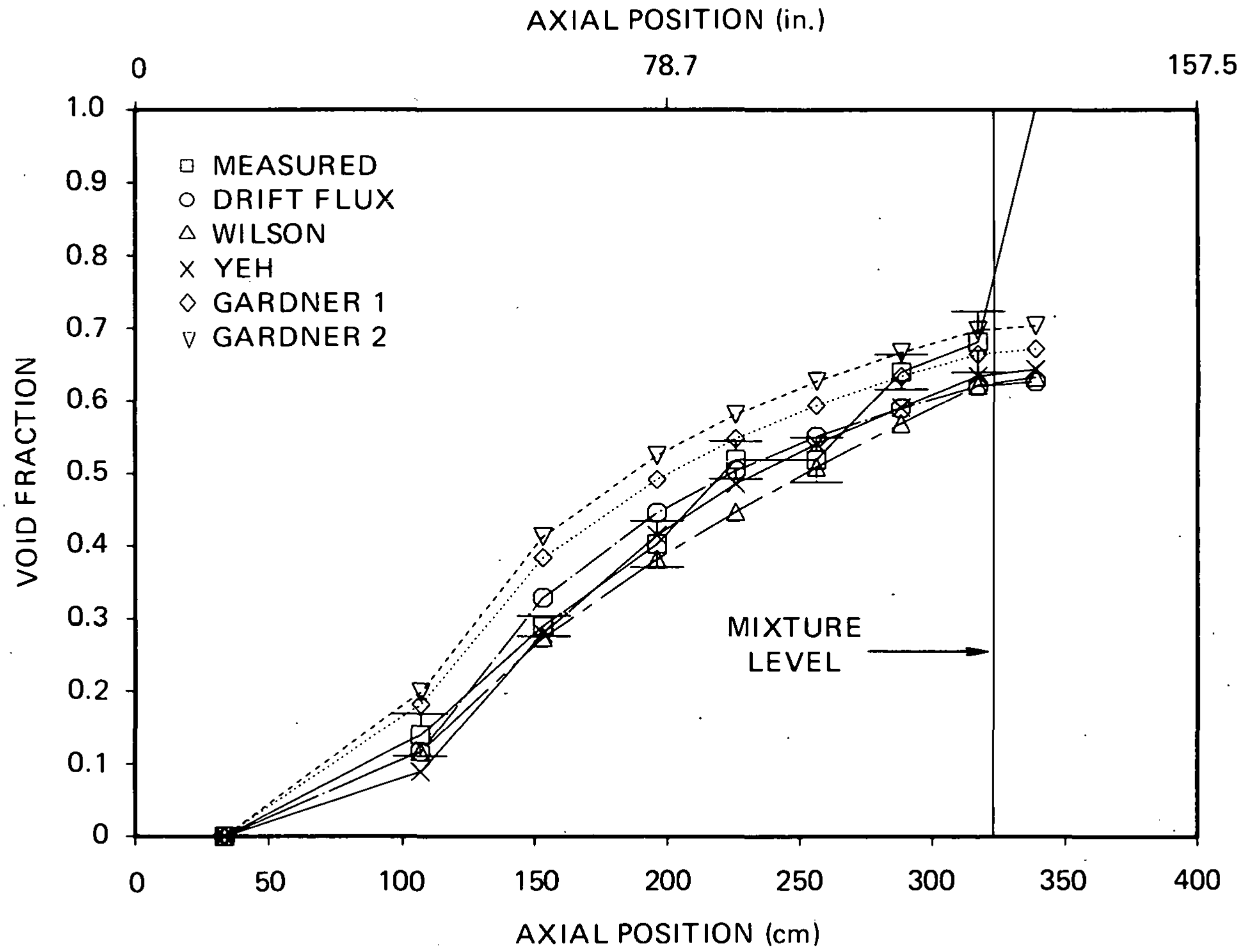

Fig. 51. Experimental and predicted void fraction profiles; test 3.09.10DD.

where

$$I_p = \int_0^1 \alpha(X)dX.$$

Tables 7 and 8 present the results of the comparisons for the 4- and 7.5-MPa data sets, respectively. Note that the Gardner correlations were not evaluated, because they consistently overpredicted the local void fractions. Several points concerning the format of the tables bear mention. First, the mixture levels appearing in the tables are in reference to the BOHL rather than the beginning of bulk boiling. Second, deviations from experimentally determined mixture levels are presented in terms of actual deviations, in centimeters or inches, and in terms of percent

Table 7(a). Comparisons of predicted to experimentally determined mixture level, 4-MPa data set

Test	Vapor superficial velocity at mixture level (m/s)	Mixture level (m)	Deviations from experimental (cm/%)		
			Yeh	Drift flux	Wilson
3.09.10I	1.30 ± 0.04	2.62 ± 0.04	14.68/6.49	14.68/6.49	56.62/25.04
3.09.10J	0.61 ± 0.02	2.47 ± 0.04	7.90/3.61	40.22/18.37	19.49/8.90
3.09.10K	0.15 ± 0.02	2.13 ± 0.30	−18.29/−9.92	−4.68/−2.54	−17.66/−9.58
3.09.10AA	1.04 ± 0.03	3.42 ± 0.03	1.37/0.48	31.49/11.00	39.36/13.75
3.09.10BB	0.48 ± 0.02	3.31 ± 0.04	−3.64/−1.28	39.68/14.01	5.29/1.87
3.09.10CC	0.40 ± 0.02	3.60 ± 0.02	32.37/10.17	87.04/27.35	39.92/12.55
Standard error[a,b]			11.19/5.57	29.74/11.86	33.09/14.07

[a]Standard errors defined as

$$SE = \sqrt{\frac{\sum_{i=1}^{N} (Z_{2-\phi_p} - Z_{2-\phi})_i^2}{N}} \quad \text{and} \quad \sqrt{\frac{\sum_{i=1}^{N} [(Z_{2-\phi_p} - Z_{2-\phi})/(Z_{2-\phi} - Z_{sat})]_i^2}{N}}$$

[b]Test 3.09.10CC excluded from standard error for reasons discussed in Sect. 6.4.2.

Table 7(b). Comparisons of predicted to experimentally determined mixture level, 4-MPa data set

Test	Vapor superficial velocity at mixture level (ft/s)	Mixture level (ft)	Deviations from experimental (in./%)		
			Yeh	Drift flux	Wilson
3.09.10I	4.25 ± 0.13	8.60 ± 0.13	5.78/6.49	5.78/6.49	22.29/25.04
3.09.10J	1.99 ± 0.07	8.10 ± 0.14	3.11/3.61	15.84/18.37	7.67/8.90
3.09.10K	0.50 ± 0.05	6.98 ± 0.98	−7.20/−9.92	−1.84/−2.54	−6.95/−9.58
3.09.10AA	3.40 ± 0.10	11.23 ± 0.09	0.54/0.48	12.40/11.00	15.50/13.75
3.09.10BB	1.59 ± 0.07	10.85 ± 0.12	−1.43/−1.28	15.62/14.01	2.08/1.87
3.09.10CC	1.31 ± 0.07	11.80 ± 0.08	12.74/10.17	34.27/27.35	15.72/12.55
Standard error[a,b]			4.41/5.57	11.71/11.86	13.03/14.07

[a]Standard errors defined as

$$SE = \sqrt{\frac{\sum_{i=1}^{N} (Z_{2-\phi_p} - Z_{2-\phi})_i^2}{N}} \quad \text{and} \quad \sqrt{\frac{\sum_{i=1}^{N} [(Z_{2-\phi_p} - Z_{2-\phi})/(Z_{2-\phi} - Z_{sat})]_i^2}{N}}$$

[b]Test 3.09.10CC excluded from standard error for reasons discussed in Sect. 6.4.2.

Table 8(a). Comparisons of predicted to experimentally determined mixture level, 7.5-MPa data set

Test	Vapor superficial velocity at mixture level (m/s)	Mixture level (m)	Deviations from experimental (cm/%) Yeh	Drift flux	Wilson
3.09.10L	0.73 ± 0.02	2.75 ± 0.09	−6.32/−3.06	−6.05/−2.93	−0.55/−0.27
3.09.10M	0.37 ± 0.01	2.62 ± 0.04	−4.98/−2.41	8.65/4.18	−9.17/−4.44
3.09.10N	0.12 ± 0.01	2.13 ± 0.30	1.06/0.64	7.87/4.73	−0.21/−0.13
3.09.10DD	0.46 ± 0.01	3.23 ± 0.04	−5.50/−2.35	2.91/1.25	−11.32/−4.85
3.09.10EE	0.27 ± 0.01	3.47 ± 0.03	−0.69/−0.27	12.51/4.89	−7.64/−2.99
3.09.10FF	0.12 ± 0.01	3.23 ± 0.04	−4.20/−1.77	4.20/1.77	−6.14/−2.59
Standard error[a]			4.36/2.01	7.70/3.58	7.17/3.14

[a]Standard errors defined as

$$SE = \sqrt{\frac{\sum_{i=1}^{N} (Z_{2-\phi_p} - Z_{2-\phi})_i^2}{N}} \text{ and } \sqrt{\frac{\sum_{i=1}^{N} [(Z_{2-\phi_p} - Z_{2-\phi})/(Z_{2-\phi} - Z_{sat})]_i^2}{N}}$$

Table 8(b). Comparisons of predicted to experimentally determined mixture level, 7.5-MPa data set

Test	Vapor superficial velocity at mixture level (ft/s)	Mixture level (ft)	Deviations from experimental (in./%) Yeh	Drift flux	Wilson
3.09.10L	2.39 ± 0.06	9.02 ± 0.29	−2.49/−3.06	−2.38/−2.93	−0.22/−0.27
3.09.10M	1.20 ± 0.03	8.60 ± 0.13	−1.96/−2.41	3.41/4.18	−3.61/−4.44
3.09.10N	0.40 ± 0.04	6.98 ± 0.98	0.42/0.64	3.10/4.73	−0.08/−0.13
3.09.10DD	1.50 ± 0.03	10.61 ± 0.13	−2.16/−2.35	1.15/1.25	−4.46/−4.85
3.09.10EE	0.88 ± 0.03	11.40 ± 0.08	−0.27/−0.27	4.92/4.89	−3.01/−2.99
3.09.10FF	0.40 ± 0.03	10.61 ± 0.13	−1.65/−1.77	1.65/1.77	−2.42/−2.59
Standard error[a]			1.72/2.01	3.03/3.58	2.83/3.14

[a]Standard errors defined as

$$SE = \sqrt{\frac{\sum_{i=1}^{N} (Z_{2-\phi_p} - Z_{2-\phi})_i^2}{N}} \text{ and } \sqrt{\frac{\sum_{i=1}^{N} [(Z_{2-\phi_p} - Z_{2-\phi})/(Z_{2-\phi} - Z_{sat})]_i^2}{N}}$$

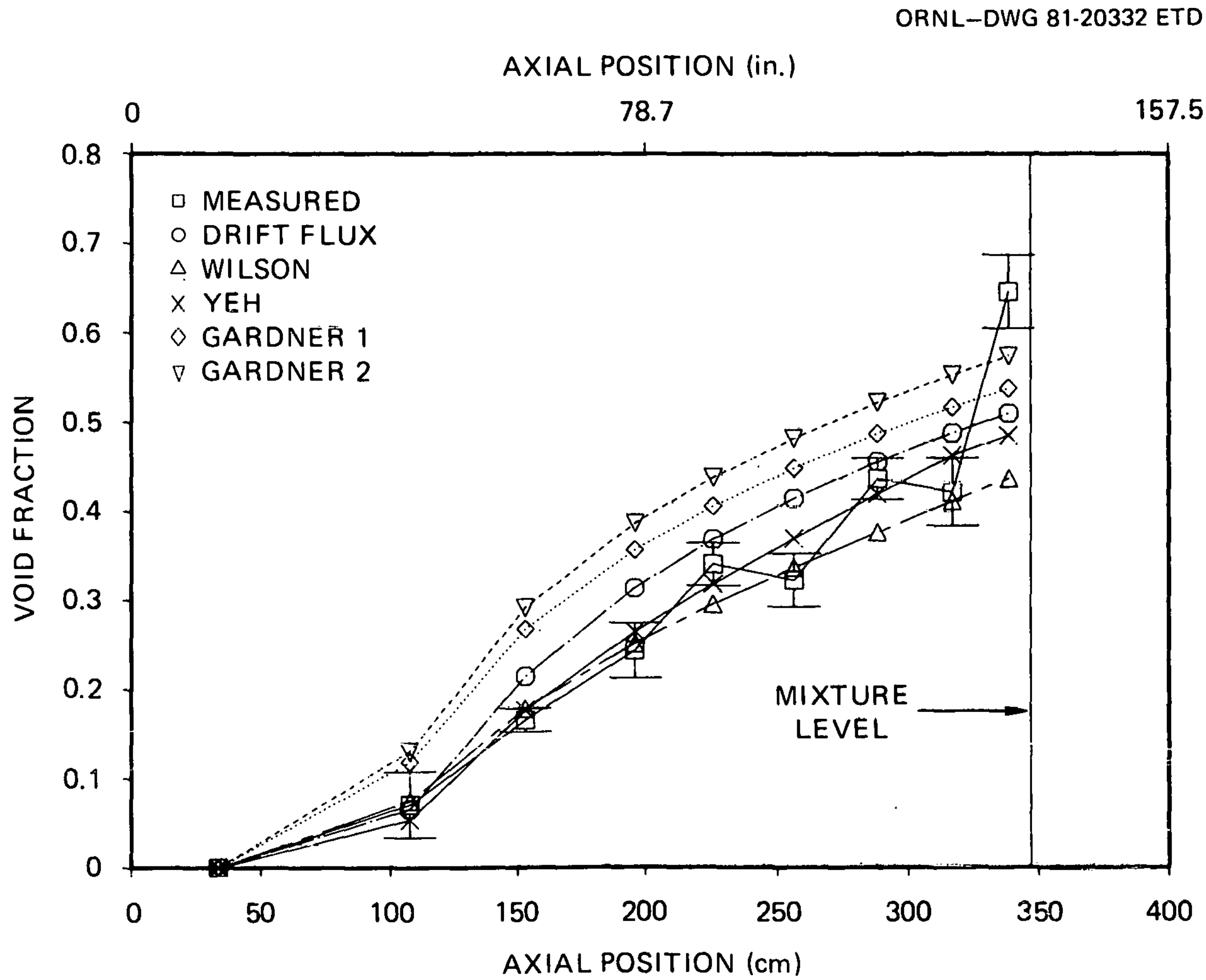

Fig. 52. Experimental and predicted void fraction profiles; test 3.09.10EE.

deviations. The percentage deviation was formulated as*

$$D = 100X \frac{Z_{2-\phi_p} - Z_{2-\phi}}{Z_{2-\phi} - Z_{sat}} \; . \qquad (49)$$

Finally, each table is presented in two versions, one using metric units and the other using English.

---

*The percentage deviations are with respect to the boiling length ($Z_{2-\phi} - Z_{sat}$). This is appropriate, because the subject correlations are used to predict boiling length rather than the sum of boiling length and Z_{sat}.

ORNL–DWG 81-20333 ETD

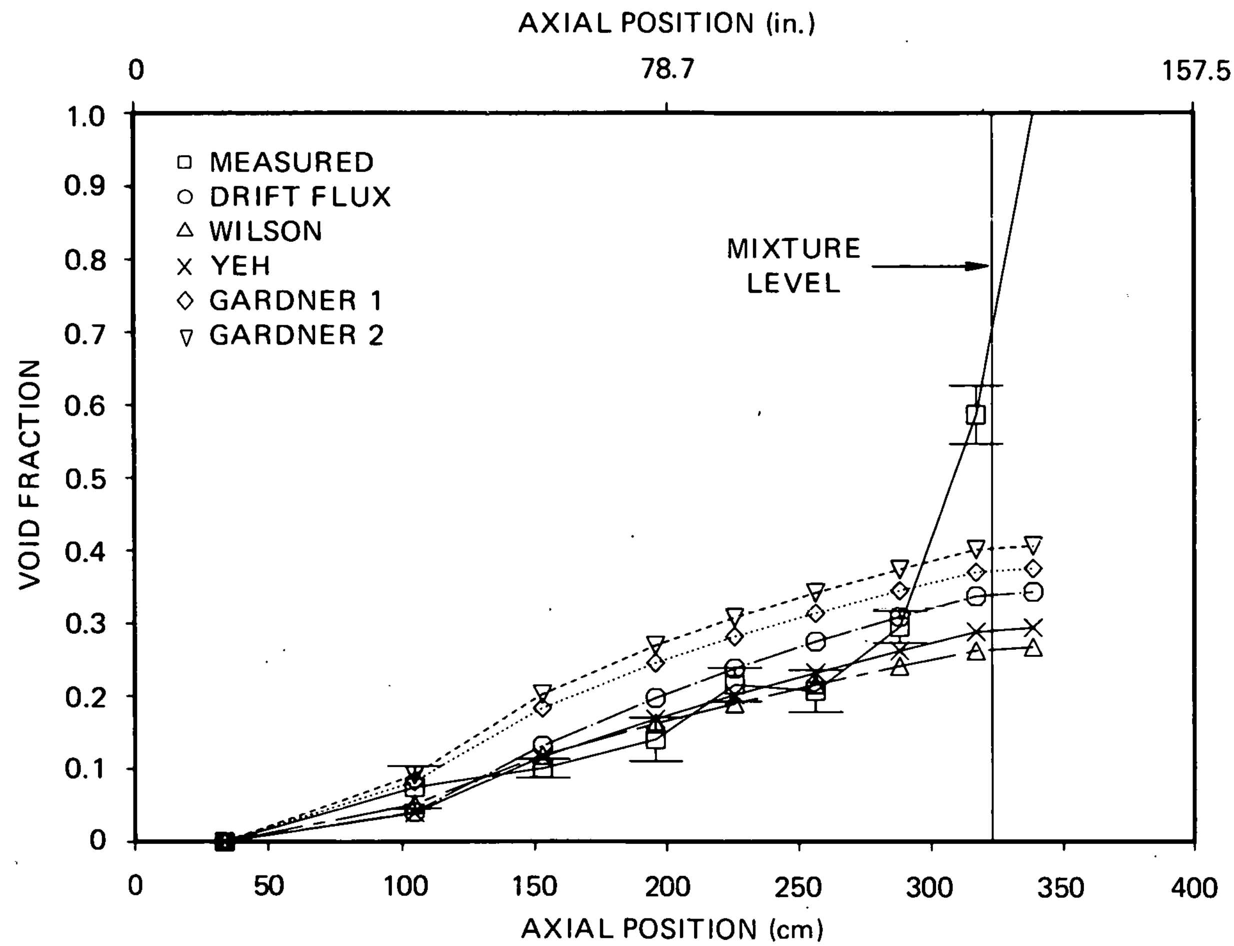

Fig. 53. Experimental and predicted void fraction profiles; test 3.09.10FF.

Of the correlations examined, the Yeh void correlation is clearly the best suited for use under conditions typical of these tests. This correlation predicts mixture level with a standard error of roughly 7% in the 4-MPa data set and 2% in the 7.5-MPa data set. The superior performance of the Yeh correlation might be expected, because it was the only correlation developed from experiments with heat addition and tests that were run in rod bundle geometry.

6.4.4 Two-phase mixture-level swell

The experimentally derived mixture-level swell is plotted against the superficial vapor velocity at the mixture level for the 7.5- and 4-MPa data sets in Figs. 54 and 55. As was reported previously,[20] mixture-level swell depends linearly on the total volumetric vapor-generation rate.*

---

*Vapor superficial velocity at mixture level is total volumetric vapor generation rate divided by flow area.

ORNL–DWG 81-20334 ETD

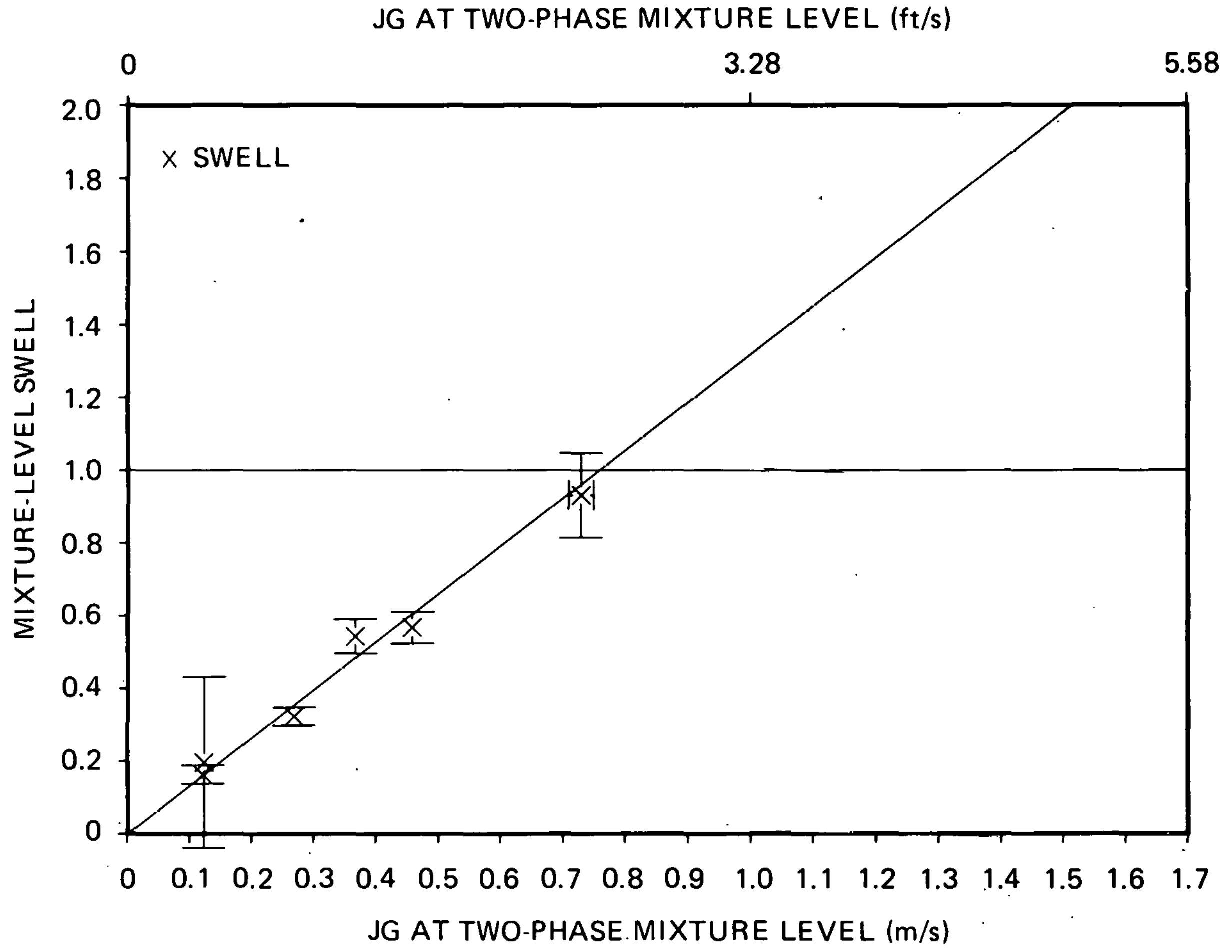

Fig. 54. Mixture level swell vs vapor superficial velocity at mixture level; 7.5 MPa data set (line represents $S = 1.32\ j_{2-\phi}$).

Least-squares fits performed on the data sets yielded the following equations:

$$S = 1.04\ j_{2-\phi} \qquad \text{(4 MPa set)} \tag{50}$$

and

$$S = 1.32\ j_{2-\phi} \qquad \text{(7.5 MPa set)}\ , \tag{51}$$

where the constraint $S = 0$ at $j_{2-\phi} = 0$ has been imposed and where $j_{2-\phi}$ is in m/s. The larger slope associated with the 7.5-MPa data set implies a decreasing drift-velocity with increasing pressure.

ORNL–DWG 81-20335 ETD

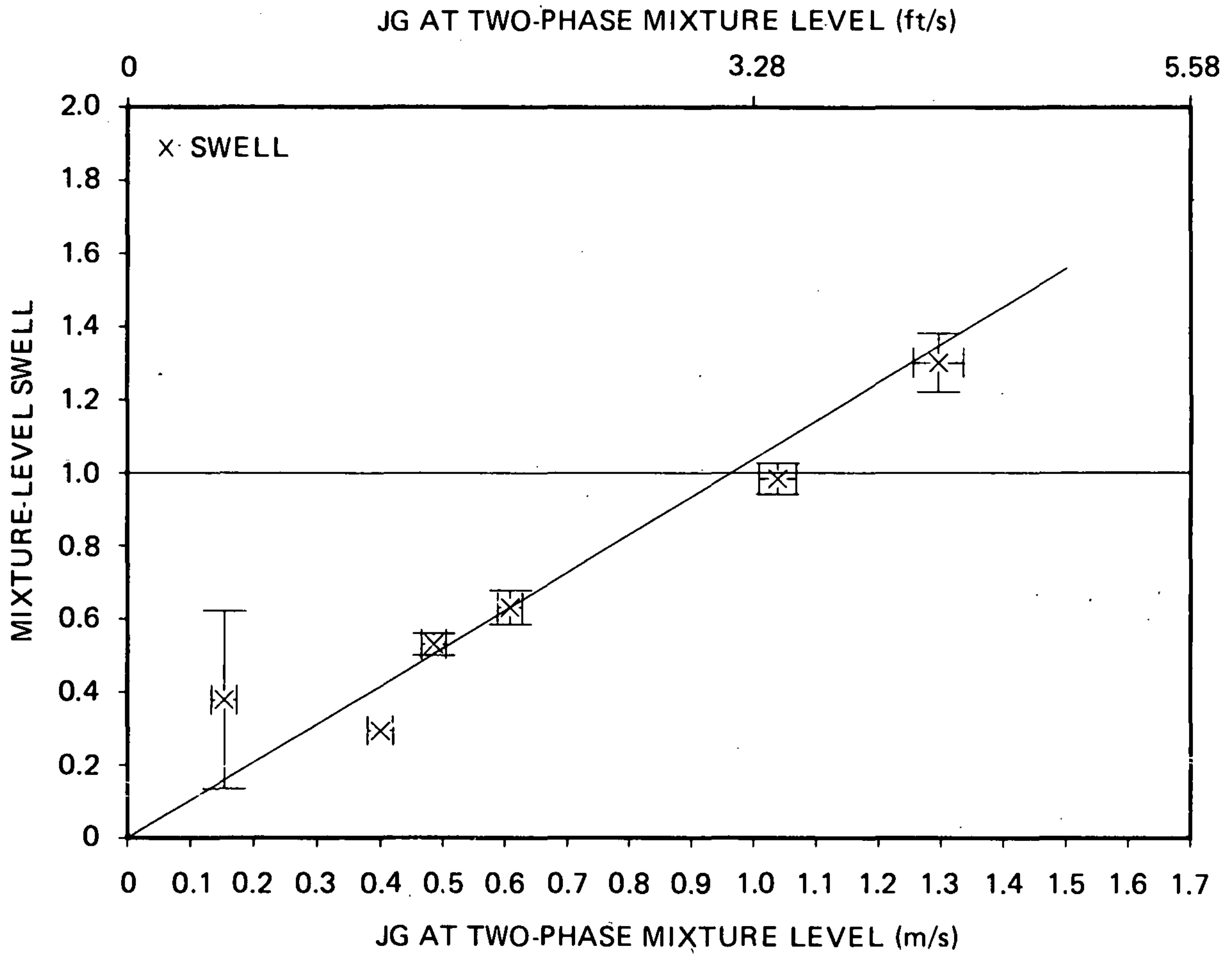

Fig. 55. Mixture level swell vs vapor superficial velocity at mixture level; 4.0 MPa data set (line represents $S = 1.04\ j_{2-\phi}$).

7. SUMMARY

A total of 12 uncovered-bundle heat transfer tests have been run in the THTF: 6 tests in January 1980 and 6 in November 1980. The tests spanned a range of linear power levels from 0.32 to 2.22 kW/m·rod (0.1 to 0.68 kW/ft·rod). Test pressures ranged from 2.6 to 7.5 MPa (375 to 1090 psia), and bundle mass fluxes varied from 3.0 to 29.7 kg/m²·s (2800 to 21,900 lb_m/h·ft²).

An extensive body of high-temperature low-flow steam-cooling data was generated. Peak cladding temperatures in excess of 1050 K (1430°F) and vapor temperatures in excess of 940 K (1250°F) were recorded. Vapor Reynolds numbers ranged from a low of 1100 to a high of 17,700. Under these conditions total heat transfer coefficients varied from 0.0045 to 0.037 W/cm²·K (8 to 65 Btu/h·ft²·°F). The lowest heat transfer coefficients were associated with the lowest flow and linear power test.

Spacer grids were observed to substantially increase heat transfer at, and downstream of, the grid. The effect was most pronounced in the high-flow tests. In the highest-flow test the heat transfer coefficient at the grid midplane was increased by more than 60% over the location 8.2 cm (3.2 in.) upstream. In many cases substantial enhancement of heat transfer occurred when the vapor was dry and highly superheated. This implies that heat transfer enhancement is not a result of desuperheating of the vapor by contact with a wet spacer.

Radiation to high-pressure steam was calculated to account for a significant fraction of the total heat transfer. This was found to be particularly true in low-flow tests where up to 65% of the heat transfer may be caused by thermal radiation.

A number of heat transfer correlations were assessed. The recommendation is that, for modified wall Reynolds numbers from 2000 to 10,000, the following correlation be used:

$$h = h_{conv} + h_{rad} ,$$

$$h_{conv} = \frac{0.021\, k_w}{D_H} Re_{mw}^{0.8}\, Pr_w^{0.4} ,$$

and

$$h_{rad} = \frac{\varepsilon' \sigma (T_w^4 - T_v^4)}{T_w - T_v} + h_{rad_{CR}} ,$$

where

$$Re_{mw} = \left(\frac{GD}{\mu_w}\right)\left(\frac{\rho_w}{\rho_v}\right)$$

and

$$\varepsilon' = \left[\frac{1}{\varepsilon_w} + \frac{1}{\varepsilon_v(T_w)} - 1\right]^{-1} .$$

The term $h_{rad_{CR}}$ accounts for radiation-to-unheated-structure and should be calculated independently for the geometry of interest. The subject correlation predicted the data to within a standard error of 11%.

For modified wall Reynolds numbers less than 2000, a best-estimate correlation cannot yet be recommended. Large variations in convective heat transfer have been observed at Reynolds numbers typical of laminar forced convection. This may indicate that, at low flow, transitions between laminar forced convection and mixed-convection regimes are possible. A constant Nusselt* number of 4.0 appears to be a lower bound to the low-flow data.

A total of 12 tests, all run in November 1980, were used for two-phase mixture-level swell and void-fraction analyses. The analyses showed that the relative expansion of the boiling length caused by the presence of vapor voids (mixture-level swell) was linearly dependent on the total volumetric vapor-generation rate. The minimum mixture swell observed in these tests was roughly 20%.

The data base generated was used to critique a number of commonly used local void-fraction models. Comparisons between sample void profiles and predictive models showed that the Yeh void correlation was best suited for use under conditions typical of the subject tests. Comparisons were made between experimentally determined mixture levels and those calculated from predictive models based on local void correlations. Again, the determination was made that, of the correlations examined, the Yeh correlation is best suited to uncovered-bundle analyses. Standard error in Yeh-correlation-predicted mixture levels at high pressure [7.5 MPa (1090 psia)] was 4.4 cm (1.7 in.); at lower pressure [4 MPa (580 psia)] standard error was 11.2 cm (4.4 in.).

---

*Vapor conductivity evaluated at heated surface temperature.

REFERENCES

1. T. M. Anklam, *ORNL Small-Break LOCA Heat Transfer Test Series I: Rod Bundle Heat Transfer Analysis*, ORNL/NUREG/TM-445 (August 1981).

2. T. M. Anklam, *ORNL Small-Break LOCA Heat Transfer Test Series I: High-Pressure Reflood Analysis*, ORNL/NUREG/TM-446 (August 1981).

3. T. M. Anklam, *ORNL Small-Break LOCA Heat Transfer Test Series I: Two-Phase Mixture Level Swell Results*, ORNL/NUREG/TM-447 (August 1981).

4. C. R. Hyman, T. M. Anklam, and M. D. White, *Experimental Investigations of Bundle Boiloff and Reflood Under High Pressure, Low Heat Flux Conditions*, ORNL 5846 (to be published).

5. D. K. Felde et al., *Facility Description — Thermal Hydraulic Test Facility (THTF) MOD3 — ORNL PWR Blowdown Heat Transfer Separate Effects Program*, ORNL/TM-7842 (to be published).

6. R. Viskanta and K. Mohanty, *TMI-2 Accident: Postulated Heat Transfer Mechanisms and Available Data Base*, NUREG/CR-2121, ANL-81-26 (April 1981).

7. B. Metais and E. R. G. Eckert, "Forced, Mixed, and Free Convection Regimes," *J. Heat Transfer* 86, 295 (May 1964).

8. D. M. McEligot et al., "Internal Low Reynolds Number Turbulent and Transitional Gas Flow with Heat Transfer," *J. Heat Transfer* 88, 239–45 (May 1966).

9. S. Wong and L. E. Hochreiter, *Analysis of the FLECHT SEASET Unblocked Bundle Steam Cooling and Boiloff Tests*, WCAP-9729 (January 1981).

10. H. C. Yeh et al., "Heat Transfer Above the Two-Phase Mixture Level Under Core Uncovering Conditions," pp. 4–31 in *Proceedings of the ANS Specialists Meeting on Small-Break Loss-of-Coolant Accident Analyses in LWRs, Monterey, Calif., August 25–27, 1981.*

11. J. B. Heineman, *An Experimental Investigation of Heat Transfer to Superheated Steam in Round and Rectangular Channels*, ANL-6213 (September 1960).

12. L. S. Tong and J. Weisman, "Thermal Analysis of Pressurized Water Reactors," p. 312, 2nd Ed., *American Nuclear Society*, LaGrange Park, Illinois, 1979.

13. C. B. Ludwig and C. C. Ferriso, "Prediction of Total Emissivity of Nitrogen Broadened and Self-Broadened Hot Water Vapor," *J. Quant. Spectrosec. Radiat. Transfer* 7, pp. 7–26, 1967.

14. G. L. Shires et al., An Experimental Study of Level Swell in a Partially Water Filled Fuel Cluster, *Nuclear Energy* 19, 381–88 (October 1980).

15. S. C. Yao et al., Heat Transfer Augmentation in Rod Bundles Near Grid Spacers, ASME Paper 80-WA/HT-62.

16. K. H. Sun et al., *The Prediction of Two-Phase Mixture Level and Hydrodynamically-Controlled Dryout Under Low Flow Conditions*, EPRI NP-1359-SR (Special Report) (March 1980).

17. J. F. Wilson, R. T. Grenda, and J. F. Patterson, The Velocity of Rising Steam in a Bubbling Two-Phase Mixture, *Trans. Am. Nucl. Soc.* 5, 151–52 (1962).

18. H. C. Yeh and J. P. Cunningham, Experiments and Void Correlation for PWR Small-Break LOCA Conditions, *Trans. Am. Nucl. Soc.* 17, 369 (1973).

19. G. C. Gardner, Fractional Vapour Content of a Liquid Pool Through Which Vapour is Bubbled, *Int. J. Multiphase Flow* 6, 399–410 (1980).

20. T. M. Anklam and M. D. White, "Experimental Investigations of Two-Phase Mixture Level Swell and Axial Void Fraction Distribution Under High Pressure, Low Heat Flux Conditions in Rod Bundle Geometry," pp. 4–67 in *Proceedings of the ANS Specialists Meeting on Small Break Loss-of-Coolant Accident Analyses in LWRs, Monterey, Calif., August 25–27, 1981.*

Appendix A

ANALYTICAL METHODOLOGY

This appendix presents the methodology used to compute the heat transfer coefficients and local fluid conditions that appear in Sect. 5 and Appendix B.

A.1 FRS Surface Temperature

The FRS surface temperature is formulated as a cross-sectional average,

$$T_{w_i} = \frac{\sum_{j=1}^{n} T_{w_{ij}}}{n} \; . \qquad \text{(A.1)}$$

The index i refers to the i'th elevation in the bundle that is instrumented with FRS sheath thermocouples (Fig. 4), and the index j refers to the j'th sheath thermocouple at elevation i. The average is restricted to FRS's at least one row removed from the unheated-bundle shroud; this was done to minimize perturbations in surface temperature caused by proximity to the relatively cold shroud wall. The total number of thermocouples considered in the average, n, varies considerably with elevation. Primary thermocouple levels may have as many as 28 thermocouples, while the intermediate levels may have as few as one. Because of the limited number of FRS thermocouples at the intermediate levels, heat transfer coefficients calculated at these elevations should be considered approximate.

Uncertainty in FRS surface temperature is formulated as

$$\Delta T_{w_i} = \sqrt{\frac{\sum_{j=1}^{n} (T_{w_i} - T_{w_{ij}})^2}{n}} \; . \qquad \text{(A.2)}$$

Errors associated with individual thermocouples are negligible in comparison with variations from the mean. Note that at intermediate thermocouple levels n may be too small to make ΔT_{w_i} a reliable indicator of uncertainty in thermocouple-level average temperature.

A.2 System Pressure

System pressure was experimentally determined from a pressure transducer in the test section upper plenum. The uncertainty in pressure is dominated by the uncertainty associated with the pressure transducer, ~207 kPa (30 psi).

A.3 Mass Flux

As noted in Sect. 5, heat transfer calculations were restricted to elevations where the rod bundle was determined to have been in dry steam cooling. It was therefore possible, assuming quasi-steady state, to compute the vapor mass flux from the measured test section outlet flow:

$$G = \frac{\dot{Q}_{outlet}\, \rho_v(P,\, T_{outlet})}{A_F} \, . \tag{A.3}$$

Note that in all of the subject tests the test section outlet flow was superheated steam; therefore, density was evaluated from measured pressure and steam temperature.

The outlet volumetric flow was measured by two instruments. For volumetric flows greater than 1265 cm^3/s (20 gpm), flow was measured with a 5.1-cm (2-in.) tungsten carbide-bearing turbine meter. At flows lower than 1262 cm^3/s (20 gpm), a 1.27-cm (0.5-in.) low-flow orifice meter was used. The uncertainty in the turbine meter output was 4.1% of output. Uncertainty in the orifice meter output was 54 cm^3/s (0.85 gpm). The uncertainty in vapor density was computed by propagating uncertainties in pressure and outlet temperature through the properties search.*

A.4 Heat Flux

The FRS surface heat flux is based on the square of the data-scan average FRS current and the temperature-dependent Inconel heater resistance:

$$q''_{net} = \frac{(\bar{I})^2\, r}{\pi\, D_{FRS}\, L_{FRS}} - q''_{heat\text{-}up} \, . \tag{A.4}$$

---

*Appendix C contains a discussion of the methodology used in uncertainty calculations.

Strictly speaking, the current term should be the data-scan average of the square of the current. However, the current is generally quite stable in the subject tests; therefore, substitution of the square of the average current is reasonable and considerably easier from a data management standpoint. The resistance per unit length of the heater, r/L_{FRS}, has been experimentally measured for THTF FRS's. The resulting curve fits were

$$r/L_{FRS} = [0.6062 + (3.833 \times 10^{-5})\ T]/12.05$$

for

$$T_{FRS} \leq 700\ K\ (800°F)\ ;$$

$$r/L_{FRS} = [0.7279 - (2.662 \times 10^{-4})\ T + (1.903 \times 10^{-7})\ T^2]/12.05$$

for

$$700\ K\ (800°F) < T_{FRS} \leq 772\ K\ (930°F)\ ;$$

$$r/L_{FRS} = [-0.2712 + (2.398 \times 10^{-3})\ T - (2.074 \times 10^{-6})\ T^2 + (5.963 \times 10^{-10})\ T^3]/12.05$$

for

$$772\ K\ (930°F) < T_{FRS} \leq 866\ K\ (1100°F)\ ;$$

$$r/L_{FRS} = 0.054$$

for

$$866\ K\ (1100°F) < T_{FRS} \leq 1005\ K\ (1350°F)\ ;$$

and

$$r/L_{FRS} = [0.7362 - 1.332 \times 10^{-4}\ T + 5.195 \times 10^{-8}\ T^2]/12.05$$

for

$$1005\ K\ (1350°F) < T_{FRS} \leq 1366\ K\ (2000°F)\ ,$$

where r/L_{FRS} is in Ω/ft and T_{FRS} is in °F.

The last term on the right hand side of Eq. (A.4) is a correction for transient heat-up or cooldown of the FRS's:*

$$q''_{heat-up} = \frac{(C_p\ V\rho')_{FRS}}{\pi\ D_{FRS}} \left(\frac{dT_w}{dt}\right) . \qquad (A.5)$$

*Correction for transient heat-up or cooldown was, in most cases, less than 10% of steady-state heat flux.

Note that $(C_p V\rho)'_{FRS}$ represents the heat capacity/length of FRS. Also, the assumption was made that the heat-up rate of a sheath thermocouple, dT_w/dt, is representative of the heat-up rate for an entire FRS cross section. This was justified because of the low heat-up rates experimentally observed. Axial conduction was negligible for the majority of axial locations and thus was ignored. However, FRS thermocouple level G is quite close to the EOHL, and axial conduction may be significant at this elevation. Axial conduction is estimated to cause the experimentally determined heat transfer coefficients at level G to be ~5 to 10% too high.

An uncertainty in the heat flux at all levels of roughly 5.5% is induced by uncertainties in Inconel resistance and FRS dimensions. Uncertainties caused by variations in current are generally negligible.

A.5 Vapor Temperature

Local vapor temperature was calculated in two different ways. In the first method, a cross-sectional average vapor temperature was calculated from vapor temperatures measured in selected subchannels at each of the primary thermocouple levels and at the EOHL. At elevations between the primary levels the vapor temperature was deduced from a linear interpolation of the enthalpy at the primary levels.

In the second method an average enthalpy at the EOHL was calculated from vapor temperature measurements taken by the subchannel thermocouple rake (Sect. 3.2). An energy balance was then employed to extrapolate the experimentally determined enthalpy downward to lower elevations in the bundle. Vapor temperature was then calculated from enthalpy using a state search. Comparisons of vapor temperatures calculated by the two methods provide a consistency check on the experimental data.

A.5.1 Method 1

The first step in method 1 was to calculate the cross-sectional average vapor temperature for each of the primary thermocouple levels and the EOHL. The vapor temperature at the EOHL was derived as a weighted average of temperatures measured by the subchannel thermocouple rake

$$T_{v_{EOHL}} = \frac{A_1\ T_{1_{EOHL}} + A_2\ T_{2_{EOHL}}}{A_1 + A_2} , \tag{A.6}$$

where T_1 is the average measured temperature of subchannels surrounded by four heated rods, and T_2 is the average measured temperature of subchannels adjacent to an unheated rod (Fig. 3). The variables A_1 and A_2 are the total numbers of subchannels surrounded by four heated rods and adjacent to an unheated rod, respectively. Note that subchannels adjacent to the unheated shroud are not included in the average, because FRS's adjacent to the shroud were not used in computing average surface temperature. Uncertainty in $T_{v_{EOHL}}$ was calculated as the standard deviation from the mean. Errors associated with individual thermocouples are negligibly small in comparison with actual vapor temperature deviations from the mean.

Cross-sectional average vapor temperatures at the primary levels were deduced from temperature measurements taken by thermocouple array rods. The thermocouple array rods (Sect. 3.2) measure vapor temperatures in subchannels adjacent to an unheated rod; therefore,

$$T_{2_i} = \frac{\sum_{j=1}^{n} T_{2_{ij}}}{n} , \qquad (A.7)$$

where n, the number of thermocouples, is 4. Uncertainty is calculated as the standard deviation from the average. This temperature was used in conjunction with the temperatures at the EOHL to compute a cross-sectional average vapor temperature for subchannels not adjacent to the shroud:

$$T_{v_i} = \left[\frac{T_v - T_{sat}}{T_2 - T_{sat}}\right]_{EOHL} (T_{2_i} - T_{sat}) + T_{sat} , \qquad (A.8)$$

where T_{2_i} has been corrected for radiative heating of the fluid thermocouples.

Implied in Eq. (A.8) is the assumption that the ratio of vapor superheat in an "average" channel to that in a partially unheated type-2 subchannel is invariant with respect to elevation in the uncovered bundle. Uncertainty was computed by propagating uncertainties in individual terms through Eq. (A.8).

The second step in method 1 was to determine the cross-sectional average vapor temperature at the intermediate thermocouple levels. As fluid temperature was not measured at intermediate levels, the intermediate-level vapor temperatures were deduced from a linear interpolation of primary-level enthalpies:

$$h_i \, (P, T_{v_i}) = \left[\frac{h_J - h_I}{Z_J - Z_I}\right] (Z - Z_I) + h_I . \qquad (A.9)$$

The index i refers to the i'th level, I to the I'th primary level, and J to the I + 1 primary level. Once the enthalpy was known it was a simple matter to deduce vapor temperature from a properties search.

Intermediate-level vapor temperatures were computed only for elevations bracketed by primary levels that experimentally indicated vapor superheat. Note that all primary-level enthalpies were based on vapor temperature measurements corrected for radiative heating of the fluid thermocouples. Uncertainties in intermediate-level vapor temperatures were determined by propagating uncertainties in individual terms through Eq. (A.9) and the properties search.

As noted in Sect. 5, vapor temperatures calculated from method 1 appear to be valid for high-flow tests. However, in low-flow tests the thermocouple array rods are not thought to accurately measure vapor temperature. Therefore, vapor temperatures computed via method 1 were used only for comparison purposes. Method 2, which relies on an energy balance, was used to calculate the vapor temperatures used in the heat transfer analysis.

A.5.2 Method 2

Method 2 employs an energy balance to extrapolate the vapor enthalpy at the EOHL downward into the heated bundle:

$$h_i(P, T_{v_i}) = h_{EOHL}(P, T_{v_{EOHL}}) - \frac{C}{\dot{m}} \int_{Z_i}^{Z_{EOHL}} (q' - q'_{loss})\, dZ \ . \qquad (A.10)$$

In Eq. (A.10) both h_i and h_{EOHL} refer to subchannels that are not directly adjacent to the unheated shroud (internal subchannels). The correction factor C adjusts the energy balance so that it applies only to subchannels that are not adjacent to the shroud:

$$C = \left[\frac{h - h_g}{h_{ave} - h_g}\right]_{EOHL} \ . \qquad (A.11)$$

Implicit in Eq. (A.10) is the assumption that C, the ratio of enthalpy superheat in internal subchannels to that for the entire cross section, is invariant with respect to elevation. Physically, the effect of C is to flatten the radial enthalpy profile as the elevation approaches the mixture level.

Enthalpies at the EOHL were derived from weighted average temperatures. For internal subchannels, average temperature was calculated from Eq. (A.6). The cross-sectional average temperature is a weighted average over all subchannel types, such that

$$T_v = \frac{\sum_{i=1}^{4} A_i T_i}{\sum_{i=1}^{4} A_i} \ , \qquad (A.12)$$

where the index 3 refers to a subchannel adjacent to a wall, and 4 refers to a corner subchannel. The average temperature for the internal subchannels was corrected for radiative heating of the fluid thermocouples (discussed in the next subsection).

Uncertainty in the internal subchannel enthalpy at the EOHL was derived from the standard deviation of the vapor temperature over the internal subchannels where vapor temperature was measured. The physical significance of this standard deviation is that it is an estimate of actual variations in vapor temperatures over the internal subchannels at the EOHL; it is not indicative of temperature measurement errors.

The heat loss q'_{loss} was estimated from the response of thermocouples embedded in the bundle shroud at 10 elevations. Thus, separation of the bundle into 10 axial nodes, each node having associated with it a pair of embedded thermocouples, is convenient. The integral in Eq. (A.10) is rewritten as a sum,

$$h_i = h_{EOHL} - \frac{C}{\dot{m}} \sum_{j=1}^{n} (q'_j - q'_{loss_j}) \, \Delta Z_j \,, \tag{A.13}$$

where ΔZ_j is the length associated with the j'th set of shroud wall thermocouples. A more detailed account of the calculation of q'_{loss} can be found in a later section.

Finally, vapor temperature was computed from the enthalpy using a properties search. Uncertainty in vapor temperature was computed by propagating uncertainties in h_{EOHL}, $\dot{m}$, and q' through Eq. (A.10) and the properties search. Note that the enthalpy was extrapolated to the lowest primary thermocouple elevation experimentally indicating vapor superheat.

A.5.3 Radiation correction to fluid thermocouples

Because of the high FRS surface temperatures and low flows extant in these tests, radiative heating of fluid thermocouples can cause significant errors in measured vapor temperatures. As a result, the measured vapor temperature was corrected for radiative heating effects. The correction is based on a steady-state energy balance:

$$\begin{bmatrix}\text{Net radiative heat transfer} \\ \text{to fluid thermocouple}\end{bmatrix} - \begin{bmatrix}\text{Convection from thermocouple} \\ \text{to vapor}\end{bmatrix} = 0 \,. \tag{A.14}$$

The thermocouple-to-vapor and thermocouple-to-unheated-surface temperature differences were small enough so that radiative interaction between the thermocouple, vapor, and unheated surfaces could be neglected. Mathematically, the radiative interchange was modeled as a two-node radiation problem with absorbing vapor:

$$R\sigma \, [T_w^4 - T_{TC}^4] - h_{conv} \, A_{TC} \, [T_{TC} - T_v] = 0 \,; \tag{A.15}$$

$$R = \left[\frac{1 - \varepsilon_{TC}}{A_{TC}\ \varepsilon_{TC}} + \frac{1}{A_{TC}\ F_{TC-w}\ (1 - \alpha_v)} + \frac{1 - \varepsilon_w}{A_w\ \varepsilon_w}\right]^{-1} .$$

The surface emissivity assumed was that for oxidized stainless steel; 0.5 ± 0.1 (Ref. 1). The vapor absorptivity was taken as the average of the absorptivity evaluated at the FRS surface temperature and that evaluated at the thermocouple temperature. Vapor absorptivity was evaluated at the high-pressure limit for water vapor[2] and adjusted using Penner's rule.[3] An allowance of ±25% was made for uncertainty.

The correction was applied to two different thermocouple types: thermocouple array rod thermocouples, which are oriented perpendicular to the vapor flow, and subchannel rake thermocouples, which are oriented parallel to the vapor flow. Thermocouple array-rod thermocouples are partially shielded from radiation by the unheated thermocouple array rod; the thermocouple-to-heated-wall view factor was estimated at 0.75 ± 0.15. The convective heat transfer coefficient for the thermocouple array-rod thermocouples was computed from a correlation recommended by Scadron[4] with allowance for a ±30% uncertainty,

$$h_{conv} = \frac{k_v}{D_{TC}} (0.478)\ Re_v^{0.5}\ Pr_v^{0.3} . \tag{A.16}$$

The correction applied to the subchannel rake thermocouples was based on an energy balance applied to the tip of the thermocouple. The tip of the thermocouple was slightly above or just inside the heated length. As a result, most of the radiative heating probably took place near the tip. The tip-to-heated-rod view factor was estimated at 0.85 ± 0.15. The convective heat transfer coefficient was assumed to be 70% of the heat transfer coefficient for the stagnation point on an axisymmetric blunt body (the rounded tip of the thermocouple):[5]

$$h_{conv} = \frac{0.92\ k_v}{D_{TC}}\ Re_v^{0.5}\ Pr_v^{0.4} . \tag{A.17}$$

The 70% factor was applied because previous experimental work has shown that the average heat transfer coefficient on the leading edge of a sphere is roughly 70% of that at the stagnation point.[6] A ±30% allowance was made for uncertainty.

The uncertainty in the vapor temperature caused by radiative heating effects was estimated by propagating uncertainties in individual quantities through Eq. (A.15).

A.6 Calculation of Heat Losses

Use of an energy balance to calculate vapor temperature requires computation of bundle heat losses [Eq. (A.10)]. In the case of the THTF, pairs of thermocouples were embedded in the shroud box walls at various elevations (Fig. 7). Each pair was embedded in such a way that one of the thermocouples was close to the inner surface of the shroud box and one thermocouple was close to the outer surface (Fig. 6). The difference in temperature between the two thermocouples divided by the separation was the temperature gradient; calculation of local heat loss was thus straightforward:

$$q'_{loss} = -\left(\frac{\Delta T}{\Delta X}\right) k_{ss} \left(\frac{1 + \eta}{2}\right) P_{shroud} , \qquad (A.18)$$

where the conductivity of stainless steel was evaluated from a temperature-dependent curve fit.[7] The term η corrects for the fact that two sides of the shroud are 2.54 cm (1 in.) thick, and the other two sides are 1.91 cm (0.75 in.) thick. If the thermocouples were embedded in the thicker wall, then heat loss through the thinner wall was greater and

$$\eta = \frac{2.54 \text{ cm}}{1.91 \text{ cm}} = 1.33 .$$

Similar arguments apply if the thermocouples were in the 1.91-cm (0.75-in.) wall; $\eta = 1/1.33 = 0.75$.

Once the local linear heat loss was known, a length of shroud box was associated with each thermocouple pair. This length is simply defined as the distance from a point midway between the thermocouple pair and the next lowest pair and a point midway between the subject pair and the next highest pair. The result of this scheme was that the shroud box was divided into a set of nodes, each node having a constant rate of heat loss. If the thermometry in a node failed, as occurred in several nodes, the nodal heat flux was formulated as the average of the heat fluxes in the two adjacent nodes. Total heat loss over a length of bundle was

$$q_{loss} = \sum_{i=1}^{n} q'_{loss_i} \Delta Z_i , \qquad (A.19)$$

which is the needed input to Eq. (A.10).*

Note that experimental procedure was such that heat loss resulting from transient shroud-box heat-up was minimal and therefore not considered.

---

*Total bundle heat losses varied from a low of about 2% of bundle power in the highest power tests to roughly 17% in the lowest power tests.

A.7 Radiation Heat Flux

The total radiation heat flux is composed of two components: (1) radiation from FRS's to high-pressure steam and (2) radiation from FRS's to unheated FRS's. Because calculations were restricted to rods at least one row removed from the bundle shroud, radiation from FRS's to the shroud was not considered. This seems justified in that experimental observations do not indicate the presence of a distinct radial temperature gradient as one moves from the innermost to the penultimate row of rods.

A.7.1 Radiation to vapor

The Hottel empirical method was used to compute the radiative heat flux from FRS's to high-pressure steam.[8] The method relies on the use of an effective emissivity,

$$q''_{w-v} = \varepsilon'\sigma[T_w^4 - T_v^4] \ , \tag{A.20}$$

where the effective emissivity (ε') is given by

$$\varepsilon' = \left[\frac{1}{\varepsilon_w} + \frac{1}{\alpha_v(T_w)} - 1\right]^{-1} . \tag{A.21}$$

Implicit in the model is the assumption that vapor absorptivity is equal to vapor emissivity. Under conditions typical of these tests this assumption is quite good. The difference between absorptivity and emissivity is generally less than 10% and in many cases is less than 3%. Because absorption of radiation by the steam was the dominant process, the absorptivity of the vapor evaluated at the FRS temperature was used in Eq. (A.21). All radiative properties for the vapor were evaluated at the high-pressure limit[2] using Penner's rule.[3] Uncertainty in the radiative properties of the vapor was assumed to be ±25%. The FRS surface emissivity was taken to be that for oxidized stainless steel: 0.5 ± 0.1 (Ref. 1). The uncertainty in the radiative flux to the vapor was computed by propagating uncertainties in individual terms through Eq. (20).

A.7.2 Radiation to unheated rods

Calculation of the radiative heat flux from heated to unheated rods was performed as a two-node radiation problem with an absorbing vapor. The vapor absorptivity was evaluated at the heated surface temperature, and a steady-state energy balance was used to calculate the unheated-rod surface temperature. A two-equation system was solved for the radiative heat flux[9]

$$q''_{w-cw} = \frac{\sigma R}{A_w}(T_w^4 - T_{cw}^4) \ , \tag{A.22}$$

where

$$R = \left[\frac{1 - \varepsilon_w}{A_w \varepsilon_w} + \frac{1}{A_w F_{w-cw} [1 - \alpha_v (T_w)]} + \frac{1 - \varepsilon_{cw}}{A_{cw} \varepsilon_{cw}}\right]^{-1} ,$$

and

$$q''_{w-cw} - h_{conv} (T_{cw} - T_v) = 0 , \qquad (A.23)$$

where

$$h_{conv} = 0.021 \frac{k_{cw}}{D_{cw}} Re_{MW}^{0.8} Pr_w^{0.4} .$$

The emissivity of the unheated rod was assumed equal to that of the heated rods; $\varepsilon_{cw} = 0.5 \pm 0.1$. All surface areas and the heated-rod-to-unheated-rod view factor are expressed as a sum for all rods in the bundle that are at least one row removed from the bundle shroud. Mathematically,

$$A_w = \sum_{i=1}^{n} A_{w_i} ; A_{cw} = \sum_{j=1}^{K} A_{cw_j} ; F_{w-cw} = \sum_{j=1}^{K} \sum_{i=1}^{n} F_{i-j} . \qquad (A.24)$$

The view factor for a heated and unheated rod on pitch is 0.1352 and on diagonal is 0.0913. All other heated-to-unheated-rod configurations were assumed to have a view factor of 0.0. View factors were evaluated using the Hottel crossed string method.[3] The convective heat transfer coefficient was evaluated from a correlation recommended by ORNL for convection to superheated steam.

In most cases the uncertainty in the radiative flux was dominated by uncertainties in vapor absorptivities and surface emissivities. Accordingly, uncertainty was estimated by propagating uncertainties in emissivity and absorptivity through Eq. (A.22). Total uncertainty in the radiation heat flux was calculated as the vectorial sum of the uncertainty in radiation to steam and the uncertainty in radiation to unheated rods.

A.8 Heat Transfer Coefficient

Total, convective, and radiative heat transfer coefficients are defined in the conventional manner:

$$h_{tot} = \frac{q''_{tot}}{T_w - T_v} ; \qquad (A.25)$$

$$h_{conv} = \frac{q''_{tot} - q''_{rad}}{T_w - T_v} ; \quad (A.26)$$

and

$$h_{rad} = \frac{q''_{rad}}{T_w - T_v} , \quad (A.27)$$

where all quantities are cross-sectional averages. Uncertainty was estimated by propagating uncertainties in q''_{tot}, q''_{rad}, and $(T_w - T_v)$ through the appropriate equation.

The procedures for estimating uncertainties in q''_{tot} and q''_{rad} are straightforward and have been discussed; estimation of the uncertainty in $(T_w - T_v)$ is somewhat more complex. The reason is that the individual uncertainties in T_w and T_v are a combination of uncertainties caused by actual local variations of temperature and uncertainties resulting from measurement or calculational uncertainties, for example, the uncertainty induced by radiative heating of the fluid thermocouples. Uncertainties formulated in this way are appropriate when temperature is used to evaluate physical properties, because uncertainty in temperature translates into a range of physical properties that might be observed. For example, a vapor temperature uncertainty of ± 50 K (90°F) would translate into a range of vapor Reynolds numbers that might be observed because of viscosity variations.

However, uncertainty in $(T_w - T_v)$ should not be formulated in terms of individual uncertainties in T_w and T_v because while individual variations in T_w and T_v are quite large, variations in $(T_w - T_v)$ are much smaller. Instead, the relative uncertainty in $(T_w - T_v)$ is formulated as

$$\frac{\Delta (T_w - T_v)}{(T_w - T_v)} = \sqrt{\varepsilon^2 + \frac{\Delta T_v^2 + \Delta T_w^2}{(T_w - T_v)^2}} , \quad (A.28)$$

where ΔT_v and ΔT_w refer only to uncertainties associated with measurement or calculation and not actual temperature variations. The quantity ε is the percentage variation in $(T_w - T_v)$, which was experimentally observed at the EOHL. In other words, ε represents uncertainty caused by actual variations in $(T_w - T_v)$, while ΔT_v and ΔT_w represent the uncertainties associated with measurement or calculational technique.

The quantity ε was calculated from temperature measurements taken near the EOHL. At the 3.62-m (11.88-ft) elevation there are six FRS's instrumented with sheath thermocouples for which all the surrounding subchannels were monitored for vapor temperature, allowing an average

$(T_w - T_v)$ and standard deviation to be calculated. The quantity ε was formulated as,

$$\varepsilon = \frac{\sigma_{T_w - T_v}}{(T_w - T_v)} , \tag{A.29}$$

where $\sigma_{T_w - T_v}$ is the standard deviation in rod-to-vapor temperature difference at the 3.62-m (11.88-ft) elevation. Note that implicit in Eq. (A.28) is the assumption that ε is invariant with respect to elevation.

A.9 Vapor Reynolds Number

The vapor Reynolds number is defined in terms of the bundle average mass flux:

$$Re_v = \frac{D_H G}{\mu_v} . \tag{A.30}$$

A.10 Film Reynolds Number

The film Reynolds number is defined as

$$Re_f = \frac{D_H G}{\mu_f} . \tag{A.31}$$

A.11 Wall Reynolds Number

The wall Reynolds number is defined as

$$Re_w = \frac{D_H G}{\mu_w} . \tag{A.32}$$

A.12 Modified Wall Reynolds Number

The modified wall Reynolds number is generally used to correlate heat transfer data in which fluid property variations across the boundary layer are important:

$$Re_{MW} = \frac{D_H\ G}{\mu_w}\left(\frac{\rho_w}{\rho_v}\right) \ . \qquad (A.33)$$

A.13 Grashof Number

The Grashof number is defined in terms of the subchannel hydraulic diameter:

$$Gr = \frac{\rho_f{}^2 \beta g \Delta T D_H{}^3}{\mu_f{}^2} \ . \qquad (A.34)$$

References

1. E. M. Sparrow and R. D. Cess, *Radiation Heat Transfer*, p. 45, Brookes/Cole, Belmont, Calif., 1966.

2. C. B. Ludwig and C. C. Ferriso, "Prediction of Total Emissivity of Nitrogen-Broadened and Self-Broadened Hot Water Vapor," *J. Quant. Spectrosc. Radiat. Transfer* 7, pp. 7–26, 1967.

3. H. C. Hottel and A. F. Sarofim, *Radiative Transfer*, pp. 31, 231, McGraw-Hill, New York, 1967.

4. M. D. Scadron and I. Warshawsky, *Experimental Determination of Time Constants and Nusselt Number for Bare-Wire Thermocouples in High Velocity Air Streams and Analytic Approximations of Conduction and Radiation Errors*, NACA TN 2599 (January 1952).

5. W. M. Kays, *Convective Heat and Mass Transfer*, p. 211, McGraw-Hill, New York, 1966.

6. G. L. Hayward and D. C. Pei, "Local Heat Transfer from a Single Sphere to a Turbulent Air Stream," *Int. J. of Heat and Mass Transfer* 21, pp. 35–42, 1978.

7. L. J. Ott and R. A. Hedrick, *ORTCAL — A Code for THTF Heater Rod Thermocouple Calibration*, ORNL/NUREG-51 (February 1979).

8. L. S. Tong and J. Weisman, *Thermal Analysis of Pressurized Water Reactors*, 2nd Ed., p. 312, American Nuclear Society, LaGrange Park, Ill., 1979.

9. T. M. Anklam, *ORNL Small-Break LOCA Heat Transfer Test Series I: Rod Bundle Heat Transfer Analysis*, ORNL/NUREG/TM-445 (August 1981).

Appendix B

UNCOVERED-BUNDLE HEAT TRANSFER RESULTS

(Standard International Units)

Appendix B presents the uncovered-bundle heat transfer results discussed in this report. Section B.1 presents the quantities in metric units; Sect. B.2 presents the same results in Standard English Engineering Units.

Heat transfer coefficients and local fluid conditions are presented as bundle average quantities for each FRS thermocouple level in the steam-cooling region. The word DELTA or +OR- preceding a word, abbreviation, or number means that the subject quantity is an uncertainty.* For example, TVAP refers to vapor temperature; thus, DELTA TVAP refers to uncertainty in vapor temperature.

The results are presented on a test-by-test basis from 3.09.10I to 3.09.10N. The first set of results shown is a system parameter summary for the test. Format and nomenclature are self-explanatory. The following nine pages contain results of a local nature. At the top of the page is listed the appropriate test number.

Listed below are definitions for abbreviations used in the tables. Note that a quantity in a table listed as zero usually means that the appropriate calculation was not applicable.

<u>Abbreviations and Definitions</u>

Level	FRS thermocouple level starting with 1 at level A and 21 at level G; levels H, S, Y, and U not counted
Elevation	Elevation with respect to BOHL
TVAP	Vapor temperature
No. of TCs	Number of thermocouples included in the average surface temperature
TW	Heated FRS surface temperature
Q''/Q''_{ss}	Multiplier for surface heat flux to correct for transient heat-up or cooldown
Q''/HTRAN	Heat flux used for heat transfer coefficient calculation, based only on rods at least one row removed from shroud box
HEXP	Experimentally determined heat transfer coefficient
REV	Vapor Reynolds number

*Calculated uncertainties were based on 2-σ instrumentation error bands.

REF	Film Reynolds number
QRAD	Radiation heat flux to steam
HCONV	Convective heat transfer coefficient
HRAD	Radiation heat transfer coefficient
REW	Modified wall Reynolds number
QCROD	Radiation flux to unheated rods on a per rod basis
GRX	Grashof number
PRV	Vapor Prandtl number
PRF	Film Prandtl number
HW-TRAN	W correlation for transition to turbulent flow
HW-LAM	W correlation for laminar flow
HW-TUR	W correlation for turbulent flow
HCE-TUR	CE correlation for turbulent flow
HB&W	B&W correlation
HORNL	The convective heat transfer coefficient computed by the ORNL recommended correlation
HEINEMAN	The convective heat transfer coefficient computed by Heineman correlation
McELIGOT	The convective heat transfer coefficient computed by the McEligot correlation
TFIL	Film temperature
HCE-TRAN	CE correlation for transition flow
HCE-LAM	CE correlation for laminar flow

B.1 Metric Units

THIS PAGE

WAS INTENTIONALLY

LEFT BLANK

TEST

3.09.10I

SYSTEM PARAMETER SUMMARY

SYSTEM PRESSURE	.450308E+01	+OR-	.211212E+00	MPA
INLET MASS FLOW	.000000E+00	+OR-	.000000E+00	KG/S
OUTLET MASS FLOW	.183960E+00	+OR-	.123608E-01	KG/S
MASS FLUX - BASED ON OUTLET FLOW	.297614E+02	+OR-	.199975E+01	KG/(M**2)S
MASS FLUX - BASED ON INLET FLOW	.000000E+00	+OR-	.000000E+00	KG/(M**2)S
INLET TEMPERATURE	.473025E+03	+OR-	.259115E+03	KELVIN
OUTLET TEMPERATURE	.774098E+03	+OR-	.259238E+03	KELVIN
BUNDLE POWER	.487359E+03	+OR-	.256083E+02	KW
AVERAGE LINEAR POWER/ROD	.222061E+01	+OR-	.116682E+00	KW/M
FRACTIONAL HEAT LOSS	.176706E-01			

HEAT TRANSFER CALCULATIONS: TEST 3.09.10I

LEVEL	ELEVATION (METER)	TVAP (KELVIN)	DELTA TVAP (KELVIN)	NO. OF TC S	TW (KELVIN)	DELTA TW (KELVIN)	Q"/Q"SS	Q"HTRAN (W/CM**2)	DELTA Q"HTRAN (W/CM**2)
12	3.02	.606655E+03	.287578E+03	22.	.933071E+03	.261206E+03	.103039E+01	.784436E+01	.417147E+00
13	3.12	.636710E+03	.287261E+03	5.	.950543E+03	.265298E+03	.103603E+01	.785936E+01	.425887E+00
14	3.20	.659745E+03	.283442E+03	4.	.972220E+03	.260025E+03	.104566E+01	.798209E+01	.395869E+00
15	3.27	.684118E+03	.287423E+03	4.	.978929E+03	.267208E+03	.103909E+01	.786334E+01	.433982E+00
16	3.34	.706575E+03	.286283E+03	1.	.912223E+03	.257540E+03	.103700E+01	.750233E+01	.361732E+00
17	3.40	.723024E+03	.286717E+03	2.	.952954E+03	.256870E+03	.103665E+01	.772733E+01	.432532E+00
18	3.45	.738697E+03	.287705E+03	3.	.101439E+04	.261927E+03	.103685E+01	.789233E+01	.383192E+00
19	3.50	.754629E+03	.287486E+03	6.	.103111E+04	.263894E+03	.103892E+01	.784797E+01	.405759E+00
20	3.57	.778067E+03	.286541E+03	6.	.105281E+04	.271424E+03	.104281E+01	.791692E+01	.419047E+00
21	3.62	.792378E+03	.285986E+03	17.	.106223E+04	.269890E+03	.104006E+01	.791904E+01	.411883E+00

HEAT TRANSFER CALCULATIONS: TEST 3.09.101

LEVEL	ELEVATION (METER)	HEXP (W/CM**2-K)	DELTA HEXP (W/CM**2-K)	REV	DELTA REV	REF	DELTA REF
12	3.02	.240463E-01	.180341E-02	.166143E+05	.169224E+04	.126253E+05	.117367E+04
13	3.12	.250582E-01	.178936E-02	.154790E+05	.131300E+04	.122215E+05	.109879E+04
14	3.20	.255601E-01	.170356E-02	.148966E+05	.126120E+04	.118637E+05	.105578E+04
15	3.27	.266886E-01	.183857E-02	.143288E+05	.118164E+04	.116269E+05	.100657E+04
16	3.34	.365034E-01	.247028E-02	.138413E+05	.111365E+04	.119669E+05	.986604E+03
17	3.40	.336277E-01	.228049E-02	.135040E+05	.108302E+04	.115311E+05	.947758E+03
18	3.45	.286462E-01	.164679E-02	.131972E+05	.106171E+04	.109904E+05	.911312E+03
19	3.50	.284026E-01	.168318E-02	.128989E+05	.102776E+04	.107763E+05	.884783E+03
20	3.57	.288330E-01	.169687E-02	.124833E+05	.975510E+03	.104934E+05	.853113E+03
21	3.62	.293632E-01	.169090E-02	.122421E+05	.946309E+03	.103505E+05	.827901E+03

HEAT TRANSFER CALCULATIONS: TEST 3.09.10I

LEVEL	ELEVATION (METER)	QRAD (W/CM**2)	DELTA QRAD (W/CM**2)	HCONV (W/CM**2-K)	DELTA HCONV (W/CM**2-K)
12	3.02	.102049E+01	.210055E+00	.202275E-01	.205587E-02
13	3.12	.107175E+01	.226707E+00	.208910E-01	.209459E-02
14	3.20	.115776E+01	.239794E+00	.210410E-01	.206184E-02
15	3.27	.115358E+01	.250451E+00	.219204E-01	.222850E-02
16	3.34	.743823E+00	.166732E+00	.321111E-01	.274005E-02
17	3.40	.920267E+00	.200443E+00	.287638E-01	.261549E-02
18	3.45	.125543E+01	.268156E+00	.231023E-01	.218499E-02
19	3.50	.132468E+01	.285673E+00	.225671E-01	.226765E-02
20	3.57	.141022E+01	.322171E+00	.225788E-01	.239538E-02
21	3.62	.143565E+01	.324119E+00	.228808E-01	.242370E-02

HEAT TRANSFER CALCULATIONS: TEST 3.09.10I

LEVEL	ELEVATION (METER)	HRAD (W/CM**2-K)	DELTA HRAD (W/CM**2-K)	REW	DELTA REW	QCRODM (W/CM**2)	DELTA QCRODM (W/CM**2)
12	3.02	.381875E-02	.987071E-03	.613912E+04	.677873E+03	.225257E+00	.105136E+00
13	3.12	.416722E-02	.108881E-02	.631926E+04	.670225E+03	.235278E+00	.109338E+00
14	3.20	.451913E-02	.116150E-02	.631415E+04	.648733E+03	.253502E+00	.117442E+00
15	3.27	.476813E-02	.125932E-02	.651651E+04	.659018E+03	.251266E+00	.116038E+00
16	3.34	.439237E-02	.118559E-02	.788310E+04	.733859E+03	.158914E+00	.731354E-01
17	3.40	.486386E-02	.128063E-02	.738185E+04	.691719E+03	.197404E+00	.907173E-01
18	3.45	.554392E-02	.143606E-02	.663147E+04	.636462E+03	.272077E+00	.124715E+00
19	3.50	.583553E-02	.151958E-02	.656837E+04	.628516E+03	.287742E+00	.131600E+00
20	3.57	.625419E-02	.169071E-02	.651191E+04	.629413E+03	.307050E+00	.139954E+00
21	3.62	.648240E-02	.173643E-02	.652506E+04	.622891E+03	.312610E+00	.142188E+00

HEAT TRANSFER CALCULATIONS: TEST 3.09.101

LEVEL	ELEVATION (METER)	GRX	DELTA GRX	PRV	DELTA PRV	PRF	DELTA PRF
12	3.02	.181900E+07	.350846E+06	.110880E+01	.564282E-01	.925812E+00	.198768E-01
13	3.12	.146163E+07	.273724E+06	.105717E+01	.530511E-01	.916617E+00	.156391E-01
14	3.20	.123815E+07	.228360E+06	.101751E+01	.411946E-01	.909534E+00	.128475E-01
15	3.27	.104792E+07	.192192E+06	.986046E+00	.298754E-01	.905302E+00	.107154E-01
16	3.34	.854000E+06	.168733E+06	.964287E+00	.223558E-01	.911488E+00	.105928E-01
17	3.40	.781831E+06	.145619E+06	.951620E+00	.188658E-01	.903682E+00	.881689E-02
18	3.45	.726296E+06	.127910E+06	.941541E+00	.164353E-01	.895400E+00	.729563E-02
19	3.50	.656674E+06	.114502E+06	.932884E+00	.139704E-01	.892480E+00	.650935E-02
20	3.57	.567700E+06	.100780E+06	.922410E+00	.110003E-01	.888900E+00	.561749E-02
21	3.62	.519126E+06	.897406E+05	.917054E+00	.959796E-02	.887207E+00	.505745E-02

HEAT TRANSFER CALCULATIONS: TEST 3.09.10I

LEVEL	ELEVATION (METER)	HW-TRAN (W/CM**2-K)	DELTA HW-TRAN (W/CM**2-K)	HW-LAM (W/CM**2-K)	DELTA HW-LAM (W/CM**2-K)	HW-TUR (W/CM**2-K)	DELTA HW-TUR (W/CM**2-K)
12	3.02	.000000E+00	.000000E+00	.000000E+00	.000000E+00	.215282E-01	.174381E-02
13	3.12	.000000E+00	.000000E+00	.000000E+00	.000000E+00	.220194E-01	.161866E-02
14	3.20	.000000E+00	.000000E+00	.000000E+00	.000000E+00	.226907E-01	.168884E-02
15	3.27	.000000E+00	.000000E+00	.000000E+00	.000000E+00	.234600E-01	.169336E-02
16	3.34	.000000E+00	.000000E+00	.000000E+00	.000000E+00	.242568E-01	.173894E-02
17	3.40	.000000E+00	.000000E+00	.000000E+00	.000000E+00	.247685E-01	.174140E-02
18	3.45	.000000E+00	.000000E+00	.000000E+00	.000000E+00	.253227E-01	.174734E-02
19	3.50	.000000E+00	.000000E+00	.000000E+00	.000000E+00	.259013E-01	.174638E-02
20	3.57	.000000E+00	.000000E+00	.000000E+00	.000000E+00	.257710E-01	.173074E-02
21	3.62	.000000E+00	.000000E+00	.000000E+00	.000000E+00	.273049E-01	.171859E-02

HEAT TRANSFER CALCULATIONS: TEST 3.09.10I

LEVEL	ELEVATION (METER)	HCE-TUR (W/CM**2-K)	DELTA HCE-TUR (W/CM**2-K)	HB&W (W/CM**2-K)	DELTA HB&W (W/CM**2-K)	HORNL (W/CM**2-K)	DELTA HORNL (W/CM**2-K)
12	3.02	.248348E-01	.249958E-02	.248348E-01	.249958E-02	.163136E-01	.145222E-02
13	3.12	.241908E-01	.224176E-02	.241908E-01	.224176E-02	.171085E-01	.147532E-02
14	3.20	.240784E-01	.226826E-02	.240784E-01	.226826E-02	.176129E-01	.145427E-02
15	3.27	.241091E-01	.219461E-02	.241091E-01	.219461E-02	.182273E-01	.150690E-02
16	3.34	.242295E-01	.212376E-02	.242295E-01	.212376E-02	.193423E-01	.144331E-02
17	3.40	.243578E-01	.213100E-02	.243578E-01	.213100E-02	.194384E-01	.145886E-02
18	3.45	.245036E-01	.216358E-02	.245036E-01	.216358E-02	.193694E-01	.149791E-02
19	3.50	.246701E-01	.214393E-02	.246701E-01	.214393E-02	.196381E-01	.152020E-02
20	3.57	.249399E-01	.209139E-02	.249399E-01	.209139E-02	.200413E-01	.160384E-02
21	3.62	.251154E-01	.206217E-02	.251154E-01	.206217E-02	.203082E-01	.159556E-02

HEAT TRANSFER CALCULATIONS: TEST 3.09.10I

LEVEL	ELEVATION (METER)	HEINEMAN (W/CM**2-K)	DELTA HEINEMAN (W/CM**2-K)	MCELIGOT (W/CM**2-K)	DELTA MCELIGOT (W/CM**2-K)
12	3.02	.210725E-01	.245109E-02	.182855E-01	.184765E-02
13	3.12	.213042E-01	.235587E-02	.180786E-01	.169159E-02
14	3.20	.215327E-01	.234487E-02	.181117E-01	.174264E-02
15	3.27	.216954E-01	.225841E-02	.184032E-01	.172113E-02
16	3.34	.214646E-01	.205075E-02	.194710E-01	.175783E-02
17	3.40	.217637E-01	.206978E-02	.193729E-01	.174872E-02
18	3.45	.221754E-01	.214189E-02	.190932E-01	.174212E-02
19	3.50	.223503E-01	.211966E-02	.192710E-01	.173115E-02
20	3.57	.225913E-01	.210199E-02	.195769E-01	.169612E-02
21	3.62	.227174E-01	.204922E-02	.198066E-01	.167936E-02

HEAT TRANSFER CALCULATIONS: TEST 3.09.10I

LEVEL	ELEVATION (METER)	TFIL (KELVIN)	DELTA TFIL (KELVIN)	HCE-TRAN (W/CM**2-K)	DELTA HCE-TRAN (W/CM**2-K)	HCE-LAM (W/CM**2-K)	DELTA HCE-LAM (W/CM**2-K)
12	3.02	.769863E+03	.302822E+03	.000000E+00	.000000E+00	.000000E+00	.000000E+00
13	3.12	.793626E+03	.301107E+03	.000000E+00	.000000E+00	.000000E+00	.000000E+00
14	3.20	.815983E+03	.301425E+03	.000000E+00	.000000E+00	.000000E+00	.000000E+00
15	3.27	.831524E+03	.299530E+03	.000000E+00	.000000E+00	.000000E+00	.000000E+00
16	3.34	.809399E+03	.293409E+03	.000000E+00	.000000E+00	.000000E+00	.000000E+00
17	3.40	.837989E+03	.294481E+03	.000000E+00	.000000E+00	.000000E+00	.000000E+00
18	3.45	.876544E+03	.297325E+03	.000000E+00	.000000E+00	.000000E+00	.000000E+00
19	3.50	.892868E+03	.297029E+03	.000000E+00	.000000E+00	.000000E+00	.000000E+00
20	3.57	.915439E+03	.296982E+03	.000000E+00	.000000E+00	.000000E+00	.000000E+00
21	3.62	.927305E+03	.295605E+03	.000000E+00	.000000E+00	.000000E+00	.000000E+00

THIS PAGE

WAS INTENTIONALLY

LEFT BLANK

TEST

3.09.10 J

SYSTEM PARAMETER SUMMARY

SYSTEM PRESSURE	.420079E+01	+OR-	.206836E+00	MPA
INLET MASS FLOW	.799134E-01	+OR-	.379818E-02	KG/S
OUTLET MASS FLOW	.782442E-01	+OR-	.538945E-02	KG/S
MASS FLUX - BASED ON OUTLET FLOW	.126585E+02	+OR-	.871914E+00	KG/(M**2)S
MASS FLUX - BASED ON INLET FLOW	.129285E+02	+OR-	.614475E+00	KG/(M**2)S
INLET TEMPERATURE	.480339E+03	+OR-	.259114E+03	KELVIN
OUTLET TEMPERATURE	.728433E+03	+OR-	.259339E+03	KELVIN
BUNDLE POWER	.234083E+03	+OR-	.124731E+02	KW
AVERAGE LINEAR POWER/ROD	.106658E+01	+OR-	.568325E-01	KW/M
FRACTIONAL HEAT LOSS	.516742E-01			

HEAT TRANSFER CALCULATIONS: TEST 3.09.10J

LEVEL	ELEVATION (METER)	TVAP (KELVIN)	DELTA TVAP (KELVIN)	NO. OF TC S	TW (KELVIN)	DELTA TW (KELVIN)	Q"/Q"SS	Q"HTRAN (W/CM**2)	DELTA Q"HTRAN (W/CM**2)
12	3.02	.629279E+03	.281900E+03	22.	.931686E+03	.265905E+03	.100000E+01	.370499E+01	.202707E+00
13	3.12	.662795E+03	.279473E+03	5.	.958129E+03	.267518E+03	.100000E+01	.369402E+01	.211762E+00
14	3.20	.687561E+03	.278680E+03	4.	.973569E+03	.262654E+03	.100000E+01	.371641E+01	.191866E+00
15	3.27	.712224E+03	.278442E+03	4.	.969363E+03	.267311E+03	.100000E+01	.368904E+01	.217204E+00
16	3.34	.736075E+03	.277034E+03	1.	.911710E+03	.255450E+03	.100000E+01	.350107E+01	.175054E+00
17	3.40	.753549E+03	.276096E+03	2.	.930967E+03	.257682E+03	.100000E+01	.363104E+01	.223279E+00
18	3.45	.769984E+03	.276679E+03	3.	.977494E+03	.256610E+03	.100000E+01	.369830E+01	.185759E+00
19	3.50	.786077E+03	.277369E+03	6.	.100292E+04	.258645E+03	.100000E+01	.367536E+01	.201348E+00
20	3.57	.811058E+03	.276448E+03	6.	.102676E+04	.265272E+03	.100000E+01	.369620E+01	.207618E+00
21	3.62	.826241E+03	.275987E+03	17.	.102922E+04	.271474E+03	.100000E+01	.370017E+01	.200092E+00

HEAT TRANSFER CALCULATIONS: TEST 3.03.10J

LEVEL	ELEVATION (METER)	HEXP (W/CM**2-K)	DELTA HEXP (W/CM**2-K)	REV	DELTA REV	REF	DELTA REF
12	3.02	.122591E-01	.116034E-02	.670124E+04	.554123E+03	.529799E+04	.449488E+03
13	3.12	.125155E-01	.113296E-02	.631570E+04	.487724E+03	.508809E+04	.409789E+03
14	3.20	.130010E-01	.108296E-02	.607130E+04	.460779E+03	.495619E+04	.386784E+03
15	3.27	.143551E-01	.127133E-02	.584545E+04	.439040E+03	.489173E+04	.379071E+03
16	3.34	.199458E-01	.176733E-02	.564204E+04	.415576E+03	.499926E+04	.371943E+03
17	3.40	.204784E-01	.185418E-02	.550158E+04	.400364E+03	.488262E+04	.358593E+03
18	3.45	.178330E-01	.136438E-02	.537557E+04	.391541E+03	.469470E+04	.345198E+03
19	3.50	.169597E-01	.133071E-02	.525754E+04	.383617E+03	.457839E+04	.337551E+03
20	3.57	.171459E-01	.131988E-02	.508407E+04	.366496E+03	.444870E+04	.326176E+03
21	3.62	.182402E-01	.136891E-02	.498404E+04	.357122E+03	.440360E+04	.325478E+03

HEAT TRANSFER CALCULATIONS: TEST 3.09.10J

LEVEL	ELEVATION (METER)	QRAD (W/CM**2)	DELTA QRAD (W/CM**2)	HCONV (W/CM**2-K)	DELTA HCONV (W/CM**2-K)
12	3.02	.969309E+00	.204666E+00	.835146E-02	.155695E-02
13	3.12	.105715E+01	.225668E+00	.815738E-02	.161658E-02
14	3.20	.110004E+01	.227589E+00	.832355E-02	.161962E-02
15	3.27	.102527E+01	.222657E+00	.951399E-02	.180660E-02
16	3.34	.659055E+00	.143217E+00	.154021E-01	.214207E-02
17	3.40	.709826E+00	.153445E+00	.156351E-01	.225040E-02
18	3.45	.924689E+00	.194454E+00	.124370E-01	.194192E-02
19	3.50	.103438E+01	.217978E+00	.111837E-01	.198794E-02
20	3.57	.110720E+01	.242326E+00	.109288E-01	.209171E-02
21	3.62	.106985E+01	.254488E+00	.118591E-01	.223029E-02

HEAT TRANSFER CALCULATIONS: TEST 3.09.10J

LEVEL	ELEVATION (METER)	HRAD (W/CM**2-K)	DELTA HRAD (W/CM**2-K)	REW	DELTA REW	QCRODM (W/CM**2)	DELTA QCRODM (W/CM**2)
12	3.02	.390760E-02	.103813E-02	.277752E+04	.303659E+03	.211663E+00	.955304E-01
13	3.12	.435813E-02	.115313E-02	.280023E+04	.296709E+03	.229173E+00	.102538E+00
14	3.20	.467750E-02	.120432E-02	.283298E+04	.290279E+03	.237048E+00	.105391E+00
15	3.27	.484111E-02	.128355E-02	.298347E+04	.299628E+03	.218820E+00	.967617E-01
16	3.34	.454370E-02	.121038E-02	.353481E+04	.329308E+03	.138500E+00	.610728E-01
17	3.40	.484330E-02	.127527E-02	.347345E+04	.322464E+03	.148945E+00	.653521E-01
18	3.45	.539606E-02	.138184E-02	.320935E+04	.301242E+03	.194374E+00	.847480E-01
19	3.50	.577601E-02	.147686E-02	.311160E+04	.292505E+03	.217350E+00	.942562E-01
20	3.57	.621709E-02	.162271E-02	.306670E+04	.289236E+03	.233041E+00	.100299E+00
21	3.62	.638111E-02	.176076E-02	.311478E+04	.296465E+03	.224616E+00	.962866E-01

HEAT TRANSFER CALCULATIONS: TEST 3.09.10J

LEVEL	ELEVATION (METER)	GRX	DELTA GRX	PRV	DELTA PRV	PRF	DELTA PRF
12	3.02	.133639E+07	.223005E+06	.105657E+01	.430917E-01	.919632E+00	.147886E-01
13	3.12	.104871E+07	.160073E+06	.100483E+01	.284319E-01	.909860E+00	.103667E-01
14	3.20	.882628E+06	.124789E+06	.976443E+00	.205155E-01	.904494E+00	.810487E-02
15	3.27	.740172E+06	.110321E+06	.955428E+00	.153508E-01	.902057E+00	.711119E-02
16	3.34	.567559E+06	.887869E+05	.939991E+00	.112944E-01	.906188E+00	.647438E-02
17	3.40	.505677E+06	.755476E+05	.930916E+00	.914605E-02	.901722E+00	.545045E-02
18	3.45	.480904E+06	.665467E+05	.923697E+00	.804788E-02	.895263E+00	.462163E-02
19	3.50	.440745E+06	.611010E+05	.917616E+00	.720201E-02	.891668E+00	.418334E-02
20	3.57	.377583E+06	.534204E+05	.909689E+00	.568392E-02	.887986E+00	.357146E-02
21	3.62	.337049E+06	.536949E+05	.905583E+00	.498210E-02	.886784E+00	.352550E-02

HEAT TRANSFER CALCULATIONS: TEST 3.09.10J

LEVEL	ELEVATION (METER)	HW-TRAN (W/CM**2-K)	DELTA HW-TRAN (W/CM**2-K)	HW-LAM (W/CM**2-K)	DELTA HW-LAM (W/CM**2-K)	HW-TUR (W/CM**2-K)	DELTA HW-TUR (W/CM**2-K)
12	3.02	.000000E+00	.000000E+00	.000000E+00	.000000E+00	.130142E-01	.768025E-03
13	3.12	.000000E+00	.000000E+00	.000000E+00	.000000E+00	.137239E-01	.740246E-03
14	3.20	.000000E+00	.000000E+00	.000000E+00	.000000E+00	.142920E-01	.736189E-03
15	3.27	.000000E+00	.000000E+00	.000000E+00	.000000E+00	.147858E-01	.757508E-03
16	3.34	.000000E+00	.000000E+00	.000000E+00	.000000E+00	.150604E-01	.760516E-03
17	3.40	.000000E+00	.000000E+00	.000000E+00	.000000E+00	.155169E-01	.750693E-03
18	3.45	.000000E+00	.000000E+00	.000000E+00	.000000E+00	.160934E-01	.755534E-03
19	3.50	.000000E+00	.000000E+00	.000000E+00	.000000E+00	.165949E-01	.770194E-03
20	3.57	.000000E+00	.000000E+00	.000000E+00	.000000E+00	.173147E-01	.772124E-03
21	3.62	.176421E-01	.163448E-02	.000000E+00	.000000E+00	.000000E+00	.000000E+00

HEAT TRANSFER CALCULATIONS: TEST 3.09.10J

LEVEL	ELEVATION (METER)	HCE-TUR (W/CM**2-K)	DELTA HCE-TUR (W/CM**2-K)	HB&W (W/CM**2-K)	DELTA HB&W (W/CM**2-K)	HORNL (W/CM**2-K)	DELTA HORNL (W/CM**2-K)
12	3.02	.000000E+00	.000000E+00	.121154E-01	.102679E-02	.860586E-02	.766220E-03
13	3.12	.000000E+00	.000000E+00	.120447E-01	.944370E-03	.898903E-02	.779020E-03
14	3.20	.000000E+00	.000000E+00	.120879E-01	.920628E-03	.926728E-02	.766332E-03
15	3.27	.000000E+00	.000000E+00	.121760E-01	.911013E-03	.960363E-02	.789273E-03
16	3.34	.000000E+00	.000000E+00	.122903E-01	.881694E-03	.101416E-01	.756321E-03
17	3.40	.000000E+00	.000000E+00	.123867E-01	.864181E-03	.102810E-01	.764886E-03
18	3.45	.000000E+00	.000000E+00	.124846E-01	.874094E-03	.102942E-01	.773588E-03
19	3.50	.000000E+00	.000000E+00	.125854E-01	.885920E-03	.103891E-01	.783071E-03
20	3.57	.000000E+00	.000000E+00	.127489E-01	.870941E-03	.105918E-01	.811570E-03
21	3.62	.000000E+00	.000000E+00	.128511E-01	.864349E-03	.107583E-01	.850814E-03

HEAT TRANSFER CALCULATIONS: TEST 3.09.10J

LEVEL	ELEVATION (METER)	HEINEMAN (W/CM**2-K)	DELTA HEINEMAN (W/CM**2-K)	MCELIGOT (W/CM**2-K)	DELTA MCELIGOT (W/CM**2-K)
12	3.02	.102867E-01	.101962E-02	.909187E-02	.778084E-03
13	3.12	.104375E-01	.941035E-03	.914741E-02	.730209E-03
14	3.20	.105418E-01	.892937E-03	.927558E-02	.721901E-03
15	3.27	.105954E-01	.884460E-03	.952988E-02	.730053E-03
16	3.34	.105070E-01	.802091E-03	.100834E-01	.740134E-03
17	3.40	.106031E-01	.785530E-03	.101755E-01	.725684E-03
18	3.45	.107695E-01	.799970E-03	.101174E-01	.724583E-03
19	3.50	.108792E-01	.812876E-03	.101737E-01	.733035E-03
20	3.57	.110076E-01	.811117E-03	.103460E-01	.722331E-03
21	3.62	.110537E-01	.829725E-03	.105135E-01	.722025E-03

HEAT TRANSFER CALCULATIONS: TEST 3.09.10J

LEVEL	ELEVATION (METER)	TFIL (KELVIN)	DELTA TFIL (KELVIN)	HCE-TRAN (W/CM**2-K)	DELTA HCE-TRAN (W/CM**2-K)	HCE-LAM (W/CM**2-K)	DELTA HCE-LAM (W/CM**2-K)
12	3.02	.780482E+03	.293591E+03	.108686E-01	.240207E-02	.000000E+00	.000000E+00
13	3.12	.810462E+03	.289658E+03	.104652E-01	.196398E-02	.000000E+00	.000000E+00
14	3.20	.830575E+03	.287002E+03	.102600E-01	.176195E-02	.000000E+00	.000000E+00
15	3.27	.840794E+03	.286582E+03	.101069E-01	.164040E-02	.000000E+00	.000000E+00
16	3.34	.823893E+03	.281019E+03	.100203E-01	.148966E-02	.000000E+00	.000000E+00
17	3.40	.842258E+03	.279904E+03	.993263E-02	.139442E-02	.000000E+00	.000000E+00
18	3.45	.873739E+03	.281031E+03	.983520E-02	.137112E-02	.000000E+00	.000000E+00
19	3.50	.894497E+03	.282053E+03	.975810E-02	.136048E-02	.000000E+00	.000000E+00
20	3.57	.918910E+03	.282000E+03	.966077E-02	.127633E-02	.000000E+00	.000000E+00
21	3.62	.927731E+03	.283461E+03	.961018E-02	.123678E-02	.000000E+00	.000000E+00

126

THIS PAGE

WAS INTENTIONALLY

LEFT BLANK

TEST

3.09.10K

SYSTEM PARAMETER SUMMARY

SYSTEM PRESSURE	.400692E+01	+OR-	.206877E+00	MPA
INLET MASS FLOW	.137488E-01	+OR-	.386970E-02	KG/S
OUTLET MASS FLOW	.193361E-01	+OR-	.160184E-02	KG/S
MASS FLUX - BASED ON OUTLET FLOW	.312822E+01	+OR-	.259149E+00	KG/(M**2)S
MASS FLUX - BASED ON INLET FLOW	.222430E+01	+OR-	.626046E+00	KG/(M**2)S
INLET TEMPERATURE	.466468E+03	+OR-	.259117E+03	KELVIN
OUTLET TEMPERATURE	.638619E+03	+OR-	.259236E+03	KELVIN
BUNDLE POWER	.695667E+02	+OR-	.435457E+01	KW
AVERAGE LINEAR POWER/ROD	.316974E+00	+OR-	.198412E-01	KW/M
FRACTIONAL HEAT LOSS	.175532E+00			

HEAT TRANSFER CALCULATIONS: TEST 3.09.10K

LEVEL	ELEVATION (METER)	TVAP (KELVIN)	DELTA TVAP (KELVIN)	NO. OF TC S	TW (KELVIN)	DELTA TW (KELVIN)	Q"/Q"SS	Q"HTRAN (W/CM**2)	DELTA Q"HTRAN (W/CM**2)
5	2.42	.565336E+03	.308364E+03	28.	.768316E+03	.268021E+03	.972225E+00	.108859E+01	.698199E-01
6	2.51	.597368E+03	.308086E+03	2.	.790347E+03	.257048E+03	.977813E+00	.109002E+01	.624730E-01
7	2.58	.622641E+03	.305603E+03	2.	.815314E+03	.255598E+03	.975756E+00	.111153E+01	.637219E-01
8	2.66	.648816E+03	.304746E+03	5.	.839620E+03	.268862E+03	.980469E+00	.111510E+01	.626391E-01
9	2.84	.706920E+03	.300866E+03	1.	.868739E+03	.255405E+03	.981044E+00	.109180E+01	.556448E-01
10	2.89	.726059E+03	.300984E+03	3.	.888227E+03	.270903E+03	.977747E+00	.110517F+01	.648300E-01
11	2.97	.753179E+03	.301007E+03	4.	.914797E+03	.263825E+03	.977040E+00	.112283E+01	.593299E-01
12	3.02	.772719E+03	.299021E+03	22.	.915549E+03	.270715E+03	.960045E+00	.108756E+01	.703197E-01
13	3.12	.809211E+03	.295409E+03	5.	.934066E+03	.267718E+03	.958717E+00	.108795E+01	.646747E-01
14	3.20	.833851E+03	.297174E+03	4.	.943869E+03	.267960E+03	.953312E+00	.107704E+01	.610596E-01
15	3.27	.854821E+03	.298260E+03	4.	.961158E+03	.260486E+03	.927879E+00	.105792E+01	.609566E-01
16	3.34	.876297E+03	.296640E+03	1.	.963127E+03	.255702E+03	.926923E+00	.103157E+01	.556448E-01
17	3.40	.891573E+03	.295517E+03	2.	.987453E+03	.261490E+03	.916793E+00	.104654E+01	.638550E-01
18	3.45	.902684E+03	.294690E+03	3.	.995097E+03	.276282E+03	.919178E+00	.104534E+01	.656608E-01
19	3.50	.912934E+03	.293992E+03	6.	.997882E+03	.273057E+03	.901293E+00	.102807E+01	.638995E-01
20	3.57	.926789E+03	.293147E+03	6.	.997631E+03	.270618E+03	.876808E+00	.997103E+00	.637536E-01
21	3.62	.934966E+03	.292704E+03	17.	.999645E+03	.281693E+03	.874654E+00	.989527E+00	.700269E-01

HEAT TRANSFER CALCULATIONS: TEST 3.09.10K

LEVEL	ELEVATION (METER)	HEXP (W/CM**2-K)	DELTA HEXP (W/CM**2-K)	REV	DELTA REV	REF	DELTA REF
5	2.42	.488496E-02	.106347E-02	.193471E+04	.311253E+03	.152757E+04	.218534E+03
6	2.51	.565179E-02	.134053E-02	.178668E+04	.262599E+03	.148717E+04	.199635E+03
7	2.53	.577246E-02	.129301E-02	.168379E+04	.212981E+03	.143124E+04	.180954E+03
8	2.66	.584775E-02	.124763E-02	.159663E+04	.185088E+03	.137902E+04	.169386E+03
9	2.84	.675110E-02	.141378E-02	.145757E+04	.157825E+03	.129709E+04	.143649E+03
10	2.89	.681903E-02	.136324E-02	.141620E+04	.151791E+03	.126378E+04	.140143E+03
11	2.97	.695163E-02	.135240E-02	.136137E+04	.143778E+03	.122019E+04	.131685E+03
12	3.02	.761897E-02	.152794E-02	.132437E+04	.136264E+03	.120448E+04	.127371E+03
13	3.12	.871900E-02	.163899E-02	.126032E+04	.124190E+03	.116382E+04	.116824E+03
14	3.20	.979561E-02	.175847E-02	.122040E+04	.120675E+03	.113971E+04	.114657E+03
15	3.27	.995471E-02	.180371E-02	.118835E+04	.117493E+03	.111407E+04	.111065E+03
16	3.34	.118876E-01	.213845E-02	.115720E+04	.112337E-03	.109891E+04	.107181E+03
17	3.40	.109217E-01	.172769E-02	.113600E+04	.108966E-03	.107421E+04	.103761E+03
18	3.45	.113184E-01	.170100E-02	.112106E+04	.106639E-03	.106289E+04	.104227E+03
19	3.50	.121097E-01	.176028E-02	.110762E+04	.104625E+03	.105516E+04	.101963E+03
20	3.57	.140836E-01	.202241E-02	.108995E+04	.102087E+03	.104721E+04	.998077E+02
21	3.62	.153083E-01	.223764E-02	.107978E+04	.100682E+03	.104134E+04	.101568E+03

HEAT TRANSFER CALCULATIONS: . TEST 3.09.10K

LEVEL	ELEVATION (METER)	QRAD (W/CM**2)	DELTA QRAD (W/CM**2)	HCONV (W/CM**2-K)	DELTA HCONV (W/CM**2-K)
5	2.42	.466271E+00	.124434E+00	.235947E-02	.139717E-02
6	2.51	.433779E+00	.120614E+00	.294590E-02	.168659E-02
7	2.58	.480510E+00	.130959E+00	.277582E-02	.169421E-02
8	2.66	.526210E+00	.153866E+00	.253992E-02	.175139E-02
9	2.84	.526729E+00	.156392E+00	.286339E-02	.201997E-02
10	2.89	.566295E+00	.184296E+00	.265314E-02	.209955E-02
11	2.97	.620481E+00	.191316E+00	.238377E-02	.215927E-02
12	3.02	.568174E+00	.199521E+00	.289388E-02	.243281E-02
13	3.12	.545285E+00	.197084E+00	.354648E-02	.264692E-02
14	3.20	.508795E+00	.211633E+00	.432945E-02	.297810E-02
15	3.27	.522910E+00	.218118E+00	.415195E-02	.312807E-02
16	3.34	.443671E+00	.214656E+00	.586946E-02	.365528E-02
17	3.40	.520285E+00	.227729E+00	.453752E-02	.334374E-02
18	3.45	.516040E+00	.265867E+00	.475485E-02	.374640E-02
19	3.50	.484002E+00	.255330E+00	.541873E-02	.388386E-02
20	3.57	.412402E+00	.246772E+00	.725596E-02	.441988E-02
21	3.62	.382464E+00	.288050E+00	.837809E-02	.537401E-02

HEAT TRANSFER CALCULATIONS: TEST 3.09.10K

LEVEL	ELEVATION (METER)	HRAD (W/CM**2-K)	DELTA HRAD (W/CM**2-K)	REW	DELTA REW	QCRODM (W/CM**2)	DELTA QCRODM (W/CM**2)
5	2.42	.252548E-02	.906154E-03	.845141E+03	.107060E+03	.965233E-01	.400894E-01
6	2.51	.270588E-02	.102351E-02	.914889E+03	.106492E+03	.880856E-01	.360358E-01
7	2.58	.299664E-02	.109474E-02	.905653E+03	.103093E+03	.965145E-01	.388206E-01
8	2.66	.330784E-02	.122915E-02	.896835E+03	.102711E+03	.104557E+00	.412770E-01
9	2.84	.388771E-02	.144274E-02	.925715E+03	.995241E+02	.102000E+00	.388785E-01
10	2.89	.416590E-02	.159677E-02	.910747E+03	.100361E+03	.103876E+00	.400297E-01
11	2.97	.456786E-02	.168329E-02	.891997E+03	.955925E+02	.117323E+00	.428612E-01
12	3.02	.472509E-02	.189314E-02	.916748E+03	.989555E+02	.106305E+00	.384545E-01
13	3.12	.517252E-02	.207843E-02	.924969E+03	.975357E+02	.108140E+00	.353222E-01
14	3.20	.546616E-02	.240351E-02	.935085E+03	.977785E+02	.922158E-01	.320025E-01
15	3.27	.580277E-02	.255567E-02	.924463E+03	.948147E+02	.937688E-01	.319688E-01
16	3.34	.601813E-02	.296447E-02	.945600E+03	.957958E+02	.785640E-01	.264763E-01
17	3.40	.638420E-02	.286281E-02	.913780E+03	.931634E+02	.914640E-01	.316566E-01
18	3.45	.656356E-02	.333798E-02	.911045E+03	.965970E+02	.901528E-01	.311020E-01
19	3.50	.669100E-02	.346205E-02	.916710E+03	.956875E+02	.840396E-01	.289496E-01
20	3.57	.682766E-02	.393004E-02	.932085E+03	.959830E+02	.709882E-01	.244397E-01
21	3.62	.693018E-02	.488600E-02	.936849E+03	.100701E+03	.655028E-01	.225403E-01

HEAT TRANSFER CALCULATIONS: TEST 3.09.10K

LEVEL	ELEVATION (METER)	GRX	DELTA GRX	PRV	DELTA PRV	PRF	DELTA PRF
5	2.42	.212296E+07	.775700E+06	.118666E+01	.123843E+00	.983454E+00	.546257E-01
6	2.51	.156704E+07	.576463E+06	.110274E+01	.854914E-01	.967108E+00	.428166E-01
7	2.58	.125413E+07	.430863E+06	.105760E+01	.705714E-01	.948208E+00	.317153E-01
8	2.66	.100803E+07	.345217E+06	.102034E+01	.573882E-01	.933792E+00	.246115E-01
9	2.84	.611559E+06	.202775E+06	.956610E+00	.269930E-01	.915946E+00	.149908E-01
10	2.89	.532988E+06	.184144E+06	.943769E+00	.222091E-01	.909971E+00	.132484E-01
11	2.97	.440776E+06	.146294E+06	.929506E+00	.172017E-01	.903016E+00	.107302E-01
12	3.02	.363781E+06	.131396E+06	.921342E+00	.140238E-01	.900717E+00	.970600E-02
13	3.12	.265584E+06	.967498E+05	.909384E+00	.983869E-02	.895217E+00	.738812E-02
14	3.20	.209839E+06	.885302E+05	.903048E+00	.860903E-02	.892235E+00	.679818E-02
15	3.27	.180234E+06	.774154E+05	.898462E+00	.768382E-02	.889271E+00	.601778E-02
16	3.34	.137107E+06	.676743E+05	.894379E+00	.650259E-02	.887618E+00	.531191E-02
17	3.40	.134665E+06	.596298E+05	.891793E+00	.578393E-02	.885076E+00	.464754E-02
18	3.45	.122921E+06	.615667E+05	.890059E+00	.531004E-02	.883974E+00	.463108E-02
19	3.50	.108839E+06	.562945E+05	.888560E+00	.491269E-02	.883245E+00	.426894E-02
20	3.57	.873169E+05	.514854E+05	.886674E+00	.442822E-02	.882514E+00	.392183E-02
21	3.62	.774577E+05	.558133E+05	.885633E+00	.416753E-02	.881987E+00	.410815E-02

HEAT TRANSFER CALCULATIONS: TEST 3.09.10K

LEVEL	ELEVATION (METER)	HW-TRAN (W/CM**2-K)	DELTA HW-TRAN (W/CM**2-K)	HW-LAM (W/CM**2-K)	DELTA HW-LAM (W/CM**2-K)	HW-TUR (W/CM**2-K)	DELTA HW-TUR (W/CM**2-K)
5	2.42	.000000E+00	.000000E+00	.402229E-02	.320719E-03	.000000E+00	.000000E+00
6	2.51	.000000E+00	.000000E+00	.428344E-02	.338304E-03	.000000E+00	.000000E+00
7	2.58	.000000E+00	.000000E+00	.466643E-02	.347185E-03	.000000E+00	.000000E+00
8	2.66	.000000E+00	.000000E+00	.508495E-02	.380436E-03	.000000E+00	.000000E+00
9	2.84	.000000E+00	.000000E+00	.592054E-02	.379718E-03	.000000E+00	.000000E+00
10	2.89	.000000E+00	.000000E+00	.629710E-02	.421331E-03	.000000E+00	.000000E+00
11	2.97	.000000E+00	.000000E+00	.684987E-02	.430134E-03	.000000E+00	.000000E+00
12	3.02	.000000E+00	.000000E+00	.710213E-02	.441426E-03	.000000E+00	.000000E+00
13	3.12	.000000E+00	.000000E+00	.775063E-02	.425199E-03	.000000E+00	.000000E+00
14	3.20	.000000E+00	.000000E+00	.818345E-02	.461650E-03	.000000E+00	.000000E+00
15	3.27	.000000E+00	.000000E+00	.865387E-02	.475711E-03	.000000E+00	.000000E+00
16	3.34	.000000E+00	.000000E+00	.898977E-02	.468006E-03	.000000E+00	.000000E+00
17	3.40	.000000E+00	.000000E+00	.947727E-02	.476682E-03	.000000E+00	.000000E+00
18	3.45	.000000E+00	.000000E+00	.973249E-02	.532072E-03	.000000E+00	.000000E+00
19	3.50	.000000E+00	.000000E+00	.992423E-02	.514656E-03	.000000E+00	.000000E+00
20	3.57	.000000E+00	.000000E+00	.101421E-01	.501699E-03	.000000E+00	.000000E+00
21	3.62	.000000E+00	.000000E+00	.102968E-01	.567147E-03	.000000E+00	.000000E+00

HEAT TRANSFER CALCULATIONS: TEST 3.09.10K

LEVEL	ELEVATION (METER)	HCE-TUR (W/CM**2-K)	DELTA HCE-TUR (W/CM**2-K)	HB&W (W/CM**2-K)	DELTA HB&W (W/CM**2-K)	HORNL (W/CM**2-K)	DELTA HORNL (W/CM**2-K)
5	2.42	.000000E+00	.000000E+00	.424051E-02	.669787E-03	.266385E-02	.278044E-03
6	2.51	.000000E+00	.000000E+00	.402922E-02	.631573E-03	.284762E-02	.266157E-03
7	2.58	.000000E+00	.000000E+00	.394498E-02	.568402E-03	.293959E-02	.268245E-03
8	2.66	.000000E+00	.000000E+00	.391142E-02	.537245E-03	.303027E-02	.286377E-03
9	2.84	.000000E+00	.000000E+00	.395713E-02	.492061E-03	.325044E-02	.279744E-03
10	2.89	.000000E+00	.000000E+00	.398674E-02	.489090E-03	.330376E-02	.302526E-03
11	2.97	.000000E+00	.000000E+00	.403598E-02	.484329E-03	.337869E-02	.293121E-03
12	3.02	.000000E+00	.000000E+00	.407513E-02	.466804E-03	.345725E-02	.309509E-03
13	3.12	.000000E+00	.000000E+00	.415333E-02	.437625E-03	.357584E-02	.308925E-03
14	3.20	.000000E+00	.000000E+00	.420835E-02	.446840E-03	.365745E-02	.313551E-03
15	3.27	.000000E+00	.000000E+00	.425585E-02	.451756E-03	.371259E-02	.305988E-03
16	3.34	.000000E+00	.000000E+00	.430487E-02	.439542E-03	.379063E-02	.307316E-03
17	3.40	.000000E+00	.000000E+00	.433974E-02	.431530E-03	.381230E-02	.312780E-03
18	3.45	.000000E+00	.000000E+00	.436507E-02	.425895E-03	.384222E-02	.344352E-03
19	3.50	.000000E+00	.000000E+00	.438838E-02	.421255E-03	.387564E-02	.337206E-03
20	3.57	.000000E+00	.000000E+00	.441977E-02	.415787E-03	.392624E-02	.333907E-03
21	3.62	.000000E+00	.000000E+00	.443822E-02	.412985E-03	.395283E-02	.368701E-03

HEAT TRANSFER CALCULATIONS: TEST 3.09.10K

LEVEL	ELEVATION (METER)	HEINEMAN (W/CM**2-K)	DELTA HEINEMAN (W/CM**2-K)	MCELIGOT (W/CM**2-K)	DELTA MCELIGOT (W/CM**2-K)
5	2.42	.304553E-02	.580747E-03	.327906E-02	.511034E-03
6	2.51	.305885E-02	.538386E-03	.319856E-02	.507644E-03
7	2.58	.308552E-02	.502539E-03	.314789E-02	.462935E-03
8	2.66	.311818E-02	.489177E-03	.313957E-02	.443230E-03
9	2.84	.318290E-02	.426252E-03	.325935E-02	.419841E-03
10	2.89	.321350E-02	.431734E-03	.329118E-02	.418688E-03
11	2.97	.325706E-02	.418096E-03	.334383E-02	.416339E-03
12	3.02	.327371E-02	.405485E-03	.341835E-02	.405865E-03
13	3.12	.331902E-02	.372991E-03	.352974E-02	.334472E-03
14	3.20	.334739E-02	.377562E-03	.361162E-02	.396649E-03
15	3.27	.337877E-02	.374080E-03	.366464E-02	.402400E-03
16	3.34	.339789E-02	.359823E-03	.374924E-02	.395354E-03
17	3.40	.342995E-02	.355573E-03	.376516E-02	.386196E-03
18	3.45	.344500E-02	.368068E-03	.379599E-02	.381702E-03
19	3.50	.345541E-02	.358093E-03	.383250E-02	.378834E-03
20	3.57	.346623E-02	.348746E-03	.388958E-02	.376384E-03
21	3.62	.347430E-02	.366628E-03	.391905E-02	.374899E-03

HEAT TRANSFER CALCULATIONS: TEST 3.09.10K

LEVEL	ELEVATION (METER)	TFIL (KELVIN)	DELTA TFIL (KELVIN)	HCE-TRAN (W/CM**2-K)	DELTA HCE-TRAN (W/CM**2-K)	HCE-LAM (W/CM**2-K)	DELTA HCE-LAM (W/CM**2-K)
5	2.42	.676826E+03	.328175E+03	.000000E+00	.000000E+00	.322564E-02	.117549E-02
6	2.51	.693857E+03	.323010E+03	.000000E+00	.000000E+00	.296307E-02	.881398E-03
7	2.58	.718977E+03	.318813E+03	.000000E+00	.000000E+00	.283941E-02	.735608E-03
8	2.66	.744218E+03	.317800E+03	.000000E+00	.000000E+00	.274789E-02	.631128E-03
9	2.84	.787829E+03	.309042E+03	.000000E+00	.000000E+00	.267290E-02	.480227E-03
10	2.89	.807143E+03	.310580E+03	.000000E+00	.000000E+00	.266600E-02	.457349E-03
11	2.97	.833988E+03	.308970E+03	.000000E+00	.000000E+00	.266979E-02	.425140E-03
12	3.02	.844134E+03	.306945E+03	.000000E+00	.000000E+00	.268969E-02	.404176E-03
13	3.12	.871639E+03	.301355E+03	.000000E+00	.000000E+00	.272242E-02	.364167E-03
14	3.20	.888860E+03	.302634E+03	.000000E+00	.000000E+00	.274163E-02	.353662E-03
15	3.27	.907989E+03	.302329E+03	.000000E+00	.000000E+00	.274759E-02	.339661E-03
16	3.34	.919712E+03	.299538E+03	.000000E+00	.000000E+00	.276843E-02	.320869E-03
17	3.40	.939513E+03	.298947E+03	.000000E+00	.000000E+00	.277260E-02	.309384E-03
18	3.45	.948891E+03	.301890E+03	.000000E+00	.000000E+00	.277028E-02	.302223E-03
19	3.50	.955408E+03	.299739E+03	.000000F+00	.000000E+00	.276980E-02	.291784E-03
20	3.57	.962210E+03	.297754E+03	.000000E+00	.000000E+00	.276901E-02	.278872E-03
21	3.62	.967306E+03	.301943E+03	.000000E+00	.000000E+00	.276707E-02	.274970E-03

THIS PAGE

WAS INTENTIONALLY

LEFT BLANK

TEST

3.09.10L

SYSTEM PARAMETER SUMMARY

SYSTEM PRESSURE	.751656E+01	+OR-	.206381E+00	MPA
INLET MASS FLOW	.000000E+00	+OR-	.000000E+00	KG/S
OUTLET MASS FLOW	.179916E+00	+OR-	.100759E-01	KG/S
MASS FLUX - BASED ON OUTLET FLOW	.291071E+02	+OR-	.163009E+01	KG/(M**2)S
MASS FLUX - BASED ON INLET FLOW	.000000E+00	+OR-	.000000E+00	KG/(M**2)S
INLET TEMPERATURE	.461324E+03	+OR-	.259117E+03	KELVIN
OUTLET TEMPERATURE	.715556E+03	+OR-	.259260E+03	KELVIN
BUNDLE POWER	.475827E+03	+OR-	.253332E+02	KW
AVERAGE LINEAR POWER/ROD	.216806E+01	+OR-	.115429E+00	KW/M
FRACTIONAL HEAT LOSS	.170706E-01			

HEAT TRANSFER CALCULATIONS: TEST 3.09.10L

LEVEL	ELEVATION (METER)	TVAP (KELVIN)	DELTA TVAP (KELVIN)	NO. OF TC S	TW (KELVIN)	DELTA TW (KELVIN)	Q"/Q"SS	Q"HTRAN (W/CM**2)	DELTA Q"HTRAN (W/CM**2)
12	3.02	.574712E+03	.274697E+03	22.	.909232E+03	.275175E+03	.988237E+00	.743256E+01	.410515E+00
13	3.12	.596938E+03	.274636E+03	5.	.960180E+03	.267712E+03	.986180E+00	.739421E+01	.425150E+00
14	3.20	.614537E+03	.274109E+03	4.	.985814E+03	.265180E+03	.986635E+00	.744862E+01	.387624E+00
15	3.27	.632161E+03	.274497E+03	4.	.987984E+03	.270234E+03	.989714E+00	.741369E+01	.433141E+00
16	3.34	.649360E+03	.275611E+03	1.	.859821E+03	.255651E+03	.993061E+00	.708053E+01	.356500E+00
17	3.40	.663398E+03	.274716E+03	2.	.892403E+03	.262919E+03	.991591E+00	.731960E+01	.446626E+00
18	3.45	.676690E+03	.275166E+03	3.	.945910E+03	.257424E+03	.992250E+00	.747207E+01	.381595E+00
19	3.50	.689630E+03	.274929E+03	6.	.973096E+03	.259925E+03	.991058E+00	.741099E+01	.409230E+00
20	3.57	.708571E+03	.275536E+03	6.	.993451E+03	.266163E+03	.990621E+00	.742993E+01	.417340E+00
21	3.62	.720612E+03	.275407E+03	17.	.999945E+03	.265196E+03	.987512E+00	.741609E+01	.402807E+00

HEAT TRANSFER CALCULATIONS: TEST 3.09.10L

LEVEL	ELEVATION (METER)	HEXP (W/CM**2-K)	DELTA HEXP (W/CM**2-K)	REV	DELTA REV	REF	DELTA REF
12	3.02	.222320E-01	.155076E-02	.177180E+05	.138841E+04	.126738E+05	.881770E+03
13	3.12	.203684E-01	.138635E-02	.165996E+05	.130140E+04	.120561E+05	.801684E+03
14	3.20	.200743E-01	.125845E-02	.157614E+05	.117232E+04	.117172E+05	.756969E+03
15	3.27	.208479E-01	.135876E-02	.149561E+05	.923811E+03	.115681E+05	.753029E+03
16	3.34	.336632E-01	.219278E-02	.145082E+05	.871840E+03	.124542E+05	.782934E+03
17	3.40	.319819E-01	.227568E-02	.142166E+05	.850498E+03	.120668E+05	.751033E+03
18	3.45	.277713E-01	.167091E-02	.139329E+05	.835206E+03	.115498E+05	.715388E+03
19	3.50	.261599E-01	.164941E-02	.136660E+05	.813736E+03	.112592E+05	.692809E+03
20	3.57	.260966E-01	.164767E-02	.132912E+05	.792929E+03	.109878E+05	.684282E+03
21	3.62	.265653E-01	.163087E-02	.130624E+05	.775338E+03	.108642E+05	.669666E+03

HEAT TRANSFER CALCULATIONS: TEST 3.09.10L

LEVEL	ELEVATION (METER)	QRAD (W/CM**2)	DELTA QRAD (W/CM**2)	HCONV (W/CM**2-K)	DELTA HCONV (W/CM**2-K)
12	3.02	.103532E+01	.234667E+00	.185117E-01	.184857E-02
13	3.12	.130303E+01	.271640E+00	.160582E-01	.176686E-02
14	3.20	.144824E+01	.296314E+00	.153912E-01	.172024E-02
15	3.27	.144033E+01	.306450E+00	.159942E-01	.187210E-02
16	3.34	.677406E+00	.140680E+00	.298119E-01	.239930E-02
17	3.40	.809517E+00	.170843E+00	.277535E-01	.251764E-02
18	3.45	.108637E+01	.220421E+00	.229460E-01	.205247E-02
19	3.50	.123391E+01	.251060E+00	.209568E-01	.209121E-02
20	3.57	.133030E+01	.280644E+00	.205177E-01	.216880E-02
21	3.62	.134611E+01	.282518E+00	.208097E-01	.218127E-02

HEAT TRANSFER CALCULATIONS: TEST 3.09.10L

LEVEL	ELEVATION (METER)	HRAD (W/CM**2-K)	DELTA HRAD (W/CM**2-K)	REW	DELTA REW	QCRODM (W/CM**2)	DELTA QCRODM (W/CM**2)
12	3.02	.372025E-02	.100615E-02	.509078E+04	.518666E+03	.208426E+00	.975077E-01
13	3.12	.431027E-02	.109530E-02	.498326E+04	.446635E+03	.261697E+00	.121874E+00
14	3.20	.468305E-02	.117284E-02	.500834E+04	.422250E+03	.289421E+00	.134611E+00
15	3.27	.485372E-02	.124428E-02	.525859E+04	.431125E+03	.285695E+00	.132347E+00
16	3.34	.385125E-02	.973848E-03	.745633E+04	.521882E+03	.132646E+00	.613995E-01
17	3.40	.422845E-02	.107693E-02	.711173E+04	.504549E+03	.158234E+00	.730701E-01
18	3.45	.482527E-02	.119193E-02	.645947E+04	.454988E+03	.211909E+00	.976051E-01
19	3.50	.520309E-02	.128553E-02	.624996E+04	.440333E+03	.240108E+00	.110352E+00
20	3.57	.557887E-02	.141027E-02	.621432E+04	.441730E+03	.258053E+00	.118252E+00
21	3.62	.575559E-02	.144851E-02	.627269E+04	.439282E+03	.260649E+00	.119233E+00

HEAT TRANSFER CALCULATIONS: TEST 3.09.10L

LEVEL	ELEVATION (METER)	GRX	DELTA GRX	PRV	DELTA PRV	PRF	DELTA PRF
12	3.02	.755156E+07	.113525E+07	.145483E+01	.121626E+00	.972813E+00	.369224E-01
13	3.12	.595245E+07	.759212E+06	.132235E+01	.776629E-01	.943194E+00	.236209E-01
14	3.20	.510692E+07	.598016E+06	.125227E+01	.580397E-01	.930594E+00	.183289E-01
15	3.27	.453063E+07	.555860E+06	.120352E+01	.649964E-01	.925704E+00	.163537E-01
16	3.34	.423778E+07	.565930E+06	.114651E+01	.587733E-01	.961158E+00	.210004E-01
17	3.40	.377335E+07	.481297E+06	.110445E+01	.460377E-01	.943626E+00	.163637E-01
18	3.45	.339566E+07	.389805E+06	.107222E+01	.396920E-01	.925130E+00	.123268E-01
19	3.50	.307392E+07	.342222E+06	.104565E+01	.334126E-01	.916655E+00	.103413E-01
20	3.57	.267996E+07	.319377E+06	.101375E+01	.271294E-01	.909727E+00	.903972E-02
21	3.62	.246188E+07	.287803E+06	.997037E+00	.232914E-01	.906840E+00	.814603E-02

HEAT TRANSFER CALCULATIONS: TEST 3.09.10L

LEVEL	ELEVATION (METER)	HW-TRAN (W/CM**2-K)	DELTA HW-TRAN (W/CM**2-K)	HW-LAM (W/CM**2-K)	DELTA HW-LAM (W/CM**2-K)	HW-TUR (W/CM**2-K)	DELTA HW-TUR (W/CM**2-K)
12	3.02	.000000E+00	.000000E+00	.000000E+00	.000000E+00	.253639E-01	.165527E-02
13	3.12	.000000E+00	.000000E+00	.000000E+00	.000000E+00	.238545E-01	.127784E-02
14	3.20	.000000E+00	.000000E+00	.000000E+00	.000000E+00	.233357E-01	.116010E-02
15	3.27	.000000E+00	.000000E+00	.000000E+00	.000000E+00	.230891E-01	.100119E-02
16	3.34	.000000E+00	.000000E+00	.000000E+00	.000000E+00	.235116E-01	.109140E-02
17	3.40	.000000E+00	.000000E+00	.000000E+00	.000000E+00	.237165E-01	.109584E-02
18	3.45	.000000E+00	.000000E+00	.000000E+00	.000000E+00	.239363E-01	.110293E-02
19	3.50	.000000E+00	.000000E+00	.000000E+00	.000000E+00	.242592E-01	.110639E-02
20	3.57	.000000E+00	.000000E+00	.000000E+00	.000000E+00	.247983E-01	.114737E-02
21	3.62	.000000E+00	.000000E+00	.000000E+00	.000000E+00	.251627E-01	.115683E-02

HEAT TRANSFER CALCULATIONS: TEST 3.09.10L

LEVEL	ELEVATION (METER)	HCE-TUR (W/CM**2-K)	DELTA HCE-TUR (W/CM**2-K)	HB&W (W/CM**2-K)	DELTA HB&W (W/CM**2-K)	HCRNL (W/CM**2-K)	DELTA HORNL (W/CM**2-K)
12	3.02	.348518E-01	.287576E-02	.348518E-01	.287576E-02	.140277E-01	.123967E-02
13	3.12	.305940E-01	.209388E-02	.305940E-01	.209388E-02	.147594E-01	.110013E-02
14	3.20	.285709E-01	.182178E-02	.285709E-01	.182178E-02	.153170E-01	.106058E-02
15	3.27	.271801E-01	.156048E-02	.271801E-01	.156048E-02	.159704E-01	.110047E-02
16	3.34	.264248E-01	.153992E-02	.264248E-01	.153992E-02	.177827E-01	.100179E-02
17	3.40	.260365E-01	.149871E-02	.260365E-01	.149871E-02	.179123E-01	.104115E-02
18	3.45	.257676E-01	.150372E-02	.257676E-01	.150372E-02	.178269E-01	.100906E-02
19	3.50	.255868E-01	.148585E-02	.255868E-01	.148585E-02	.179902E-01	.102278E-02
20	3.57	.254338E-01	.149753E-02	.254338E-01	.149753E-02	.183801E-01	.108025E-02
21	3.62	.253909E-01	.148713E-02	.253909E-01	.148713E-02	.186704E-01	.107569E-02

HEAT TRANSFER CALCULATIONS: TEST 3.09.10L

LEVEL	ELEVATION (METER)	HEINEMAN (W/CM**2-K)	DELTA HEINEMAN (W/CM**2-K)	MCELIGOT (W/CM**2-K)	DELTA MCELIGOT (W/CM**2-K)
12	3.02	.214689E-01	.178710E-02	.253018E-01	.195538E-02
13	3.12	.216177E-01	.166322E-02	.220273E-01	.142147E-02
14	3.20	.217548E-01	.159082E-02	.205986E-01	.126163E-02
15	3.27	.218259E-01	.161593E-02	.198528E-01	.106762E-02
16	3.34	.215054E-01	.147270E-02	.209686E-01	.116411E-02
17	3.40	.216140E-01	.146105E-02	.204979E-01	.115131E-02
18	3.45	.218350E-01	.147059E-02	.199006E-01	.114809E-02
19	3.50	.219920E-01	.146514E-02	.196684E-01	.113998E-02
20	3.57	.221573E-01	.151283E-02	.196133E-01	.116437E-02
21	3.62	.222381E-01	.148862E-02	.196816E-01	.116726E-02

HEAT TRANSFER CALCULATIONS: TEST 3.09.10L

LEVEL	ELEVATION (METER)	TFIL (KELVIN)	DELTA TFIL (KELVIN)	HCE-TRAN (W/CM**2-K)	DELTA HCE-TRAN (W/CM**2-K)	HCE-LAM (W/CM**2-K)	DELTA HCE-LAM (W/CM**2-K)
12	3.02	.741972E+03	.288402E+03	.000000E+00	.000000E+00	.000000E+00	.000000E+00
13	3.12	.778559E+03	.286367E+03	.000000E+00	.000000E+00	.000000E+00	.000000E+00
14	3.20	.800176E+03	.284813E+03	.000000E+00	.000000E+00	.000000E+00	.000000E+00
15	3.27	.810073E+03	.285787E+03	.000000E+00	.000000E+00	.000000E+00	.000000E+00
16	3.34	.754591E+03	.281057E+03	.000000E+00	.000000E+00	.000000E+00	.000000E+00
17	3.40	.777900E+03	.280971E+03	.000000E+00	.000000E+00	.000000E+00	.000000E+00
18	3.45	.811300E+03	.281595E+03	.000000E+00	.000000E+00	.000000E+00	.000000E+00
19	3.50	.831363E+03	.281630E+03	.000000E+00	.000000E+00	.000000E+00	.000000E+00
20	3.57	.851011E+03	.283341E+03	.000000E+00	.000000E+00	.000000E+00	.000000E+00
21	3.62	.860278E+03	.282687E+03	.000000E+00	.000000E+00	.000000E+00	.000000E+00

THIS PAGE

WAS INTENTIONALLY

LEFT BLANK

TEST

3.09.10M

SYSTEM PARAMETER SUMMARY

SYSTEM PRESSURE	.695626E+01	+OR-	.206836E+00	MPA
INLET MASS FLOW	.826878E-01	+OR-	.383885E-02	KG/S
OUTLET MASS FLOW	.780733E-01	+OR-	.444501E-02	KG/S
MASS FLUX - BASED ON OUTLET FLOW	.126308E+02	+OR-	.719121E+00	KG/(M**2)S
MASS FLUX - BASED ON INLET FLOW	.133774E+02	+OR-	.621055E+00	KG/(M**2)S
INLET TEMPERATURE	.474433E+03	+OR-	.259112E+03	KELVIN
OUTLET TEMPERATURE	.746549E+03	+OR-	.259289E+03	KELVIN
BUNDLE POWER	.224455E+03	+OR-	.121239E+02	KW
AVERAGE LINEAR POWER/ROD	.102271E+01	+OR-	.552412E-01	KW/M
FRACTIONAL HEAT LOSS	.422668E-01			

HEAT TRANSFER CALCULATIONS: TEST 3.09.10M

LEVEL	ELEVATION (METER)	TVAP (KELVIN)	DELTA TVAP (KELVIN)	NO. OF TC S	TW (KELVIN)	DELTA TW (KELVIN)	Q"/Q"SS	Q"HTRAN (W/CM**2)	DELTA Q"HTRAN (W/CM**2)
12	3.02	.631011E+03	.272498E+03	22.	.849258E+03	.266511E+03	.100000E+01	.353755E+01	.197621E+00
13	3.12	.658490E+03	.271500E+03	5.	.875811E+03	.263199E+03	.100000E+01	.352368E+01	.201501E+00
14	3.20	.679156E+03	.271407E+03	4.	.901479E+03	.260563E+03	.100000E+01	.354236E+01	.182302E+00
15	3.27	.699758E+03	.270598E+03	4.	.923076E+03	.260487E+03	.100000E+01	.353615E+01	.205998E+00
16	3.34	.719427E+03	.270116E+03	1.	.875106E+03	.255507E+03	.100000E+01	.335672E+01	.167836E+00
17	3.40	.734224E+03	.269561E+03	2.	.905630E+03	.262944E+03	.100000E+01	.349330E+01	.221727E+00
18	3.45	.747820E+03	.269701E+03	3.	.946836E+03	.256144E+03	.100000E+01	.352860E+01	.181262E+00
19	3.50	.761256E+03	.269543E+03	6.	.978404E+03	.258658E+03	.100000E+01	.352447E+01	.197192E+00
20	3.57	.780799E+03	.268924E+03	6.	.100711E+04	.263556E+03	.100000E+01	.353226E+01	.198792E+00
21	3.62	.792765E+03	.269232E+03	17.	.101723E+04	.264626E+03	.100000E+01	.352834E+01	.192946E+00

HEAT TRANSFER CALCULATIONS: TEST 3.09.10M

LEVEL	ELEVATION (METER)	HEXP (W/CM**2-K)	DELTA HEXP (W/CM**2-K)	REV	DELTA REV	REF	DELTA REF
12	3.02	.162187E-01	.148622E-02	.653974E+04	.410898E+03	.552830E+04	.351108E+03
13	3.12	.162240E-01	.142416E-02	.623909E+04	.370108E+03	.532520E+04	.326088E+03
14	3.20	.159429E-01	.130870E-02	.604415E+04	.356591E+03	.516280E+04	.311534E+03
15	3.27	.158441E-01	.130197E-02	.586031E+04	.341420E+03	.502147E+04	.298105E+03
16	3.34	.215748E-01	.180290E-02	.569409E+04	.329004E+03	.511489E+04	.298098E+03
17	3.40	.203925E-01	.174604E-02	.557470E+04	.319695E+03	.496686E+04	.290254E+03
18	3.45	.177409E-01	.129503E-02	.546905E+04	.313347E+03	.479854E+04	.277291E+03
19	3.50	.162405E-01	.120602E-02	.536829E+04	.306537E+03	.466835E+04	.269260E+03
20	3.57	.156172E-01	.113511E-02	.522788E+04	.296245E+03	.453619E+04	.261578E+03
21	3.62	.157284E-01	.112158E-02	.514531E+04	.291801E+03	.447810E+04	.259042E+03

HEAT TRANSFER CALCULATIONS: TEST 3.09.10M

LEVEL	ELEVATION (METER)	QRAD (W/CM**2)	DELTA QRAD (W/CM**2)	HCONV (W/CM**2-K)	DELTA HCONV (W/CM**2-K)
12	3.02	.653220E+00	.142504E+00	.126353E-01	.176709E-02
13	3.12	.724945E+00	.152556E+00	.122352E-01	.175738E-02
14	3.20	.811350E+00	.167203E+00	.115826E-01	.171260E-02
15	3.27	.882506E+00	.181319E+00	.111267E-01	.175927E-02
16	3.34	.585473E+00	.123170E+00	.170967E-01	.213733E-02
17	3.40	.700601E+00	.151114E+00	.155261E-01	.215067E-02
18	3.45	.896941E+00	.183118E+00	.123743E-01	.185324E-02
19	3.50	.105867E+01	.215805E+00	.104362E-01	.186803E-02
20	3.57	.119628E+01	.249380E+00	.932642E-02	.193204E-02
21	3.62	.122855E+01	.258770E+00	.921568E-02	.197713E-02

HEAT TRANSFER CALCULATIONS: TEST 3.09.10M

LEVEL	ELEVATION (METER)	HRAD (W/CM**2-K)	DELTA HRAD (W/CM**2-K)	REW	DELTA REW	QCRODM (W/CM**2)	DELTA QCRODM (W/CM**2)
12	3.02	.358340E-02	.955916E-03	.320636E+04	.249740E+03	.128378E+00	.581180E-01
13	3.12	.398877E-02	.102963E-02	.321063E+04	.237610E+03	.141373E+00	.634990E-01
14	3.20	.436028E-02	.110467E-02	.315656E+04	.227765E+03	.157460E+00	.702952E-01
15	3.27	.471747E-02	.118318E-02	.312789E+04	.222540E+03	.170357E+00	.756012E-01
16	3.34	.447811E-02	.114792E-02	.364941E+04	.246637E+03	.111255E+00	.492298E-01
17	3.40	.486642E-02	.125567E-02	.347783E+04	.239765E+03	.133031E+00	.585835E-01
18	3.45	.536660E-02	.132567E-02	.323361E+04	.220575E+03	.170456E+00	.746762E-01
19	3.50	.580437E-02	.142655E-02	.308207E+04	.211472E+03	.200975E+00	.876086E-01
20	3.57	.629081E-02	.156343E-02	.298992E+04	.207336E+03	.226561E+00	.981234E-01
21	3.62	.651272E-02	.162823E-02	.298185E+04	.206704E+03	.232447E+00	.100317E+00

HEAT TRANSFER CALCULATIONS: TEST 3.09.10M

LEVEL	ELEVATION (METER)	GRX	DELTA GRX	PRV	DELTA PRV	PRF	DELTA PRF
12	3.02	.415757E+07	.545971E+06	.117799E+01	.518310E-01	.967738E+00	.220457E-01
13	3.12	.327724E+07	.378872E+06	.109809E+01	.382272E-01	.946234E+00	.149813E-01
14	3.20	.277414E+07	.298438E+06	.105168E+01	.292958E-01	.932311E+00	.114209E-01
15	3.27	.236554E+07	.239651E+06	.101602E+01	.216617E-01	.922234E+00	.883586E-02
16	3.34	.183897E+07	.211836E+06	.989537E+00	.165481E-01	.928755E+00	.855422E-02
17	3.40	.170314E+07	.195744E+06	.973418E+00	.134006E-01	.918720E+00	.719181E-02
18	3.45	.162103E+07	.154691E+06	.960923E+00	.115282E-01	.909071E+00	.556917E-02
19	3.50	.151354E+07	.138052E+06	.950376E+00	.980352E-02	.902637E+00	.473725E-02
20	3.57	.134357E+07	.125325E+06	.937617E+00	.762678E-02	.896849E+00	.403657E-02
21	3.62	.124081E+07	.120353E+06	.931030E+00	.687883E-02	.894510E+00	.382465E-02

HEAT TRANSFER CALCULATIONS: TEST 3.09.10M

LEVEL	ELEVATION (METER)	HW-TRAN (W/CM**2-K)	DELTA HW-TRAN (W/CM**2-K)	HW-LAM (W/CM**2-K)	DELTA HW-LAM (W/CM**2-K)	HW-TUR (W/CM**2-K)	DELTA HW-TUR (W/CM**2-K)
12	3.02	.000000E+00	.000000E+00	.000000E+00	.000000E+00	.134862E-01	.561680E-03
13	3.12	.000000E+00	.000000E+00	.000000E+00	.000000E+00	.138739E-01	.548542E-03
14	3.20	.000000E+00	.000000E+00	.000000E+00	.000000E+00	.142834E-01	.556352E-03
15	3.27	.000000E+00	.000000E+00	.000000E+00	.000000E+00	.147301E-01	.555423E-03
16	3.34	.000000E+00	.000000E+00	.000000E+00	.000000E+00	.149709E-01	.573699E-03
17	3.40	.000000E+00	.000000E+00	.000000E+00	.000000E+00	.153562E-01	.571236E-03
18	3.45	.000000E+00	.000000E+00	.000000E+00	.000000E+00	.157898E-01	.566078E-03
19	3.50	.000000E+00	.000000E+00	.000000E+00	.000000E+00	.162192E-01	.564869E-03
20	3.57	.000000E+00	.000000E+00	.000000E+00	.000000E+00	.167973E-01	.567087E-03
21	3.62	.000000E+00	.000000E+00	.000000E+00	.000000E+00	.171224E-01	.577792E-03

HEAT TRANSFER CALCULATIONS: TEST 3.09.10M

LEVEL	ELEVATION (METER)	HCE-TUR (W/CM**2-K)	DELTA HCE-TUR (W/CM**2-K)	HB&W (W/CM**2-K)	DELTA HB&W (W/CM**2-K)	HORNL (W/CM**2-K)	DELTA HORNL (W/CM**2-K)
12	3.02	.000000E+00	.000000E+00	.136003E-01	.775892E-03	.885473E-02	.577061E-03
13	3.12	.000000E+00	.000000E+00	.131472E-01	.722707E-03	.920358E-02	.558374E-03
14	3.20	.000000E+00	.000000E+00	.129756E-01	.712487E-03	.941050E-02	.549780E-03
15	3.27	.000000E+00	.000000E+00	.128907E-01	.693280E-03	.962318E-02	.553687E-03
16	3.34	.000000E+00	.000000E+00	.128672E-01	.682066E-03	.101867E-01	.551834E-03
17	3.40	.000000E+00	.000000E+00	.128773E-01	.671938E-03	.102277E-01	.576815E-03
18	3.45	.000000E+00	.000000E+00	.129029E-01	.673188E-03	.102041E-01	.557678E-03
19	3.50	.000000E+00	.000000E+00	.129407E-01	.670480E-03	.102359E-01	.564438E-03
20	3.57	.000000E+00	.000000E+00	.130129E-01	.661900E-03	.103635E-01	.586410E-03
21	3.62	.000000E+00	.000000E+00	.130651E-01	.666660E-03	.104730E-01	.595036E-03

HEAT TRANSFER CALCULATIONS: TEST 3.09.10M

LEVEL	ELEVATION (METER)	HEINEMAN (W/CM**2-K)	DELTA HEINEMAN (W/CM**2-K)	MCELIGOT (W/CM**2-K)	DELTA MCELIGOT (W/CM**2-K)
12	3.02	.105431E-01	.715103E-03	.107045E-01	.587488E-03
13	3.12	.106042E-01	.671621E-03	.104093E-01	.562495E-03
14	3.20	.106735E-01	.657500E-03	.102837E-01	.562996E-03
15	3.27	.107531E-01	.639522E-03	.102482E-01	.554102E-03
16	3.34	.107037E-01	.608255E-03	.106527E-01	.570259E-03
17	3.40	.107926E-01	.618344E-03	.105870E-01	.558861E-03
18	3.45	.105103E-01	.608964E-03	.104703E-01	.553520E-03
19	3.50	.110121E-01	.612039E-03	.104226E-01	.547596E-03
20	3.57	.111243E-01	.617971E-03	.104620E-01	.539596E-03
21	3.62	.111762E-01	.625702E-03	.105315E-01	.545280E-03

HEAT TRANSFER CALCULATIONS: TEST 3.09.10M

LEVEL	ELEVATION (METER)	TFIL (KELVIN)	DELTA TFIL (KELVIN)	HCE-TRAN (W/CM**2-K)	DELTA HCE-TRAN (W/CM**2-K)	HCE-LAM (W/CM**2-K)	DELTA HCE-LAM (W/CM**2-K)
12	3.02	.740134E+03	.279345E+03	.123345E-01	.190957E-02	.000000E+00	.000000E+00
13	3.12	.767151E+03	.276908E+03	.115654E-01	.162718E-02	.000000E+00	.000000E+00
14	3.20	.790318E+03	.276124E+03	.111605E-01	.147440E-02	.000000E+00	.000000E+00
15	3.27	.811417E+03	.274953E+03	.108465E-01	.131037E-02	.000000E+00	.000000E+00
16	3.34	.797267E+03	.272616E+03	.106483E-01	.120735E-02	.000000E+00	.000000E+00
17	3.40	.819927E+03	.273408E+03	.104864E-01	.112995E-02	.000000E+00	.000000E+00
18	3.45	.847328E+03	.272643E+03	.103388E-01	.108824E-02	.000000E+00	.000000E+00
19	3.50	.869830E+03	.272859E+03	.102140E-01	.104607E-02	.000000E+00	.000000E+00
20	3.57	.893956E+03	.273316E+03	.100603E-01	.981372E-03	.000000E+00	.000000E+00
21	3.62	.904998E+03	.273960E+03	.997766E-02	.971615E-03	.000000E+00	.000000E+00

THIS PAGE

WAS INTENTIONALLY

LEFT BLANK

TEST

3.09.10N

SYSTEM PARAMETER SUMMARY

SYSTEM PRESSURE	.708098E+01	+OR-	.206820E+00	MPA
INLET MASS FLOW	.267890E-01	+OR-	.384625E-02	KG/S
OUTLET MASS FLOW	.284625E-01	+OR-	.168959E-02	KG/S
MASS FLUX - BASED ON OUTLET FLOW	.460472E+01	+OR-	.273345E+00	KG/(M**2)S
MASS FLUX - BASED ON INLET FLOW	.433397E+01	+OR-	.622253E+00	KG/(M**2)S
INLET TEMPERATURE	.473074E+03	+OR-	.259117E+03	KELVIN
OUTLET TEMPERATURE	.714778E+03	+OR-	.259337E+03	KELVIN
BUNDLE POWER	.104065E+03	+OR-	.559020E+01	KW
AVERAGE LINEAR POWER/ROD	.474161E+00	+OR-	.254712E-01	KW/M
FRACTIONAL HEAT LOSS	.162226E+00			

HEAT TRANSFER CALCULATIONS: TEST 3.09.10N

LEVEL	ELEVATION (METER)	TVAP (KELVIN)	DELTA TVAP (KELVIN)	NO. OF TC S	TW (KELVIN)	DELTA TW (KELVIN)	Q"/Q"SS	Q"HTRAN (W/CM**2)	DELTA Q"HTRAN (W/CM**2)
5	2.42	.588247E+03	.285885E+03	28.	.720958E+03	.258213E+03	.100000E+01	.162135E+01	.855885E-01
6	2.51	.616694E+03	.286763E+03	2.	.744622E+03	.260248E+03	.100000E+01	.161746E+01	.818031E-01
7	2.58	.640639E+03	.285234E+03	2.	.769567E+03	.256456E+03	.100000E+01	.160219E+01	.100911E+00
8	2.66	.666490E+03	.284432E+03	5.	.795132E+03	.259811E+03	.100000E+01	.164224E+01	.842071E-01
9	2.84	.725217E+03	.281852E+03	1.	.834700E+03	.255493E+03	.100000E+01	.155495E+01	.777473E-01
10	2.89	.744769E+03	.280866E+03	3.	.862501E+03	.261771E+03	.100000E+01	.165485E+01	.852376E-01
11	2.97	.771117E+03	.279643E+03	4.	.885221E+03	.258612E+03	.100000E+01	.165485E+01	.846207E-01
12	3.02	.789168E+03	.278471E+03	22.	.898452E+03	.260645E+03	.100000E+01	.164296E+01	.906000E-01
13	3.12	.824405E+03	.277348E+03	5.	.921259E+03	.261233E+03	.100000E+01	.164012E+01	.940145E-01
14	3.20	.849219E+03	.275803E+03	4.	.939301E+03	.261175E+03	.100000E+01	.164861E+01	.850098E-01
15	3.27	.870115E+03	.275366E+03	4.	.961098E+03	.260666E+03	.100000E+01	.164270E+01	.967221E-01
16	3.34	.890308E+03	.274717E+03	1.	.956150E+03	.255460E+03	.100000E+01	.155603E+01	.778017E-01
17	3.40	.905438E+03	.273236E+03	2.	.986135E+03	.259120E+03	.100000E+01	.161800E+01	.101907E+00
18	3.45	.915321E+03	.273075E+03	3.	.999748E+03	.262408E+03	.100000E+01	.163815E+01	.827497E-01
19	3.50	.924891E+03	.272975E+03	6.	.101130E+04	.261818E+03	.100000E+01	.163442E+01	.905214E-01
20	3.57	.939021E+03	.272973E+03	6.	.102597E+04	.263359E+03	.100000E+01	.164341E+01	.924405E-01
21	3.62	.947926E+03	.273071E+03	17.	.103204E+04	.267883E+03	.100000E+01	.164366E+01	.900106E-01

HEAT TRANSFER CALCULATIONS: TEST 3.09.10N

LEVEL	ELEVATION (METER)	HEXP (W/CM**2-K)	DELTA HEXP (W/CM**2-K)	REV	DELTA REV	REF	DELTA REF
5	2.42	.122245E-01	.274355E-02	.269424E+04	.295124E+03	.228933E+04	.191866E+03
6	2.51	.126512E-01	.297904E-02	.248295E+04	.240385E+03	.219682E+04	.180522E+03
7	2.58	.124345E-01	.278812E-02	.233717E+04	.178194E+03	.211825E+04	.166718E+03
8	2.66	.127737E-01	.268569E-02	.224477E+04	.167401E+03	.204099E+04	.156533E+03
9	2.84	.142112E-01	.303174E-02	.205735E+04	.145295E+03	.190708E+04	.136422E+03
10	2.89	.140646E-01	.265515E-02	.200119E+04	.138882E+03	.184836E+04	.130537E+03
11	2.97	.145118E-01	.263196E-02	.192992E+04	.131204E+03	.179107E+04	.123044E+03
12	3.02	.150430E-01	.262233E-02	.188382E+04	.126032E+03	.175629E+04	.118831E+03
13	3.12	.169442E-01	.296424E-02	.179963E+04	.118232E+03	.169512E+04	.112477E+03
14	3.20	.183121E-01	.288925E-02	.174457E+04	.112666E+03	.165254E+04	.107636E+03
15	3.27	.180657E-01	.260779E-02	.170067E+04	.109088E+03	.161215E+04	.104150E+03
16	3.34	.236469E-01	.372727E-02	.166024E+04	.105688E+03	.159818E+04	.101932E+03
17	3.40	.200624E-01	.249930E-02	.163115E+04	.102649E+03	.155822E+04	.984474E+02
18	3.45	.194148E-01	.208166E-02	.161267E+04	.101269E+03	.153817E+04	.974380E+02
19	3.50	.189263E-01	.192274E-02	.159517E+04	.100002E+03	.152057E+04	.960404E+02
20	3.57	.189115E-01	.178527E-02	.157000E+04	.982699E+02	.149719E+04	.946669E+02
21	3.62	.195517E-01	.179103E-02	.155453E+04	.972628E+02	.148532E+04	.949667E+02

HEAT TRANSFER CALCULATIONS: TEST 3.09.10N

LEVEL	ELEVATION (METER)	QRAD (W/CM**2)	DELTA QRAD (W/CM**2)	HCONV (W/CM**2-K)	DELTA HCONV (W/CM**2-K)
5	2.42	.276441E+00	.742709E-01	.974478E-02	.289085E-02
6	2.51	.300073E+00	.850113E-01	.986610E-02	.316419E-02
7	2.58	.336394E+00	.913607E-01	.934190E-02	.300849E-02
8	2.66	.374000E+00	.102111E+00	.933393E-02	.295587E-02
9	2.84	.387921E+00	.110692E+00	.100366E-01	.339779E-02
10	2.89	.456171E+00	.126505E+00	.950455E-02	.309086E-02
11	2.97	.483916E+00	.130737E+00	.952877E-02	.312182E-02
12	3.02	.490309E+00	.134804E+00	.977737E-02	.316175E-02
13	3.12	.481136E+00	.139846E+00	.111268E-01	.358302E-02
14	3.20	.481365E+00	.141232E+00	.120638E-01	.358563E-02
15	3.27	.521729E+00	.149884E+00	.113749E-01	.340882E-02
16	3.34	.387587E+00	.131040E+00	.167812E-01	.452444E-02
17	3.40	.510126E+00	.146767E+00	.127044E-01	.341840E-02
18	3.45	.553675E+00	.161197E+00	.117867E-01	.318033E-02
19	3.50	.584198E+00	.165974E+00	.110650E-01	.308150E-02
20	3.57	.612591E+00	.177770E+00	.107244E-01	.309222E-02
21	3.62	.605554E+00	.196943E+00	.111898E-01	.333823E-02

HEAT TRANSFER CALCULATIONS: TEST 3.09.10N

LEVEL	ELEVATION (METER)	HRAD (W/CM**2-K)	DELTA HRAD (W/CM**2-K)	REW	DELTA REW	QCRODM (W/CM**2)	DELTA QCRODM (W/CM**2)
5	2.42	.247974E-02	.911014E-03	.147519E+04	.118993E+03	.524492E-01	.229538E-01
6	2.51	.278508E-02	.106652E-02	.150698E+04	.115697E+03	.560014E-01	.240147E-01
7	2.56	.309260E-02	.113022E-02	.149322E+04	.110729E+03	.620877E-01	.263443E-01
8	2.66	.343973E-02	.123460E-02	.147583E+04	.108217E+03	.682283E-01	.285144E-01
9	2.84	.417453E-02	.153410E-02	.149115E+04	.104976E+03	.688443E-01	.278805E-01
10	2.89	.456000E-02	.158228E-02	.143582E+04	.102306E+03	.803648E-01	.321282E-01
11	2.97	.498303E-02	.167885E-02	.141717E+04	.992396E+02	.843232E-01	.331992E-01
12	3.02	.526559E-02	.176636E-02	.141174E+04	.988979E+02	.847885E-01	.330425E-01
13	3.12	.581746E-02	.201279E-02	.140908E+04	.979748E+02	.819662E-01	.313147E-01
14	3.20	.624829E-02	.212344E-02	.139911E+04	.967622E+02	.811576E-01	.305524E-01
15	3.27	.669081E-02	.219534E-02	.136962E+04	.943699E+02	.866614E-01	.329245E-01
16	3.34	.686577E-02	.256476E-02	.142187E+04	.963805E+02	.641997E-01	.236277E-01
17	3.40	.735796E-02	.233217E-02	.135627E+04	.925566E+02	.832823E-01	.301747E-01
18	3.45	.762812E-02	.240441E-02	.133328E+04	.918060E+02	.899580E-01	.323312E-01
19	3.50	.786136E-02	.240805E-02	.131624E+04	.904208E+02	.946849E-01	.337786E-01
20	3.57	.818711E-02	.252481E-02	.129826E+04	.895441E+02	.988717E-01	.349035E-01
21	3.62	.836187E-02	.281709E-02	.129559E+04	.910634E+02	.974056E-01	.341871E-01

HEAT TRANSFER CALCULATIONS: TEST 3.09.10N

LEVEL	ELEVATION (METER)	GRX	DELTA GRX	PRV	DELTA PRV	PRF	DELTA PRF
5	2.42	.665183E+07	.183725E+07	.133031E+01	.117620E+00	.111142E+01	.811422E-01
6	2.51	.466011E+07	.133603E+07	.122026E+01	.886712E-01	.105202E+01	.599613E-01
7	2.58	.360449E+07	.956864E+06	.115476E+01	.822398E-01	.101056E+01	.423259E-01
8	2.66	.279319E+07	.722580E+06	.108258E+01	.579207E-01	.978595E+00	.303704E-01
9	2.84	.154635E+07	.405440E+06	.984723E+00	.260108E-01	.939027E+00	.157134E-01
10	2.89	.137746E+07	.335566E+06	.964985E+00	.200413E-01	.926393E+00	.123043E-01
11	2.97	.110955E+07	.257885E+06	.944618E+00	.143497E-01	.916081E+00	.925607E-02
12	3.02	.948933E+06	.221061E+06	.933741E+00	.114005E-01	.910614E+00	.780168E-02
13	3.12	.687485E+06	.170644E+06	.917514E+00	.783029E-02	.902168E+00	.592044E-02
14	3.20	.554536E+06	.137269E+06	.908887E+00	.596138E-02	.897023E+00	.474843E-02
15	3.27	.488350E+06	.116522E+06	.902880E+00	.498305E-02	.892607E+00	.402304E-02
16	3.34	.336893E+06	.101869E+06	.897914E+00	.418920E-02	.891175E+00	.354972E-02
17	3.40	.359517E+06	.847212E+05	.894632E+00	.351540E-02	.887322E+00	.294174E-02
18	3.45	.350593E+06	.825425E+05	.892662E+00	.326813E-02	.885520E+00	.282544E-02
19	3.50	.337173E+06	.764309E+05	.890872E+00	.305785E-02	.884006E+00	.261425E-02
20	3.57	.312140E+06	.724099E+05	.888421E+00	.279801E-02	.882093E+00	.244545E-02
21	3.62	.289334E+06	.773658E+05	.886984E+00	.266155E-02	.881163E+00	.254728E-02

HEAT TRANSFER CALCULATIONS: TEST 3.09.10N

LEVEL	ELEVATION (METER)	HW-TRAN (W/CM**2-K)	DELTA HW-TRAN (W/CM**2-K)	HW-LAM (W/CM**2-K)	DELTA HW-LAM (W/CM**2-K)	HW-TUR (W/CM**2-K)	DELTA HW-TUR (W/CM**2-K)
5	2.42	.000000E+00	.000000E+00	.407273E-02	.161836E-03	.000000E+00	.000000E+00
6	2.51	.000000E+00	.000000E+00	.436254E-02	.187298E-03	.000000E+00	.000000E+00
7	2.58	.000000E+00	.000000E+00	.469326E-02	.193855E-03	.000000E+00	.000000E+00
8	2.66	.000000E+00	.000000E+00	.508602E-02	.208430E-03	.000000E+00	.000000E+00
9	2.84	.000000E+00	.000000E+00	.597161E-02	.217348E-03	.000000E+00	.000000E+00
10	2.89	.000000E+00	.000000E+00	.640877E-02	.227502E-03	.000000E+00	.000000E+00
11	2.97	.000000E+00	.000000E+00	.691260E-02	.224495E-03	.000000E+00	.000000E+00
12	3.02	.000000E+00	.000000E+00	.725375E-02	.225274E-03	.000000E+00	.000000E+00
13	3.12	.000000E+00	.000000E+00	.792547E-02	.231125E-03	.000000E+00	.000000E+00
14	3.20	.000000E+00	.000000E+00	.844242E-02	.226066E-03	.000000E+00	.000000E+00
15	3.27	.000000E+00	.000000E+00	.896200E-02	.229785E-03	.000000E+00	.000000E+00
16	3.34	.000000E+00	.000000E+00	.921273E-02	.220083E-03	.000000E+00	.000000E+00
17	3.40	.000000E+00	.000000E+00	.976082E-02	.215882E-03	.000000E+00	.000000E+00
18	3.45	.000000E+00	.000000E+00	.100657E-01	.230147E-03	.000000E+00	.000000E+00
19	3.50	.000000E+00	.000000E+00	.103489E-01	.231008E-03	.000000E+00	.000000E+00
20	3.57	.000000E+00	.000000E+00	.107491E-01	.244771E-03	.000000E+00	.000000E+00
21	3.62	.000000E+00	.000000E+00	.109686E-01	.278562E-03	.000000E+00	.000000E+00

HEAT TRANSFER CALCULATIONS: TEST 3.09.10N

LEVEL	ELEVATION (METER)	HCE-TUR (W/CM**2-K)	DELTA HCE-TUR (W/CM**2-K)	HB&W (W/CM**2-K)	DELTA HB&W (W/CM**2-K)	HORNL (W/CM**2-K)	DELTA HORNL (W/CM**2-K)
5	2.42	.000000E+00	.000000E+00	.701427E-02	.670705E-03	.400713E-02	.265693E-03
6	2.51	.000000E+00	.000000E+00	.632256E-02	.555866E-03	.419462E-02	.262947E-03
7	2.58	.000000E+00	.000000E+00	.600726E-02	.468545E-03	.430308E-02	.257183E-03
8	2.66	.000000E+00	.000000E+00	.585362E-02	.453982E-03	.441608E-02	.262228E-03
9	2.84	.000000E+00	.000000E+00	.575503E-02	.419425E-03	.470899E-02	.265711E-03
10	2.89	.000000E+00	.000000E+00	.576539E-02	.408380E-03	.475214E-02	.275481E-03
11	2.97	.000000E+00	.000000E+00	.579875E-02	.395698E-03	.485502E-02	.273423E-03
12	3.02	.000000E+00	.000000E+00	.583084E-02	.385081E-03	.492988E-02	.279397E-03
13	3.12	.000000E+00	.000000E+00	.590771E-02	.375288E-03	.507884E-02	.286177E-03
14	3.20	.000000E+00	.000000E+00	.596918E-02	.363950E-03	.517459E-02	.289822E-03
15	3.27	.000000E+00	.000000E+00	.602380E-02	.361139E-03	.523643E-02	.291512E-03
16	3.34	.000000E+00	.000000E+00	.607818E-02	.357260E-03	.536060E-02	.290898E-03
17	3.40	.000000E+00	.000000E+00	.611956E-02	.348637E-03	.536726E-02	.294545E-03
18	3.45	.000000E+00	.000000E+00	.614679E-02	.348077E-03	.538702E-02	.301284E-03
19	3.50	.000000E+00	.000000E+00	.617324E-02	.347894E-03	.541002E-02	.301086E-03
20	3.57	.000000E+00	.000000E+00	.621238E-02	.348480E-03	.544924E-02	.306129E-03
21	3.62	.000000E+00	.000000E+00	.623706E-02	.349395E-03	.548104E-02	.320676E-03

HEAT TRANSFER CALCULATIONS: TEST 3.09.10N

LEVEL	ELEVATION (METER)	HEINEMAN (W/CM**2-K)	DELTA HEINEMAN (W/CM**2-K)	MCELIGOT (W/CM**2-K)	DELTA MCELIGOT (W/CM**2-K)
5	2.42	.462651E-02	.430293E-03	.578524E-02	.515127E-03
6	2.51	.455063E-02	.427656E-03	.525378E-02	.440448E-03
7	2.58	.452310E-02	.405330E-03	.500461E-02	.371873E-03
8	2.66	.452201E-02	.393834E-03	.489340E-02	.375151E-03
9	2.84	.456776E-02	.356515E-03	.489802E-02	.363957E-03
10	2.89	.460315E-02	.351861E-03	.489175E-02	.354348E-03
11	2.97	.464509E-02	.336643E-03	.494165E-02	.345410E-03
12	3.02	.467375E-02	.328291E-03	.498966E-02	.337444E-03
13	3.12	.472949E-02	.318508E-03	.510269E-02	.331704E-03
14	3.20	.477195E-02	.307884E-03	.518229E-02	.322694E-03
15	3.27	.481479E-02	.304550E-03	.523328E-02	.320148E-03
16	3.34	.483016E-02	.295938E-03	.535522E-02	.320805E-03
17	3.40	.487562E-02	.291457E-03	.535402E-02	.310193E-03
18	3.45	.489924E-02	.294777E-03	.537017E-02	.309123E-03
19	3.50	.492039E-02	.293718E-03	.539035E-02	.308687E-03
20	3.57	.494909E-02	.296104E-03	.542658E-02	.309222E-03
21	3.62	.496392E-02	.305351E-03	.545778E-02	.310560E-03

HEAT TRANSFER CALCULATIONS: TEST 3.09.10N

LEVEL	ELEVATION (METER)	TFIL (KELVIN)	DELTA TFIL (KELVIN)	HCE-TRAN (W/CM**2-K)	DELTA HCE-TRAN (W/CM**2-K)	HCE-LAM (W/CM**2-K)	DELTA HCE-LAM (W/CM**2-K)
5	2.42	.654602E+03	.292084E+03	.560638E-02	.203986E-02	.000000E+00	.000000E+00
6	2.51	.680658E+03	.292600E+03	.467380E-02	.134052E-02	.000000E+00	.000000E+00
7	2.58	.705103E+03	.290271E+03	.419584E-02	.102454E-02	.000000E+00	.000000E+00
8	2.66	.730811E+03	.289241E+03	.386699E-02	.827928E-03	.000000E+00	.000000E+00
9	2.84	.779959E+03	.284954E+03	.342250E-02	.585137E-03	.000000E+00	.000000E+00
10	2.89	.803635E+03	.284552E+03	.331484E-02	.535785E-03	.000000E+00	.000000E+00
11	2.97	.828169E+03	.282519E+03	.000000E+00	.000000E+00	.328474E-02	.427107E-03
12	3.02	.843810E+03	.281326E+03	.000000E+00	.000000E+00	.328268E-02	.402580E-03
13	3.12	.872832E+03	.279869E+03	.000000E+00	.000000E+00	.329403E-02	.365358E-03
14	3.20	.894260E+03	.278052E+03	.000000E+00	.000000E+00	.330208E-02	.339443E-03
15	3.27	.915606E+03	.277448E+03	.000000E+00	.000000E+00	.329808E-02	.318236E-03
16	3.34	.923229E+03	.275729E+03	.000000E+00	.000000E+00	.331365E-02	.301033E-03
17	3.40	.945786E+03	.274705E+03	.000000E+00	.000000E+00	.331023E-02	.287067E-03
18	3.45	.957534E+03	.275390E+03	.000000E+00	.000000E+00	.329640E-02	.276303E-03
19	3.50	.968096E+03	.275117E+03	.000000E+00	.000000E+00	.328603E-02	.266509E-03
20	3.57	.982498E+03	.275603E+03	.000000E+00	.000000E+00	.327517E-02	.254537E-03
21	3.62	.989985E+03	.277624E+03	.000000E+00	.000000E+00	.327151E-02	.248826E-03

THIS PAGE

WAS INTENTIONALLY

LEFT BLANK

B.2 Standard English Engineering Units

THIS PAGE

WAS INTENTIONALLY

LEFT BLANK

TEST

3.09.10I

SYSTEM PARAMETER SUMMARY

SYSTEM PRESSURE	.653188E+03	+OR-	.306371E+02	PSIA
INLET MASS FLOW	.000000E+00	+OR-	.000000E+00	LBM/HR
OUTLET MASS FLOW	.146000E+04	+OR-	.981016E+02	LBM/HR
MASS FLUX - BASED ON OUTLET FLOW	.219439E+05	+OR-	.147447E+04	LBM/(FT**2)HR
MASS FLUX - BASED ON INLET FLOW	.000000E+00	+OR-	.000000E+00	LBM/(FT**2)HR
INLET TEMPERATURE	.392045E+03	+OR-	.700668E+01	DEGREES F
OUTLET TEMPERATURE	.933976E+03	+OR-	.722793E+01	DEGREES F
BUNDLE POWER	.166278E+07	+OR-	.873704E+05	BTU/HR
AVERAGE LINEAR POWER/ROD	.676849E+00	+OR-	.355650E-01	KW/FT
FRACTIONAL HEAT LOSS	.176706E-01			

HEAT TRANSFER CALCULATIONS: TEST 3.09.10I

LEVEL	ELEVATION (FEET)	TVAP (DEG. F)	DELTA TVAP (DEG. F)	NO. OF TC S	TW (DEG. F)	DELTA TW (DEG. F)	Q"/Q"SS	Q"HTRAN (BTU/HR-FT**2)	DELTA Q"HTRAN (BTU/HR-FT**2)
12	9.91	.632578E+03	.582410E+02	22.	.122013E+04	.107710E+02	.103039E+01	.248782E+05	.132298E+04
13	10.23	.686677E+03	.576694E+02	5.	.125158E+04	.181369E+02	.103603E+01	.249258E+05	.135069E+04
14	10.48	.728142E+03	.597956E+02	4.	.129060E+04	.864531E+01	.104566E+01	.253150E+05	.125549E+04
15	10.73	.772013E+03	.579512E+02	4.	.130267E+04	.215738E+02	.103909E+01	.249384E+05	.137636E+04
16	10.97	.812435E+03	.559096E+02	1.	.118260E+04	.417223E+01	.103700E+01	.237935E+05	.114723E+04
17	11.14	.842044E+03	.566398E+02	2.	.125592E+04	.296650E+01	.103665E+01	.245071E+05	.137177E+04
18	11.32	.870254E+03	.584585E+02	3.	.136650E+04	.120690E+02	.103685E+01	.250320E+05	.121529E+04
19	11.48	.898932E+03	.580754E+02	6.	.139659E+04	.156088E+02	.103892E+01	.243897E+05	.128686E+04
20	11.73	.941121E+03	.563743E+02	6.	.143566E+04	.291637E+02	.104281E+01	.251084E+05	.132900E+04
21	11.88	.966880E+03	.553747E+02	17.	.145262E+04	.264015E+02	.104006E+01	.251151E+05	.130628E+04

HEAT TRANSFER CALCULATIONS: TEST 3.09.10I

LEVEL	ELEVATION (FEET)	HEXP (BTU/HR-FT**2-F)	DELTA HEXP (BTU/HR-FT**2-F)	REV	DELTA REV	REF	DELTA REF
12	9.91	.423424E+02	.317557E+01	.166143E+05	.169224E+04	.126258E+05	.117367E+04
13	10.23	.441243E+02	.315084E+01	.154790E+05	.131300E+04	.122215E+05	.109879E+04
14	10.48	.450081E+02	.299975E+01	.148966E+05	.126120E+04	.118637E+05	.105578E+04
15	10.73	.469952E+02	.323748E+01	.143288E+05	.118164E+04	.116269E+05	.100657E+04
16	10.97	.642779E+02	.434985E+01	.138413E+05	.111365E+04	.119669E+05	.986604E+03
17	11.14	.592141E+02	.401566E+01	.135040E+05	.108302E+04	.115311E+05	.947758E+03
18	11.32	.504423E+02	.289979E+01	.131972E+05	.106171E+04	.109904E+05	.911312E+03
19	11.43	.500135E+02	.296387E+01	.128989E+05	.102776E+04	.107763E+05	.884783E+03
20	11.73	.507713E+02	.298797E+01	.124833E+05	.975510E+03	.104934E+05	.853113E+03
21	11.88	.517046E+02	.297745E+01	.122421E+05	.946309E+03	.103505E+05	.827901E+03

HEAT TRANSFER CALCULATIONS: TEST 3.09.101

LEVEL	ELEVATION (FEET)	QRAD (BTU/HR-FT**2)	DELTA QRAD (BTU/HR-FT**2)	HCONV (BTU/HR-FT**2-F)	DELTA HCONV (BTU/HR-FT**2-F)
12	9.91	.323648E+04	.666185E+03	.356181E+02	.362012E+01
13	10.23	.339902E+04	.718997E+03	.367864E+02	.368831E+01
14	10.48	.367182E+04	.760502E+03	.370505E+02	.363064E+01
15	10.73	.365857E+04	.794301E+03	.385991E+02	.392411E+01
16	10.97	.235902E+04	.528787E+03	.565435E+02	.482489E+01
17	11.14	.291861E+04	.635702E+03	.506494E+02	.460555E+01
18	11.32	.398157E+04	.850451E+03	.406802E+02	.384750E+01
19	11.48	.420120E+04	.906006E+03	.397378E+02	.399304E+01
20	11.73	.447248E+04	.102176E+04	.397584E+02	.421796E+01
21	11.88	.455314E+04	.102794E+04	.402901E+02	.426783E+01

HEAT TRANSFER CALCULATIONS: TEST 3.09.10I

LEVEL	ELEVATION (FEET)	HRAD (BTU/HR-FT**2-F)	DELTA HRAD (BTU/HR-FT**2-F)	REW	DELTA REW	QCROD (BTU/HR-FT**2)	DELTA QCROD (BTU/HR-FT**2)
12	9.31	.672434E+01	.173811E+01	.613912E+04	.677873E+03	.714398E+03	.333436E+03
13	10.23	.733794E+01	.191725E+01	.631926E+04	.670225E+03	.746178E+03	.346762E+03
14	10.48	.795761E+01	.204525E+01	.631415E+04	.648733E+03	.803978E+03	.372465E+03
15	10.73	.839607E+01	.221750E+01	.651651E+04	.659078E+03	.796885E+03	.368013E+03
16	10.97	.773440E+01	.208767E+01	.788310E+04	.733859E+03	.503993E+03	.231948E+03
17	11.14	.856464E+01	.225511E+01	.738185E+04	.691719E+03	.626063E+03	.287708E+03
18	11.32	.976214E+01	.252872E+01	.663147E+04	.636462E+03	.862887E+03	.395532E+03
19	11.48	.102756E+02	.267579E+01	.656837E+04	.628516E+03	.912568E+03	.417366E+03
20	11.73	.110128E+02	.297712E+01	.651191E+04	.629413E+03	.973802E+03	.443860E+03
21	11.88	.114147E+02	.305764E+01	.652506E+04	.622891E+03	.991438E+03	.450946E+03

HEAT TRANSFER CALCULATIONS: TEST 3.09.10I

LEVEL	ELEVATION (FEET)	GRX	DELTA GRX	PRV	DELTA PRV	PRF	DELTA PRF
12	9.91	.181900E+07	.350846E+06	.110880E+01	.564282E-01	.925812E+00	.198768E-01
13	10.23	.146163E+07	.273724E+06	.105717E+01	.530511E-01	.916617E+00	.156391E-01
14	10.48	.123815E+07	.228360E+06	.101751E+01	.411946E-01	.909534E+00	.128475E-01
15	10.73	.104792E+07	.192192E+06	.986046E+00	.298754E-01	.905302E+00	.107154E-01
16	10.97	.854000E+06	.168733E+06	.964287E+00	.223558E-01	.911488E+00	.105928E-01
17	11.14	.781331E+06	.145619E+06	.951620E+00	.188658E-01	.903682E+00	.881689E-02
18	11.32	.726296E+06	.127910E+06	.941541E+00	.164353E-01	.895400E+00	.729563E-02
19	11.48	.656674E+06	.114502E+06	.932884E+00	.139704E-01	.892430E+00	.650935E-02
20	11.73	.567700E+06	.100780E+06	.922410E+00	.110003E-01	.888900E+00	.561749E-02
21	11.88	.519126E+06	.897406E+05	.917054E+00	.959796E-02	.887207E+00	.505745E-02

HEAT TRANSFER CALCULATIONS: TEST 3.09.10I

LEVEL	ELEVATION (FEET)	HW-TRAN (BTU/HR-FT**2-F)	DELTA HW-TRAN (BTU/HR-FT**2-F)	HW-LAM (BTU/HR-FT**2-F)	DELTA HW-LAM (BTU/HR-FT**2-F)	HW-TUR (BTU/HR-FT**2-F)	DELTA HW-TUR (BTU/HR-FT**2-F)
12	9.91	.000000E+00	.000000E+00	.000000E+00	.000000E+00	.379084E+02	.307062E+01
13	10.23	.000000E+00	.000000E+00	.000000E+00	.000000E+00	.387733E+02	.285025E+01
14	10.48	.000000E+00	.000000E+00	.000000E+00	.000000E+00	.399555E+02	.297383E+01
15	10.73	.000000E+00	.000000E+00	.000000E+00	.000000E+00	.413101E+02	.298180E+01
16	10.97	.000000E+00	.000000E+00	.000000E+00	.000000E+00	.427132E+02	.306206E+01
17	11.14	.000000E+00	.000000E+00	.000000E+00	.000000E+00	.436142E+02	.306639E+01
18	11.32	.000000E+00	.000000E+00	.000000E+00	.000000E+00	.445901E+02	.307685E+01
19	11.48	.000000E+00	.000000E+00	.000000E+00	.000000E+00	.456089E+02	.307515E+01
20	11.73	.000000E+00	.000000E+00	.000000E+00	.000000E+00	.471403E+02	.304761E+01
21	11.88	.000000E+00	.000000E+00	.000000E+00	.000000E+00	.480805E+02	.302621E+01

HEAT TRANSFER CALCULATIONS: TEST 3.09.10I

LEVEL	ELEVATION (FEET)	HCE-TUR (BTU/HR-FT**2-F)	DELTA HCE-TUR (BTU/HR-FT**2-F)	HB&W (BTU/HR-FT**2-F)	DELTA HB&W (BTU/HR-FT**2-F)	HORNL (BTU/HR-FT**2-F)	DELTA HORNL (BTU/HR-FT**2-F)
12	9.91	.437309E+02	.440145E+01	.437309E+02	.440145E+01	.287261E+02	.255717E+01
13	10.23	.425969E+02	.394745E+01	.425969E+02	.394745E+01	.301256E+02	.259784E+01
14	10.48	.423989E+02	.399413E+01	.423989E+02	.399413E+01	.310140E+02	.256078E+01
15	10.73	.424531E+02	.386443E+01	.424531E+02	.386443E+01	.320960E+02	.265346E+01
16	10.97	.426651E+02	.373968E+01	.426651E+02	.373968E+01	.340593E+02	.254149E+01
17	11.14	.428910E+02	.375242E+01	.428910E+02	.375242E+01	.342285E+02	.256887E+01
18	11.32	.431478E+02	.380979E+01	.431478E+02	.380979E+01	.341070E+02	.263763E+01
19	11.48	.434410E+02	.377519E+01	.434410E+02	.377519E+01	.345802E+02	.267688E+01
20	11.73	.439161E+02	.368267E+01	.439161E+02	.368267E+01	.352902E+02	.282416E+01
21	11.88	.442250E+02	.363123E+01	.442250E+02	.363123E+01	.357602E+02	.280959E+01

HEAT TRANSFER CALCULATIONS: TEST 3.09.10I

LEVEL	ELEVATION (FEET)	HEINEMAN (BTU/HR-FT**2-F)	DELTA HEINEMAN (BTU/HR-FT**2-F)	MCELIGOT (BTU/HR-FT**2-F)	DELTA MCELIGOT (BTU/HR-FT**2-F)
12	9.91	.371060E+02	.431606E+01	.321985E+02	.325348E+01
13	10.23	.375140E+02	.414839E+01	.318341E+02	.297939E+01
14	10.48	.379164E+02	.412901E+01	.318924E+02	.306858E+01
15	10.73	.382029E+02	.397678E+01	.324059E+02	.303069E+01
16	10.97	.377964E+02	.361111E+01	.342859E+02	.309532E+01
17	11.14	.383232E+02	.364462E+01	.341132E+02	.307927E+01
18	11.32	.390481E+02	.377160E+01	.336207E+02	.306766E+01
19	11.48	.393561E+02	.373245E+01	.339338E+02	.304834E+01
20	11.73	.397805E+02	.370134E+01	.344725E+02	.298665E+01
21	11.88	.400024E+02	.360841E+01	.348769E+02	.295713E+01

HEAT TRANSFER CALCULATIONS: TEST 3.09.10I

LEVEL	ELEVATION (FEET)	TFIL (DEG. F)	DELTA TFIL (DEG. F)	HCE-TRAN (BTU/HR-FT**2-F)	DELTA HCE-TRAN (BTU/HR-FT**2-F)	HCE-LAM (BTU/HR-FT**2-F)	DELTA HCE-LAM (BTU/HR-FT**2-F)
12	9.91	.926353E+03	.856798E+02	.000000E+00	.000000E+00	.000000E+00	.000000E+00
13	10.23	.969127E+03	.825932E+02	.000000E+00	.000000E+00	.000000E+00	.000000E+00
14	10.48	.100937E+04	.831655E+02	.000000E+00	.000000E+00	.000000E+00	.000000E+00
15	10.73	.103734E+04	.797539E+02	.000000E+00	.000000E+00	.000000E+00	.000000E+00
16	10.97	.997518E+03	.687367E+02	.000000E+00	.000000E+00	.000000E+00	.000000E+00
17	11.14	.104898E+04	.706651E+02	.000000E+00	.000000E+00	.000000E+00	.000000E+00
18	11.32	.111838E+04	.757853E+02	.000000E+00	.000000E+00	.000000E+00	.000000E+00
19	11.48	.114776E+04	.752524E+02	.000000E+00	.000000E+00	.000000E+00	.000000E+00
20	11.73	.118839E+04	.751680E+02	.000000E+00	.000000E+00	.000000E+00	.000000E+00
21	11.88	.120975E+04	.726894E+02	.000000E+00	.000000E+00	.000000E+00	.000000E+00

THIS PAGE

WAS INTENTIONALLY

LEFT BLANK

TEST

3.09.10 J

SYSTEM PARAMETER SUMMARY

SYSTEM PRESSURE	.609340E+03	+OR-	.300023E+02	PSIA
INLET MASS FLOW	.634233E+03	+OR-	.301443E+02	LBM/HR
OUTLET MASS FLOW	.620986E+03	+OR-	.427734E+02	LBM/HR
MASS FLUX - BASED ON OUTLET FLOW	.933342E+04	+OR-	.642885E+03	LBM/(FT**2)HR
MASS FLUX - BASED ON INLET FLOW	.953253E+04	+OR-	.453069E+03	LBM/(FT**2)HR
INLET TEMPERATURE	.405210E+03	+OR-	.700564E+01	DEGREES F
OUTLET TEMPERATURE	.851780E+03	+OR-	.740935E+01	DEGREES F
BUNDLE POWER	.798647E+06	+OR-	.425558E+05	BTU/HR
AVERAGE LINEAR POWER/ROD	.325097E+00	+OR-	.173227E-01	KW/FT
FRACTIONAL HEAT LOSS	.516742E-01			

HEAT TRANSFER CALCULATIONS: TEST 3.09.10J

LEVEL	ELEVATION (FEET)	TVAP (DEG. F)	DELTA TVAP (DEG. F)	NO. OF TC S	TW (DEG. F)	DELTA TW (DEG. F)	Q"/Q"SS	Q"HTRAN (BTU/HR-FT**2)	DELTA Q"HTRAN (BTU/HR-FT**2)
12	9.91	.673302E+03	.480192E+02	22.	.121763E+04	.192284E+02	.100000E+01	.117503E+05	.642881E+03
13	10.23	.733631E+03	.436519E+02	5.	.126523E+04	.221315E+02	.100000E+01	.117155E+05	.671600E+03
14	10.48	.778210E+03	.422234E+02	4.	.129306E+04	.133771E+02	.100000E+01	.117365E+05	.608498E+03
15	10.73	.822603E+03	.417957E+02	4.	.128545E+04	.217600E+02	.100000E+01	.116997E+05	.688858E+03
16	10.97	.865535E+03	.392620E+02	1.	.118168E+04	.410022E+00	.100000E+01	.111036E+05	.555180E+03
17	11.14	.896988E+03	.375725E+02	2.	.121634E+04	.442722E+01	.100000E+01	.115158E+05	.708125E+03
18	11.32	.926571E+03	.386215E+02	3.	.130009E+04	.249887E+01	.100000E+01	.117291E+05	.589131E+03
19	11.48	.955538E+03	.398645E+02	6.	.134585E+04	.616183E+01	.100000E+01	.116563E+05	.638570E+03
20	11.73	.100051E+04	.382062E+02	6.	.138877E+04	.180890E+02	.100000E+01	.117224E+05	.658455E+03
21	11.88	.102783E+04	.373760E+02	17.	.139320E+04	.292536E+02	.100000E+01	.117350E+05	.634588E+03

HEAT TRANSFER CALCULATIONS: TEST 3.09.10J

LEVEL	ELEVATION (FEET)	HEXP (BTU/HR-FT**2-F)	DELTA HEXP (BTU/HR-FT**2-F)	REV	DELTA REV	REF	DELTA REF
12	9.91	.215867E+02	.204321E+01	.670124E+04	.554128E+03	.529799E+04	.449488E+03
13	10.23	.220382E+02	.199501E+01	.631570E+04	.487724E+03	.508809E+04	.409789E+03
14	10.48	.228532E+02	.150695E+01	.607130E+04	.460779E+03	.495619E+04	.386784E+03
15	10.73	.252775E+02	.223866E+01	.584545E+04	.439040E+03	.489173E+04	.379071E+03
16	10.97	.351220E+02	.311204E+01	.564204E+04	.415576E+03	.499926E+04	.371943E+03
17	11.14	.360599E+02	.326498E+01	.550158E+04	.400354E+03	.488262E+04	.358593E+03
18	11.32	.314017E+02	.240251E+01	.537557E+04	.391541E+03	.469470E+04	.345198E+03
19	11.48	.296639E+02	.234321E+01	.525754E+04	.383617E+03	.457839E+04	.337551E+03
20	11.73	.301917E+02	.232414E+01	.508407E+04	.366496E+03	.444870E+04	.326176E+03
21	11.88	.321196E+02	.241047E+01	.498404E+04	.357122E+03	.440360E+04	.325478E+03

HEAT TRANSFER CALCULATIONS: TEST 3.09.10J

LEVEL	ELEVATION (FEET)	QRAD (BTU/HR-FT**2)	DELTA QRAD (BTU/HR-FT**2)	HCONV (BTU/HR-FT**2-F)	DELTA HCONV (BTU/HR-FT**2-F)
12	9.91	.307415E+04	.649094E+03	.147059E+02	.274160E+01
13	10.23	.335274E+04	.715701E+03	.143641E+02	.284659E+01
14	10.48	.348875E+04	.721793E+03	.146567E+02	.285195E+01
15	10.73	.325163E+04	.706153E+03	.167529E+02	.318119E+01
16	10.97	.209018E+04	.454210E+03	.271211E+02	.377192E+01
17	11.14	.225120E+04	.486648E+03	.275314E+02	.396266E+01
18	11.32	.293263E+04	.616706E+03	.218999E+02	.341947E+01
19	11.48	.328051E+04	.691313E+03	.196931E+02	.350051E+01
20	11.73	.351146E+04	.768534E+03	.192442E+02	.368324E+01
21	11.88	.339299E+04	.807105E+03	.208823E+02	.392725E+01

HEAT TRANSFER CALCULATIONS: TEST 3.09.10J

LEVEL	ELEVATION (FEET)	HRAD (BTU/HR-FT**2-F)	DELTA HRAD (BTU/HR-FT**2-F)	REW	DELTA REW	QCROD (BTU/HR-FT**2)	DELTA QCROD (BTU/HR-FT**2)
12	9.91	.688078E+01	.132801E+01	.277752E+04	.303659E+03	.671286E+03	.302973E+03
13	10.23	.767411E+01	.203052E+01	.280023E+04	.296709E+03	.726818E+03	.325196E+03
14	10.48	.823648E+01	.212065E+01	.283298E+04	.290279E+03	.751795E+03	.334246E+03
15	10.73	.852459E+01	.226017E+01	.298347E+04	.299628E+03	.693982E+03	.306878E+03
16	10.97	.800089E+01	.213133E+01	.353481E+04	.329308E+03	.439250E+03	.193691E+03
17	11.14	.852845E+01	.224558E+01	.347345E+04	.322464E+03	.472378E+03	.207263E+03
18	11.32	.950178E+01	.243325E+01	.320935E+04	.301242E+03	.616454E+03	.268777E+03
19	11.48	.101706E+02	.260057E+01	.311160E+04	.292505E+03	.689322E+03	.298932E+03
20	11.73	.109475E+02	.265738E+01	.306670E+04	.289236E+03	.739087E+03	.318097E+03
21	11.88	.112363E+02	.310048E+01	.311478E+04	.296465E+03	.712365E+03	.305371E+03

HEAT TRANSFER CALCULATIONS: TEST 3.09.10J

LEVEL	ELEVATION (FEET)	GRX	DELTA GRX	PRV	DELTA PRV	PRF	DELTA PRF
12	9.91	.133639E+07	.223005E+06	.105657E+01	.430917E-01	.919632E+00	.147886E-01
13	10.23	.104871E+07	.160073E+06	.100483E+01	.284319E-01	.909860E+00	.103667E-01
14	10.48	.882628E+06	.124789E+06	.976443E+00	.205155E-01	.904494E+00	.810487E-02
15	10.73	.740172E+06	.110321E+06	.955428E+00	.153508E-01	.902057E+00	.711119E-02
16	10.97	.567559E+06	.887869E+05	.939991E+00	.112944E-01	.906188E+00	.647438E-02
17	11.14	.505677E+06	.755476E+05	.930916E+00	.914605E-02	.901722E+00	.545045E-02
18	11.32	.480904E+06	.665467E+05	.923697E+00	.804788E-02	.895263E+00	.462163E-02
19	11.48	.440745E+06	.611010E+05	.917616E+00	.720201E-02	.891668E+00	.418334E-02
20	11.73	.377583E+06	.534204E+05	.909689E+00	.568392E-02	.887986E+00	.357146E-02
21	11.88	.337049E+06	.536949E+05	.905583E+00	.498210E-02	.886784E+00	.352550E-02

HEAT TRANSFER CALCULATIONS: TEST 3.09.10J

LEVEL	ELEVATION (FEET)	HW-TRAN (BTU/HR-FT**2-F)	DELTA HW-TRAN (BTU/HR-FT**2-F)	HW-LAM (BTU/HR-FT**2-F)	DELTA HW-LAM (BTU/HR-FT**2-F)	HW-TUR (BTU/HR-FT**2-F)	DELTA HW-TUR (BTU/HR-FT**2-F)
12	9.91	.000000E+00	.000000E+00	.000000E+00	.000000E+00	.229164E+02	.135239E+01
13	10.23	.000000E+00	.000000E+00	.000000E+00	.000000E+00	.241661E+02	.130348E+01
14	10.48	.000000E+00	.000000E+00	.000000E+00	.000000E+00	.251665E+02	.129634E+01
15	10.73	.000000E+00	.000000E+00	.000000E+00	.000000E+00	.260360E+02	.133388E+01
16	10.97	.000000E+00	.000000E+00	.000000E+00	.000000E+00	.265194E+02	.133917E+01
17	11.14	.000000E+00	.000000E+00	.000000E+00	.000000E+00	.273234E+02	.132188E+01
18	11.32	.000000E+00	.000000E+00	.000000E+00	.000000E+00	.283384E+02	.133040E+01
19	11.48	.000000E+00	.000000E+00	.000000E+00	.000000E+00	.292215E+02	.135621E+01
20	11.73	.000000E+00	.000000E+00	.000000E+00	.000000E+00	.304889E+02	.135961E+01
21	11.88	.310655E+02	.287811E+01	.000000E+00	.000000E+00	.000000E+00	.000000E+00

HEAT TRANSFER CALCULATIONS: TEST 3.09.10J

LEVEL	ELEVATION (FEET)	HCE-TUR (BTU/HR-FT**2-F)	DELTA HCE-TUR (BTU/HR-FT**2-F)	HB&W (BTU/HR-FT**2-F)	DELTA HB&W (BTU/HR-FT**2-F)	HORNL (BTU/HR-FT**2-F)	DELTA HORNL (BTU/HR-FT**2-F)
12	9.91	.000000E+00	.000000E+00	.213337E+02	.180805E+01	.151538E+02	.134922E+01
13	10.23	.000000E+00	.000000E+00	.212092E+02	.166292E+01	.158286E+02	.137176E+01
14	10.48	.000000E+00	.000000E+00	.212852E+02	.162111E+01	.163185E+02	.134941E+01
15	10.73	.000000E+00	.000000E+00	.214404E+02	.160418E+01	.169108E+02	.138981E+01
16	10.97	.000000E+00	.000000E+00	.216416E+02	.155255E+01	.178581E+02	.133179E+01
17	11.14	.000000E+00	.000000E+00	.218115E+02	.152171E+01	.181035E+02	.134687E+01
18	11.32	.000000E+00	.000000E+00	.219838E+02	.153917E+01	.181267E+02	.136219E+01
19	11.48	.000000E+00	.000000E+00	.221613E+02	.155999E+01	.182938E+02	.137889E+01
20	11.73	.000000E+00	.000000E+00	.224492E+02	.153362E+01	.186509E+02	.142907E+01
21	11.88	.000000E+00	.000000E+00	.226292E+02	.152201E+01	.189440E+02	.149818E+01

HEAT TRANSFER CALCULATIONS: TEST 3.09.10J

LEVEL	ELEVATION (FEET)	HEINEMAN (BTU/HR-FT**2-F)	DELTA HEINEMAN (BTU/HR-FT**2-F)	MCELIGOT (BTU/HR-FT**2-F)	DELTA MCELIGOT (BTU/HR-FT**2-F)
12	9.91	.181135E+02	.179543E+01	.160096E+02	.137011E+01
13	10.23	.183791E+02	.165704E+01	.161074E+02	.128581E+01
14	10.48	.185628E+02	.157235E+01	.163331E+02	.127118E+01
15	10.73	.186572E+02	.155742E+01	.167809E+02	.128553E+01
16	10.97	.185014E+02	.141238E+01	.177555E+02	.130328E+01
17	11.14	.186708E+02	.138322E+01	.179178E+02	.127784E+01
18	11.32	.189637E+02	.140865E+01	.178155E+02	.127590E+01
19	11.48	.191569E+02	.143137E+01	.179146E+02	.129078E+01
20	11.73	.193830E+02	.142827E+01	.182181E+02	.127193E+01
21	11.88	.194641E+02	.146104E+01	.185130E+02	.127139E+01

HEAT TRANSFER CALCULATIONS: TEST 3.09.10J

LEVEL	ELEVATION (FEET)	TFIL (DEG. F)	DELTA TFIL (DEG. F)	HCE-TRAN (BTU/HR-FT**2-F)	DELTA HCE-TRAN (BTU/HR-FT**2-F)	HCE-LAM (BTU/HR-FT**2-F)	DELTA HCE-LAM (BTU/HR-FT**2-F)
12	9.91	.945468E+03	.690630E+02	.191382E+02	.422974E+01	.000000E+00	.000000E+00
13	10.23	.999431E+03	.619837E+02	.184279E+02	.345833E+01	.000000E+00	.000000E+00
14	10.48	.103564E+04	.572028E+02	.180666E+02	.310258E+01	.000000E+00	.000000E+00
15	10.73	.105403E+04	.564482E+02	.177970E+02	.288854E+01	.000000E+00	.000000E+00
16	10.97	.102361E+04	.464337E+02	.176445E+02	.262310E+01	.000000E+00	.000000E+00
17	11.14	.105666E+04	.444277E+02	.174901E+02	.245539E+01	.000000E+00	.000000E+00
18	11.32	.111333E+04	.464553E+02	.173185E+02	.241436E+01	.000000E+00	.000000E+00
19	11.48	.115070E+04	.482945E+02	.171828E+02	.239563E+01	.000000E+00	.000000E+00
20	11.73	.119464E+04	.482002E+02	.170114E+02	.224746E+01	.000000E+00	.000000E+00
21	11.88	.121052E+04	.508305E+02	.169223E+02	.217781E+01	.000000E+00	.000000E+00

THIS PAGE

WAS INTENTIONALLY

LEFT BLANK

TEST

3.09.10K

SYSTEM PARAMETER SUMMARY

SYSTEM PRESSURE	.581218E+03	+OR-	.300083E+02	PSIA
INLET MASS FLOW	.109117E+03	+OR-	.307119E+02	LBM/HR
OUTLET MASS FLOW	.153461E+03	+OR-	.127130E+02	LBM/HR
MASS FLUX - BASED ON OUTLET FLOW	.230652E+04	+OR-	.191077E+03	LBM/(FT**2)HR
MASS FLUX - BASED ON INLET FLOW	.164003E+04	+OR-	.461600E+03	LBM/(FT**2)HR
INLET TEMPERATURE	.380243E+03	+OR-	.701085E+01	DEGREES F
OUTLET TEMPERATURE	.690114E+03	+OR-	.722437E+01	DEGREES F
BUNDLE POWER	.237348E+06	+OR-	.148569E+05	BTU/HR
AVERAGE LINEAR POWER/ROD	.966149E-01	+OR-	.604766E-02	KW/FT
FRACTIONAL HEAT LOSS	.175532E+00			

HEAT TRANSFER CALCULATIONS: TEST 3.09.10K

LEVEL	ELEVATION (FEET)	TVAP (DEG. F)	DELTA TVAP (DEG. F)	NO. OF TC S	TW (DEG. F)	DELTA TW (DEG. F)	Q"/Q"SS	Q"HTRAN (BTU/HR-FT**2)	DELTA Q"HTRAN (BTU/HR-FT**2)
5	7.94	.558204E+03	.956547E+02	28.	.959569E+03	.230386E+02	.972225E+00	.345246E+04	.221432E+03
6	8.24	.615862E+03	.951543E+02	2.	.963224E+03	.328599E+01	.977813E+00	.345697E+04	.198132E+03
7	8.47	.661353E+03	.906851E+02	2.	.100817E+04	.676476E+00	.975756E+00	.352519E+04	.202093E+03
8	8.73	.708469E+03	.891436E+02	5.	.105192E+04	.245512E+02	.980469E+00	.353652E+04	.198659E+03
9	9.31	.813055E+03	.821585E+02	1.	.110433E+04	.328807E+00	.981044E+00	.346262E+04	.176477E+03
10	9.49	.847505E+03	.823712E+02	3.	.113941E+04	.282250E+02	.977747E+00	.350502E+04	.205607E+03
11	9.74	.896322E+03	.824124E+02	4.	.118723E+04	.154853E+02	.977040E+00	.356104E+04	.188164E+03
12	9.91	.931494E+03	.788386E+02	22.	.118859E+04	.278862E+02	.960045E+00	.344919E+04	.223018E+03
13	10.23	.997180E+03	.723360E+02	5.	.122192E+04	.224924E+02	.958717E+00	.345043E+04	.205115E+03
14	10.48	.104153E+04	.755135E+02	4.	.123956E+04	.229273E+02	.953312E+00	.341581E+04	.193650E+03
15	10.73	.107928E+04	.774683E+02	4.	.127068E+04	.947404E+01	.927879E+00	.335518E+04	.193323E+03
16	10.97	.111794E+04	.745525E+02	1.	.127423E+04	.862801E+00	.926923E+00	.327160E+04	.176477E+03
17	11.14	.114543E+04	.725303E+02	2.	.131801E+04	.112820E+02	.916793E+00	.331910E+04	.202515E+03
18	11.32	.116543E+04	.710425E+02	3.	.133177E+04	.379083E+02	.919178E+00	.331527E+04	.208242E+03
19	11.48	.118388E+04	.697854E+02	6.	.133679E+04	.321029E+02	.901293E+00	.326051E+04	.202656E+03
20	11.73	.120882E+04	.682639E+02	6.	.133634E+04	.277126E+02	.876808E+00	.316230E+04	.202193E+03
21	11.88	.122354E+04	.674666E+02	17.	.133996E+04	.476469E+02	.874654E+00	.313827E+04	.222089E+03

HEAT TRANSFER CALCULATIONS: TEST 3.09.10K

LEVEL	ELEVATION (FEET)	HEXP (BTU/HR-FT**2-F)	DELTA HEXP (BTU/HR-FT**2-F)	REV	DELTA REV	REF	DELTA REF
5	7.94	.860179E+01	.187264E+01	.193471E+04	.311253E+03	.152757E+04	.218534E+03
6	8.24	.955208E+01	.236050E+01	.178668E+04	.262595E+03	.148717E+04	.199635E+03
7	8.47	.101646E+02	.227684E+01	.168379E+04	.212981E+03	.143124E+04	.180954E+03
8	8.73	.102972E+02	.219692E+01	.159663E+04	.185088E+03	.137902E+04	.169386E+03
9	9.31	.118878E+02	.248949E+01	.145757E+04	.157825E+03	.129709E+04	.143649E+03
10	9.49	.120075E+02	.240049E+01	.141620E+04	.151791E+03	.126378E+04	.140143E+03
11	9.74	.122409E+02	.236141E+01	.136137E+04	.143778E+03	.122019E+04	.131685E+03
12	9.91	.134160E+02	.269050E+01	.132437E+04	.136264E+03	.120448E+04	.127371E+03
13	10.23	.153531E+02	.288605E+01	.126032E+04	.124190E+03	.116382E+04	.116824E+03
14	10.48	.172488E+02	.309644E+01	.122040E+04	.120675E+03	.113971E+04	.114657E+03
15	10.73	.175290E+02	.317611E+01	.118835E+04	.117493E+03	.111407E+04	.111065E+03
16	10.97	.209325E+02	.376553E+01	.115720E+04	.112337E+03	.109891E+04	.107181E+03
17	11.19	.192318E+02	.304225E+01	.113600E+04	.108966E+03	.107421E+04	.103761E+03
18	11.32	.199303E+02	.299525E+01	.112106E+04	.106639E+03	.106289E+04	.104227E+03
19	11.48	.213237E+02	.309963E+01	.110762E+04	.104625E+03	.105516E+04	.101963E+03
20	11.73	.247995E+02	.356120E+01	.108995E+04	.102087E+03	.104721E+04	.998077E+02
21	11.88	.269559E+02	.394019E+01	.107978E+04	.100682E+03	.104134E+04	.101568E+03

HEAT TRANSFER CALCULATIONS: TEST 3.09.10K

LEVEL	ELEVATION (FEET)	QRAD (BTU/HR-FT**2)	DELTA QRAD (BTU/HR-FT**2)	HCONV (BTU/HR-FT**2-F)	DELTA HCONV (BTU/HR-FT**2-F)
5	7.94	.147877E+04	.394641E+03	.415474E+01	.246025E+01
6	8.24	.137572E+04	.382525E+03	.518736E+01	.296987E+01
7	8.47	.152393E+04	.415335E+03	.488787E+01	.298329E+01
8	8.73	.166887E+04	.487985E+03	.447247E+01	.308398E+01
9	9.31	.167051E+04	.495993E+03	.504206E+01	.355690E+01
10	9.49	.179599E+04	.584493E+03	.467184E+01	.369704E+01
11	9.74	.196784E+04	.606755E+03	.419752E+01	.380220E+01
12	9.91	.180195E+04	.632778E+03	.509576E+01	.428387E+01
13	10.23	.172936E+04	.625049E+03	.624491E+01	.466088E+01
14	10.48	.161363E+04	.671191E+03	.762361E+01	.524405E+01
15	10.73	.165840E+04	.691757E+03	.731105E+01	.550813E+01
16	10.97	.140709E+04	.680777E+03	.103354E+02	.643648E+01
17	11.14	.165007E+04	.722237E+03	.799000E+01	.588791E+01
18	11.32	.163661E+04	.843193E+03	.837269E+01	.659693E+01
19	11.48	.153500E+04	.809774E+03	.954169E+01	.683899E+01
20	11.73	.130793E+04	.782632E+03	.127768E+02	.778286E+01
21	11.88	.121298E+04	.913546E+03	.147528E+02	.946295E+01

HEAT TRANSFER CALCULATIONS: TEST 3.09.10K

LEVEL	ELEVATION (FEET)	HRAD (BTU/HR-FT**2-F)	DELTA HRAD (BTU/HR-FT**2-F)	REW	DELTA REW	QCROD (BTU/HR-FT**2)	DELTA QCROD (BTU/HR-FT**2)
5	7.94	.444705E+01	.159562E+01	.845141E+03	.107060E+03	.306122E+03	.127143E+03
6	8.24	.476472E+01	.180223E+01	.914889E+03	.106492E+03	.279362E+03	.114287E+03
7	8.47	.527670E+01	.192770E+01	.905653E+03	.103093E+03	.306094E+03	.123119E+03
8	8.73	.582468E+01	.216437E+01	.896835E+03	.102711E+03	.331602E+03	.130909E+03
9	9.31	.684577E+01	.254048E+01	.925715E+03	.995241E+02	.323490E+03	.123302E+03
10	9.49	.733561E+01	.281172E+01	.910747E+03	.100361E+03	.345298E+03	.126953E+03
11	9.74	.804343E+01	.296405E+01	.891997E+03	.955925E+02	.372087E+03	.135934E+03
12	9.91	.832028E+01	.333358E+01	.916748E+03	.989555E+02	.357143E+03	.121958E+03
13	10.23	.910815E+01	.365986E+01	.924969E+03	.975357E+02	.317592E+03	.112024E+03
14	10.48	.962522E+01	.423228E+01	.935085E+03	.977785E+02	.292461E+03	.101495E+03
15	10.73	.102179E+02	.450020E+01	.924463E+03	.948147E+02	.297386E+03	.101389E+03
16	10.97	.105972E+02	.522006E+01	.945600E+03	.957958E+02	.249164E+03	.839690E+02
17	11.14	.112418E+02	.504105E+01	.913780E+03	.931634E+02	.290076E+03	.100398E+03
18	11.32	.115576E+02	.587775E+01	.911045E+03	.965970E+02	.285918E+03	.986393E+02
19	11.48	.117820E+02	.609623E+01	.916710E+03	.956875E+02	.266530E+03	.918132E+02
20	11.73	.120227E+02	.692031E+01	.932085E+03	.959830F+02	.225138F+03	.775099E+02
21	11.88	.122032E+02	.860362E+01	.936849E+03	.100701E+03	.207741E+03	.714862E+02

HEAT TRANSFER CALCULATIONS: TEST 3.09.10K

LEVEL	ELEVATION (FEET)	GRX	DELTA GRX	PRV	DELTA PRV	PRF	DELTA PRF
5	7.94	.212296E+07	.775700E+06	.118666E+01	.123843E+00	.983454E+00	.546257E-01
6	8.24	.156704E+07	.576463E+06	.110274E+01	.854914E-01	.967108E+00	.428166E-01
7	8.47	.125413E+07	.430863E+06	.105760E+01	.705714E-01	.948208E+00	.317153E-01
8	8.73	.100803E+07	.345217E+06	.102034E+01	.573882E-01	.933792E+00	.246115E-01
9	9.31	.611559E+06	.202775E+06	.956610E+00	.269930E-01	.915946E+00	.149908E-01
10	9.49	.532988E+06	.184144E+06	.943769E+00	.222091E-01	.909971E+00	.132484E-01
11	9.74	.440776E+06	.146294E+06	.929506E+00	.172017E-01	.903016E+00	.107302E-01
12	9.91	.363781E+06	.131396E+06	.921342E+00	.140238E-01	.900717E+00	.970000E-02
13	10.23	.265584E+06	.967498E+05	.909384E+00	.983869E-02	.895217E+00	.738812E-02
14	10.48	.209839E+06	.885302E+05	.903048E+00	.860903E-02	.892235E+00	.679818E-02
15	10.73	.180234E+06	.774154E+05	.898462E+00	.768382E-02	.889271E+00	.601778E-02
16	10.97	.137107E+06	.676743E+05	.894379E+00	.650259E-02	.887618E+00	.531191E-02
17	11.14	.134665E+06	.596298E+05	.891793E+00	.578393E-02	.885076E+00	.464754E-02
18	11.32	.122921E+06	.615667E+05	.890059E+00	.531004E-02	.883974E+00	.463108E-02
19	11.48	.108839E+06	.562945E+05	.888560E+00	.491269E-02	.883245E+00	.426894E-02
20	11.73	.873169E+05	.514854E+05	.886674E+00	.442822E-02	.882514E+00	.392183E-02
21	11.88	.774577E+05	.558133E+05	.885633E+00	.416753E-02	.881987E+00	.410815E-02

HEAT TRANSFER CALCULATIONS: TEST 3.09.10K

LEVEL	ELEVATION (FEET)	HW-TRAN (BTU/HR-FT**2-F)	DELTA HW-TRAN (BTU/HR-FT**2-F)	HW-LAM (BTU/HR-FT**2-F)	DELTA HW-LAM (BTU/HR-FT**2-F)	HW-TUR (BTU/HR-FT**2-F)	DELTA HW-TUR (BTU/HR-FT**2-F)
5	7.94	.000000E+00	.000000E+00	.708275E+01	.564745E+00	.000000E+00	.000000E+00
6	8.24	.000000E+00	.000000E+00	.754259E+01	.595710E+00	.000000E+00	.000000E+00
7	8.47	.000000E+00	.000000E+00	.821699E+01	.611349E+00	.000000E+00	.000000E+00
8	8.73	.000000E+00	.000000E+00	.895395E+01	.669899E+00	.000000E+00	.000000E+00
9	9.31	.000000E+00	.000000E+00	.104253E+02	.668635E+00	.000000E+00	.000000E+00
10	9.49	.000000E+00	.000000E+00	.110884E+02	.741910E+00	.000000E+00	.000000E+00
11	9.74	.000000E+00	.000000E+00	.120618E+02	.757411E+00	.000000E+00	.000000E+00
12	9.91	.000000E-00	.000000E+00	.125060E+02	.777296E+00	.000000E+00	.000000E+00
13	10.23	.000000E+00	.000000E+00	.136479E+02	.748722E+00	.000000E+00	.000000E+00
14	10.48	.000000E+00	.000000E+00	.144100E+02	.812908E+00	.000000E+00	.000000E+00
15	10.73	.000000E+00	.000000E+00	.152384E+02	.837669E+00	.000000E+00	.000000E+00
16	10.97	.000000E+00	.000000E+00	.158299E+02	.824100E+00	.000000E+00	.000000E+00
17	11.14	.000000E+00	.000000E+00	.166883E+02	.839377E+00	.000000E+00	.000000E+00
18	11.32	.000000E+00	.000000E+00	.171377E+02	.936912E+00	.000000E+00	.000000E+00
19	11.48	.000000E+00	.000000E+00	.174753E+02	.906245E+00	.000000E+00	.000000E+00
20	11.73	.000000E+00	.000000E+00	.178590E+02	.883429E+00	.000000E+00	.000000E+00
21	11.88	.000000E+00	.000000E-00	.181313E+02	.998674E+00	.000000E+00	.000000E+00

HEAT TRANSFER CALCULATIONS: TEST 3.09.10K

LEVEL	ELEVATION (FEET)	HCE-TUR (BTU/HR-FT**2-F)	DELTA HCE-TUR (BTU/HR-FT**2-F)	HB&W (BTU/HR-FT**2-F)	DELTA HB&W (BTU/HR-FT**2-F)	HORNL (BTU/HR-FT**2-F)	DELTA HORNL (BTU/HR-FT**2-F)
5	7.94	.000000E+00	.000000E+00	.746700E+01	.117941E+01	.469071E+01	.489599E+00
6	8.24	.000000E+00	.000000E+00	.709495E+01	.111212E+01	.501429E+01	.468669E+00
7	8.47	.000000E+00	.000000E+00	.694660E+01	.100088E+01	.517624E+01	.472346E+00
8	8.73	.000000E+00	.000000E+00	.688751E+01	.946021E+00	.533592E+01	.504273E+00
9	9.31	.000000E+00	.000000E+00	.696800E+01	.866456E+00	.572361E+01	.492593E+00
10	9.49	.000000E+00	.000000E+00	.702015E+01	.861226E+00	.581750E+01	.532710E+00
11	9.74	.000000E+00	.000000E+00	.710685E+01	.852843E+00	.594944E+01	.516149E+00
12	9.91	.000000E+00	.000000E+00	.717578E+01	.821983E+00	.608778E+01	.545006E+00
13	10.23	.000000E+00	.000000E+00	.731349E+01	.770603E+00	.629660E+01	.543978E+00
14	10.48	.000000E+00	.000000E+00	.741037E+01	.786829E+00	.644031E+01	.552124E+00
15	10.73	.000000E+00	.000000E+00	.749408E+01	.795486E+00	.653741E+01	.538805E+00
16	10.97	.000000E+00	.000000E+00	.758033E+01	.773977E+00	.667481E+01	.541145E+00
17	11.14	.000000E+00	.000000E+00	.764174E+01	.759869E+00	.671298E+01	.550765E+00
18	11.32	.000000E+00	.000000E+00	.768634E+01	.749948E+00	.676567E+01	.606360E+00
19	11.48	.000000E+00	.000000E+00	.772738E+01	.741777E+00	.682450E+01	.593777E+00
20	11.73	.000000E+00	.000000E+00	.778266E+01	.732148E+00	.691362E+01	.587968E+00
21	11.88	.000000E+00	.000000E+00	.781515E+01	.727215E+00	.696044E+01	.649236E+00

HEAT TRANSFER CALCULATIONS: TEST 3.09.10K

LEVEL	ELEVATION (FEET)	HEINEMAN (BTU/HR-FT**2-F)	DELTA HEINEMAN (BTU/HR-FT**2-F)	MCELIGOT (BTU/HR-FT**2-F)	DELTA MCELIGOT (BTU/HR-FT**2-F)
5	7.94	.536280E+01	.102262E+01	.577400E+01	.899867E+00
6	8.24	.538625E+01	.948030E+00	.563226E+01	.893897E+00
7	8.47	.543320E+01	.884908E+00	.554304E+01	.815170E+00
8	8.73	.549072E+01	.861379E+00	.552839E+01	.780471E+00
9	9.31	.560468E+01	.750576E+00	.573931E+01	.739287E+00
10	9.49	.565857E+01	.760229E+00	.579535E+01	.737256E+00
11	9.74	.573527E+01	.736215E+00	.588806E+01	.733120E+00
12	9.91	.576458E+01	.714008E+00	.601929E+01	.714677E+00
13	10.23	.584438E+01	.656790E+00	.621542E+01	.677006E+00
14	10.48	.589433E+01	.664838E+00	.635961E+01	.698448E+00
15	10.73	.594958E+01	.658708E+00	.645296E+01	.708575E+00
16	10.97	.598326E+01	.633602E+00	.660194E+01	.696169E+00
17	11.14	.603970E+01	.626119E+00	.662997E+01	.680042E+00
18	11.32	.606622E+01	.648121E+00	.668426E+01	.672128E+00
19	11.48	.608455E+01	.630556E+00	.674855E+01	.667079E+00
20	11.73	.610359E+01	.614098E+00	.684905E+01	.662765E+00
21	11.88	.611730E+01	.645585E+00	.690095E+01	.660150E+00

HEAT TRANSFER CALCULATIONS: TEST 3.09.10K

LEVEL	ELEVATION (FEET)	TFIL (DEG. F)	DELTA TFIL (DEG. F)	HCE-TRAN (BTU/HR-FT**2-F)	DELTA HCE-TRAN (BTU/HR-FT**2-F)	HCE-LAM (BTU/HR-FT**2-F)	DELTA HCE-LAM (BTU/HR-FT**2-F)
5	7.94	.758887E+03	.131314E+03	.000000E+00	.000000E+00	.567994E+01	.206989E+01
6	8.24	.789543E+03	.122019E+03	.000000E+00	.000000E+00	.521760E+01	.155203E+01
7	8.47	.834759E+03	.114464E+03	.000000E+00	.000000E+00	.499984E+01	.129531E+01
8	8.73	.880192E+03	.112640E+03	.000000E+00	.000000E+00	.483868E+01	.111134E+01
9	9.31	.958692E+03	.968755E+02	.000000E+00	.000000E+00	.470664E+01	.845618E+00
10	9.49	.993457E+03	.996435E+02	.000000E+00	.000000E+00	.469449E+01	.805334E+00
11	9.74	.104178E+04	.967454E+02	.000000E+00	.000000E+00	.470116E+01	.748618E+00
12	9.91	.106004E+04	.931017E+02	.000000E+00	.000000E+00	.473621E+01	.711703E+00
13	10.23	.110955E+04	.830383E+02	.000000E+00	.000000E+00	.479383E+01	.641252E+00
14	10.48	.114055E+04	.853408E+02	.000000E+00	.000000E+00	.482775E+01	.622753E+00
15	10.73	.117498E+04	.847914E+02	.000000E+00	.000000E+00	.483815E+01	.598100E+00
16	10.97	.119608E+04	.797680E+02	.000000E+00	.000000E+00	.487485E+01	.565009E+00
17	11.14	.123172E+04	.787044E+02	.000000E+00	.000000E+00	.488219E+01	.544786E+00
18	11.32	.124860E+04	.840013E+02	.000000E+00	.000000E+00	.487811E+01	.532177E+00
19	11.48	.126033E+04	.802209E+02	.000000E+00	.000000E+00	.487726E+01	.513794E+00
20	11.73	.127258E+04	.765568E+02	.000000E+00	.000000E+00	.487587E+01	.491058E+00
21	11.88	.128175E+04	.840976E+02	.000000E+00	.000000E+00	.487246E+01	.484187E+00

THIS PAGE

WAS INTENTIONALLY

LEFT BLANK

TEST

3.09.10L

SYSTEM PARAMETER SUMMARY

SYSTEM PRESSURE	.109031E+04	+OR-	.300088E+02	PSIA
INLET MASS FLOW	.000000E+00	+OR-	.000000E+00	LBM/HR
OUTLET MASS FLOW	.142791E+04	+OR-	.799672E+02	LBM/HR
MASS FLUX - BASED ON OUTLET FLOW	.214614E+05	+OR-	.120191E+04	LBM/(FT**2)HR
MASS FLUX - BASED ON INLET FLOW	.000000E+00	+OR-	.000000E+00	LBM/(FT**2)HR
INLET TEMPERATURE	.370983E+03	+OR-	.700971E+01	DEGREES F
OUTLET TEMPERATURE	.828601E+03	+OR-	.726803E+01	DEGREES F
BUNDLE POWER	.162343E+07	+OR-	.864321E+05	BTU/HR
AVERAGE LINEAR POWER/ROD	.660833E+00	+OR-	.351830E-01	KW/FT
FRACTIONAL HEAT LOSS	.170706E-01			

HEAT TRANSFER CALCULATIONS: TEST 3.09.10L

LEVEL	ELEVATION (FEET)	TVAP (DEG. F)	DELTA TVAP (DEG. F)	NO. OF TC S	TW (DEG. F)	DELTA TW (DEG. F)	Q"/Q"SS	Q"HTRAN (BTU/HR-FT**2)	DELTA Q"HTRAN (BTU/HR-FT**2)
12	9.91	.575082E+03	.350553E+02	22.	.117722E+04	.359145E+02	.988237E+00	.235722E+05	.130194E+04
13	10.23	.615089E+03	.349451E+02	5.	.126892E+04	.224813E+02	.986180E+00	.234506E+05	.134836E+04
14	10.48	.646767E+03	.339954E+02	4.	.131507E+04	.179236E+02	.986635E+00	.236232E+05	.122934E+04
15	10.73	.678490E+03	.346945E+02	4.	.131897E+04	.270209E+02	.989714E+00	.235124E+05	.137370E+04
16	10.97	.709448E+03	.367005E+02	1.	.108828E+04	.771157E+00	.993061E+00	.224558E+05	.113063E+04
17	11.14	.734717E+03	.350888E+02	2.	.114692E+04	.138546E+02	.991591E+00	.232140E+05	.141647E+04
18	11.32	.758642E+03	.358985E+02	3.	.124324E+04	.396335E+01	.992250E+00	.236976E+05	.121022E+04
19	11.48	.781934E+03	.354724E+02	6.	.129217E+04	.846464E+01	.991058E+00	.235038E+05	.129787E+04
20	11.73	.816027E+03	.365646E+02	6.	.132881E+04	.196939E+02	.990621E+00	.235639E+05	.132359E+04
21	11.88	.837701E+03	.365326E+02	17.	.134050E+04	.179523E+02	.987512E+00	.235200E+05	.127749E+04

HEAT TRANSFER CALCULATIONS: TEST 3.09.10L

LEVEL	ELEVATION (FEET)	HEXP (BTU/HR-FT**2-F)	DELTA HEXP (BTU/HR-FT**2-F)	REV	DELTA REV	REF	DELTA REF
12	9.91	.391477E+02	.273070E+01	.177180E+05	.138841E+04	.126738E+05	.881770E+03
13	10.23	.358663E+02	.244127E+01	.165996E+05	.130140E+04	.120561E+05	.801684E+03
14	10.48	.353483E+02	.221596E+01	.157614E+05	.117232E+04	.117172E+05	.756969E+03
15	10.73	.367105E+02	.246304E+01	.149561E+05	.923811E+03	.115681E+05	.753029E+03
16	10.97	.592766E+02	.386120E+01	.145082E+05	.871840E+03	.124542E+05	.782934E+03
17	11.14	.563162E+02	.400719E+01	.142166E+05	.850498E+03	.120668E+05	.751033E+03
18	11.32	.489017E+02	.294226E+01	.139329E+05	.835206E+03	.115498E+05	.715388E+03
19	11.48	.460643E+02	.290441E+01	.136660E+05	.813736E+03	.112592E+05	.692809E+03
20	11.73	.459528E+02	.290134E+01	.132912E+05	.792929E+03	.109878E+05	.684282E+03
21	11.88	.467781E+02	.287176E+01	.130624E+05	.775338E+03	.108642E+05	.669666E+03

HEAT TRANSFER CALCULATIONS: TEST 3.09.10L

LEVEL	ELEVATION (FEET)	QRAD (BTU/HR-FT**2)	DELTA QRAD (BTU/HR-FT**2)	HCONV (BTU/HR-FT**2-F)	DELTA HCONV (BTU/HR-FT**2-F)
12	9.91	.328351E+04	.744242E+03	.325968E+02	.325509E+01
13	10.23	.413253E+04	.861500E+03	.282764E+02	.311121E+01
14	10.48	.459306E+04	.939753E+03	.271020E+02	.302913E+01
15	10.73	.456798E+04	.971901E+03	.281637E+02	.329653E+01
16	10.97	.214838E+04	.446164E+03	.524950E+02	.422487E+01
17	11.14	.256737E+04	.541827E+03	.488704E+02	.443324E+01
18	11.32	.344540E+04	.699062E+03	.404050E+02	.361413E+01
19	11.48	.391331E+04	.796232E+03	.369023E+02	.368235E+01
20	11.73	.421903E+04	.890056E+03	.361291E+02	.381898E+01
21	11.83	.426916E+04	.896000E+03	.366432E+02	.384093E+01

HEAT TRANSFER CALCULATIONS: TEST 3.09.10L

LEVEL	ELEVATION (FEET)	HRAD (BTU/HR-FT**2-F)	DELTA HRAD (BTU/HR-FT**2-F)	REW	DELTA REW	QCROD (BTU/HR-FT**2)	DELTA QCROD (BTU/HR-FT**2)
12	9.91	.655089E+01	.177170E+01	.509078E+04	.518665E+03	.661019E+03	.309244E+03
13	10.23	.758984E+01	.192869E+01	.498326E+04	.446635E+03	.829966E+03	.386520E+03
14	10.43	.824625E+01	.206522E+01	.500834E+04	.422250E+03	.917894E+03	.426918E+03
15	10.75	.854678E+01	.219102E+01	.525859E+04	.431125E+03	.906076E+03	.419736E+03
16	10.97	.678157E+01	.171482E+01	.745633E+04	.521882E+03	.420684E+03	.194727E+03
17	11.14	.744576E+01	.189633E+01	.711173E+04	.504549E+03	.501836E+03	.231740E+03
18	11.32	.849669E+01	.209883E+01	.645947E+04	.454986E+03	.672065E+03	.309553E+03
19	11.48	.916198E+01	.226366E+01	.624996E+04	.440333E+03	.761499E+03	.349978E+03
20	11.73	.982369E+01	.248330E+01	.621432E+04	.441730E+03	.818412E+03	.375035E+03
21	11.88	.101349E+02	.255865E+01	.627269E+04	.439282E+03	.826643E+03	.378146E+03

HEAT TRANSFER CALCULATIONS: TEST 3.09.10L

LEVEL	ELEVATION (FEET)	GRX	DELTA GRX	PRV	DELTA PRV	PRF	DELTA PRF
12	9.91	.755156E+07	.113525E+07	.145483E+01	.121626E+00	.972813E+00	.369224E-01
13	10.23	.595245E+07	.759212E+06	.132235E+01	.776629E-01	.943194E+00	.236209E-01
14	10.48	.510692E+07	.598016E+06	.125227E+01	.580397E-01	.930594E+00	.183289E-01
15	10.73	.453063E+07	.555860E+06	.120352E+01	.649964E-01	.925704E+00	.163537E-01
16	10.97	.423778E+07	.565930E+06	.114651E+01	.587733E-01	.961158E+00	.210004E-01
17	11.14	.377335E+07	.481297E+06	.110445E+01	.460377E-01	.943626E+00	.163637E-01
18	11.32	.339566E+07	.389805E+06	.107222E+01	.396920E-01	.925130E+00	.123268E-01
19	11.48	.307392E+07	.342222E+06	.104565E+01	.334126E-01	.916655E+00	.103413E-01
20	11.73	.267996E+07	.319377E+06	.101375E+01	.271294E-01	.909727E+00	.903972E-02
21	11.88	.246188E+07	.287803E+06	.997037E+00	.232914E-01	.906840E+00	.814603E-02

HEAT TRANSFER CALCULATIONS: TEST 3.09.10L

LEVEL	ELEVATION (FEET)	HW-TRAN (BTU/HR-FT**2-F)	DELTA HW-TRAN (BTU/HR-FT**2-F)	HW-LAM (BTU/HR-FT**2-F)	DELTA HW-LAM (BTU/HR-FT**2-F)	HW-TUR (BTU/HR-FT**2-F)	DELTA HW-TUR (BTU/HR-FT**2-F)
12	9.91	.000000E+00	.000000E+00	.000000E+00	.000000E+00	.446627E+02	.291472E+01
13	10.23	.000000E+00	.000000E+00	.000000E+00	.000000E+00	.420047E+02	.225012E+01
14	10.48	.000000E+00	.000000E+00	.000000E+00	.000000E+00	.410912E+02	.204279E+01
15	10.73	.000000E+00	.000000E+00	.000000E+00	.000000E+00	.406571E+02	.176297E+01
16	10.97	.000000E+00	.000000E+00	.000000E+00	.000000E+00	.414009E+02	.192183E+01
17	11.14	.000000E+00	.000000E+00	.000000E+00	.000000E+00	.417618E+02	.192964E+01
18	11.32	.000000E+00	.000000E+00	.000000E+00	.000000E+00	.421488E+02	.194212E+01
19	11.48	.000000E+00	.000000E+00	.000000E+00	.000000E+00	.427173E+02	.194821E+01
20	11.73	.000000E+00	.000000E+00	.000000E+00	.000000E+00	.436666E+02	.202037E+01
21	11.88	.000000E+00	.000000E+00	.000000E+00	.000000E+00	.443083E+02	.203704E+01

HEAT TRANSFER CALCULATIONS: TEST 3.09.10L

LEVEL	ELEVATION (FEET)	HCE-TUR (BTU/HR-FT**2-F)	DELTA HCE-TUR (BTU/HR-FT**2-F)	HB&W (BTU/HR-FT**2-F)	DELTA HB&W (BTU/HR-FT**2-F)	HORNL (BTU/HR-FT**2-F)	DELTA HORNL (BTU/HR-FT**2-F)
12	9.91	.613696E+02	.506385E+01	.613696E+02	.506385E+01	.247011E+02	.218290E+01
13	10.23	.538722E+02	.368706E+01	.538722E+02	.368706E+01	.259894E+02	.193719E+01
14	10.48	.503098E+02	.320793E+01	.503098E+02	.320793E+01	.269713E+02	.186755E+01
15	10.73	.478606E+02	.274780E+01	.478606E+02	.274780E+01	.281218E+02	.193779E+01
16	10.97	.465307E+02	.271160E+01	.465307E+02	.271160E+01	.313131E+02	.176402E+01
17	11.14	.458470E+02	.263904E+01	.458470E+02	.263904E+01	.315413E+02	.183334E+01
18	11.32	.453734E+02	.264785E+01	.453734E+02	.264785E+01	.313908E+02	.177682E+01
19	11.48	.450552E+02	.261640E+01	.450552E+02	.261640E+01	.316785E+02	.180099E+01
20	11.73	.447858E+02	.263697E+01	.447858E+02	.263697E+01	.323649E+02	.190219E+01
21	11.88	.447102E+02	.261865E+01	.447102E+02	.261865E+01	.328761E+02	.189415E+01

HEAT TRANSFER CALCULATIONS: TEST 3.09.10L

LEVEL	ELEVATION (FEET)	HEINEMAN (BTU/HR-FT**2-F)	DELTA HEINEMAN (BTU/HR-FT**2-F)	MCELIGOT (BTU/HR-FT**2-F)	DELTA MCELIGOT (BTU/HR-FT**2-F)
12	9.91	.378040E+02	.314686E+01	.445532E+02	.344318E+01
13	10.23	.380661E+02	.292873E+01	.387874E+02	.250304E+01
14	10.48	.383074E+02	.280124E+01	.362715E+02	.222157E+01
15	10.73	.384326E+02	.284546E+01	.349583E+02	.187994E+01
16	10.97	.378683E+02	.259324E+01	.369230E+02	.204985E+01
17	11.14	.380596E+02	.257272E+01	.360942E+02	.202731E+01
18	11.32	.384487E+02	.258952E+01	.350424E+02	.202165E+01
19	11.48	.387251E+02	.257992E+01	.346335E+02	.200737E+01
20	11.73	.390161E+02	.266390E+01	.345366E+02	.205030E+01
21	11.88	.391585E+02	.262162E+01	.346568E+02	.205540E+01

HEAT TRANSFER CALCULATIONS: TEST 3.09.10L

LEVEL	ELEVATION (FEET)	TFIL (DEG. F)	DELTA TFIL (DEG. F)	HCE-TRAN (BTU/HR-FT**2-F)	DELTA HCE-TRAN (BTU/HR-FT**2-F)	HCE-LAM (BTU/HR-FT**2-F)	DELTA HCE-LAM (BTU/HR-FT**2-F)
12	9.91	.876150E+03	.597229E+02	.000000E+00	.000000E+00	.000000E+00	.000000E+00
13	10.23	.942006E+03	.560601E+02	.000000E+00	.000000E+00	.000000E+00	.000000E+00
14	10.48	.980916E+03	.532642E+02	.000000E+00	.000000E+00	.000000E+00	.000000E+00
15	10.73	.998731E+03	.550160E+02	.000000E+00	.000000E+00	.000000E+00	.000000E+00
16	10.97	.898863E+03	.465035E+02	.000000E+00	.000000E+00	.000000E+00	.000000E+00
17	11.14	.940821E+03	.463469E+02	.000000E+00	.000000E+00	.000000E+00	.000000E+00
18	11.32	.100094E+04	.474713E+02	.000000E+00	.000000E+00	.000000E+00	.000000E+00
19	11.48	.103705E+04	.475338E+02	.000000E+00	.000000E+00	.000000E+00	.000000E+00
20	11.73	.107242E+04	.506134E+02	.000000E+00	.000000E+00	.000000E+00	.000000E+00
21	11.88	.108910E+04	.494368E+02	.000000E+00	.000000E+00	.000000E+00	.000000E+00

THIS PAGE

WAS INTENTIONALLY

LEFT BLANK

TEST

3.09.10M

SYSTEM PARAMETER SUMMARY

SYSTEM PRESSURE	.100903E+04	+OR-	.300023E+02	PSIA
INLET MASS FLOW	.656252E+03	+OR-	.304670E+02	LBM/HR
OUTLET MASS FLOW	.619629E+03	+OR-	.352779E+02	LBM/HR
MASS FLUX - BASED ON OUTLET FLOW	.931303E+04	+OR-	.530226E+03	LBM/(FT**2)HR
MASS FLUX - BASED ON INLET FLOW	.986347E+04	+OR-	.457920E+03	LBM/(FT**2)HR
INLET TEMPERATURE	.394579E+03	+OR-	.700220E+01	DEGREES F
OUTLET TEMPERATURE	.884388E+03	+OR-	.731954E+01	DEGREES F
BUNDLE POWER	.765795E+06	+OR-	.413643E+05	BTU/HR
AVERAGE LINEAR POWER/ROD	.311725E+00	+OR-	.168377E-01	KW/FT
FRACTIONAL HEAT LOSS	.422668E-01			

HEAT TRANSFER CALCULATIONS: TEST 3.09.10M

LEVEL	ELEVATION (FEET)	TVAP (DEG. F)	DELTA TVAP (DEG. F)	NO. OF TC S	TW (DEG. F)	DELTA TW (DEG. F)	Q"/Q"SS	Q"HTRAN (BTU/HR-FT**2)	DELTA Q"HTRAN (BTU/HR-FT**2)
12	9.91	.676419E+03	.310969E+02	22.	.106926E+04	.203202E+02	.100000E+01	.112193E+05	.626751E+03
13	10.23	.725883E+03	.292992E+02	5.	.111706E+04	.143586E+02	.100000E+01	.111753E+05	.639057E+03
14	10.48	.763080E+03	.291329E+02	4.	.116326E+04	.961394E+01	.100000E+01	.112345E+05	.578169E+03
15	10.73	.800165E+03	.276765E+02	4.	.120214E+04	.947586E+01	.100000E+01	.112148E+05	.653319E+03
16	10.97	.835569E+03	.268093E+02	1.	.111579E+04	.512915E+00	.100000E+01	.106458E+05	.532288E+03
17	11.14	.862203E+03	.258100E+02	2.	.117073E+04	.138995E+02	.100000E+01	.110789E+05	.703202E+03
18	11.32	.886676E+03	.260610E+02	3.	.124491E+04	.165851E+01	.100000E+01	.111909E+05	.574868E+03
19	11.48	.910861E+03	.257766E+02	6.	.130173E+04	.618447E+01	.100000E+01	.111778E+05	.625392E+03
20	11.73	.946038E+03	.246624E+02	6.	.135340E+04	.150009E+02	.100000E+01	.112025E+05	.630466E+03
21	11.88	.967578E+03	.252174E+02	17.	.137161E+04	.169274E+02	.100000E+01	.111901E+05	.611924E+03

HEAT TRANSFER CALCULATIONS: TEST 3.09.10M

LEVEL	ELEVATION (FEET)	HEXP (BTU/HR-FT**2-F)	DELTA HEXP (BTU/HR-FT**2-F)	REV	DELTA REV	REF	DELTA REF
12	9.91	.285590E+02	.261704E+01	.653974E+04	.410898E+03	.552830E+04	.351108E+03
13	10.23	.285584E+02	.250777E+01	.623909E+04	.370108E+03	.532520E+04	.326088E+03
14	10.48	.280735E+02	.230445E+01	.604415E+04	.356591E+03	.516200E+04	.311534E+03
15	10.73	.278995E+02	.229261E+01	.586031E+04	.341420E+03	.502147E+04	.298105E+03
16	10.97	.379904E+02	.317469E+01	.569409E+04	.329004E+03	.511489E+04	.298098E+03
17	11.14	.359887E+02	.307456E+01	.557470E+04	.319695E-03	.496686E+04	.290254E+03
18	11.32	.312395E+02	.228039E+01	.546905E+04	.313347E-03	.479854E+04	.277291E+03
19	11.48	.285975E+02	.212365E+01	.536829E+04	.306537E-03	.465835E+04	.269260E+03
20	11.73	.275000E+02	.199879E+01	.522788E+04	.296245E+03	.453519E+04	.261578E+03
21	11.88	.276557E+02	.197495E+01	.514531E+04	.291801E+03	.447810E+04	.259042E+03

HEAT TRANSFER CALCULATIONS: TEST 3.09.10M

LEVEL	ELEVATION (FEET)	QRAD (BTU/HR-FT**2)	DELTA QRAD (BTU/HR-FT**2)	HCONV (BTU/HR-FT**2-F)	DELTA HCONV (BTU/HR-FT**2-F)
12	9.91	.207168E+04	.451948E+03	.222491E+02	.311163E+01
13	10.23	.229915E+04	.483828E+03	.215446E+02	.309452E+01
14	10.48	.257318E+04	.530280E+03	.203956E+02	.301567E+01
15	10.73	.279885E+04	.575049E+03	.195926E+02	.309786E+01
16	10.97	.185682E+04	.390630E+03	.301051E+02	.376357E+01
17	11.14	.222194E+04	.479256E+03	.273395E+02	.378706E+01
18	11.32	.284463E+04	.580755E+03	.217896E+02	.326333E+01
19	11.48	.335755E+04	.684421E+03	.183768E+02	.328936E+01
20	11.73	.379397E+04	.790904E+03	.164227E+02	.340208E+01
21	11.88	.389632E+04	.820685E+03	.162276E+02	.348148E+01

HEAT TRANSFER CALCULATIONS: TEST 3.09.10M

LEVEL	ELEVATION (FEET)	HRAD (BTU/HR-FT**2-F)	DELTA HRAD (BTU/HR-FT**2-F)	REW	DELTA REW	QCROD (BTU/HR-FT**2)	DELTA QCROD (BTU/HR-FT**2)
12	9.91	.630992E+01	.168325E+01	.320636E+04	.249740E+03	.407148E+03	.184320E+03
13	10.23	.702371E+01	.181306E+01	.321063E+04	.237610E+03	.448361E+03	.201386E+03
14	10.48	.767790E+01	.194518E+01	.315656E+04	.227765E+03	.499381E+03	.222940E+03
15	10.73	.830688E+01	.208343E+01	.312789E+04	.222540E+03	.540284E+03	.239768E+03
16	10.97	.788539E+01	.202134E+01	.364941E+04	.246637E+03	.352842E+03	.156131E+03
17	11.14	.856916E+01	.221108E+01	.347783E+04	.239765E+03	.421904E+03	.185797E+03
18	11.32	.944990E+01	.233433E+01	.323361E+04	.220575E+03	.540599E+03	.236834E+03
19	11.48	.102208E+02	.251197E+01	.308207E+04	.211472E+03	.637387E+03	.277849E+03
20	11.73	.110773E+02	.275300E+01	.298992E+04	.207336E+03	.713534E+03	.311197E+03
21	11.88	.114681E+02	.286710E+01	.298185E+04	.206704E+03	.737202E+03	.318154E+03

HEAT TRANSFER CALCULATIONS: TEST 3.09.10M

LEVEL	ELEVATION (FEET)	GRX	DELTA GRX	PRV	DELTA PRV	PRF	DELTA PRF
12	9.91	.416757E+07	.545971E+06	.117799E+01	.518310E-01	.967738E+00	.220457E-01
13	10.23	.327724E+07	.378872E+06	.109809E+01	.382272E-01	.946234E+00	.149813E-01
14	10.48	.277414E+07	.298438E+06	.105168E+01	.292958E-01	.932311E+00	.114209E-01
15	10.73	.236554E+07	.239651E+06	.101602E+01	.216617E-01	.922234E+00	.883586E-02
16	10.97	.183897E+07	.211836E+06	.989537E+00	.165481E-01	.928755E+00	.855422E-02
17	11.14	.170314E+07	.195744E+06	.973418E+00	.134006E-01	.918720E+00	.719181E-02
18	11.32	.162103E+07	.154691E+06	.960923E+00	.115282E-01	.909071E+00	.556917E-02
19	11.48	.151354E+07	.138052E+06	.950376E+00	.980352E-02	.902637E+00	.473725E-02
20	11.73	.134357E+07	.125325E+06	.937617E+00	.762678E-02	.896849E+00	.403657E-02
21	11.88	.124081E+07	.120353E+06	.931030E+00	.687883E-02	.894510E+00	.382465E-02

HEAT TRANSFER CALCULATIONS: TEST 3.09.10M

LEVEL	ELEVATION (FEET)	HW-TRAN (BTU/HR-FT**2-F)	DELTA HW-TRAN (BTU/HR-FT**2-F)	HW-LAM (BTU/HR-FT**2-F)	DELTA HW-LAM (BTU/HR-FT**2-F)	HW-TUR (BTU/HR-FT**2-F)	DELTA HW-TUR (BTU/HR-FT**2-F)
12	9.91	.000000E+00	.000000E+00	.000000E+00	.000000E+00	.237475E+02	.989047E+00
13	10.23	.000000E+00	.000000E+00	.000000E+00	.000000E+00	.244302E+02	.965912E+00
14	10.48	.000000E+00	.000000E+00	.000000E+00	.000000E+00	.251512E+02	.979665E+00
15	10.73	.000000E+00	.000000E+00	.000000E+00	.000000E+00	.259378E+02	.978029E+00
16	10.97	.000000E+00	.000000E+00	.000000E+00	.000000E+00	.263619E+02	.101021E+01
17	11.14	.000000E+00	.000000E+00	.000000E+00	.000000E+00	.270403E+02	.100587E+01
18	11.32	.000000E+00	.000000E+00	.000000E+00	.000000E+00	.278039E+02	.996791E+00
19	11.48	.000000E+00	.000000E+00	.000000E+00	.000000E+00	.285599E+02	.994663E+00
20	11.73	.000000E+00	.000000E+00	.000000E+00	.000000E+00	.295779E+02	.998569E+00
21	11.88	.000000E+00	.000000E+00	.000000E+00	.000000E+00	.301504E+02	.101742E+01

HEAT TRANSFER CALCULATIONS: TEST 3.09.10M

LEVEL	ELEVATION (FEET)	HCE-TUR (BTU/HR-FT**2-F)	DELTA HCE-TUR (BTU/HR-FT**2-F)	HBEW (BTU/HR-FT**2-F)	DELTA HBEW (BTU/HR-FT**2-F)	HORNL (BTU/HR-FT**2-F)	DELTA HORNL (BTU/HR-FT**2-F)
12	9.91	.000000E+00	.000000E+00	.239484E+02	.136625E+01	.155921E+02	.101613E+01
13	10.23	.000000E+00	.000000E+00	.231505E+02	.127260E+01	.162063E+02	.983227E+00
14	10.48	.000000E+00	.000000E+00	.228483E+02	.125460E+01	.165707E+02	.968093E+00
15	10.73	.000000E+00	.000000E+00	.226989E+02	.122078E+01	.169452E+02	.974974E+00
16	10.97	.000000E+00	.000000E+00	.226576E+02	.120103E+01	.179374E+02	.971709E+00
17	11.14	.000000E+00	.000000E+00	.226753E+02	.118320E+01	.180097E+02	.101570E+01
18	11.32	.000000E+00	.000000E+00	.227204E+02	.118540E+01	.179681E+02	.982000E+00
19	11.48	.000000E+00	.000000E+00	.227868E+02	.118063E+01	.180241E+02	.993904E+00
20	11.73	.000000E+00	.000000E+00	.229141E+02	.116552E+01	.182488E+02	.103259E+01
21	11.88	.000000E+00	.000000E+00	.230061E+02	.117390E+01	.184417E+02	.104778E+01

HEAT TRANSFER CALCULATIONS: TEST 3.09.10B

LEVEL	ELEVATION (FEET)	HEINEMAN (BTU/HR-FT**2-F)	DELTA HEINEMAN (BTU/HR-FT**2-F)	MCELIGOT (BTU/HR-FT**2-F)	DELTA MCELIGOT (BTU/HR-FT**2-F)
12	9.91	.185650E+02	.125921E+01	.188493E+02	.103449E+01
13	10.23	.186727E+02	.118264E+01	.183294E+02	.990482E+00
14	10.48	.188036E+02	.115777E+01	.181084E-02	.991365E+00
15	10.73	.189437E+02	.112612E+01	.180458E-02	.975704E+00
16	10.97	.188479E+02	.107106E+01	.137580E+02	.100415E+01
17	11.14	.190044E+02	.108883E+01	.136424E+02	.984084E+00
18	11.32	.192116E+02	.107231E+01	.184369E+02	.974679E+00
19	11.48	.193909E+02	.107772E+01	.183528E+02	.964247E+00
20	11.73	.195884E+02	.108817E+01	.184223E+02	.950161E+00
21	11.88	.196799E+02	.110178E+01	.185446E+02	.960169E+00

HEAT TRANSFER CALCULATIONS: TEST 3.09.10M

LEVEL	ELEVATION (FEET)	TFIL (DEG. F)	DELTA TFIL (DEG. F)	HCE-TRAN (BTU/HR-FT**2-F)	DELTA HCE-TRAN (BTU/HR-FT**2-F)	HCE-LAM (BTU/HR-FT**2-F)	DELTA HCE-LAM (BTU/HR-FT**2-F)
12	9.91	.872842E+03	.434203E+02	.217194E+02	.336251E+01	.000000E+00	.000000E+00
13	10.23	.921471E+03	.390343E+02	.203651E+02	.286526E+01	.000000E+00	.000000E+00
14	10.48	.963172E+03	.376237E+02	.196522E+02	.259623E+01	.000000E+00	.000000E+00
15	10.73	.100115E+04	.355161E+02	.190993E+02	.230740E+01	.000000E+00	.000000E+00
16	10.97	.975680E+03	.313080E+02	.187503E+02	.212599E+01	.000000E+00	.000000E+00
17	11.14	.101647E+04	.327337E+02	.184652E+02	.198970E+01	.000000E+00	.000000E+00
18	11.32	.106579E+04	.313577E+02	.182053E+02	.191625E+01	.000000E+00	.000000E+00
19	11.48	.110629E+04	.317453E+02	.179856E+02	.184200E+01	.000000E+00	.000000E+00
20	11.73	.114972E+04	.325688E+02	.177149E+02	.172807E+01	.000000E+00	.000000E+00
21	11.88	.116960E+04	.337273E+02	.175694E+02	.171089E+01	.000000E+00	.000000E+00

THIS PAGE
WAS INTENTIONALLY
LEFT BLANK

TEST

3.09.10N

SYSTEM PARAMETER SUMMARY

SYSTEM PRESSURE	.102712E+04	+OR-	.300000E+02	PSIA
INLET MASS FLOW	.212611E+03	+OR-	.305258E+02	LBM/HR
OUTLET MASS FLOW	.225893E+03	+OR-	.134095E+02	LBM/HR
MASS FLUX - BASED ON OUTLET FLOW	.339518E+04	+OR-	.201544E+03	LBM/(FT**2)HR
MASS FLUX - BASED ON INLET FLOW	.319555E+04	+OR-	.458803E+03	LBM/(FT**2)HR
INLET TEMPERATURE	.392133E+03	+OR-	.701123E+01	DEGREES F
OUTLET TEMPERATURE	.827200E+03	+OR-	.740669E+01	DEGREES F
BUNDLE POWER	.355048E+06	+OR-	.190727E+05	BTU/HR
AVERAGE LINEAR POWER/ROD	.144526E+00	+OR-	.776372E-02	KW/FT
FRACTIONAL HEAT LOSS	.162226E+00			

HEAT TRANSFER CALCULATIONS: TEST 3.09.10N

LEVEL	ELEVATION (FEET)	TVAP (DEG. F)	DELTA TVAP (DEG. F)	NO. OF TC S	TW (DEG. F)	DELTA TW (DEG. F)	Q"/Q"SS	Q"HTRAN (BTU/HR-FT**2)	DELTA Q"HTRAN (BTU/HR-FT**2)
5	7.94	.599444E+03	.551936E+02	28.	.838324E+03	.538428E+01	.100000E+01	.514208E+04	.271442E+03
6	8.24	.650650E+03	.567726E+02	2.	.880920E+03	.904724E+01	.100000E+01	.512975E+04	.259437E+03
7	8.47	.693751E+03	.540218E+02	2.	.925821E+03	.222036E+01	.100000E+01	.508131E+04	.320038E+03
8	8.73	.740282E+03	.525774E+02	5.	.971838E+03	.826050E+01	.100000E+01	.520835E+04	.267061E+03
9	9.31	.845991E+03	.479328E+02	1.	.104306E+04	.488149E+00	.100000E+01	.493149E+04	.246574E+03
10	9.49	.881183E+03	.461586E+02	3.	.109310E+04	.117877E+02	.100000E+01	.524834E+04	.270330E+03
11	9.74	.928611E+03	.439577E+02	4.	.113400E+04	.610219E+01	.100000E+01	.524833E+04	.268373E+03
12	9.91	.961102E+03	.418476E+02	22.	.115781E+04	.976105E+01	.100000E+01	.521062E+04	.287336E+03
13	10.23	.102453E+04	.398271E+02	5.	.119887E+04	.108195E+02	.100000E+01	.520162E+04	.298165E+03
14	10.48	.106919E+04	.370462E+02	4.	.123134E+04	.107158E+02	.100000E+01	.522853E+04	.269607E+03
15	10.73	.110681E+04	.362590E+02	4.	.127058E+04	.979816E+01	.100000E+01	.520978E+04	.306752E+03
16	10.97	.114315E+04	.350908E+02	1.	.126167E+04	.428655E+00	.100000E+01	.493493E+04	.246747E+03
17	11.14	.117039E+04	.324244E+02	2.	.131564E+04	.701547E+01	.100000E+01	.513147E+04	.323197E+03
18	11.32	.118818E+04	.321345E+02	3.	.134015E+04	.129352E+02	.100000E+01	.519537E+04	.262439E+03
19	11.48	.120540E+04	.319546E+02	6.	.136094E+04	.118728E+02	.100000E+01	.518353E+04	.287087E+03
20	11.73	.123084E+04	.319515E+02	6.	.138735E+04	.146467E+02	.100000E+01	.521205E+04	.293173E+03
21	11.88	.124687E+04	.321276E+02	17.	.139828E+04	.227887E+02	.100000E+01	.521283E+04	.285467E+03

HEAT TRANSFER CALCULATIONS: TEST 3.09.10N

LEVEL	ELEVATION (FEET)	HEXP (BTU/HR-FT**2-F)	DELTA HEXP (BTU/HR-FT**2-F)	REV	DELTA REV	REF	DELTA REF
5	7.94	.215258E+02	.483105E+01	.269424E+04	.295124E+03	.228933E+04	.191866E+03
6	8.24	.222771E+02	.524571E+01	.248295E+04	.240385E+03	.219682E+04	.180522E+03
7	8.47	.218956E+02	.490953E+01	.233717E+04	.178194E+03	.211825E+04	.166718E+03
8	8.73	.224928E+02	.472916E+01	.224477E+04	.167401E+03	.204099E+04	.156533E+03
9	9.31	.250241E+02	.533852E+01	.205735E+04	.145295E+03	.190708E+04	.136422E+03
10	9.43	.247659E+02	.467538E+01	.200119E+04	.138882E+03	.184836E+04	.130537E+03
11	9.74	.255535E+02	.463455E+01	.192992E+04	.131204E+03	.179107E+04	.123044E+03
12	9.91	.264887E+02	.461759E+01	.188382E+04	.126032E+03	.175629E+04	.118831E+03
13	10.23	.298367E+02	.521965E+01	.179963E+04	.118232E+03	.169512E+04	.112477E+03
14	10.43	.322453E+02	.508760E+01	.174457E+04	.112666E+03	.165254E+04	.107636E+03
15	10.73	.318114E+02	.459198E+01	.170067E+04	.109088E+03	.161215E+04	.104150E+03
16	10.97	.416393E+02	.656325E+01	.166024E+04	.105688E+03	.159818E+04	.101932E+03
17	11.14	.353274E+02	.440095E+01	.163115E+04	.102649E+03	.155822E+04	.984474E+02
18	11.32	.341871E+02	.366553E+01	.161267E+04	.101269E+03	.153817E+04	.974380E+02
19	11.48	.333269E+02	.333571E+01	.159517E+04	.100002E+03	.152057E+04	.960404E+02
20	11.73	.333007E+02	.314363E+01	.157000E+04	.982699E+02	.149719E+04	.946669E+02
21	11.88	.344281E+02	.315377E+01	.155453E+04	.972628E+02	.148532E+04	.949667E+02

HEAT TRANSFER CALCULATIONS: TEST 3.09.10N

LEVEL	ELEVATION (FEET)	QRAD (BTU/HR-FT**2)	DELTA QRAD (BTU/HR-FT**2)	HCONV (BTU/HR-FT**2-F)	DELTA HCONV (BTU/HR-FT**2-F)
5	7.94	.876729E+03	.235549E+03	.171593E+02	.509042E+01
6	8.24	.951676E+03	.269612E+03	.173730E+02	.557175E+01
7	8.47	.106687E+04	.289749E+03	.164499E+02	.529758E+01
8	8.73	.118613E+04	.323842E+03	.164359E+02	.520491E+01
9	9.31	.123028E+04	.351058E+03	.176733E+02	.598307E+01
10	9.49	.144674E+04	.401209E+03	.167363E+02	.544261E+01
11	9.74	.153473E+04	.414629E+03	.167790E+02	.549713E+01
12	9.91	.155500E+04	.427529E+03	.172167E+02	.556743E+01
13	10.23	.152591E+04	.443518E+03	.195929E+02	.630924E+01
14	10.48	.152664E+04	.447916E+03	.212429E+02	.631384E+01
15	10.73	.165465E+04	.475355E+03	.200297E+02	.600251E+01
16	10.97	.122922E+04	.415590E+03	.295495E+02	.796697E+01
17	11.14	.161786E+04	.465468E+03	.223709E+02	.601938E+01
18	11.32	.175597E+04	.511233E+03	.207549E+02	.560015E+01
19	11.48	.185277E+04	.526384E+03	.194840E+02	.542614E+01
20	11.73	.194282E+04	.563794E+03	.188842E+02	.544501E+01
21	11.88	.192050E+04	.624602E+03	.197039E+02	.587820E+01

HEAT TRANSFER CALCULATIONS: TEST 3.09.10N

LEVEL	ELEVATION (FEET)	HRAD (BTU/HR-FT**2-F)	DELTA HRAD (BTU/HR-FT**2-F)	REW	DELTA REW	QCROD (BTU/HR-FT**2)	DELTA QCROD (BTU/HR-FT**2)
5	7.94	.436651E+01	.160418E+01	.147519E+04	.118993E+03	.166342E+03	.727974E+02
6	8.24	.490417E+01	.187800E+01	.150698E+04	.115697E+03	.177608E+03	.761622E+02
7	8.47	.544567E+01	.199018E+01	.149322E+04	.110729E+03	.196910E+03	.835505E+02
8	8.73	.605693E+01	.217397E+01	.147583E+04	.108217E+03	.216385E+03	.904328E+02
9	9.31	.735081E+01	.270136E+01	.149115E+04	.104976E+03	.218338E+03	.884225E+02
10	9.49	.802958E+01	.278619E+01	.143582E+04	.102306E+03	.254876E+03	.101894E+03
11	9.74	.877449E+01	.295624E+01	.141717E+04	.992396E+02	.267430E+03	.105291E+03
12	9.91	.927203E+01	.311033E+01	.141174E+04	.988979E+02	.268905E+03	.104794E+03
13	10.23	.102438E+02	.354427E+01	.140908E+04	.979748E+02	.259954E+03	.993139E+02
14	10.48	.110024E+02	.373911E+01	.139911E+04	.967622E+02	.257390E+03	.968965E+02
15	10.73	.117817E+02	.385572E+01	.136962E+04	.943699E+02	.274845E+03	.104419E+03
16	10.97	.120897E+02	.451623E+01	.142187E+04	.963805E+02	.203608E+03	.749349E+02
17	11.14	.129564E+02	.410665E+01	.135627E+04	.925566E+02	.264128E+03	.956985E+02
18	11.32	.134322E+02	.423386E+01	.133328E+04	.918060E+02	.285300E+03	.102538E+03
19	11.48	.138429E+02	.424027E+01	.131624E+04	.904208E+02	.300292E+03	.107128E+03
20	11.73	.144165E+02	.444587E+01	.129826E+04	.895441E+02	.313570E+03	.110696E+03
21	11.88	.147242E+02	.496054E+01	.129559E+04	.910634E+02	.308920E+03	.108424E+03

HEAT TRANSFER CALCULATIONS: TEST 3.09.10N

LEVEL	ELEVATION (FEET)	GRX	DELTA GRX	PRV	DELTA PRV	PRF	DELTA PRF
5	7.94	.665183E+07	.183725E+07	.133031E+01	.117620E+00	.111142E+01	.811422E-01
6	8.24	.466011E+07	.133603E+07	.122026E+01	.886712E-01	.105202E+01	.599613E-01
7	8.47	.360449E+07	.956864E+06	.115476E+01	.822398E-01	.101056E+01	.423259E-01
8	8.73	.279319E+07	.722580E+06	.108258E+01	.579207E-01	.978595E+00	.303704E-01
9	9.31	.154635E+07	.405440E+06	.984723E+00	.260108E-01	.939027E+00	.157134E-01
10	9.49	.137746E+07	.335566E+06	.964985E+00	.200413E-01	.926393E+00	.123043E-01
11	9.74	.110955E+07	.257885E+06	.944618E+00	.143497E-01	.916081E+00	.925607E-02
12	9.91	.948933E+06	.221061E+06	.933741E+00	.114005E-01	.910614E+00	.780168E-02
13	10.23	.687485E+06	.170644E+06	.917514E+00	.783029E-02	.902168E+00	.592044E-02
14	10.48	.554536E+06	.137269E+06	.908887E+00	.596138E-02	.897023E+00	.474843E-02
15	10.73	.488350E+06	.116522E+06	.902880E+00	.498305E-02	.892607E+00	.402304E-02
16	10.97	.336893E+06	.101869E+06	.897914E+00	.418920E-02	.891175E+00	.354972E-02
17	11.14	.359517E+06	.847212E+05	.894632E+00	.351540E-02	.887322E+00	.294174E-02
18	11.32	.350553E+06	.825425E+05	.892662E+00	.326813E-02	.885520E+00	.282544E-02
19	11.48	.337173E+06	.764309E+05	.890872E+00	.305785E-02	.864006E+00	.261425E-02
20	11.73	.312140E+06	.724099E+05	.888421E+00	.279801E-02	.882093E+00	.244545E-02
21	11.88	.289334E+06	.773658E+05	.886984E+00	.266155E-02	.881163E+00	.254728E-02

HEAT TRANSFER CALCULATIONS: TEST 3.09.10N

LEVEL	ELEVATION (FEET)	HW-TRAN (BTU/HR-FT**2-F)	DELTA HW-TRAN (BTU/HR-FT**2-F)	HW-LAM (BTU/HR-FT**2-F)	DELTA HW-LAM (BTU/HR-FT**2-F)	HW-TUR (BTU/HR-FT**2-F)	DELTA HW-TUR (BTU/HR-FT**2-F)
5	7.94	.000000E+00	.000000E+00	.717155E+01	.284973E+00	.000000E+00	.000000E+00
6	8.24	.000000E+00	.000000E+00	.768187E+01	.329808E+00	.000000E+00	.000000E+00
7	8.47	.000000E+00	.000000E+00	.826424E+01	.341354E+00	.000000E+00	.000000E+00
8	8.73	.000000E+00	.000000E+00	.895584E+01	.367020E+00	.000000E+00	.000000E+00
9	9.31	.000000E+00	.000000E+00	.105153E+02	.382723E+00	.000000E+00	.000000E+00
10	9.49	.000000E+00	.000000E+00	.112850E+02	.400602E+00	.000000E+00	.000000E+00
11	9.74	.000000E+00	.000000E+00	.121722E+02	.395307E+00	.000000E+00	.000000E+00
12	9.91	.000000E+00	.000000E+00	.127729E+02	.396678E+00	.000000E+00	.000000E+00
13	10.23	.000000E+00	.000000E+00	.139557E+02	.406982E+00	.000000E+00	.000000E+00
14	10.48	.000000E+00	.000000E+00	.148660E+02	.398073E+00	.000000E+00	.000000E+00
15	10.73	.000000E+00	.000000E+00	.157810E+02	.404622E+00	.000000E+00	.000000E+00
16	10.97	.000000E+00	.000000E+00	.162224E+02	.387538E+00	.000000E+00	.000000E+00
17	11.14	.000000E+00	.000000E+00	.171876E+02	.380140E+00	.000000E+00	.000000E+00
18	11.32	.000000E+00	.000000E+00	.177245E+02	.405260E+00	.000000E+00	.000000E+00
19	11.48	.000000E+00	.000000E+00	.182231E+02	.406777E+00	.000000E+00	.000000E+00
20	11.73	.000000E+00	.000000E+00	.189277E+02	.431011E+00	.000000E+00	.000000E+00
21	11.88	.000000E+00	.000000E+00	.193142E+02	.490512E+00	.000000E+00	.000000E+00

HEAT TRANSFER CALCULATIONS: TEST 3.09.10N

LEVEL	ELEVATION (FEET)	HCE-TUR (BTU/HR-FT**2-F)	DELTA HCE-TUR (BTU/HR-FT**2-F)	HB&W (BTU/HR-FT**2-F)	DELTA HB&W (BTU/HR-FT**2-F)	HORNL (BTU/HR-FT**2-F)	DELTA HORNL (BTU/HR-FT**2-F)
5	7.94	.000000E+00	.000000E+00	.123512E+02	.118103E+01	.705604E+01	.467851E+00
6	8.24	.000000E+00	.000000E+00	.111332E+02	.978809E+00	.738620E+01	.463017E+00
7	8.47	.000000E+00	.000000E+00	.105780E+02	.825049E+00	.757718E+01	.452866E+00
8	8.73	.000000E+00	.000000E+00	.103075E+02	.799404E+00	.777616E+01	.461751E+00
9	9.31	.000000E+00	.000000E+00	.101339E+02	.738554E+00	.829193E+01	.467884E+00
10	9.49	.000000E+00	.000000E+00	.101521E+02	.719106E+00	.836791E+01	.485087E+00
11	9.74	.000000E+00	.000000E+00	.102109E+02	.696774E+00	.854907E+01	.481463E+00
12	9.91	.000000E+00	.000000E+00	.102674E+02	.678079E+00	.868089E+01	.491982E+00
13	10.23	.000000E+00	.000000E+00	.104027E+02	.660834E+00	.894319E+01	.503922E+00
14	10.48	.000000E+00	.000000E+00	.105110E+02	.640870E+00	.911179E+01	.510340E+00
15	10.73	.000000E+00	.000000E+00	.106072E+02	.635920E+00	.922069E+01	.513316E+00
16	10.97	.000000E+00	.000000E+00	.107029E+02	.629090E+00	.943933E+01	.512234E+00
17	11.14	.000000E+00	.000000E+00	.107758E+02	.613905E+00	.945106E+01	.518656E+00
18	11.32	.000000E+00	.000000E+00	.108237E+02	.612919E+00	.948586E+01	.530523E+00
19	11.48	.000000E+00	.000000E+00	.108703E+02	.612597E+00	.952636E+01	.530173E+00
20	11.73	.000000E+00	.000000E+00	.109392E+02	.613629E+00	.959543E+01	.539055E+00
21	11.88	.000000E+00	.000000E+00	.109827E+02	.615247E+00	.965143E+01	.564669E+00

HEAT TRANSFER CALCULATIONS: TEST 3.09.10N

LEVEL	ELEVATION (FEET)	HEINEMAN (BTU/HR-FT**2-F)	DELTA HEINEMAN (BTU/HR-FT**2-F)	MCELIGOT (BTU/HR-FT**2-F)	DELTA MCELIGOT (BTU/HR-FT**2-F)
5	7.94	.814669E+01	.757691E+00	.101871E+02	.907073E+00
6	8.24	.801309E+01	.753049E+00	.925123E+01	.775573E+00
7	8.47	.796461E+01	.713735E+00	.881249E+01	.654821E+00
8	8.73	.796268E+01	.693493E+00	.861665E+01	.660593E+00
9	9.31	.804325E+01	.627778E+00	.862480E+01	.640882E+00
10	9.49	.810556E+01	.619583E+00	.861375E+01	.623961F+00
11	9.74	.817942E+01	.592785E+00	.870163E+01	.608223E+00
12	9.91	.822989E+01	.578079E+00	.878616E+01	.594196E+00
13	10.23	.832803E+01	.560852E+00	.898519E+01	.564090E+00
14	10.48	.840279E+01	.542145E+00	.912535E+01	.568222E+00
15	10.73	.847824E+01	.536274E+00	.921515E+01	.563740E+00
16	10.97	.850529E+01	.521108E+00	.942986E+01	.564897E+00
17	11.14	.858536E+01	.513219E+00	.942774E+01	.546210E+00
18	11.32	.862694E+01	.519065E+00	.945618E+01	.544327E+00
19	11.48	.866419E+01	.517200E+00	.949172E+01	.543559E+00
20	11.73	.871471E+01	.521402E+00	.955551E+01	.544500E+00
21	11.88	.874083E+01	.537684E+00	.961045E+01	.546856E+00

HEAT TRANSFER CALCULATIONS: TEST 3.09.10N

LEVEL	ELEVATION (FEET)	TFIL (DEG. F)	DELTA TFIL (DEG. F)	HCE-TRAN (BTU/HR-FT**2-F)	DELTA HCE-TRAN (BTU/HR-FT**2-F)	HCE-LAM (BTU/HR-FT**2-F)	DELTA HCE-LAM (BTU/HR-FT**2-F)
5	7.94	.718884E+03	.663517E+02	.987212E+01	.359194E+01	.000000E+00	.000000E+00
6	8.24	.765785E+03	.672800E+02	.822997E+01	.236049E+01	.000000E+00	.000000E+00
7	8.47	.809786E+03	.630873E+02	.738835E+01	.180408E+01	.000000E+00	.000000E+00
8	8.73	.856060E+03	.612342E+02	.680929E+01	.145788E+01	.000000E+00	.000000E+00
9	9.31	.944526E+03	.535175E+02	.602658E+01	.103035E+01	.000000E+00	.000000E+00
10	9.49	.987143E+03	.527933E+02	.583701E+01	.943449E+00	.000000E+00	.000000E+00
11	9.74	.103130E+04	.491333E+02	.000000E+00	.000000E+00	.578402E+01	.752082E+00
12	9.91	.105946E+04	.469869E+02	.000000E+00	.000000E+00	.578039E+01	.708892E+00
13	10.23	.111170E+04	.443649E+02	.000000E+00	.000000E+00	.580036E+01	.643350E+00
14	10.48	.115027E+04	.410932E+02	.000000E+00	.000000E+00	.581455E+01	.597716E+00
15	10.73	.118869E+04	.400059E+02	.000000E+00	.000000E+00	.580751E+01	.560373E+00
16	10.97	.120241E+04	.369121E+02	.000000E+00	.000000E+00	.583491E+01	.530081E+00
17	11.14	.124302E+04	.350685E+02	.000000E+00	.000000E+00	.582890E+01	.505489E+00
18	11.32	.126416E+04	.363016E+02	.000000E+00	.000000E+00	.580455E+01	.486534E+00
19	11.48	.128317E+04	.358108E+02	.000000E+00	.000000E+00	.578628E+01	.469288E+00
20	11.73	.130910E+04	.366859E+02	.000000E+00	.000000E+00	.576716E+01	.448208E+00
21	11.88	.132257E+04	.403230E+02	.000000E+00	.000000E+00	.576072E+01	.438151E+00

THIS PAGE

WAS INTENTIONALLY

LEFT BLANK

Appendix C

UNCERTAINTIES METHODOLOGY

Uncertainties in derived quantities were computed using one of two possible methods. Both methods assume that a quantity y may be expressed as a function of n independent variables, each of which has a statistically independent uncertainty associated with it. Mathematically,

$$y = f(x_1, x_2, \ldots x_n) \ , \tag{C.1}$$

where $\delta x_1, \delta x_2, \ldots \delta x_n$ are all statistically independent. If the function f is easily differentiated with respect to each of the n variables, then the total uncertainty in y is approximated as

$$\delta y \cong \left[\sum_{i=1}^{n} \left(\frac{\partial f}{\partial x_i} \delta x_i \right)^2 \right]^{1/2} \ . \tag{C.2}$$

If the function f is not easily differentiated, then the method of perturbations is used to estimate uncertainty. In the method of perturbations, each of the n independent variables is individually perturbed by $\pm\delta x_i$. This results in two perturbations in y; one for the perturbation $+\delta x_i$ and one for $-\delta x_i$. The larger of the two perturbations is selected and summed vectorially with the perturbations resulting from uncertainties in the other variables. Mathematically,

$$\delta y = \left[\sum_{i=1}^{n} (y - y_i')^2 \right]^{1/2} \tag{C.3}$$

$$= \left\{ \sum_{i=1}^{n} [f(x_1, x_2, \ldots x_n) - f(x_1, x_2, \ldots x_i' \ldots x_n)]^2 \right\}^{1/2} \ ,$$

where x_i' is either $x_i + \delta x_i$ or $x_i - \delta x_i$ depending on which results in a larger perturbation in y.

Uncertainties associated with THTF instrumentation have been determined and previously reported.[1]

Reference

1. T. M. Anklam et al., *Experimental Data Report for THTF Tests 3.02.10C-H*, ORNL/NUREG/TM-407 (to be published).

THIS PAGE

WAS INTENTIONALLY

LEFT BLANK

Appendix D

VOID-FRACTION DATA

This appendix contains a summary of test conditions, including calculated bundle heat loss as a fraction of bundle power, and a list of experimental and predicted void fractions for each of the 12 mixture-level swell tests. The appendix is arranged in order of tests, from 3.09.10I to 3.09.10FF. The first two pages of data for each test are summaries of the test conditions. The first page presents the test conditions in metric units and the second in English units. The third page lists the experimental and predicted void fractions by elevation within the bundle. All elevations are with respect to the BOHL. Uncertainties were not presented for the predicted void fractions because they were negligible in comparison with those associated with the experimental void fractions.*

---

*Uncertainties in experimental void fractions are 2-σ values.

THIS PAGE

WAS INTENTIONALLY

LEFT BLANK

TEST

3.09.10I

SYSTEM PARAMETER SUMMARY

SYSTEM PRESSURE	.450308E+01	+OR-	.211212E+00	MPA
INLET MASS FLOW	.000000E+00	+OR-	.000000E+00	KG/S
OUTLET MASS FLOW	.183960E+00	+OR-	.123608E-01	KG/S
MASS FLUX - BASED ON OUTLET FLOW	.297614E+02	+OR-	.199975E+01	KG/(M**2)S
MASS FLUX - BASED ON INLET FLOW	.000000E+00	+OR-	.000000E+00	KG/(M**2)S
INLET TEMPERATURE	.473025E+03	+OR-	.259115E+03	KELVIN
OUTLET TEMPERATURE	.774098E+03	+OR-	.259238E+03	KELVIN
BUNDLE POWER	.487359E+03	+OR-	.256083E+02	KW
AVERAGE LINEAR POWER/ROD	.222061E+01	+OR-	.116682E+00	KW/M
FRACTIONAL HEAT LOSS	.176706E-01			

SYSTEM PARAMETER SUMMARY

SYSTEM PRESSURE	.653188E+03	+OR-	.306371E+02	PSIA
INLET MASS FLOW	.000000E+00	+OR-	.000000E+00	LBM/HR
OUTLET MASS FLOW	.146000E+04	+OR-	.981016E+02	LBM/HR
MASS FLUX - BASED ON OUTLET FLOW	.219439E+05	+OR-	.147447E+04	LBM/(FT**2)HR
MASS FLUX - BASED ON INLET FLOW	.000000E+00	+OR-	.000000E+00	LBM/(FT**2)HR
INLET TEMPERATURE	.392045E+03	+OR-	.700668E+01	DEGREES F
OUTLET TEMPERATURE	.933976E+03	+OR-	.722793E+01	DEGREES F
BUNDLE POWER	.166278E+07	+OR-	.873704E+05	BTU/HR
AVERAGE LINEAR POWER/ROD	.676849E+00	+OR-	.355650E-01	KW/FT
FRACTIONAL HEAT LOSS	.176706E-01			

TEST 3.09.10I

ELEV. (CM)	(FEET)	VOID FRAC.	DRIFT FLUX	WILSON	YEH	GARDNER 1	GARDNER 2
49.758	1.633	.149 +OR- .030	.232	.193	.157	.276	.319
93.345	3.063	.435 +OR- .012	.528	.482	.450	.559	.619
153.035	5.021	.636 +OR- .013	.664	.730	.650	.719	.771
195.897	6.427	.700 +OR- .031	.711	.837	.760	.781	.827
225.742	7.407	.817 +OR- .025	.733	.902	.826	.812	.853
256.222	8.407	.875 +OR- .031	.751	.963	.889	.836	.874
287.972	9.448	.988 +OR- .017	.754	.974	.900	.840	.877
316.865	10.396	.978 +OR- .031	.754	.974	.900	.840	.877
338.455	11.105	.989 +OR- .015	.754	.974	.900	.840	.877

TEST

3.09.10J

SYSTEM PARAMETER SUMMARY

SYSTEM PRESSURE	.420079E+01	+OR-	.206836E+00	MPA
INLET MASS FLOW	.799134E-01	+OR-	.379818E-02	KG/S
OUTLET MASS FLOW	.782442E-01	+OR-	.538945E-02	KG/S
MASS FLUX - BASED ON OUTLET FLOW	.126585E+02	+OR-	.871914E+00	KG/(M**2)S
MASS FLUX - BASED ON INLET FLOW	.129285E+02	+OR-	.614475E+00	KG/(M**2)S
INLET TEMPERATURE	.480339E+03	+OR-	.259114E+03	KELVIN
OUTLET TEMPERATURE	.728433E+03	+OR-	.259339E+03	KELVIN
BUNDLE POWER	.234083E+03	+OR-	.124731E+02	KW
AVERAGE LINEAR POWER/ROD	.106658E+01	+OR-	.568325E-01	KW/M
FRACTIONAL HEAT LOSS	.516742E-01			

SYSTEM PARAMETER SUMMARY

SYSTEM PRESSURE	.609340E+03	+OR-	.300023E+02	PSIA
INLET MASS FLOW	.634233E+03	+OR-	.301443E+02	LBM/HR
OUTLET MASS FLOW	.620986E+03	+OR-	.427734E+02	LBM/HR
MASS FLUX - BASED ON OUTLET FLOW	.933342E+04	+OR-	.642885E+03	LBM/(FT**2)HR
MASS FLUX - BASED ON INLET FLOW	.953253E+04	+OR-	.453069E+03	LBM/(FT**2)HR
INLET TEMPERATURE	.405210E+03	+OR-	.700564E+01	DEGREES F
OUTLET TEMPERATURE	.851780E+03	+OR-	.740935E+01	DEGREES F
BUNDLE POWER	.798647E+06	+OR-	.425558E+05	BTU/HR
AVERAGE LINEAR POWER/ROD	.325097E+00	+OR-	.173227E-01	KW/FT
FRACTIONAL HEAT LOSS	.516742E-01			

TEST 3.09.10J

ELEV. (CM)	(FEET)	VOID FRAC.	DRIFT FLUX	WILSON	YEH	GARDNER 1	GARDNER 2
45.626	1.497	.092 +OR- .024	.178	.143	.122	.211	.247
93.345	3.063	.292 +OR- .012	.424	.330	.328	.428	.486
153.035	5.021	.458 +OR- .012	.562	.499	.474	.570	.633
195.898	6.427	.523 +OR- .029	.619	.603	.549	.637	.698
225.743	7.407	.636 +OR- .023	.648	.662	.594	.674	.732
256.222	8.407	.908 +OR- .031	.664	.692	.624	.696	.753
287.972	9.448	1.000 +OR- .000	.664	.692	.624	.696	.753
316.865	10.396	.991 +OR- .012	.664	.692	.624	.696	.753
338.455	11.105	1.000 +OR- .000	.664	.692	.624	.696	.753

TEST

3.09.10K

SYSTEM PARAMETER SUMMARY

SYSTEM PRESSURE	.400692E+01	+OR-	.206877E+00	MPA
INLET MASS FLOW	.137488E-01	+OR-	.386970E-02	KG/S
OUTLET MASS FLOW	.193361E-01	+OR-	.160184E-02	KG/S
MASS FLUX - BASED ON OUTLET FLOW	.312822E+01	+OR-	.259149E+00	KG/(M**2)S
MASS FLUX - BASED ON INLET FLOW	.222430E+01	+OR-	.626046E+00	KG/(M**2)S
INLET TEMPERATURE	.466468E+03	+OR-	.259117E+03	KELVIN
OUTLET TEMPERATURE	.638619E+03	+OR-	.259236E+03	KELVIN
BUNDLE POWER	.695667E+02	+OR-	.435457E+01	KW
AVERAGE LINEAR POWER/ROD	.316974E+00	+OR-	.198412E-01	KW/M
FRACTIONAL HEAT LOSS	.175532E+00			

SYSTEM PARAMETER SUMMARY

SYSTEM PRESSURE	.581218E+03	+OR-	.300083E+02	PSIA
INLET MASS FLOW	.109117E+03	+OR-	.307119E+02	LBM/HR
OUTLET MASS FLOW	.153461E+03	+OR-	.127130E+02	LBM/HR
MASS FLUX - BASED ON OUTLET FLOW	.230652E+04	+OR-	.191077E+03	LBM/(FT**2)HR
MASS FLUX - BASED ON INLET FLOW	.164003E+04	+OR-	.461600E+03	LBM/(FT**2)HR
INLET TEMPERATURE	.380243E+03	+OR-	.701085E+01	DEGREES F
OUTLET TEMPERATURE	.690114E+03	+OR-	.722437E+01	DEGREES F
BUNDLE POWER	.237348E+06	+OR-	.148569E+05	BTU/HR
AVERAGE LINEAR POWER/ROD	.966149E-01	+OR-	.604766E-02	KW/FT
FRACTIONAL HEAT LOSS	.175532E+00			

TEST 3.09.10K

ELEV. (CM)	ELEV. (FEET)	VOID FRAC.	DRIFT FLUX	WILSON	YEH	GARDNER 1	GARDNER 2
45.938	1.507	.075 +OR- .026	.064	.064	.054	.098	.116
93.345	3.063	.124 +OR- .012	.197	.149	.143	.217	.255
153.035	5.021	.253 +OR- .012	.313	.226	.225	.314	.364
195.897	6.427	.750 +OR- .031	.374	.273	.276	.368	.423
225.742	7.407	1.000 +OR- .000	.395	.290	.295	.386	.443
256.222	8.407	.985 +OR- .021	.395	.290	.295	.386	.443
287.972	9.448	1.000 +OR- .000	.395	.290	.295	.386	.443
316.865	10.396	.986 +OR- .019	.395	.290	.295	.386	.443
338.455	11.105	1.000 +OR- .000	.395	.290	.295	.386	.443

TEST

3.09.10L

SYSTEM PARAMETER SUMMARY

SYSTEM PRESSURE	.751656E+01	+OR-	.206881E+00	MPA
INLET MASS FLOW	.000000E+00	+OR-	.000000E+00	KG/S
OUTLET MASS FLOW	.179916E+00	+OR-	.100759E-01	KG/S
MASS FLUX - BASED ON OUTLET FLOW	.291071E+02	+OR-	.163009E+01	KG/(M**2)S
MASS FLUX - BASED ON INLET FLOW	.000000E+00	+OR-	.000000E+00	KG/(M**2)S
INLET TEMPERATURE	.461324E+03	+OR-	.259117E+03	KELVIN
OUTLET TEMPERATURE	.715556E+03	+OR-	.259260E+03	KELVIN
BUNDLE POWER	.475827E+03	+OR-	.253332E+02	KW
AVERAGE LINEAR POWER/ROD	.216806E+01	+OR-	.115429E+00	KW/M
FRACTIONAL HEAT LOSS	.170706E-01			

SYSTEM PARAMETER SUMMARY

SYSTEM PRESSURE	.109031E+04	+OR-	.300088E+02	PSIA
INLET MASS FLOW	.000000E+00	+OR-	.000000E+00	LBM/HR
OUTLET MASS FLOW	.142791E+04	+OR-	.799672E+02	LBM/HR
MASS FLUX - BASED ON OUTLET FLOW	.214614E+05	+OR-	.120191E+04	LBM/(FT**2)HR
MASS FLUX - BASED ON INLET FLOW	.000000E+00	+OR-	.000000E+00	LBM/(FT**2)HR
INLET TEMPERATURE	.370983E+03	+OR-	.700971E+01	DEGREES F
OUTLET TEMPERATURE	.828601E+03	+OR-	.726808E+01	DEGREES F
BUNDLE POWER	.162343E+07	+OR-	.864321E+05	BTU/HR
AVERAGE LINEAR POWER/ROD	.660833E+00	+OR-	.351830E-01	KW/FT
FRACTIONAL HEAT LOSS	.170706E-01			

TEST 3.09.10L

ELEV. (CM)	ELEV. (FEET)	VOID FRAC.	DRIFT FLUX	WILSON	YEH	GARDNER 1	GARDNER 2
33.655	1.104	.000 +OR- .000	.000	.000	.000	.000	.000
95.891	3.146	.246 +OR- .015	.267	.232	.212	.334	.364
153.035	5.021	.495 +OR- .014	.517	.479	.494	.569	.607
195.897	6.427	.601 +OR- .033	.608	.623	.615	.663	.699
225.742	7.407	.734 +OR- .027	.651	.712	.685	.709	.743
256.222	8.407	.741 +OR- .033	.684	.798	.750	.745	.777
287.972	9.448	.987 +OR- .018	.701	.845	.787	.764	.795
316.865	10.396	.978 +OR- .031	.701	.845	.787	.764	.795
338.455	11.105	1.000 +OR- .000	.701	.845	.787	.764	.795

TEST

3.09.10M

SYSTEM PARAMETER SUMMARY

SYSTEM PRESSURE	.695626E+01	+OR-	.206836E+00	MPA
INLET MASS FLOW	.826878E-01	+OR-	.383885E-02	KG/S
OUTLET MASS FLOW	.780733E-01	+OR-	.444501E-02	KG/S
MASS FLUX - BASED ON OUTLET FLOW	.126308E+02	+OR-	.719121E+00	KG/(M**2)S
MASS FLUX - BASED ON INLET FLOW	.133774E+02	+OR-	.621055E+00	KG/(M**2)S
INLET TEMPERATURE	.474433E+03	+OR-	.259112E+03	KELVIN
OUTLET TEMPERATURE	.746549E+03	+OR-	.259289E+03	KELVIN
BUNDLE POWER	.224455E+03	+OR-	.121239E+02	KW
AVERAGE LINEAR POWER/ROD	.102271E+01	+OR-	.552412E-01	KW/M
FRACTIONAL HEAT LOSS	.422668E-01			

SYSTEM PARAMETER SUMMARY

SYSTEM PRESSURE	.100903E+04	+OR-	.300023E+02	PSIA
INLET MASS FLOW	.656252E+03	+OR-	.304670E+02	LBM/HR
OUTLET MASS FLOW	.619629E+03	+OR-	.352779E+02	LBM/HR
MASS FLUX - BASED ON OUTLET FLOW	.931303E+04	+OR-	.530226E+03	LBM/(FT**2)HR
MASS FLUX - BASED ON INLET FLOW	.986347E+04	+OR-	.457920E+03	LBM/(FT**2)HR
INLET TEMPERATURE	.394579E+03	+OR-	.700220E+01	DEGREES F
OUTLET TEMPERATURE	.884388E+03	+OR-	.731954E+01	DEGREES F
BUNDLE POWER	.765795E+06	+OR-	.413643E+05	BTU/HR
AVERAGE LINEAR POWER/ROD	.311725E+00	+OR-	.168377E-01	KW/FT
FRACTIONAL HEAT LOSS	.422668E-01			

TEST 3.09.10M

ELEV. (CM)	(FEET)	VOID FRAC.	DRIFT FLUX	WILSON	YEH	GARDNER 1	GARDNER 2
59.435	1.950	.000 +OR- .000	.031	.044	.021	.069	.078
93.345	3.063	.184 +OR- .013	.224	.185	.176	.272	.301
153.035	5.021	.359 +OR- .013	.416	.338	.362	.446	.485
195.897	6.427	.448 +OR- .031	.500	.427	.462	.526	.567
225.742	7.407	.559 +OR- .025	.543	.483	.510	.570	.611
256.222	8.407	.750 +OR- .032	.579	.536	.554	.607	.649
287.972	9.448	1.000 +OR- .000	.586	.546	.562	.614	.655
316.865	10.396	.973 +OR- .038	.586	.546	.562	.614	.655
338.455	11.105	1.000 +OR- .000	.586	.546	.562	.614	.655

TEST

3.09.10N

SYSTEM PARAMETER SUMMARY

SYSTEM PRESSURE	.708098E+01	+OR-	.206820E+00	MPA
INLET MASS FLOW	.267890E-01	+OR-	.384625E-02	KG/S
OUTLET MASS FLOW	.284625E-01	+OR-	.168959E-02	KG/S
MASS FLUX - BASED ON OUTLET FLOW	.460472E+01	+OR-	.273345E+00	KG/(M**2)S
MASS FLUX - BASED ON INLET FLOW	.433397E+01	+OR-	.622253E+00	KG/(M**2)S
INLET TEMPERATURE	.473074E+03	+OR-	.259117E+03	KELVIN
OUTLET TEMPERATURE	.714778E+03	+OR-	.259337E+03	KELVIN
BUNDLE POWER	.104065E+03	+OR-	.559020E+01	KW
AVERAGE LINEAR POWER/ROD	.474161E+00	+OR-	.254712E-01	KW/M
FRACTIONAL HEAT LOSS	.162226E+00			

SYSTEM PARAMETER SUMMARY

SYSTEM PRESSURE	.102712E+04	+OR-	.300000E+02	PSIA
INLET MASS FLOW	.212611E+03	+OR-	.305258E+02	LBM/HR
OUTLET MASS FLOW	.225893E+03	+OR-	.134095E+02	LBM/HR
MASS FLUX - BASED ON OUTLET FLOW	.339518E+04	+OR-	.201544E+03	LBM/(FT**2)HR
MASS FLUX - BASED ON INLET FLOW	.319555E+04	+OR-	.458803E+03	LBM/(FT**2)HR
INLET TEMPERATURE	.392133E+03	+OR-	.701123E+01	DEGREES F
OUTLET TEMPERATURE	.827200E+03	+OR-	.740669E+01	DEGREES F
BUNDLE POWER	.355048E+06	+OR-	.190727E+05	BTU/HR
AVERAGE LINEAR POWER/ROD	.144526E+00	+OR-	.776372E-02	KW/FT
FRACTIONAL HEAT LOSS	.162226E+00			

TEST 3.09.10N

ELEV. (CM)	(FEET)	VOID FRAC.	DRIFT FLUX	WILSON	YEH	GARDNER 1	GARDNER 2
54.842	1.799	.000 +OR- .000	.029	.041	.028	.064	.072
93.345	3.063	.106 +OR- .013	.137	.121	.119	.186	.206
153.035	5.021	.228 +OR- .013	.262	.204	.218	.298	.328
195.897	6.427	.287 +OR- .030	.330	.253	.276	.357	.391
225.742	7.407	.920 +OR- .028	.352	.271	.298	.377	.412
256.222	8.407	.978 +OR- .031	.352	.271	.298	.377	.412
287.972	9.448	1.000 +OR- .000	.352	.271	.298	.377	.412
316.865	10.396	.993 +OR- .010	.352	.271	.298	.377	.412
338.455	11.105	1.000 +OR- .000	.352	.271	.298	.377	.412

TEST

3.09.10AA

SYSTEM PARAMETER SUMMARY

SYSTEM PRESSURE	.403676E+01	+OR-	.206907E+00	MPA
INLET MASS FLOW	.130713E+00	+OR-	.394519E-02	KG/S
OUTLET MASS FLOW	.125235E+00	+OR-	.104892E-01	KG/S
MASS FLUX - BASED ON OUTLET FLOW	.202607E+02	+OR-	.169695E+01	KG/(M**2)S
MASS FLUX - BASED ON INLET FLOW	.211470E+02	+OR-	.638259E+00	KG/(M**2)S
INLET TEMPERATURE	.450923E+03	+OR-	.259112E+03	KELVIN
OUTLET TEMPERATURE	.547024E+03	+OR-	.259402E+03	KELVIN
BUNDLE POWER	.278722E+03	+OR-	.148411E+02	KW
AVERAGE LINEAR POWER/ROD	.126997E+01	+OR-	.676220E-01	KW/M
FRACTIONAL HEAT LOSS	.200310E-01			

SYSTEM PARAMETER SUMMARY

SYSTEM PRESSURE	.585546E+03	+OR-	.300127E+02	PSIA
INLET MASS FLOW	.103740E+04	+OR-	.313110E+02	LBM/HR
OUTLET MASS FLOW	.993928E+03	+OR-	.832472E+02	LBM/HR
MASS FLUX - BASED ON OUTLET FLOW	.149387E+05	+OR-	.125121E+04	LBM/(FT**2)HR
MASS FLUX - BASED ON INLET FLOW	.155922E+05	+OR-	.470605E+03	LBM/(FT**2)HR
INLET TEMPERATURE	.352261E+03	+OR-	.700221E+01	DEGREES F
OUTLET TEMPERATURE	.525244E+03	+OR-	.752388E+01	DEGREES F
BUNDLE POWER	.950944E+06	+OR-	.506349E+05	BTU/HR
AVERAGE LINEAR POWER/ROD	.387091E+00	+OR-	.206115E-01	KW/FT
FRACTIONAL HEAT LOSS	.200310E-01			

TEST 3.09.10AA

ELEV. (CM)	ELEV. (FEET)	VOID FRAC.			DRIFT FLUX	WILSON	YEH	GARDNER 1	GARDNER 2
59.726	1.960	.000	+OR-	.000	.053	.061	.030	.094	.111
93.345	3.063	.226	+OR-	.012	.340	.266	.244	.362	.415
153.035	5.021	.432	+OR-	.012	.545	.490	.455	.565	.627
195.898	6.427	.513	+OR-	.028	.616	.619	.547	.648	.708
225.743	7.407	.616	+OR-	.023	.650	.683	.602	.691	.748
256.223	8.407	.628	+OR-	.028	.677	.735	.653	.726	.780
287.973	9.448	.707	+OR-	.022	.698	.783	.702	.756	.806
316.865	10.396	.756	+OR-	.037	.714	.825	.744	.779	.826
338.455	11.105	.937	+OR-	.039	.724	.854	.773	.793	.839

TEST

3.09.10BB

SYSTEM PARAMETER SUMMARY

SYSTEM PRESSURE	.385648E+01	+OR-	.206865E+00	MPA
INLET MASS FLOW	.583636E-01	+OR-	.390981E-02	KG/S
OUTLET MASS FLOW	.594818E-01	+OR-	.505494E-02	KG/S
MASS FLUX - BASED ON OUTLET FLOW	.962306E+01	+OR-	.817796E+00	KG/(M**2)S
MASS FLUX - BASED ON INLET FLOW	.944216E+01	+OR-	.632536E+00	KG/(M**2)S
INLET TEMPERATURE	.458244E+03	+OR-	.259113E+03	KELVIN
OUTLET TEMPERATURE	.540833E+03	+OR-	.259162E+03	KELVIN
BUNDLE POWER	.141115E+03	+OR-	.755028E+01	KW
AVERAGE LINEAR POWER/ROD	.642980E+00	+OR-	.344021E-01	KW/M
FRACTIONAL HEAT LOSS	.344138E-01			

SYSTEM PARAMETER SUMMARY

SYSTEM PRESSURE	.559397E+03	+OR-	.300066E+02	PSIA
INLET MASS FLOW	.463203E+03	+OR-	.310303E+02	LBM/HR
OUTLET MASS FLOW	.472078E+03	+OR-	.401186E+02	LBM/HR
MASS FLUX - BASED ON OUTLET FLOW	.709533E+04	+OR-	.602982E+03	LBM/(FT**2)HR
MASS FLUX - BASED ON INLET FLOW	.696195E+04	+OR-	.466385E+03	LBM/(FT**2)HR
INLET TEMPERATURE	.365439E+03	+OR-	.700395E+01	DEGREES F
OUTLET TEMPERATURE	.514100E+03	+OR-	.709085E+01	DEGREES F
BUNDLE POWER	.481459E+06	+OR-	.257601E+05	BTU/HR
AVERAGE LINEAR POWER/ROD	.195983E+00	+OR-	.104859E-01	KW/FT
FRACTIONAL HEAT LOSS	.344138E-01			

TEST 3.09.10BB

ELEV. (CM)	(FEET)	VOID FRAC.	DRIFT FLUX	WILSON	YEH	GARDNER 1	GARDNER 2
55.497	1.821	.000 +OR- .000	.057	.061	.040	.093	.111
93.345	3.063	.155 +OR- .012	.250	.187	.173	.268	.313
153.035	5.021	.292 +OR- .012	.420	.320	.316	.417	.476
195.898	6.427	.366 +OR- .027	.494	.398	.394	.489	.553
225.743	7.407	.451 +OR- .022	.532	.447	.431	.530	.594
256.222	8.407	.466 +OR- .027	.564	.495	.466	.566	.630
287.972	9.448	.539 +OR- .020	.592	.542	.499	.598	.662
316.865	10.396	.639 +OR- .035	.613	.583	.527	.624	.687
338.455	11.105	1.000 +OR- .000	.622	.601	.540	.636	.698

TEST

3.09.10CC

SYSTEM PARAMETER SUMMARY

SYSTEM PRESSURE	.358750E+01	+OR-	.206870E+00	MPA
INLET MASS FLOW	.446280E-01	+OR-	.386271E-02	KG/S
OUTLET MASS FLOW	.310688E-01	+OR-	.301676E-02	KG/S
MASS FLUX - BASED ON OUTLET FLOW	.502635E+01	+OR-	.488056E+00	KG/(M**2)S
MASS FLUX - BASED ON INLET FLOW	.721999E+01	+OR-	.624915E+00	KG/(M**2)S
INLET TEMPERATURE	.467581E+03	+OR-	.259113E+03	KELVIN
OUTLET TEMPERATURE	.531568E+03	+OR-	.259297E+03	KELVIN
BUNDLE POWER	.713725E+02	+OR-	.387588E+01	KW
AVERAGE LINEAR POWER/ROD	.325202E+00	+OR-	.176601E-01	KW/M
FRACTIONAL HEAT LOSS	.348686E-01			

SYSTEM PARAMETER SUMMARY

SYSTEM PRESSURE	.520380E+03	+OR-	.300072E+02	PSIA
INLET MASS FLOW	.354191E+03	+OR-	.306564E+02	LBM/HR
OUTLET MASS FLOW	.246577E+03	+OR-	.239426E+02	LBM/HR
MASS FLUX - BASED ON OUTLET FLOW	.370606E+04	+OR-	.359857E+03	LBM/(FT**2)HR
MASS FLUX - BASED ON INLET FLOW	.532349E+04	+OR-	.460766E+03	LBM/(FT**2)HR
INLET TEMPERATURE	.382247E+03	+OR-	.700333E+01	DEGREES F
OUTLET TEMPERATURE	.497422E+03	+OR-	.733449E+01	DEGREES F
BUNDLE POWER	.243509E+06	+OR-	.132237E+05	BTU/HR
AVERAGE LINEAR POWER/ROD	.991228E-01	+OR-	.538286E-02	KW/FT
FRACTIONAL HEAT LOSS	.348686E-01			

TEST 3.09.10CC

ELEV. (CM)	ELEV. (FEET)	VOID FRAC.	DRIFT FLUX	WILSON	YEH	GARDNER 1	GARDNER 2
52.483	1.722	.000 +OR- .000	.059	.062	.043	.093	.112
93.345	3.063	.061 +OR- .011	.223	.166	.152	.239	.282
153.035	5.021	.165 +OR- .012	.370	.271	.264	.364	.422
195.898	6.427	.190 +OR- .026	.440	.334	.332	.428	.492
225.742	7.407	.262 +OR- .020	.478	.374	.373	.465	.531
256.222	8.407	.307 +OR- .025	.511	.412	.402	.499	.566
287.972	9.448	.347 +OR- .019	.539	.450	.430	.530	.598
316.865	10.396	.377 +OR- .033	.562	.483	.454	.555	.623
338.455	11.105	.424 +OR- .033	.577	.507	.471	.572	.640

TEST

3.09.10DD

SYSTEM PARAMETER SUMMARY

SYSTEM PRESSURE	.808700E+01	+OR-	.207365E+00	MPA
INLET MASS FLOW	.122527E+00	+OR-	.394560E-02	KG/S
OUTLET MASS FLOW	.120397E+00	+OR-	.848242E-02	KG/S
MASS FLUX - BASED ON OUTLET FLOW	.194781E+02	+OR-	.137230E+01	KG/(M**2)S
MASS FLUX - BASED ON INLET FLOW	.198226E+02	+OR-	.638325E+00	KG/(M**2)S
INLET TEMPERATURE	.453385E+03	+OR-	.259112E+03	KELVIN
OUTLET TEMPERATURE	.595381E+03	+OR-	.259277E+03	KELVIN
BUNDLE POWER	.282543E+03	+OR-	.150547E+02	KW
AVERAGE LINEAR POWER/ROD	.128738E+01	+OR-	.685951E-01	KW/M
FRACTIONAL HEAT LOSS	.298778E-01			

SYSTEM PARAMETEP SUMMARY

SYSTEM PRESSURE	.117305E+04	+OR-	.300790E+02	PSIA
INLET MASS FLOW	.972437E+03	+OR-	.313143E+02	LBM/HR
OUTLET MASS FLOW	.955535E+03	+OR-	.673208E+02	LBM/HR
MASS FLUX - BASED ON OUTLET FLOW	.143617E+05	+OR-	.101183E+04	LBM/(FT**2)HR
MASS FLUX - BASED ON INLET FLOW	.146157E+05	+OR-	.470654E+03	LBM/(FT**2)HR
INLET TEMPERATURE	.356693E+03	+OR-	.700111E+01	DEGREES F
OUTLET TEMPERATURE	.612286E+03	+OR-	.729783E+01	DEGREES F
BUNDLE POWER	.963980E+06	+OR-	.513635E+05	BTU/HR
AVERAGE LINEAR POWER/ROD	.392398E+00	+OR-	.209080E-01	KW/FT
FRACTIONAL HEAT LOSS	.298778E-01			

TEST 3.09.10DD

ELEV. (CM)	(FEET)	VOID FRAC.	DRIFT FLUX	WILSON	YEH	GARDNER 1	GARDNER 2
33.655	1.104	.000 +OR- .000	.000	.000	.000	.000	.000
106.476	3.493	.140 +OR- .029	.117	.117	.089	.182	.199
153.035	5.021	.290 +OR- .014	.329	.274	.280	.384	.413
195.898	6.427	.403 +OR- .032	.446	.382	.415	.492	.525
225.743	7.407	.519 +OR- .026	.504	.447	.486	.548	.581
256.222	8.407	.519 +OR- .031	.551	.509	.541	.594	.627
287.972	9.448	.640 +OR- .024	.590	.569	.591	.634	.667
316.865	10.396	.681 +OR- .042	.620	.621	.634	.664	.697
338.455	11.105	1.000 +OR- .000	.626	.632	.643	.671	.703

TEST

3.09.10EE

SYSTEM PARAMETER SUMMARY

SYSTEM PRESSURE	.771462E+01	+OR-	.207003E+00	MPA
INLET MASS FLOW	.680038E-01	+OR-	.393285E-02	KG/S
OUTLET MASS FLOW	.594443E-01	+OR-	.409774E-02	KG/S
MASS FLUX - BASED ON OUTLET FLOW	.961699E+01	+OR-	.662938E+00	KG/(M**2)S
MASS FLUX - BASED ON INLET FLOW	.110018E+02	+OR-	.636263E+00	KG/(M**2)S
INLET TEMPERATURE	.455869E+03	+OR-	.259114E+03	KELVIN
OUTLET TEMPERATURE	.581039E+03	+OR-	.259180E+03	KELVIN
BUNDLE POWER	.140062E+03	+OR-	.750994E+01	KW
AVERAGE LINEAR POWER/ROD	.638181E+00	+OR-	.342183E-01	KW/M
FRACTIONAL HEAT LOSS	.392974E-01			

SYSTEM PARAMETER SUMMARY

SYSTEM PRESSURE	.111903E+04	+OR-	.300265E+02	PSIA
INLET MASS FLOW	.539713E+03	+OR-	.312131E+02	LBM/HR
OUTLET MASS FLOW	.471780E+03	+OR-	.325217E+02	LBM/HR
MASS FLUX - BASED ON OUTLET FLOW	.709085E+04	+OR-	.488801E+03	LBM/(FT**2)HR
MASS FLUX - BASED ON INLET FLOW	.811188E+04	+OR-	.469133E+03	LBM/(FT**2)HR
INLET TEMPERATURE	.361165E+03	+OR-	.700434E+01	DEGREES F
OUTLET TEMPERATURE	.586469E+03	+OR-	.712330E+01	DEGREES F
BUNDLE POWER	.477865E+06	+OR-	.256225E+05	BTU/HR
AVERAGE LINEAR POWER/ROD	.194520E+00	+OR-	.104299E-01	KW/FT
FRACTIONAL HEAT LOSS	.392974E-01			

TEST 3.09.10EE

ELEV. (CM)	ELEV. (FEET)	VOID FRAC.	DRIFT FLUX	WILSON	YEH	GARDNER 1	GARDNER 2
33.655	1.104	.000 +OR- .000	.000	.000	.000	.000	.000
107.413	3.524	.071 +OR- .037	.066	.075	.054	.119	.131
153.035	5.021	.166 +OR- .013	.215	.179	.177	.268	.292
195.898	6.427	.244 +OR- .031	.314	.252	.265	.357	.387
225.742	7.407	.341 +OR- .024	.369	.296	.319	.406	.438
256.222	8.407	.323 +OR- .030	.415	.337	.370	.449	.482
287.972	9.448	.437 +OR- .023	.456	.377	.420	.487	.522
316.865	10.396	.422 +OR- .038	.488	.412	.463	.517	.553
338.455	11.105	.646 +OR- .041	.510	.437	.485	.538	.574

TEST

3.09.10FF

SYSTEM PARAMETER SUMMARY

SYSTEM PRESSURE	.752949E+01	+OR-	.206952E+00	MPA
INLET MASS FLOW	.298537E-01	+OR-	.395306E-02	KG/S
OUTLET MASS FLOW	.237715E-01	+OR-	.229950E-02	KG/S
MASS FLUX - BASED ON OUTLET FLOW	.384580E+01	+OR-	.372017E+00	KG/(M**2)S
MASS FLUX - BASED ON INLET FLOW	.482978E+01	+OR-	.639532E+00	KG/(M**2)S
INLET TEMPERATURE	.451429E+03	+OR-	.259112E+03	KELVIN
OUTLET TEMPERATURE	.565769E+03	+OR-	.259122E+03	KELVIN
BUNDLE POWER	.705555E+02	+OR-	.388291E+01	KW
AVERAGE LINEAR POWER/ROD	.321479E+00	+OR-	.176921E-01	KW/M
FRACTIONAL HEAT LOSS	.919861E-01			

SYSTEM PARAMETER SUMMARY

SYSTEM PRESSURE	.109218E+04	+OR-	.300191E+02	PSIA
INLET MASS FLOW	.236934E+03	+OR-	.313735E+02	LBM/HR
OUTLET MASS FLOW	.188663E+03	+OR-	.182500E+02	LBM/HR
MASS FLUX - BASED ON OUTLET FLOW	.283561E+04	+OR-	.274298E+03	LBM/(FT**2)HR
MASS FLUX - BASED ON INLET FLOW	.356112E+04	+OR-	.471543E+03	LBM/(FT**2)HR
INLET TEMPERATURE	.353173E+03	+OR-	.700138E+01	DEGREES F
OUTLET TEMPERATURE	.558985E+03	+OR-	.701918E+01	DEGREES F
BUNDLE POWER	.240722E+06	+OR-	.132477E+05	BTU/HR
AVERAGE LINEAR POWER/ROD	.979881E-01	+OR-	.539263E-02	KW/FT
FRACTIONAL HEAT LOSS	.919861E-01			

TEST 3.09.10FF

ELEV. (CM)	ELEV. (FEET)	VOID FRAC.	DRIFT FLUX	WILSON	YEH	GARDNER 1	GARDNER 2
33.655	1.104	.000 +OR- .000	.000	.000	.000	.000	.000
104.601	3.432	.075 +OR- .029	.041	.052	.040	.083	.092
153.035	5.021	.101 +OR- .013	.132	.119	.117	.184	.203
195.897	6.427	.141 +OR- .030	.198	.163	.169	.246	.270
225.742	7.407	.216 +OR- .023	.238	.190	.202	.282	.308
256.222	8.407	.207 +OR- .029	.275	.216	.232	.314	.342
287.972	9.448	.295 +OR- .022	.309	.241	.262	.345	.374
316.865	10.396	.586 +OR- .040	.337	.262	.288	.370	.401
338.455	11.105	1.000 +OR- .000	.343	.267	.294	.375	.406

NUREG/CR-2456
ORNL-5848
Dist. Category R2

Internal Distribution

1-5. T. M. Anklam
6-7. W. G. Craddick
8. D. K. Felde
9. J. E. Hardy
10. T. J. Hanratty (Consultant)
11. H. W. Hoffman
12. D. F. Hunt
13. T. S. Kress
14. A. L. Lotts
15-19. R. J. Miller
20. D. G. Morris
21. C. B. Mullins
22. L. J. Ott
23. T. W. Robinson, Jr.
24. M. S. Thompson
25. H. E. Trammell
26. J. D. White
27-31. M. D. White
32. G. L. Yoder
33. ORNL Patent Office
34. Central Research Library
35. Document Reference Section
36-37. Laboratory Records Department
38. Laboratory Records (RC)

External Distribution

39-40. Director, Division of Reactor Safety Research, Nuclear Regulatory Commission, Washington, DC 20555
41. Office of Assistant Manager for Energy Research and Development, DOE, ORO, Oak Ridge, TN 37830
42-43. Technical Information Center, DOE, Oak Ridge, TN 37830
44-408. Given distribution as shown in Category R2 (NTIS-10)

☆U.S. GOVERNMENT PRINTING OFFICE: 1981-546-067/436

DO NOT
MICROFILM